Zebrafish Targeted Mutagenesis to Unveil Normal Physiological Functions of, and Interactions between, Prion Protein (PrP) and Amyloid Precursor Protein (APP): Relevance to Alzheimer's disease

by

Patricia Lee Anna Leighton

A thesis submitted in partial fulfillment of the requirements for the degree of

Doctor of Philosophy

in

Physiology, Cell and Developmental Biology

Department of Biological Sciences

University of Alberta

© Patricia Lee Anna Leighton, 2017

Abstract

Much of the work on Prion Protein (PrP^C) and Amyloid Precursor Protein (APP) biology has focused on the contributions of their misfolded forms or aggregated metabolites to prion diseases and Alzheimer's disease, respectively. As subversion/partial loss of some normal functions are also likely contributors to these disease states, it is also important to understand the normal functions of these proteins in healthy organisms. Zebrafish are an attractive model organism for uncovering conserved (and hence important) functions of PrP^C and APP because their CNS resembles that of mammals, and their genetic tractability can be harnessed to identify protein functional domains (eg. by 'rescuing' a phenotype in loss-of-function mutants with modified mRNAs). Here we created loss-of-function mutants of zebrafish homologs of PrP^C and APP (prp1 and appa) to identify normal functions of these proteins, using Tal-Effector Nuclease gene targeting. We also bred the $prp1^{-/-}$ mutants to our existing $prp2^{-/-}$ mutants to test for redundancy between prp1 and prp2, and created compound $prp1^{-/-}$;$appa^{-/-}$ mutants to identify functional interactions between PrP^C and APP. We did not observe overt phenotypes in any of the single mutants or compound mutants generated, likely due to genetic and/or physiological redundancy. We went on to challenge the prion protein mutants first with acute loss of a second gene and later with a convulsant. We also looked for subtle phenotypes in neural development by examining an accessible neural tissue in zebrafish larvae- the posterior lateral line, and searched for cognitive deficits in adult $prp2^{-/-}$ mutants using behavioural tests.

We found that acute loss of *appa*, achieved using morpholino gene knockdown, in $prp1^{-/-}$ mutants produced an early developmental phenotype. These developmental defects could be partly reversed or 'rescued' by delivering either *prp1* mRNA or mouse *Prnp* to one-cell staged zebrafish embryos. These experiments confirmed our previous finding that *prp1* and *appa*

interact genetically. We also found that *prp1* and *prp2* have redundant roles in modulating neural activity (measured indirectly by quantifying *c-fos* abundance) during exposure to the convulsant, PTZ. Further, both *prp1* and *prp2* participate in the development of the zebrafish lateral line neuromasts. Finally, using an object recognition test and novel object approach test, we showed that zebrafish lacking the *prp2* paralog have age-dependent deficits in object recognition memory and cognitive appraisal.

The zebrafish PrP^C and APP loss-of-function mutants and assays that we have developed herein will be used to further dissect the molecular mechanisms through which these proteins participate in neural development, neural activity, and ultimately memory and cognition. For example, 'rescue' experiments, wherein modified versions of *Prnp* and *APP* mRNA are injected into zebrafish embryos, can be used to determine which PrP^C and APP protein domains mediate their normal functions. Such information will be useful for the design of Alzheimer's disease and prion disease therapeutics.

Preface

This thesis is an original work by Patricia L.A. Leighton. The research project, of which this thesis is a part, received ethics approval from the University of Alberta Animal Policy and Welfare Committee. The author has met and exceeded the mandatory training requirements for animal users set out by the Canadian Council on Animal Care (CCAC) on the Care and Use of Animals in Research, Teaching and Testing.

A version of Chapter 1 of this thesis has been published as:

Leighton, P. L., Allison, W. T., 2016. Protein Misfolding in Prion and Prion-Like Diseases: Reconsidering a Required Role for Protein Loss-of-Function. J Alzheimers Dis. 54, 3-29.

Patricia L.A. Leighton was responsible for manuscript composition. W. Ted Allison was the supervisory author and was involved in concept formation and editing of the manuscript.

A portion of Chapter 2 of this thesis (Figure 2.15 and associated text) has been published in:

Kaiser, D., et al., 2012. Amyloid beta precursor protein and prion protein have a conserved interaction affecting cell adhesion and CNS development. PloS One. 7.

Patricia L.A. Leighton sub-cloned '*appa-i2*' and '*appb-i3*' into the pCS2+ plasmid, generated and analyzed the data in Supplemental Figure 6 of the manuscript (Figure 2.15 of this thesis) and assisted in the writing and editing of the manuscript. Gavin Neil performed the RNA extractions and RT-qPCR presented in Chapter 2 and synthesized some of the 'rescue' mRNA. Hao Wang generated some of the constructs used for the production of the 'rescue' mRNA. Natasha Lifeso and Ria Rana assisted with genotyping.

A portion of Chapter 3 has been published in:

Fleisch, V., et al., 2013. Targeted mutation of the gene encoding prion protein in zebrafish reveals a conserved role in neuron excitability. Neurobiology of disease. 55, 11-25.

Patricia L.A. Leighton performed and analyzed the behavioural experiments in Figure 6 and Supplementary Figure 8 of the manuscript (Figures 3.2-3.4 of this thesis), analyzed the RT-qPCR data and assisted in the writing and editing of the manuscript. PTZ treatments for the RT-qPCR data presented in Chapter 3 were performed by Dr. Richard Kanyo. The RNA extractions and RT-qPCR were performed by Dr. Richard Kanyo and Gavin Neil and initially analyzed by Dr.

Richard Kanyo. Hao Wang generated some of the constructs used to generate the 'rescue' mRNA and Gavin Neil synthesized some of the 'rescue' mRNAs.

A portion of Chapter 4 (Figure 4.3A in this thesis) has been published in:

Huc-Brandt, S., et al., 2014. Zebrafish prion protein PrP2 controls collective migration process during lateral line sensory system development. PLoS One. 9, e113331.

This manuscript was part of an international research collaboration led by Dr. Mireille Rossel at Université Montpellier, France. Patricia L.A. Leighton performed the experiment in Figure 2A-D in the manuscript (Figure 4.3A in this thesis), generated, prepared and shipped tissues from $prp1^{ua5001/ua5001}$ larvae described elsewhere in the manuscript and assisted in writing and editing the manuscript. Natasha Lifeso, Niall Pollock and Kirklin Maclise assisted with collection of the data presented in Chapter 4.

The entirety of Chapter 5 has been prepared for submission to Dis Model Mech. under the title:

"An Ancient Conserved Role for Prion Protein in Learning and Memory". Authors: Patricia L.A. Leighton, Nathan J. Nadolski, Adam Morrill, Trevor J. Hamilton and W. Ted Allison.

This manuscript was part of a research collaboration between the Allison Lab and the Hamilton Lab at MacEwan University, Edmonton, AB Canada. Patricia L.A. Leighton assisted with data collection, analyzed the data and composed and edited the manuscript. Nathan J. Nadolski and Adam Morrill also performed experiments and some initial analyses. Trevor J. Hamilton and W. Ted Allison were the supervisory authors, were involved in concept formation and edited the manuscript.

Chapter 6 and Appendix A are original works by Patricia L.A. Leighton.

Acknowledgements

Table of Contents

List of Tables

List of Figures

List of Common Abbreviations

°C	Degrees Celsius
aa	Amino acid
AD	Alzheimer's disease
ALS	Amyotrophic lateral sclerosis
ANOVA	Analysis of variance
AREB	Animal Research Ethics Board
bp	base pair
BCIP	5-Bromo-4-chloro-3-indoyl phosphate
BSE	Bovine spongiform encephalopathy
CaMPARI	Calcium-Modulated Photoactivatable Ratiometric Integrator
CCAC	Canadian Council on Animal Care
cDNA	Complementary deoxyribonucleic acid
CJD	Creutzfeldt–Jakob disease
CNS	Central Nervous System
CRISPR	Clustered regularly interspaced short palindromic repeats
Ct	Cycle threshold (for quantitative polymerase chain reaction)
CuBD	Copper binding domain
CWD	Chronic wasting disease
DEPC	Diethyl pyrocarbonate
DIG	Digoxigenin
DMSO	Dimethyl sulfoxide
DNA	Deoxyribonucleic acid
DNase	Deoxyribonuclease
dpf	Days post-fertilization
E	Exploration (object preference test)
E3	Zebrafish embryo growth medium
Edin	Edinburgh line of $Prnp^{-/-}$ mice
EDTA	Ethylenediaminetetraacetic acid
ENU	N-ethyl-N-nitrosourea
ER	Endoplasmic reticulum

F0	Parental generation
F1	First filial generation
FFI	Fatal familial insomnia
fmol	Femtomole
Fm43fx	Fixable analog of (*N*-(3-Triethylammoniumpropyl)-4-(4-(Dibutylamino) Styryl) Pyridinium Dibromide) membrane stain
g	Gravity (Acceleration of centrifuge)
G	Needle gauge
GFLD	Growth factor like domain
GoF	Gain-of-function
GPI	Glycophosphatidylinositol
GSS	Gerstmann–Sträussler–Scheinker syndrome
HD	Huntington's disease
hpf	Hours post-fertilization
HRM	High resolution melt analysis
HRP	Horseradish peroxidase
iCJD	Iatrogenic Creutzfeldt–Jakob disease
KCl	Potassium chloride
kDa	Kilodalton
KO	Knockout
L	Liter
LiCl	Lithium chloride
LoF	Loss-of-function
M	Moles per liter
MeOH	Methanol
mg	Milligram
MgCl2	Magnesium chloride
MIQUE	Minimum information for publication of quantitative real-time PCR experiments
mL	Milliliters
mM	Millimoles per liter

MO	Morpholino
mRNA	Messenger ribonucleic acid
MS222	Tricaine methanesulphonate
N2A Cells	Neuro2a cells (mouse neuroblastoma cell line)
NaCl	Sodium chloride
NaOH	Sodium hydroxide
NBT	Nitroblue tetrazolium
NCBI	National Center for Biotechnology Information
NFT	Neurofibrillary tangles
ng	Nano-gram
Ngsk	Nagasaki line of $Prnp^{-/-}$ mice
nL	Nano-liter
NMDA	N-Methyl-D-aspartate
NMJ	Neuromuscular junction
NOA	Novel object approach
NOR	Novel object recognition
NSC	Neural stem cells
PBS	Phosphate buffered saline
PBS^{3+}	Phosphate buffered saline containing 1% dimethyl sulfoxide, 1% Tween20 and 1% Triton
PBST	Phosphate buffered saline with 0.1% Tween20
PCR	Polymerase chain reaction
PD	Parkinson's disease
PFA	Paraformaldehyde
pg	picogram
PLL	Posterior lateral line
PTU	1-phenol-2-thiourea
PTZ	Pentylenetetrazole
qPCR	Real-time quantitative polymerase chain reaction
RFLP	Restriction fragment length polymorphism
RIN	Ribonucleic acid integrity number

RML	Rocky Mountain Laboratory/Chandler mouse adapted scrapie prion strain
RNA	Ribonucleic acid
RNA Seq	Ribonucleic acid-sequencing
RPM	Revolutions per minute
RQ	Relative quantity (for quantitative polymerase chain reaction)
RT-PCR	Reverse transcriptase polymerase chain reaction
RVD	Repeat variable diresidue
s	Seconds
sCJD	Sporadic Creutzfeldt–Jakob disease
SDS	Sodium dodecyl sulfate
SDS-PAGE	Sodium dodecyl sulfate- polyacrylamide gel electrophoresis
SE	Standard error of the mean
siRNA	Small interfering ribonucleic acid
SSC	Saline sodium citrate
T1	Training trial (object preference test)
T2	Testing trial (object preference test)
TALEN	Transcription activator-like effector nuclease
TBD	To be determined
TBST	Tris buffered saline with 0.1% Tween
TGN	Trans-Golgi Network
TILLING	Targeting induced local lesions in genomes
TME	Transmissible mink encephalopathy
Tris-HCl	Tris base mixed with hydrocholoric acid
ua	Designates alleles generated at the University of Alberta
UAS	Upstream activating sequence
UK	United Kingdom
U of A	University of Alberta
USA	United States of America
vCJD	Variant Creutzfeldt–Jakob disease
wt	Wild type
ZFIN	The Zebrafish Model Organism Database

ZFN	Zinc finger nuclease
Zrch	Zurich lines of *Prnp*$^{-/-}$ mice
µg	Microgram
µL	Microliter
µmol	Micromoles per liter

List of Gene Names

APLP1	Amyloid precursor-like protein 1 (humans)
APLP2	Amyloid precursor-like protein 2 (humans)
aplp1	*amyloid precursor-like protein 1* (zebrafish)
aplp2	*amyloid precursor-like protein 1* (zebrafish)
APP	Amyloid precursor protein (Humans, non-human primates, domestic species)
App	Amyloid precursor protein (Mice and rats)
appa	*amyloid precursor protein a* (Fish)
appb	*amyloid precursor protein b* (Fish)
appl	amyloid precursor protein-like (Fruit flies)
atoh1a	*atonal bHLH transcription factor 1a* (Zebrafish)
bdnf	*brain derived neurotrophic factor* (Zebrafish)
c-fos	FBJ osteosarcoma oncogene (Mice) [also *Fos*]
c-fos	*v-fos FBJ murine osteosarcoma viral oncogene homolog Ab* (Fish) [also *fosab*]
egfp	enhanced green fluorescent protein
elavl3	*ELAV like neuron-specific RNA binding protein 3* (Zebrafish)
Eno2	*enolase 2* (Zebrafish promoter sequence)
GFAP	*glial fibrillary acidic protein* (Zebrafish promoter sequence)
HTT	Huntingtin (Humans)
Htt	Huntingtin (mice)
MAPT	Microtubule associated protein tau (Humans)
Mapt	Microtubule associated protein tau (Mice and Fruit flies)
mib1	*mindbomb E3 ubiquitin protein ligase 1* (Zebrafish)
npas4	*bHLH-PAS-domain-containing transcription factor* (zebrafish)
Prnd	Doppel (Mice) [also Prion protein dublet]
PRNP	Prion protein (Humans, non-human primates, domestic species)
Prnp	Prion protein (Mice and rats)
prp1	*prion protein 1* (Fish) [also *prion protein b*, *prnpb*]
prp2	*prion protein 2* (Fish) [also *prion protein, related sequence 3*, *prnprs3*]
PSEN1	Presenilin 1 (Humans)
PSEN2	Presenilin 2 (Humans)

sef   *interleukin 17 receptor D* (Zebrafish) [also *il17rd*]

SNCA   Alpha synuclein

SOD1   Copper-zinc superoxide dismutase (humans)

Sod1   Copper-zinc superoxide dismutase (mice)

Sprn   *Shadoo* (Mice) [Also shadow of Prion protein]

TP53   Tumor protein p53 (humans)

tp53   *tumor protein p53* (zebrafish)

List of Protein/Peptide Names

Aβ   Amyloid beta

ADAM10   A Disintegrin and metalloproteinase domain-containing protein 10

ADAM17   A Disintegrin and metalloproteinase domain-containing protein 17

AICD   Amyloid precursor protein intracellular domain

AMPA receptor   α-amino-3-hydroxy-5-methyl-4-isoxazolepropionic acid receptor

APLP1   Amyloid precursor-like protein 1

APLP2   Amyloid precursor-like protein 2

APP   Amyloid precursor protein

appa   amyloid precursor protein a (zebrafish)

appb   amyloid precursor protein b (zebrafish)

atp2b1a   ATPase, Ca^{2+} transporting, plasma membrane 1a (zebrafish)

BACE1   β-site APP cleaving enzyme

BDNF   Brain-derived neurotrophic factor

C9ORF72   Chromosome 9 open reading frame 72

CTFα   Amyloid precursor protein C-terminal fragment alpha

CTFβ   Amyloid precursor protein C-terminal fragment beta

dkkb1   dickkopf WNT signaling pathway inhibitor 1b (zebrafish)

DPP6   Dipeptidyl aminopeptidase-like protein 6

EGFR   Epidermal growth factor receptor

ERK1   Mitogen-activated protein kinase 3

ERK2   Mitogen-activated protein kinase 1

FGF   Fibroblast growth factor

fgf3   fibroblast growth factor 3 (zebrafish)

fgf10a   fibroblast growth factor 10a (zebrafish)

FYN   FYN proto-oncogene, Src family tyrosine kinase

FUS   Fused in Sarcoma RNA binding protein

GFP   Green fluorescent protein

GluR1   Glutamate receptor 1

GluR2   Glutamate receptor 2

GSK3β   Glycogen synthase kinase 3 beta

Lnγ1	Laminin gamma-1
LRP	Lipoprotein receptor-related proteins
Lyn	Tyrosine-protein kinase Lyn proto-oncogene
NCAM	Neural cell adhesion molecule
MAP kinase	Mitogen-activated protein kinase
mGluR1	Metabotrophic glutamate receptor 1
mGluR5	Metabotrophic glutamate receptor 5
MK-801	Dizocilpine
p3	Amyloid beta- peptide $(A\beta)_{17-40/42}$
PKA	Protein kinase A
PKC	Protein kinase C
PrP^C	Cellular prion protein
PrP^{Sc}	Misfolded (scrapie) prion protein
prp1	prion protein 1 (zebrafish)
prp2	prion protein 2 (zebrafish)
PSD-95	Post-synaptic density-95
RFP	Red fluorescent protein
sAPPα	Soluble amyloid precursor protein alpha
sAPPβ	Soluble amyloid precursor protein beta
SOD1	Copper-zinc superoxide dismutase
SRC	SRC proto-oncogene, non-receptor tyrosine kinase
Std Ctrl MO	Standard control morpholino
STI1	Stress-inducible phosphoprotein 1
TARDBP	TAR DNA-binding protein 43
YFP	Yellow fluorescent protein
ZO1	Zonula occludens-1

Chapter 1. Introduction and Literature Review[1]

1.1 Introduction

1.1.1 Overview of Prion Diseases and the Prion Protein

Prion diseases are progressive, invariably fatal neurodegenerative diseases that naturally affect a number of mammalian species including sheep and goats (scrapie), mink (Transmissible Mink Encephalopathy (TME)), cervids (chronic wasting disease (CWD)), cattle (bovine spongiform encephalopathy (BSE) or mad cow disease) and humans (reviewed in (Prusiner, 1991)). Human versions of the disease include Kuru, Fatal Familial Insomnia (FFI), Gerstmann-Sträussler-Scheinker disease (GSS) and sporadic, iatrogenic and variant forms of Creutzfeldt-Jakob disease (sCJD, iCJD and vCJD). Disease pathology typical to most prion diseases includes spongiform degeneration, neuronal loss, astrogliosis and deposits of misfolded prion protein (PrP) (Budka et al., 1995; Scott et al., 1990; Williams and Young, 1980; Wood et al., 1997). The clinical features of human prion diseases are wide-ranging and vary within and between subtypes. These features include, but are not limited to, dementia, ataxia, involuntary movements and disruptions in the sleep-wake cycle (reviewed in (Collins et al., 2004)).

Prion diseases are a unique disease class due to the nature of the disease agent. The pathogens underlying prion diseases are infectious proteins or proteinaceous infectious particles (prions; as coined by S.B. Prusiner), as opposed to bacteria, viruses or viroids (Prusiner, 1982). The disease can originate sporadically or from genetic or infectious routes (reviewed in (Watts and Prusiner, 2014)). A major insight into the nature of the infectious pathogen came when a protease resistant protein was identified in scrapie infected hamster brains that was not present in uninfected brains (Bolton et al., 1982). The protein was later purified and the N-terminal amino acids of the peptide were sequenced (Oesch et al., 1985; Prusiner et al., 1984). 5'-[^{32}P]-labeled probes were then designed based on the peptide sequence and subsequently used to screen a cDNA library produced from scrapie infected hamster samples. One such cDNA clone was identified and found to contain the *Prnp* gene sequence, and *Prnp* was also found in the nuclear genome of healthy hamsters (Oesch et al., 1985). Hence the normal form of the prion

2

prion, $\underline{C}$ellular prion protein (PrP^C), and the disease form, PrP $\underline{S}$crapie (PrP^{Sc}), were identified as conformational isoforms (reviewed in (Prusiner, 1991)).

Crucial open questions in the prion field include what the nature of PrP^{Sc} is and how PrP^{Sc} replicates. While it has been established that PrP^{Sc} has a much higher β sheet content than PrP^C (Pan et al., 1993), researchers have faced difficulty in elucidating the structure of PrP^{Sc} molecules because the molecules are insoluble and have a high propensity to aggregate (reviewed in (Requena and Wille, 2014)). Recently, Vázquez-Fernández found, using electron cryomicroscopy, that a four-rung β-solenoid is a feature of the PrP^{Sc} structure (Vázquez-Fernández et al., 2016). Thus far, two models have been proposed to explain how PrP^{Sc} replicates. In the template directed misfolding model, partially unfolded PrP^C intermediates result from stochastic changes to PrP^C structure. These partially unfolded PrP^C molecules then form dimers with PrP^{Sc} molecules, which template the conversion of the PrP^C intermediates into PrP^{Sc} molecules (Cohen et al., 1994; Prusiner et al., 1990). An alternative model of prion replication is non-catalytic nucleated polymerization. In this model, PrP^C monomers are slowly converted to PrP^{Sc} monomers, which eventually form a PrP^{Sc} nucleus. This process is energetically unfavorable. In the prion disease state, PrP^{Sc} aggregates serve as pre-formed PrP^{Sc} seeds. Once a PrP^{Sc} nucleus is formed, it rapidly converts to an ordered PrP^{Sc} aggregate (Cohen et al., 1994; Come et al., 1993; Lansbury and Caughey, 1995).

Other key characteristics of prion diseases include prion strains and the species barrier. Prion strains are distinct isolates that produce recognizably different phenotypes in identical hosts. Strain-specific phenotypes are characterized by incubation time, biochemical profile (for example, the proteinase K digestion pattern) and histological profile (Aguzzi et al., 2007). The species barrier is a term used to describe the lack of disease phenotype or prolonged incubation period that occurs when a prion isolate originating in one species is introduced to a new species. Contributors to the species barrier include differences in the primary sequence between host PrP^C molecules and the PrP^{Sc} agent, as well as prion strain (Bruce et al., 1994; Scott et al., 1989).

Prion diseases have attracted much government and public attention in recent years due to their tremendous implications for the food industry, the medical system and the environment. BSE was first identified in cattle in 1985, and became an epidemic in the

UK in the early 1990s. The outbreak likely arose from incorporating carcass waste from scrapie-infected sheep and BSE-infected cattle into animal feed (Fraser et al., 1992a). The epidemic caused tragic loss for farm families and costs to the government exceeded £4 billion (Leiss and Nicol, 2006). In 2003, the BSE problem spread to North America upon the identification of BSE in a beef cow on a northern Alberta farm. The economic costs, largely resulting from the blockage of beef exports, exceeded $7 billion CAD ((Le Roy and Klein, 2003-12); reviewed in (McLachlan and Yestrau, 2008)). About 10 years after the discovery of BSE, vCJD was first reported in the UK (Will et al., 1996), and consumption of beef or beef products was later identified as a high risk factor for vCJD (Ward et al., 2006). As of April 2014, 177 cases of definite or probable vCJD had been identified in the UK (with a peak of 28 cases in 2000) and the worldwide total was 228. All genotyped cases in the UK were homozygous for methionine at codon 129, thus there is concern that the incubation period for individuals with other codon 129 genotypes may be longer and leaves potential for a second wave of vCJD onset (reviewed in (Diack et al., 2014)). There is also risk of prion disease transmission through blood transfusion and infected blood products, and three cases of probable vCJD cases due to blood transfusion have been identified in the UK (Hewitt et al., 2006) (reviewed in (Urwin et al., 2016)). Iatrogenic CJD can be transmitted through the use of contaminated surgical instruments, thus the World Health Organization advises the use of disposable surgical instruments and/or more stringent sterilization techniques for cases where prion diseases are suspected (Thomas et al., 2013).

CWD is the only prion disease known to affect free-ranging wildlife, and is an alarming ecological problem. The disease currently affects white tail deer, mule deer, elk and moose (reviewed in (Kurt and Sigurdson, 2016)). The disease was first identified in the western USA in the 1960s and has continuously expanded into other areas in North America (Kuznetsova et al., 2014) and is also present in Korea and Norway (Benestad et al., 2016; Lee et al., 2013). In Canada, CWD was first identified in captive elk, while the first case of CWD in a free-ranging animal was discovered in a Saskatchewan mule deer in 2000. There is concern that the disease will be transmitted to caribou as infected deer migrate into the southernmost part of the caribou range (reviewed in (Kuznetsova et al., 2014)). Some non-cervid species, including ferrets and squirrel monkeys, are

experimentally susceptible to CWD. While humans have certainly been orally exposed to CWD (e.g. by eating infected venison), so far there is no evidence that humans are susceptible to this form of prion disease (reviewed in (Kurt and Sigurdson, 2016)). Overall, learning more about prion disease pathology and the role of PrP^C in healthy brains is critical for developing effective disease management strategies.

1.1.2 PrP^C and its family members

PrP^C is a conserved glycophosphatidylinositol (GPI)- anchored membrane protein (Stahl et al., 1987), though alternative topologies including a secreted form and transmembrane forms exist (Hay et al., 1987a; Hay et al., 1987b). The human *PRNP* gene, located on chromosome 20, encodes a 253 amino acid protein. PrP^C is made up of a disordered N-terminus and a globular c-terminal domain that is structurally conserved among vertebrates (Calzolai et al., 2005; Zahn et al., 2000). Notable domains within the N-terminus of the protein include the octapeptide repeats (residues 51-90) and the hydrophobic domain (residues 112-145) (Figure 1.1). The octarepeat region of mammals consists of four or five repeats of PHGGGWGQ (reviewed in (Millhauser, 2007)), which bind Copper II selectively over other divalent cations (Hornshaw et al., 1995). The histidine residues coordinate this copper binding (Burns et al., 2002). The hydrophobic domain overlaps with binding sites for several of PrP^C's ligands including StiI (Zanata et al., 2002), SOD1 (Sakudo et al., 2005) and others (reviewed in (Marc et al., 2007). The C-terminus has two putative glycosylation sites (N181 and N197 in the hamster sequence) and a disulphide bond, formed between C179 and C214 in the hamster sequence (Haraguchi et al., 1989; Turk et al., 1988). The pro-peptide of hamster PrP^C is 254 amino acids long (reviewed in (Prusiner, 1991)), and it becomes 209 amino acids long after removal of the N-terminal signal peptide and 23 C-terminal amino acids that signal the attachment of the GPI anchor (Stahl et al., 1987; Turk et al., 1988). PrP^C is the substrate of multiple cleavage enzymes. ADAM10 cleaves near the C-terminus, releasing the protein from its GPI anchor. ADAM8 appears to be one candidate enzyme responsible for □1 cleavage at Lys109□His 110 (mouse sequence), which produces the N1 and C1 fragments (reviewed in (McDonald et al., 2014)). N1 has anti-apoptotic roles (Guillot-Sestier et al., 2009), while C1 has pro-apoptotic roles (Sunyach et al., 2007) and

protects against PrP[Sc] propagation (Westergard et al., 2011). Recently, an additional □-cleavage site (□2) was identified at Ala-119□Val-120, with cleavage mediated by ADAM10 and ADAM17 (McDonald et al., 2014). □-cleavage occurs at multiple sites within and immediately C-terminal to the octarepeats and produces the N2 and C2 fragments. These fragments are produced by both reactive oxygen species and ADAM10 (McDonald et al., 2014).
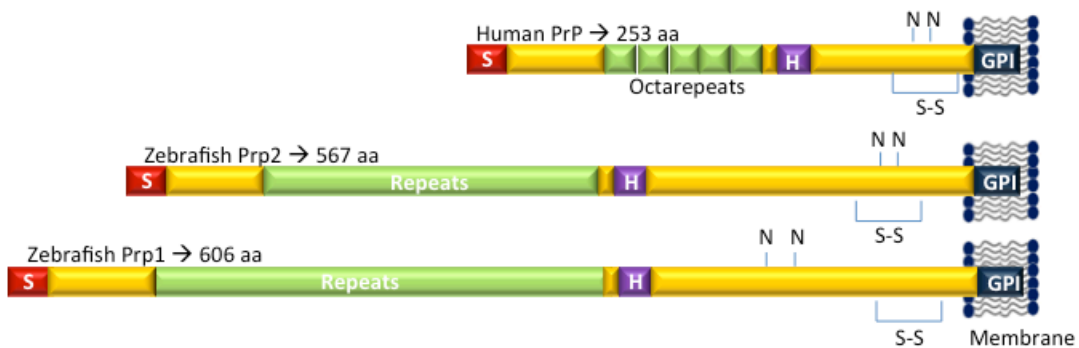
Figure 1.1. Line diagrams of Human PrP[C] and Zebrafish prp1 and prp2 show conservation of PrP[C] at the protein domain level

Like mammalian PrP[C], the zebrafish prion proteins have repetitive regions (Repeats; though they are longer and not as ordered as the octarepeats in mammals), a hydrophobic domain (H), and disulphide bonds (S—S) and N-linked glycosylation sites (N) near the C-terminus. All proteins have a signal peptide (S) and are anchored to the cell membrane by a GPI anchor (GPI).

Other members of the prion protein gene family include Doppel and Shadoo. Doppel is encoded by the *Prnd* gene, which is located downstream of *Prnp* (on chromosome 2 in mice), and it shares 25% identify with PrP^C (Moore et al., 1999). The C-terminal globular domain is structurally conserved between PrP^C and Doppel (Mo et al., 2001). *Prnd* mRNA is primarily expressed in the testis of adult males, but is upregulated in the central nervous system (CNS) of two lines of *Prnp*$^{-/-}$ mice (Ngsk and Rcm0 lines) that exhibit ataxia. Thus overexpression of *Prnd* is thought to produce the neurodegenerative phenotype in the Ngsk and Rcm0 *Prnp*$^{-/-}$ lines (Moore et al., 1999). The *Sprn* gene, which encodes the Shadoo protein, is not on the same chromosome as the genes *Prnp* and *Prnd*. It is instead located on chromosome 7 in mice. Like *Prnp*, *Sprn* is expressed in embryos and adult brain and retina (Premzl et al., 2003). Shadoo's N-terminus is structurally similar to PrP^C including a conserved N-terminal signal sequence and hydrophobic domain (Premzl et al., 2003). Like PrP^C, Shadoo has a GPI anchor and N-linked glycosylation sites (Premzl et al., 2003). Further, Shadoo has neuroprotective properties resembling those of PrP^C (Watts et al., 2007). Acute loss of Shadoo, through small interfering ribonucleic acid (siRNA) knockdown produces an embryonic lethal phenotype in *Prnp*$^{-/-}$ mice (Young et al., 2009), and Shadoo is downregulated during prion infection (Watts et al., 2007). This, along with overlapping expression patterns, points to functional redundancy between PrP^C and Shadoo that may be lost during prion infection. Double *Prnp*$^{-/-}$;*Sprn* mice, however, do not display an overt phenotype (Daude et al., 2012). Thus it is likely that other genes compensate for loss of *Prnp* function.

1.1.3 Overview of Alzheimer's disease and Amyloid Precursor Protein

Alois Alzheimer, a German physician, first publicly described what is now known as Alzheimer's disease (AD) in 1906. His 51-year old female patient, Auguste D, displayed a number of neurological symptoms including memory and psychosocial impairments, disorientation and hallucinations. After her death he discovered amyloid plaques and neurofibrillary tangles in her brain (reviewed in (Maurer et al., 1997)). It was later found that the plaques were composed of amyloid beta (Aβ) peptides (Glenner, 2012; Masters et al., 1985a), while neurofibrillary tangles (NFT) were composed of the tau protein (Goedert et al., 1988)(reviewed in (Hardy, 2006)). To this day, Aβ peptides and tau remain important diagnostic markers of AD (reviewed in (Scheltens et al., 2016)).

Several observations in the 1980s and 1990s suggested that the Amyloid Precursor Protein (APP) was a central molecule in AD pathology, and led to the formulation of the Amyloid Cascade Hypothesis, which proposes that APP metabolites work upstream of tau to produce AD phenotypes (Hardy and Allsop, 1991). First, the Aβ peptides found in AD plaques were found to be a likely proteolytic product of the larger APP protein, encoded by the *APP* gene (Kang et al., 1987). Second, human *APP* was localized to chromosome 21 (Goldgaber et al., 1987), the chromosome found in triplicate or partial triplicate in Down's syndrome patients (reviewed in (Aula et al., 1973)). AD and Down's syndrome brains share similar amyloid pathology (Masters et al., 1985b). Finally, it was discovered that some cases of AD were familial and caused by mutations in the *APP* gene (Goate et al., 1991). Other familial cases of AD were found to be associated with mutations in *APP* proteolytic enzymes including *PSEN1* and *PSEN2* (reviewed in (Hardy, 2006)). The sequence of events producing AD phenotypes has been debated since the formation of the Amyloid Cascade Hypothesis (for review see (Karran and De Strooper, 2016) and '*Complex roles for gain- and loss-of-function in AD Etiology*' in section 1.3, below). Regardless of its position in the sequence of events underlying AD, APP remains a central protein in AD and is a logical target for AD therapeutics (for examples see (Huang and Mucke, 2012; Rosenkranz et al., 2013; Selkoe, 2011)). Thus it is important to gain insight into its role in both AD pathophysiology and its role in healthy brains.

AD has tremendous socioeconomic implications. The risk of developing AD increases with age (Kawas et al., 2000), thus developed countries with aging populations are expected to experience increases in the number of AD patients in the coming decades. In 2010, the estimated number of global AD patients was 35 million and this number is predicted to reach 115 million by 2050 (Prince et al., 2013). People living with AD have a reduced quality of life, as do their caregivers who experience reduced emotional health, financial pressures and employment changes such as reduced work hours (Black et al., 2010). Further, the monetary cost to society is substantial. In Canada alone, the projected total costs to care for people with AD and other dementias in 2016 is $10.4 billion, and the annual costs are predicted to double by 2031 (In: Prevalence and Monetary Costs of Dementia in Canada (2016)). As there are currently no known preventative measures for

AD and treatment options are limited, further research into the AD mechanism and roles of APP in healthy brains is warranted.

1.1.4 APP and its family members

APP is a type I transmembrane domain glycoprotein with an extensive N-terminal domain and a short cytoplasmic tail (Bayer et al., 1999; Kang et al., 1987). Due to alternative splicing of the *APP* gene, at least 8 isoforms of the protein exist (reviewed in (Bayer et al., 1999)). Starting from the N-terminus, APP is composed of the E1 region, the acidic region, the carbohydrate domain including the E2 domain and a linker domain, the transmembrane region and the APP intracellular domain (AICD). The amyloid β (Aβ) region overlaps with the carbohydrate domain and the transmembrane domain (Figure 1.2), reviewed in (Reinhard et al., 2005)). Some isoforms of APP (APP_{751} and APP_{770} in humans) have a Kunitz-type protease inhibitor domain between the acidic region and the E2 domain that may protect APP and neighbouring proteins from protease degradation (Tanzi et al., 1988); reviewed in (Reinhard et al., 2005). The E1 region is made up of the growth factor like domain (GFLD) and the copper-binding domain (CuBD) (reviewed in (Reinhard et al., 2005)). The heparin-binding domain within the GFLD was found to mediate neurite outgrowth (Small et al., 1994), and the GFLD also binds to the extracellular matrix (Ohsawa et al., 2001; Small et al., 1999) and participates in cell-cell adhesion (Soba et al., 2005). The CuBD has been demonstrated to bind copper (Hesse et al., 1994) and reduce Copper (II) to Copper (I) (Multhaup et al., 1996). The carbohydrate domain is composed of the E2 region, which participates in extracellular matrix adhesion (reviewed in (Small et al., 1999)) and has growth-promoting properties (Jin et al., 1994; Ninomiya et al., 1993), and a linker domain. Finally, the AICD has been implicated in diverse functions including G protein (Nishimoto et al., 1993), kinase (Tarr et al., 2002) and calcium mediated signalling (Leissring et al., 2002), transcriptional regulation (Cao and Sudhof, 2001; Kimberly et al., 2005), and apoptosis (Kim et al., 2003; Kinoshita et al., 2002). APP is the substrate of multiple enzymes and can be broken into several protein fragments. The non-amyloidogenic pathway yields sAPPα, CTFα, p3 and the AICD, while the amyloidogenic pathway yields sAPPβ, CTFβ, Aβ peptides of various lengths and the AICD (Figure 1.3). The APP protein family includes the amyloid

precursor-like proteins, APLP1 and APLP2. These are structurally similar to APP, but lack the Aβ region (reviewed in (Bayer et al., 1999)).
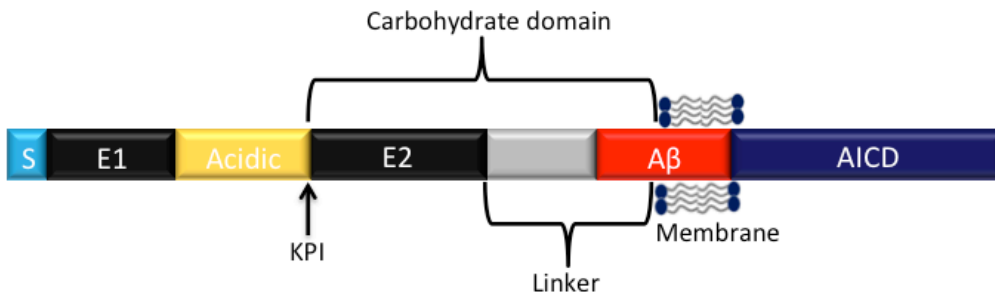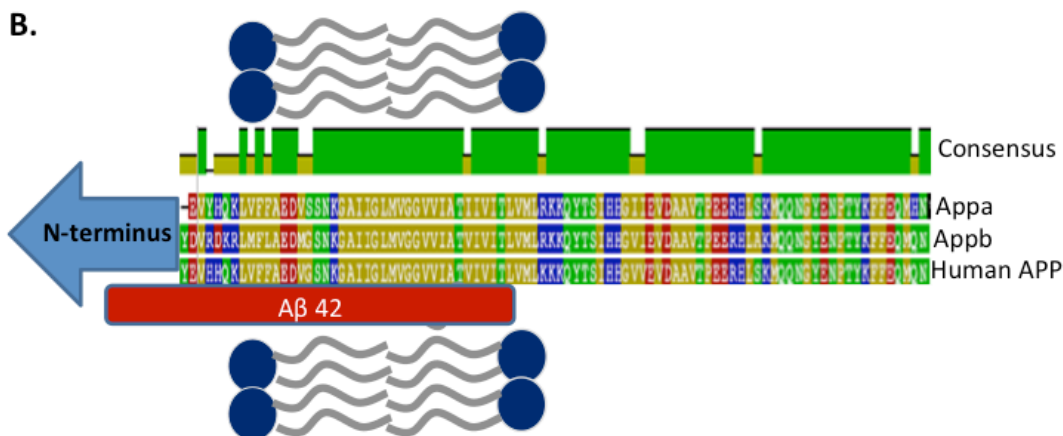
Figure 1.2. APP is conserved between fish and mammals at the amino acid level

A. Line diagram of APP highlighting its structural features. An acidic region separates the two largest divisions of the N-terminus- the E1 region and the carbohydrate domain. The carbohydrate domain consists of the E2 domain and a linker domain. The amyloid β region (Aβ) is partly housed within the transmembrane domain. The APP intracellular domain (AICD) is found at the C-terminus. A Kunitz-type protease inhibitor domain (KPI) is present in some isoforms of APP (APP_{751} and APP_{770} in humans). S refers to the signal peptide.

B. An alignment of the amino acid sequences of Human APP695 and zebrafish appa and appb reveals a high level of conservation among these proteins within the transmembrane region and C-terminus (>90%). Along the entire lengths of these proteins, they share ~70% identity (Musa et al., 2001).

A. Non-Amyloidogenic Pathway

sAPP-α

1. α-secretase

2. γ-secretase

α-secretase cleavage site

γ-secretase cleavage site

CTF-α

p3

AICD

B. Amyloidogenic Pathway

sAPP-β

Aβ

1. β-secretase

2. γ-secretase

β-Secretase cleavage site

γ-Secretase cleavage site

CTF-β

AICD
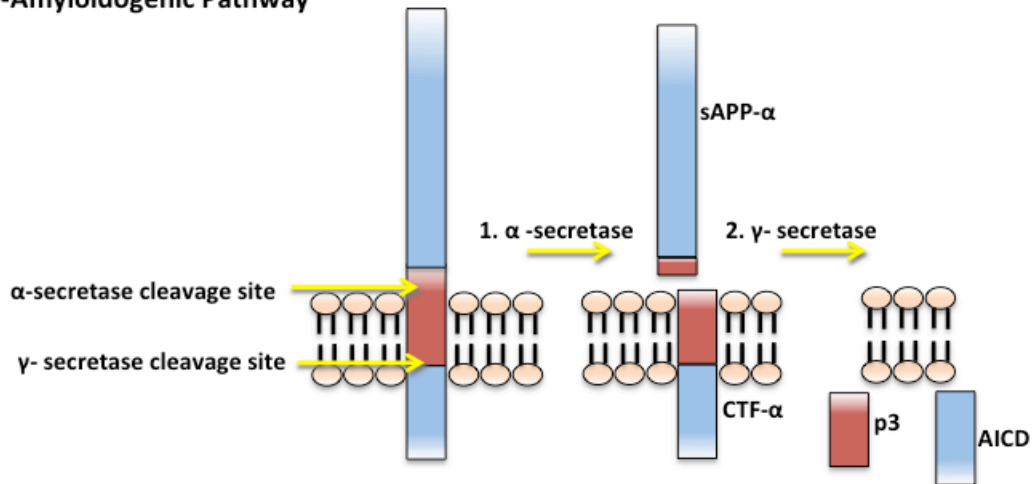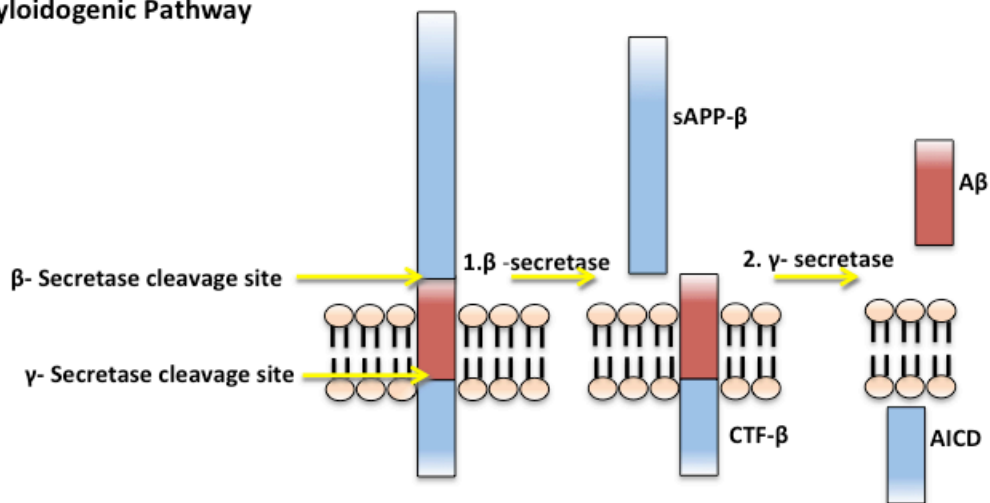
Figure 1.3. APP is processed through the non-amyloidogenic pathway and the amyloidogenic pathway[2]

A. Cleavage by α-secretase yields sAPP-α and CTF-α (1). CTF-α is then processed by the γ-secretase complex to produce p3 and AICD (2). **B.** Cleavage by β-secretase yields sAPP-β and CTF-β (1). CTF-β is then processed by the γ-secretase complex to produce Aβ peptides of varying lengths (which aggregate into neurotoxic oligomers) and the AICD (2).

1.1.5 Physiological functions of PrP and APP in healthy individuals

Despite intense study of the contributions of PrP^{Sc} to prion diseases and APP cleavage products (i.e. A$\square$ oligomers) to AD since the 1980s, the physiological functions of PrP^{C} and APP in healthy individuals remain enigmatic. Research efforts are complicated by the existence of multiple metabolites of both proteins. While a number of putative functions have been assigned to both proteins (Tables 1.1 and 1.2), the molecular mechanisms underlying many of these functions remain unclear. A useful starting point for uncovering gene function is performing an analysis of a gene's interactome. Intriguingly, it was found that PrP and APP are members of each other's interactomes (Bai et al., 2008; Schmitt-Ulms et al., 2004). While progress in uncovering *in vivo* functions of *PRNP* and *APP* was slowed by the lack of overt phenotypes in *Prnp* and *APP* knockout mice (Bueler et al., 1992; Manson et al., 1994; Muller et al., 1994; Zheng et al., 1995), examination of subtler phenotypes suggested that PrP and APP might be involved in overlapping cellular functions. These phenotypes included increased susceptibility to convulsants (Rangel et al., 2007; Steinbach et al., 1998; Walz et al., 1999), deficits in synaptic transmission (Khosravani et al., 2008; Wang et al., 2005) and age-dependent cognitive deficits (Coitinho et al., 2003; Dawson et al., 1999; Muller et al., 1994). Contrasting the lack of overt phenotypes in mouse *Prnp* knockouts, gene knockdown of zebrafish *prp1* (one of the zebrafish homologs of PRNP) resulted in a severe developmental phenotype characterized by aberrant cell adhesion and dysregulation of of E-cadherin and $\square$-catenin during gastrulation (Malaga-Trillo et al., 2009). In addition, gene knockdown of the zebrafish *appb* paralog produced fish with a shortened body axis, possibly pointing to disruptions in the convergent-extension process, which begins during gastrulation. APP could plausibly participate in convergent extension through direct regulation of cell adhesion or migration, or indirectly through regulation of a signalling pathway such as non-canonical Wnt signalling (Joshi et al., 2009).

The above findings, together with an exciting report of an interaction between PrP^{C} and A$\square$ oligomers (Lauren et al., 2009) the year before my arrival in the Allison lab, prompted my colleagues to test the hypothesis that zebrafish PrP and APP interact to mediate neuroprotection and cell adhesion in developing zebrafish. They found a specific

genetic interaction between the zebrafish *prp1* and *appa* paralogs upon deploying morpholino gene knockdown technology (Kaiser et al., 2012). Co-knockdown of *appa* and *prp1* using low doses of each morpholino (0.5 ng of each) resulted in developmental defects that could be partially rescued with ectopic overexpression of *appa* mRNA or human *APP* mRNA, but could not be rescued with *appb* mRNA. Similarly, ectopically expressed *prp1* mRNA and mouse *Prnp* mRNA rescued the phenotypes produced by *appa*/*prp1* co-knockdown, but *prp2* mRNA did not (Kaiser et al., 2012). All of the zebrafish studies described above deployed morpholino gene knockdown technology, which transiently disrupt mRNA splicing or protein translation. Thus to study the roles of APP and PrP in older fish, I sought to engineer corresponding genetic mutants.

Table 1.1. Putative functions of PrP^C and its interactome[3]

Broad Function	Specific Function	Interacting proteins	Downstream pathway
Cell adhesion	-Embryonic cell adhesion [1, 2]	-Src kinases [1, 2]	-Ca^{2+}-independent homophilic interactions [1] -Ca^{2+}-dependent, Trafficking of E-cadherin, β-catenin, F-actin to plasma membrane [1, 2]
	-Zebrafish lateral line [3]		E-cadherin, β-catenin [3]
	-Neuritogenesis (growth cone formation) [4]	-Reggie, Fyn/MAP kinase [4]	-N-cadherin [4]
Neurite Out-growth	-Neurite outgrowth [5]	-Integrins/ caveolin 1/Fyn [5]	-Raf/Ras→Erk1/2 [5]
	-Neurite outgrowth [6]	-NCAM→Fyn [6]	-TBD
	-Neurite outgrowth [7]	-Lnγ1 →mGluRI/MgluR5 [7]	-Phospholipase C, Ca^{2+} mobilization, protein-kinase C (PKC), extracellular signal-regulated kinase (ERK1/2) [7]
Regulation of neurotransmission	-Regulation of NMDA receptors [8, 9]		
	-Regulation of Kv4.2 channels [10]	-DPP6 [10]	
Metal homeostasis	Zinc uptake at the synapse [11]	-AMPA receptors (GluR2 and/or GluR1) [11]	-Inhibits tyrosine phosphatase activity [11]
Regulation of protein processing	APP processing [12,13]	-APP, BACE [12.13]	-TBD

TBD- To be determined

Table 1.1 References:

1 (Malaga-Trillo et al., 2009), 2 (Sempou et al., 2016), 3 (Huc-Brandt et al., 2014), 4 (Bodrikov et al., 2011), 5 (Pantera et al., 2009), 6 (Santuccione et al., 2005), 7 (Beraldo et al., 2011), 8 (Khosravani et al., 2008), 9 (Fleisch et al., 2013),10 (Mercer et al., 2013), 11 (Watt et al., 2012), 12 (Schmitz et al., 2014b), 13 (Parkin et al., 2007)

Table 1.2. Phenotypes resulting from loss of prion-like proteins[4]

Disease	Gene	Loss-of-function Animal Models		
		Drosophila	Zebrafish	Mice
AD	*MAPT*	*Mapt* **knockdown** -3% viable to adulthood [1] -Photoreceptor defects [1] -Neuronal degeneration [1]		*Mapt*^{-/-} -No overt phenotype [2-4] -Axon defects [2-3, 5] -Axonal transport defects (e.g., iron transport [6] -Motor deficits [6-8] -Cognitive deficits [8-9] (age and strain dependent)
	APP	*App*^{-/-} -Defective locomotion [10] -Memory impairments [11]	*Appa* **knockdown** -Developmental defects [12] -CNS apoptosis [12] *Appb* **knockdown** -Developmental defects [12-13] -Defects in motor axon outgrowth [14-15] -Locomotion defects and defects in NMJ synapse formation [15] -CNS apoptosis [12]	*APP* **KO** -No overt phenotype [17-18] -Reduced brain and/or body mass [16-19] -Reduced grip strength [18-19] -Increased seizure susceptibility [20] -Age-dependent cognitive deficits [17,21] **Conditional *APP* KO in muscle & motor neurons** -Aberrant patterning of NMJ synapses [22] -Mislocalization of high affinity choline transporter affects choline vesicle release [22]
	APP, APLP1, APLP2			*APP*^{-/-}; *APLP2*^{-/-} -Postnatal lethality [23] -Defects in NMJ structure and synaptic transmission [24] *APP*^{-/-}; *APLP1*^{-/-}; *APLP2*^{-/-} Postnatal lethality, brain structure defects [25]
ALS	*SOD1*			*Sod1*^{-/-} **mice** -Develop normally [26] -Mitochondrial oxidative stress [27] -More sensitive to neuronal injury [26] -Disruption of neuromuscular junctions [28] -Accelerated skeletal muscle denervation (reviewed in [28])
HD	*HTT*			*Htt*^{-/-} **mice** -Perinatal lethality and defects in brain development [29] -Apoptotic cell death in the testes (reviewed in [29]

Table 1.2 References

1 (Bolkan and Kretzschmar, 2014), 2 (Harada et al., 1994), 3 (Dawson et al., 2001), 4 (Fujio et al., 2007), 5 (Takei et al., 2000), 6 (Lei et al., 2012), 7 (Ikegami et al., 2000), 8 (Lei et al., 2014), 9 (Ma et al., 2014), 10 (Luo et al., 1992), 11 (Bourdet et al., 2015), 12 (Kaiser et al., 2012), 13 (Joshi et al., 2009), 14 (Song and Pimplikar, 2012), 15 (Abramsson et al., 2013), 16 (Magara et al., 1999), 17 (Muller et al., 1994), 18 (Zheng et al., 1995), 19 (Mallm et al., 2010), 20 (Steinbach et al., 1998), 21 (Dawson et al., 1999), 22 (Wang et al., 2009), 23 (Heber et al., 2000), 24 (Wang et al., 2005), 25 (Herms et al., 2004), 26 (Reaume et al., 1996), 27 (Fischer et al., 2012), 28 (Grad et al., 2011), 29 (Cattaneo et al., 2005)

1.2 Objectives, rationale and hypotheses

1.2.1 Objectives

My overall objective was to uncover conserved physiological functions of PrP^C and APP that might become disrupted during prion diseases and AD. As others in the lab had identified a genetic interaction between zebrafish homologs of *PRNP* and *APP* (Kaiser et al., 2012), I also sought to further characterize this interaction. To accomplish these goals, I used targeted mutagenesis to disrupt the zebrafish *Prnp* and *APP* genes and performed multiple phenotypic analyses on the resulting mutants.

1.2.2 Why zebrafish?

Zebrafish are an effective *in vivo* model for the study of genetic and protein interactions within the CNS for multiple reasons. They are relatively convenient to work with because they have a sequenced and annotated genome, their eggs are fertilized externally (and hence embryos are accessible to genetic manipulations), and they produce large numbers of offspring year-round. Despite some important differences in brain structure between fish and mammals, the overall architecture of their nervous system resembles that of mammals and the major neurotransmitter systems are conserved (Norton and Bally-Cuif, 2010; Panula et al., 2010; Rodriguez et al., 2002a). Further, CNS development can be easily visualized since embryos are transparent and develop externally, and embryos and larvae are suited to high throughput phenotypic screens. A key disadvantage of using zebrafish to study neurodegenerative diseases is that they have a long lifespan compared to other model organisms, living up to 5.5 years (Gerhard et al., 2002).

Importantly for the current work, zebrafish possess homologs of both *PRNP* and *APP* that are fairly conserved with those in mammals (Kaiser et al., 2012). One disadvantage of using zebrafish to study the function of these genes is that the fish have two copies of each gene (*prp1* and *prp2* are homologs of *PRNP*; *appa* and *appb* are homologs of *APP*); thus both copies must be disrupted to most closely resemble the biology a mammalian gene knockout. Further, when multiple paralogs of a gene are present in an organism, analysis of gene function can complicated by subfunctionalization and neofunctionalization. Zebrafish *prp1* (ZFIN ID ZDB-GENE-041221; alternate name

prnpb) is located on chromosome 10, and *prp2* (ZFIN ID: ZDB-GENE-041221-3; alternate name *prnprs3*) is located on chromosome 25. Both *prp1* and *prp2* have 2 exons, with their complete ORF contained within the 2nd exon. Both proteins are conserved with tetrapod PrP at the domain level in that they have an N-terminal signal peptide, a repetitive region (though longer and less patterned than the mammalian octarepeats), a hydrophobic domain, cysteine residues potentially involved in disulphide bond formation, and putative GPI anchor signals (Figure 1, (Cotto et al., 2005)). Both proteins also have putative N-glycosylation sites (Cotto et al., 2005) and it has been experimentally shown that prp1 is glycosylated and contains a GPI anchor (Miesbauer et al., 2006; Salta et al., 2014). Both proteins also have C-terminal motifs that are conserved with mammalian PrP. Within these motifs, prp1 has 25% identity to human PrP^C and prp2 has 33% identity to human PrP^C (Cotto et al., 2005).

Experiments examining expression of *prp1* and *prp2* during early development have produced inconsistent results. One group detected high levels of *prp1* expression at 2.5 hpf with low expression in the forebrain and eyes by 30 hpf (Malaga-Trillo et al., 2009), while another group did not detect *prp1* in cranial ganglia and the floorplate until 48 hpf (Cotto et al., 2005). Conversely, Malaga-Trillo *et al.* (2009) did not detect *prp2* in 2.5 hpf blastula stage embryos (Malaga-Trillo et al., 2009), while Cotto *et al.* (2005) detected high levels of *prp2* in 3.5 hpf blastula stage embryos (Cotto et al., 2005). Both studies reported expression of *prp2* in the CNS of zebrafish larvae beginning at 24 hpf including in the telencephalon, mesencephalon, rhomencephalon and hair cells of the posterior lateral line (Cotto et al., 2005; Malaga-Trillo et al., 2009)**.**

The zebrafish homologs of *APP* include *appa* (ZFIN ID: ZDB-GENE-000616-13), located on chromosome 1, and *appb* (ZFIN ID: ZDB-GENE-020220-1) located on chromosome 9. *appa* and *appb* have 70% identify at the amino acid level. Both genes share ~ 70% identify with human APP-695, and are even more conserved in the A☐42 (80% for *appa*; 71% for *appb*), transmembrane (95% for *appa*; 100% for *appb*) and cytoplasmic regions (91% for *appa*; 94% for *appb*; Figure 2B). Both genes share less than 50% identify with the APP family members APPLP1 and APPLP2. *Appa* and *appb* are both expressed by mid gastrula stages and are expressed in the telencephalon, diencephalon and posterior lateral line ganglia by 24hpf. *Appa* is also expressed in the

lens of the eye, the otic vesicles and the somites by 24 hpf, while *appb* is expressed in the mesencephalon and spinal cord (Musa et al., 2001).

1.2.3 Outline of thesis and hypotheses

This thesis is comprised of 6 chapters and 1 appendix. The remainder of Chapter 1 consists of a synthesis in which the balances of gain- and loss- of protein function in prion diseases and prion-like diseases (including AD) are discussed. Its main purposes are 1) to highlight how loss of PrP^C function in prion disease has been overshadowed by the infamous replication and gain-of-function of PrP^{Sc}, and 2) to discuss why consideration of protein loss-of-function is important for developing treatment strategies for prion and prion-like diseases. In Chapter 2, I describe the generation of mutant alleles of zebrafish *appa* and *prp1*, and the generation of double $prp1^{-/-};prp2^{-/-}$ mutants and double $prp1^{-/-};appa^{-/-}$ mutants. I also compare the developmental phenotypes to those identified in *appa* and *prp1* morphants. I found that loss of *prp1* (in $prp1^{-/-}$ mutants) sensitizes the fish to knockdown of *appa*, confirming a genetic interaction between *appa* and *prp1*. Chapters 3 and 4 address the hypotheses that PrP^C has conserved roles in neuroprotection and CNS development, respectively, while Chapter 5 addresses the hypothesis that PrP^C has conserved functions in memory and cognitive appraisal. In Chapter 6, I summarize my findings and propose future experiments. Finally, Appendix 1 describes my efforts towards generating a zebrafish model of AD.

1.3 Literature Review: Protein Misfolding in Prion and Prion-Like Diseases: Reconsidering a Required Role for Protein Loss-of-Function

Prion diseases are incurable neurological diseases that produce a wide range of devastating symptoms in several mammalian species including humans (Creutzfeldt-Jakob Disease or CJD, Fatal Familial Insomnia or FFI, Kuru, etc.), cattle (bovine spongiform encephalopathy or BSE), and cervids (chronic wasting disease or CWD). Prion diseases are a unique and fascinating disease class because a normal protein (Cellular prion protein, or PrP^C) becomes misfolded and gain-of-function mechanisms associated with this misfolding not only propagate further PrP^C misfolding in neighboring cells and tissues, but can also infect other organisms.

The principal focus of prion research has typically centered on the mechanisms of its infamous gain-of-function, and the concept of propagated misfolding has very recently inspired novel re-consideration of similar neurodegenerative diseases, such as Alzheimer's disease (AD), Huntington's disease (HD), Parkinson's disease (PD), and amyotrophic lateral sclerosis (ALS), which are now considered to be prion-like in their etiology (defined below). Given that prion diseases have taught/inspired the field about important disease mechanisms, we speculated that the reverse ought to now be possible. We turned to prion-like diseases (especially HD, ALS, and AD) for inspiration to further our understanding of classic prion diseases and to seek out commonalities that might inform or inspire new therapeutic strategies for this class of devastating neurodegenerative diseases. Given this context, and our consideration of other recent developments in the prion field, it seemed timely to reconsider the issue of protein loss-of-function in prion diseases; thus we examine herein the balance of loss- versus gain-of-function in prion diseases and prion-like diseases.

We were prompted to evaluate the contribution of loss of PrP^C function in prion diseases in part because very little is known about the role of PrP^C in healthy brains and such knowledge is critical for implementing appropriate disease management strategies. Intriguingly, PrP^C has recently been implicated in AD, e.g., by serving as a receptor for the neurotoxic species of amyloid beta (Aβ) oligomers (Lauren et al., 2009). Because PrP^C has been highly conserved through hundreds of millions of years of evolution, and is robustly expressed in the CNS, it undoubtedly plays an important part in organism physiology. It follows then, that conversion of PrP^C into a misfolded form lacking its normal function (typically denoted 'PrP^{Sc}' after <u>Sc</u>rapie, the prototypical prion disease of sheep) ought to disrupt normal organism physiology at some point(s) during the disease course. Indeed, PrP^C has several neuroprotective functions that may be lost during disease progression (reviewed in (Steele et al., 2007; Winklhofer et al., 2008)). PrP^{Sc} could also interact with PrP^C in a dominant negative fashion to obscure its normal function (Solomon et al., 2010). Further, there is potential for haploinsufficiency in individuals who are heterozygous for familial *PRNP* mutations. It is notable, however, that aged humans (>80 years) heterozygous for early frame-shift mutations in *PRNP* exhibit no overt CNS phenotypes (Minikel et al., 2016). From an alternative perspective, disrupting

normally folded PrP^C itself has been proposed as a promising therapeutic strategy (Chung et al., 2010; Lauren, 2014), and thus it is critical to question whether such strategies would unintentionally potentiate loss-of-function aspects of etiology and thereby accelerate neurodegenerative disease or produce treatment side effects. If this outcome were anticipated, strategies to mitigate PrP^C misfolding or the toxicity of PrP^{Sc} might be advisable as more viable therapeutic strategies. Knowledge of when during prion disease progression PrP^C loss-of-function is a major contributor will also influence disease management strategies.

The dominant hypothesis in the field is that toxicity in prion diseases is mediated primarily through a gain-of-toxic-function (i.e., a neomorphic prion protein conformation is causal to disease. The neomorphic protein conformation may be encoded by *PRNP* mutation or induced by infection (reviewed in (Poggiolini et al., 2013)). Gain-of-function and loss-of-function are often intertwined, as is the case in HD and ALS, which we outline later. As loss-of-function remains largely overlooked in prion diseases (although see (Steele et al., 2007; Winklhofer et al., 2008)), we examine where/when loss-of-function contributes to prion-like diseases with the aim of inspiring future studies into the role of loss-of-function in prion diseases. Thus in this section we explore a family of alternate hypotheses, schematized in Figure 1.4, including:

1) Prion diseases are gain-of-function diseases. New functions gained by prion protein misfolding are sufficient to produce disease phenotypes, i.e., loss-of-function is not required;

2) Gain-of-function initiates disease and is required for spread to new sites and/or individuals, but loss-of-function is both required and sufficient at end stages (e.g., is directly causal of neuron death, from which it follows that gain-of-function is not required at end stages of the etiology); and

3) Gain-of-function initiates disease spread, and a combination of gain- and loss-of-function occurs at many stages of disease.
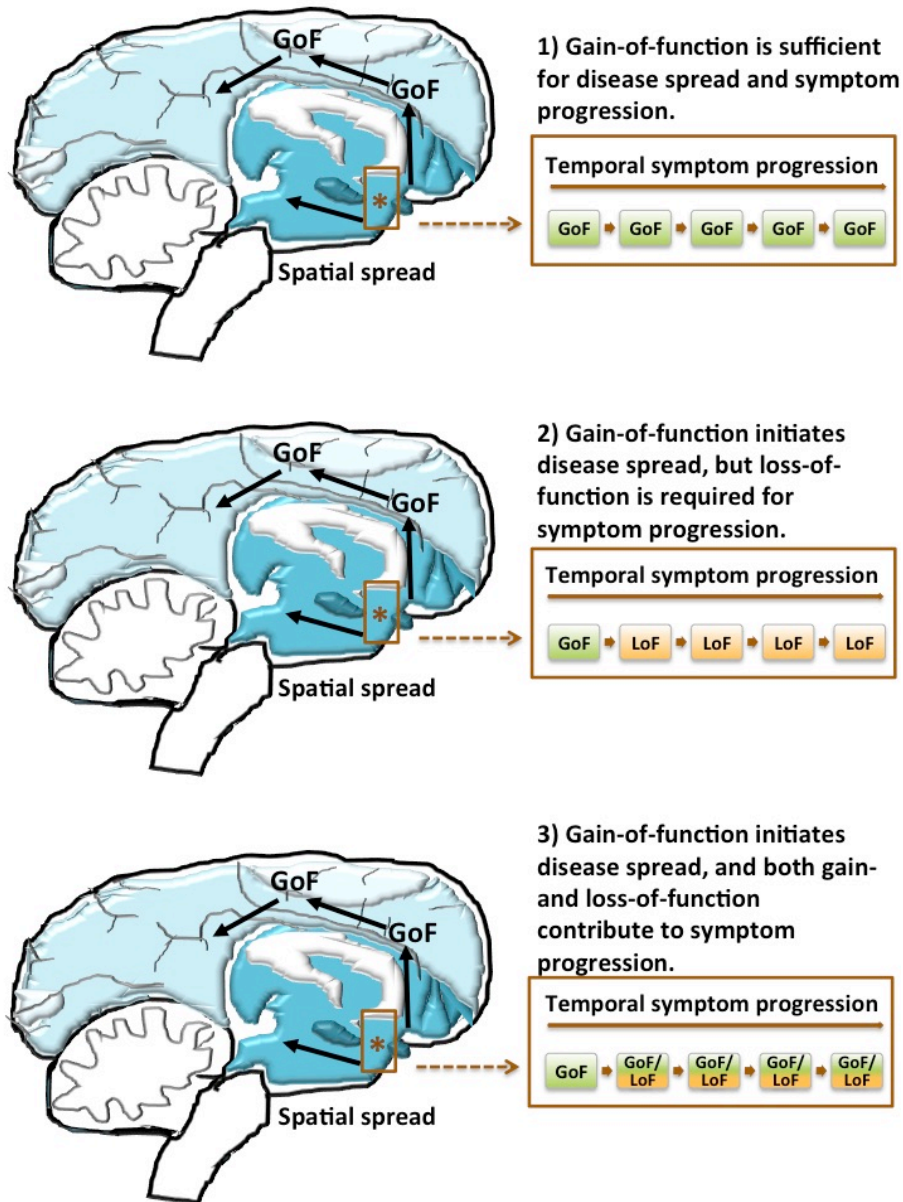
Figure 1.4. Potential causes of prion and prion-like disease spread to new sites within the brain and putative causes of temporal symptom progression at nucleation sites[5]

In all models we propose that gain-of-function initiates spread between brain regions. **Model 1**. Gain-of-function produces neuron cell death and disease symptoms at all stages of disease. **Model 2**. Gain-of-function initiates disease at the nucleation site, but loss-of-function produces symptoms at subsequent disease stages. **Model 3**. Gain-of-function initiates disease at the nucleation site, and gain- and loss-of-function work in concert to produce symptoms at subsequent disease stages. We hypothesize that loss-of-function has an early role in prion diseases and prion-like diseases as illustrated in models 2 or 3. The example given is the regional spread of AD pathology through the brain. Darker areas of the brain represent more severely affected regions (Partially modeled after Figure 3 in (Brundin et al., 2010)).

1.3.1 Untangling gain-of-function versus loss-of-function in prion-like diseases

Prion diseases have served as inspiration for untangling the mechanisms involved in other disparate neurodegenerative diseases. After S.B. Prusiner's discovery that misfolded PrP was the infectious agent in prion diseases (Prusiner, 1982), protein aggregates began to be viewed as a cause rather than simply as signs and symptoms of disease. Experimental prion diseases in animals faithfully recapitulated natural disease course and symptom onset, and led scientists to question whether similar disease processes (e.g., self-propagation of protein misfolding) could be occurring in other neurodegenerative diseases. Experimental methods were subsequently borrowed from the prion field, leading other diseases to be classified as being prion-like (Table 1.3). If prion-like diseases have important loss-of-function components, they may provide unique insight on how to experimentally separate the loss- and gain-of-function components of other diseases, including classical prion diseases that continue to threaten the health, ecology and socioeconomic well being of many regions internationally. There has been spirited debate regarding which of the diseases qualify as being 'prion-like' (Aguzzi and Rajendran, 2009; Frost and Diamond, 2010; Goedert et al., 2014; Hall and Patuto, 2012; Marciniuk et al., 2013), though the list is now broadly accepted to include AD, PD, other tauopathies, HD, and ALS. For the purposes of this review, we consider a disease to be prion-like if it includes the following main features: 1) intramolecular conversion of a native protein into a misfolded form; 2) the misfolded conformer causes misfolding of the normal protein via either template directed misfolding or nucleated polymerization (reviewed in (Horwich and Weissman, 1997)); 3) secretion of misfolded protein and uptake/ interaction with neighboring cells leads to toxicity (Figure 1.5); and 4) the propensity to experimentally seed the transmission of misfolded protein from one site to a distant site (Aguzzi and Rajendran, 2009; Brundin et al., 2010; Costanzo and Zurzolo, 2013; Frost and Diamond, 2010; Goedert et al., 2014; Grad et al., 2015; Hall and Patuto, 2012; Marciniuk et al., 2013; Morales et al., 2015; Oueslati et al., 2014). Spread of misfolded protein proteins between organisms may occur, but is not required within our definition of a prion-like disease. We compare several diseases in our analysis, and our logic assumes that prion-like mechanisms are at play in each. We also note that the proteins that become misfolded and/or aggregated in these diseases (huntingtin, SOD1,

Aβ, and tau) have many putative functions that are expected to be lost when they become misfolded (Table 1.2). Although familial cases of these diseases are generally autosomal dominant (Table 1.3), loss-of-function may occur through haploinsufficiency or dominant negative mechanisms. In the following sections we discuss the balance of gain- versus loss-of-function in HD, ALS, and AD.
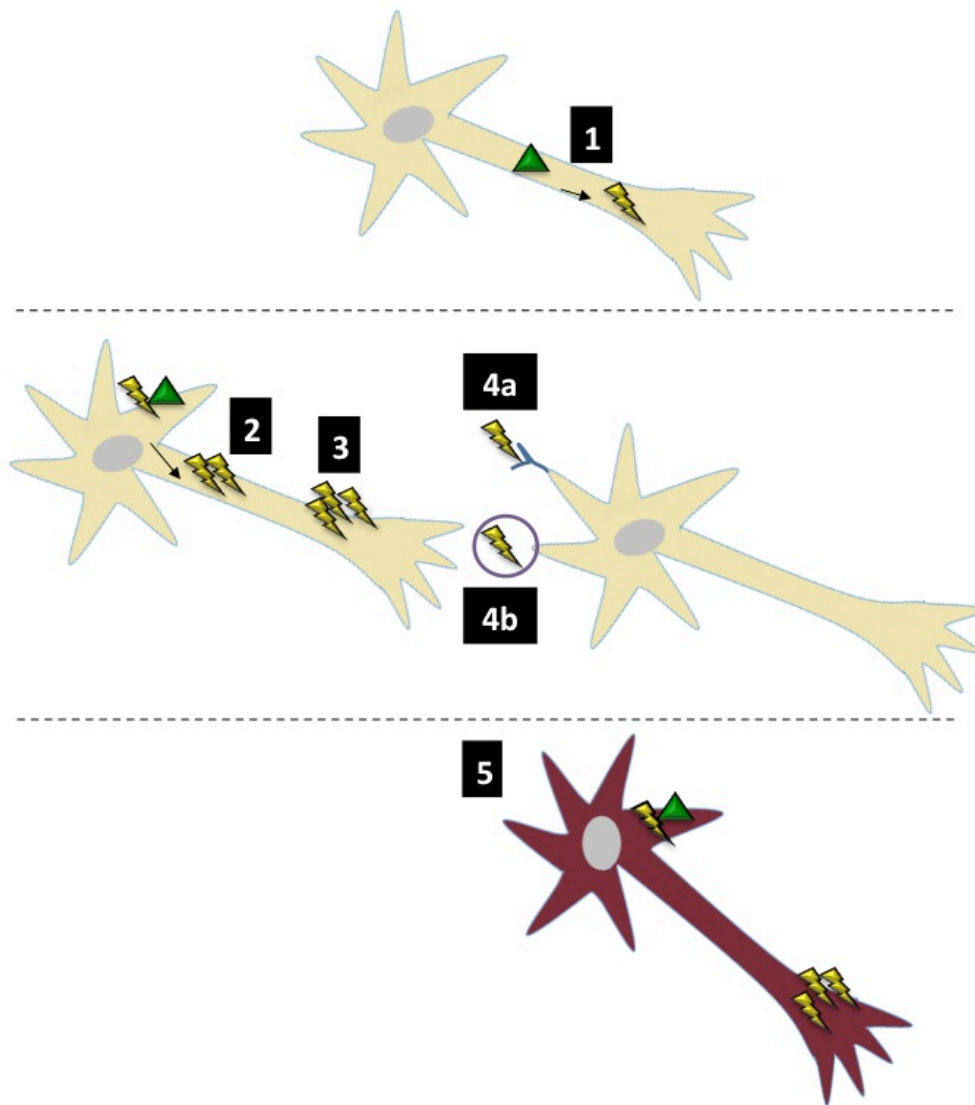
Figure 1.5. Features of prion-like disease[6]

1) Induction of native protein into a misfolded protein (may be spontaneous or driven by altered kinetics of a mutant version of the protein); 2) Misfolded protein propagates misfolding of the native form into the misfolded form within a cell (e.g. within a neuron);

---

[6] Reprinted from Journal of Alzheimer's Disease, Vol 54, Patricia L.A. Leighton and W.Ted Allison, Protein Misfolding in Prion and Prion-Like Diseases: Reconsidering a Required Role for Protein Loss-of-Function, Pages 3-29, Copyright (2016), with permission from IOS Press.
The publication is available at IOS Press through http://dx.doi.org/10.3233/JAD-160361

3) Aggregation of the misfolded form into oligomers and fibrils; 4) The misfolded protein exits the cell (e.g. through exosomes) and interacts with surface receptors of a neighbouring cell or is taken up by neighbouring cells; 5) Misfolded protein propagates in the neighbouring cell leading to cell death.

Table 1.3. Characteristics common to prion disease and prion-like diseases[7]

Disease	Protein: Native form, Misfolded form/aggregated form	Nature of misfolded/aggregated form	Gene encoding the aggregated protein, mode of inheritance	Location of intracellular aggregates	Extracellular aggregate seed site; spreads to	Experimentally Transmissible?
Prion	PrP^C, PrP^{Sc}	-β-sheet rich	*PRNP*, Autosomal dominant or sporadic (reviewed in [1])	Cell surface, endosomes, lysosomes, associated with lipid rafts (reviewed in [2])	Various; Various	Yes (reviewed in [3])
AD	APP, Aβ aggregates	-β-sheet rich	*APP*, Autosomal dominant or sporadic (reviewed in [1])	Early endosomes and/or TGN [4]	Various; Anatomically connected regions	Yes (For example [5-6]
	Tau, hyper-phosphorylated tau	-β-sheets [7-8]	*MAPT*, Autosomal dominant or sporadic (reviewed in [1])	Cytosol [7]	Entorhinal cortex; Dentate gyrus, other axonally connected regions (reviewed in [9]).	Yes (For example [10-15])
HD	Huntingtin, Mutant huntingtin with ≥35-40 poly-Q repeats [16]	-β-sheet rich -Stable [16]	*HTT*, Autosomal dominant [17]	Nucleus and cytosol [16]	Cortical areas; Striatum [16]	Yes* Spread of transgenic huntingtin in *Drosophila* [18]
ALS	SOD1, misfolded wild type or mutant SOD1	-SOD1 aggregates -Less stable than wild type [19-20]	*SOD1*, Depends on mutation	Cytosol, ER/Golgi, outer membrane of extracellular vesicles [19]	NMJ (possibly originates in skeletal muscle [21]	Yes [22-23]

Table 1.3 References: 1 (Winklhofer et al., 2008), 2 (Poggiolini et al., 2013), 3 (Prusiner, 1989), 4 (van der Kant and Goldstein, 2015), 5 (Kane et al., 2000), 6 (Meyer-

---

Luehmann et al., 2006), 7 (Hall and Patuto, 2012), 8 (Novak et al., 2011), 9 (Walker et al., 2013), 10 (Clavaguera et al., 2009), 11 (Clavaguera et al., 2013), 12 (Lasagna-Reeves et al., 2012), 13 (Iba et al., 2015), 14 (Ahmed et al., 2014), 15 (Peeraer et al., 2015), 16 (Costanzo and Zurzolo, 2013), 17 (Jacobsen et al., 2011), 18 (Pearce et al., 2015), 19 (Grad et al., 2015), 20 (Borchelt et al., 1994), 21 (Redler and Dokholyan, 2012), 22 (Ayers et al., 2014), 23 (Bidhendi et al., 2016)

We begin by considering HD because it represents an example where experiments have unambiguously categorized it as being primarily a gain-of-function disease, and this serves as a good context from which to contrast the remaining disease comparators. We then discuss familial cases of ALS associated with SOD1 misfolding, wherein experiments demonstrate a substantial role for SOD1 loss-of-function early during disease progression. We end the section with a consideration of AD to illustrate that there is much to be learned about the intertwined roles of gain- versus loss-of-function in other prion-like diseases. We will also discuss AD as a topical case study in how protein misfolding can instigate loss-of-function by inducing disruptions to the protein-protein interactions that underpin healthy neurons as well as normal learning and memory.

Huntington disease etiology is dominated by gain-of-function outcomes during huntingtin misfolding, but loss-of-function cannot be excluded as a contributor

HD is a classic example of an autosomal dominant disease dominated by its toxic gain-of-function component, the latter having been repeatedly demonstrated experimentally; yet even in this disease some aspects of etiology appear to be due to the loss of normally folded huntingtin. HD is a fatal neurodegenerative disease characterized by motor deficits including chorea and loss of coordination, cognitive decline (especially deficits in executive function), and psychiatric and behavioral symptoms (Walker, 2007). The disease is caused by an excess of CAG (poly-glutamine) repeat expansions in one copy of the gene *HTT* (Jacobsen et al., 2011). Huntingtin is required for embryogenesis (Cattaneo et al., 2005) and is ubiquitously expressed, with expression enriched most highly in the brain and testes (Leavitt et al., 2001). Huntingtin is proteolytically cleaved to produce N-terminal fragments. N-terminal fragments with polyglutamine tract expansions aggregate into inclusions and cause cytoplasmic and/or nuclear pathogenesis (Leavitt et al., 2001). While huntingtin is typically excluded from the nucleus, it was recently found that disruption of the N17 domain (the nuclear exclusion signal) in small N-terminal fragments causes them to accumulate and aggregate in the nucleus (Gu et al., 2015).

HD has recently been classified as a prion-like disease (Table 1.3). While it has been shown to be prion-like in cell culture, evidence of *in vivo* prion-like spread remains

sparse. Mutant huntingtin was taken up by cells in culture and could seed the conversion of labeled huntingtin (reviewed in (Costanzo and Zurzolo, 2013)). Further, mutant huntingtin aggregates are transferred between cultured cells by direct contact and the aggregates are likely spread through tunneling nanotubes (Costanzo et al., 2013). It was recently found that aggregates of fluorescently labeled mutant huntingtin in *Drosophila* olfactory receptor neurons could seed the conversion of wild type huntingtin expressed in adjacent phagocytic glia (Pearce et al., 2015).

Experimental evidence demonstrates that toxic gain-of-function is undoubtedly important in HD. A humanized mouse model of HD (mice that have one copy of the human mutant *HTT* gene, one copy of the human wild type *HTT* gene, and lack the mouse *Htt* gene) recapitulates features of HD neuropathology including forebrain atrophy, reductions in cortical and striatal volume and further displays psychiatric, motor learning, object recognition, and spatial learning deficits (Southwell et al., 2013). Jacobsen et al. (2011) experimentally demonstrated that gain-of-function is at play in HD by assessing gene expression profiles in *Htt^{-/-}* cells compared to similar cells expressing an allelic series of mouse *Htt* with increasing CAG length (an aspect of huntingtin known to be causal of increased disease severity). Because the CAG repeat expressing cells affected had a largely distinct set of genes and biological pathways affected from those in the *Htt^{-/-}* cells, it can be it can be concluded that HD follows a simple toxic gain-of-function mechanism that does not involve a detectable loss-of-function component (Jacobsen et al., 2011). Thus gain-of-function is clear in HD because 1) it has a prion-like mechanism for disease spread; 2) mice expressing mutant human *HTT* recapitulate features of HD; and 3) expression of mutant *Htt* in cell lines affects different cellular pathways compared to when the *Htt* gene is knocked out.

Despite unambiguous evidence for gain-of-function mechanisms dominating HD progression, perhaps more so than for any other of the prion-like diseases, several other lines of inquiry show that loss-of-function might also play important roles in the disease. First, neurodegeneration is observed when the huntingtin protein is disrupted. For example, neurodegeneration occurs in mouse adult forebrain neurons when *Htt* is conditionally ablated (Dragatsis et al., 2000). Further, transgenically expressed mutant human *HTT* induces apoptotic death in the testes of *Htt^{-/-}* mice, and this apoptosis is

reduced in transgenic mice with an $Htt^{+/-}$ background and absent in transgenic mice with an $Htt^{+/+}$ background (Leavitt et al., 2001). This indicates that wild type *Htt* is protective, and loss of normally folded huntingtin in the disease state induces cell death (i.e., Haploinsufficiency/ gene ablation induces a cell death phenotype), thus loss-of-function appears detrimental to disease outcomes.

Mechanistically, effects of huntingtin loss-of-function may be related to the roles of wild type huntingtin in transcription and trafficking of brain derived neurotrophic factor (BDNF). BDNF promotes survival and differentiation of striatal neurons and protects against glutamate excitoxicity (Nakao et al., 1995). BDNF levels are reduced in both mouse $Htt^{-/-}$ neural stem cells and in mouse neural stem cells with knock-in of mutant mouse *Htt* (knock-in of one copy of *Htt* with glutamine expansion), compared to BDNF levels in mouse $Htt^{+/+}$ neural stem cells (Conforti et al., 2013). Reduced BDNF levels are also observed in patients with HD (Zuccato et al., 2001). Huntingtin is further involved in the intracellular trafficking of BDNF, and mutant huntingtin is unable to perform this function, likely contributing to neuronal apoptosis observed in HD (Gauthier et al., 2004). Wild type huntingtin also associates with PSD-95 to regulate NMDA receptors. As mutant huntingtin is unable to bind PSD-95, NMDA receptors in mutant *HTT* expressing cells become sensitized leading to excitoxicity (Sun et al., 2001).

In sum, loss-of-function is likely occurring in HD as indicated by 1) the induction of neuron death upon conditional ablation of *Htt* (Dragatsis et al., 2000)*; 2)* the ability of wild type huntingtin to reverse phenotypes imparted by a mutant *HTT* allele (Leavitt et al., 2001); 3) the shared reduction in BDNF levels in both *Htt* loss-of-function models (Conforti et al., 2013; Zuccato et al., 2001) and HD patients; and 4) the inability of mutant huntingtin to perform functions inherent of wild type huntingtin (Gauthier et al., 2004; Sun et al., 2001).

While it is clear that polyQ expansion is a requirement for HD pathology (e.g., loss of one copy of the gene is insufficient to cause disease) (Ambrose et al., 1994), subtle aspects of HD, such as reduction of BDNF levels are phenocopied in loss-of-function models (Conforti et al., 2013). Hence careful comparison between diseased animals and loss-of-function animal models can provide insight into where/when loss-of-function may be occurring in the diseased state.

We selected HD as the exemplar among prion- and prion-like disease wherein gain-of-function mechanisms are most dominant, unambiguous, and most thoroughly demonstrated by experimental evidence. Even in this extreme case, however, we cannot conclude that gain-of-function is sufficient for disease progression, as loss-of-function appears itself to recapitulate many symptoms and cellular/molecular events in HD progression.

We next consider an opposing example in this spectrum of prion-like diseases, ALS, wherein loss-of-function is clearly occurring early in disease progression.

Etiology of ALS unambiguously acts through loss-of-function during SOD1 misfolding, however gain-of-function is also required

ALS is a devastating neuromuscular disease caused by prion-like spread of misfolded proteins in the neuromuscular system. Familial mutations have been identified in the *SOD1, TARDBP, C9ORF72,* and *FUS* genes, and bone morphogenetic protein modifier genes affect susceptibility (reviewed in (DuVal et al., 2014)). While familial genetics of ALS involve various loci, SOD1 appears central to disease progression regardless of genetic source or sporadic incidence. Wild type SOD1 misfolds and causes disease if overexpressed (Graffmo et al., 2013) and misfolded SOD1 is present in sporadic ALS and other familial forms not associated with SOD1 mutation (Pokrishevsky et al., 2012). The normal function of SOD1 is to act as an antioxidant by catalyzing the conversion of superoxide free radicals to oxygen and water (McCord and Fridovich, 1969). ALS is characterized by muscle weakness and paralysis due to loss of upper and lower motor neurons and defects at neuromuscular junctions. Death usually occurs within 3-5 years of disease onset due to loss of respiratory muscle activity. Misfolding of SOD1 triggers disease in prominent forms of ALS, but loss of SOD1 function, via dominant negative mechanisms, also contributes to pathology early in the disease course (reviewed in (Saccon et al., 2013)).

ALS has been classified as a prion-like disease in cell culture models (Grad and Cashman, 2014; Grad et al., 2015; Grad et al., 2011; Grad et al., 2014a; Grad et al., 2014b; Zeineddine et al., 2015), and *in vivo* (Ayers et al., 2014; Bidhendi et al., 2016). In the former *in vivo* study SOD1 was fused to a fluorescent protein (Ayers et al., 2014), but

it has recently been shown that untagged SOD1 can also propagate aggregates and disease in transgenic mice expressing human SOD1[G85R] (Bidhendi et al., 2016). Mutant SOD1 causes wild type SOD1 to misfold through nucleation dependent polymerization (Chattopadhyay et al., 2008; Chia et al., 2010). ALS phenotypes were propagated between cells in mice expressing SOD1[G85R] fused to an YFP reporter (Ayers et al., 2014). When postnatal mice heterozygous for the SOD1[G85R]-YFP transgene were injected with inoculum from terminal stage SOD1 mice, they developed hind-limb paralysis coincident with inclusion-like structures containing YFP accumulated in their spinal cord, brainstem and thalamus. Mice expressing untagged versions of SOD1[G85R] were less vulnerable to motor neuron degeneration than the YFP-tagged versions (Ayers et al., 2014). Two other strains of untagged SOD1 (human SOD1[G85R] and human SOD1[D90A]), however, were recently found to cause motor neuron degeneration and ALS-like symptoms in hemizygous transgenic mice expressing human SOD1[G85R] (Bidhendi et al., 2016). Thus toxicity is likely dependent on the strain of the inoculum.

Several lines of evidence suggest that neurodegeneration and physiological phenotypes in ALS can be caused by a toxic-gain-of function mechanism associated with misfolded SOD1. Mouse models overexpressing SOD1 with various familial mutations exhibit neurodegeneration in similar patterns to what is seen in human ALS cases (for examples see (Gurney et al., 1994; Jonsson et al., 2004; Wong et al., 1995); for review see (Turner and Talbot, 2008)). Similar results are observed when familial mutants of SOD1 are expressed in rats (reviewed in (Joyce et al., 2011)), zebrafish (DuVal et al., 2014; McGown et al., 2013; Ramesh et al., 2010), or invertebrate models (reviewed in (Joyce et al., 2011)). Mice expressing human SOD1[G93A] also have changes in their motor system physiology that are similar to what is seen in ALS patients including reduction in motor unit function (Shefner et al., 1999). Zebrafish expressing mutant human *SOD1* also recapitulate features of ALS including defects at the neuromuscular junction (DuVal et al., 2014; McGown et al., 2013; Ramesh et al., 2010), decreased muscular endurance in a swim tunnel test (DuVal et al., 2014; Ramesh et al., 2010), and paralysis at end of life stages (Ramesh et al., 2010). Disease is not caused by SOD1 loss-of-function because when that function is replaced, symptoms are not alleviated: e.g., addition of wild type human SOD1 either has no effect or reduces the survival of transgenic mouse models

expressing mutant SOD1 (reviewed in (Turner and Talbot, 2008)). $Sod1^{-/-}$ mice do not have motor neuron degeneration (Reaume et al., 1996), arguing against a simple loss of SOD1 function underlying this disease phenotype. Along this same line of reasoning, reducing levels of murine SOD1 did not significantly change survival time or axon survival in transgenic mice expressing $SOD1^{G85R}$ (Bruijn et al., 1998). In sum, gain-of-function in ALS is evidenced by 1) the ability of mutant human SOD1 to recapitulate ALS phenotypes (McGown et al., 2013; Ramesh et al., 2010; Shefner et al., 1999); 2) the inability of wild type murine *Sod1* to modulate survival time and axon phenotypes in mutant human *SOD1* transgenic mice (Bruijn et al., 1998); and 3) the inability of *Sod1* knockout to induce key features of ALS etiology such as motor neuron degeneration (Reaume et al., 1996) (though the latter point is debated below).

A large body of evidence argues for a disease-modifying role of SOD1 loss-of-function early in the ALS disease process. SOD1's antioxidant activity is reduced in patients with most fALS mutations, due to a combination of reduced intrinsic protein activity and the reduced half-life of mutant SOD1 in the tissues compared to wild type SOD1 (even mutant forms that retain their intrinsic activity *in vitro* have reduced activity *in vivo*) (Saccon et al., 2013). Axon outgrowth defects of $SOD1^{-/-}$ primary motor neuron cultures can be rescued by addition of an antioxidant, which supports a role for SOD1 loss-of-function playing a role in disease (Fischer et al., 2012). Wild type SOD1 co-aggregates with mutant SOD1 in mouse models (Prudencio et al., 2010); thus normal functions of properly folded SOD1 might be lost in a dominant negative fashion when the protein is misfolded. Additional functions of SOD1 are listed in Table 1.2.

A role for loss of SOD1 function in ALS is supported by observations that loss-of-function is sufficient to mimic several ALS symptoms. $Sod1^{-/-}$ knockout mice display features that are similar to those in ALS and/or ALS mouse models including a reduction in motor neuron units (Shefner et al., 1999) , muscle denervation, selective damage to the distal-most part of motor neuron axons (Fischer et al., 2012), and disruption of mitochondrial function (Fischer et al., 2011). As in mouse models of familial ALS, fast muscle fibers are more vulnerable to denervation than slow twitch muscle fibers in $Sod1^{-/-}$ knockout mice (Fischer et al., 2012; Pun et al., 2006). Further, glutamate transport is disrupted in ALS, and *Sod1* deficient mice are more susceptible to glutamate-induced

excitotoxicity (Rothstein et al., 1995; Schwartz et al., 1998). While normally developing (uninjured) $Sod1^{-/-}$ mice do not display motor neuron degeneration, motor neurons in $Sod1^{-/-}$ mice are more vulnerable to tissue injury (Reaume et al., 1996).

Further exemplifying the intertwined gain- and loss-of-function components of ALS, one $SOD1$ familial mutation (D83G) has been observed in mice that both phenocopies aspects of other transgenic mouse ALS models and also phenocopies features of $Sod1^{-/-}$ mice particularly well. $Sod1^{D83G}$ is a point mutation that was induced by N-ethyl-N-nitrosourea in mouse $Sod1$. This mutation renders the protein dismutase inactive due to a disruption in the zinc-binding site. This mutated Sod1 protein is present at lower levels than wild type Sod1 (Joyce et al., 2015). A gain-of-function phenotype induced by this allele (and typically seen in ALS patients and human $SOD1$ transgenic mouse models) includes loss of upper and lower motor neurons. Loss-of-function phenotypes in $Sod1^{D83G}$, which are also seen in $Sod1^{-/-}$ mice, include peripheral axonopathy, mitochondrial defects, neuromuscular junction damage, loss of motor force, and the development of liver cancer (Joyce et al., 2015). Thus the $SOD1^{D83G}$ mutation clearly produces loss-of-function phenotypes.

In addition to causing subtle defects in ALS pathology as described above, loss of normally folded SOD1 during the ALS disease course may also exacerbate gain-of-toxic-function mechanisms. Misfolded SOD1 molecules may lose their enzymatic activities contributing to oxidative stress. As oxidation is known to dissociate dimers of both mutant and wild type SOD1 into monomers (Rakhit et al., 2004), which are more prone to misfolding than dimers, this may lead to increased misfolding and production of SOD1 aggregates (reviewed in (Saccon et al., 2013)).

Most strikingly, loss of SOD1 function is conclusively prominent in ALS etiology because mutant and misfolded SOD1 are inherently unstable. This ironic inversion of events relative to prion protein misfolding biology (wherein misfolded protein is notoriously stable and difficult to eradicate, including from surgical tools or from the environment) is typified by normally folded SOD1 being extremely stable relative to most proteins (Bonaccorsi di Patti et al., 2002). Since mutant SOD1 is infamously unstable (Borchelt et al., 1994; Broom et al., 2015; Khare et al., 2006; Lindberg et al.,

2002; Rodriguez et al., 2002b; Stathopulos et al., 2006), individual molecules likely don't persist for long to cause tissue damage, but newly misfolded SOD1 takes its place.

We conclude that prion-like propagation of SOD1 misfolding in ALS has an unambiguous and substantial loss-of-function component in its etiology. However, even in this extreme example of loss-of-function in a prion-like disease, both gain- and loss-of-function mechanisms work together to propagate disease. The disease is not entirely loss-of-function because *Sod1$^{-/-}$* mice do not exhibit all features of ALS, while animal models expressing human *SOD1* with familial mutations exhibit motor neuron degeneration and other classic symptoms. Further, phenotypes in these transgenic mice cannot be reversed by addition of wild type SOD1. Thus the gain-of-function component minimally exists insofar that misfolded proteins can operate to propagate misfolding (and spread disease). Dominant negative mechanisms are at work early in the disease to disrupt the normal functions of SOD1 (including protection of tissues from oxidative stress), leading to the multitude of phenotypes shared by ALS patients and *Sod1$^{-/-}$* mice.

Complex roles for gain- and loss-of-function in AD Etiology

AD is a prion-like disease wherein the balance of toxic gain-of-function versus loss-of-function remains ambiguous. This ambiguity can be largely attributed to the many putative functions of its keystone protein culprits: amyloid precursor protein (APP), the various cleavage products of APP, and the isoforms of microtubule associated protein, tau (MAPT). Amyloid β (Aβ) peptides are formed by sequential cleavage of APP by β and γ secretases (Figure 1.3). The prevailing toxic gain-of-function hypothesis in the field is the Amyloid Cascade Hypothesis, which proposes that Aβ has an early role in disease and induces tau pathology (Hardy and Allsop, 1991). Thus APP, Aβ peptides and tau have been proposed as targets for AD drug development (Huang and Mucke, 2012; Rosenkranz et al., 2013; Selkoe, 2011). It is important to consider how loss of the normal roles of these proteins may impact disease progression so that appropriate therapeutic interventions can be developed.

Aβ oligomers and misfolded tau have prion-like properties. It has long been established that Aβ forms fibrillar and oligomeric intermediates *in vitro* (for examples, see (Fraser et al., 1992b; Walsh et al., 1997)). Further, Aβ$_{42}$ (which is more abundant in

AD patients than in healthy individuals) is more prone to aggregation than $A\beta_{40}$ (reviewed in (Rauk, 2009)). Some familial mutations in APP (e.g., the Arctic mutation) result in $A\beta$ strains that are more prone to aggregation than wild type $A\beta$ (reviewed in (Watts et al., 2014)). More recently it has been shown that pyroglutamylated $A\beta$ can seed the conversion of $A\beta$ into oligomers that are toxic to cells in culture (Nussbaum et al., 2012). $A\beta$ oligomers can also seed the oligomerization of tau *in vitro* (Lasagna-Reeves et al., 2010). Polymerization of wild type tau can be induced *in vitro* by polyanionic compounds, and mutations in the tau gene (*MAPT*) enhance tau's ability to polymerize (for review see (Gamblin et al., 2003)). Of special relevance to the prion-like aspects of AD are the findings that both $A\beta$ and tau aggregates from exogenous sources can propagate protein misfolding/aggregation in mouse models of AD and tauopathies. Brain homogenates from AD patients and APP transgenic mice, when appropriately delivered, can seed the misfolding and spread of $A\beta$ in APP transgenic mice (Kane et al., 2000; Meyer-Luehmann et al., 2006). Likewise, tau pathology can be seeded by exogenous tau aggregates in mouse models of tauopathy (Ahmed et al., 2014; Clavaguera et al., 2013; Clavaguera et al., 2009; Iba et al., 2013; Iba et al., 2015; Peeraer et al., 2015) and in wild type mice (Lasagna-Reeves et al., 2012). In some tauopathy models, the spread of tau pathology is associated with neurodegeneration (Iba et al., 2015; Peeraer et al., 2015). In sum, both $A\beta$ and tau exhibit prion-like mechanisms *in vitro* and *in vivo.*

APP cleavage products contribute to AD pathology through toxic gain-of-function mechanisms. APP can be cleaved through several different pathways (Figure 1.3). There is some evidence that $A\beta$ oligomers disrupt synaptic plasticity *in vivo* (Walsh et al., 2002). $A\beta_{42}$ promotes glial cell formation (Fonseca et al., 2013), and this could exacerbate disease by increasing astrogliosis (reviewed in (Birch, 2014)). Numerous mouse models have been developed that overexpress mutant forms of human APP and these models recapitulate some aspects of AD in humans, though typically do not exhibit detectable neuron loss (reviewed in (Spires and Hyman, 2005)). For example, PDAPP mice have dystrophic neurites, gliosis, reduced synapse number, and extracellular plaque pathology with regional spread mimicking that of AD (Games et al., 1995), but do not exhibit neuron loss in the entorhinal cortex or in first region of the hippocampus (the CA1 region) (Irizarry et al., 1997). PDAPP mice and TgCRND8 mice also present with

memory deficits as assessed by the Morris water maze (Chen et al., 2000; Chishti et al., 2001).

Tau also contributes to AD pathology through toxic gain-of-function. Tau that is aberrantly phosphorylated inhibits association of normal tau with tubulin, causing breakdown of axon microtubules (Alonso et al., 1994). Several lines of tau overexpressing mice have been generated and some of these phenocopy aspects of AD (reviewed in (Spires and Hyman, 2005)). For example JNPL3 mice, which express P301L mutant tau (mutation found in patients with frontotemporal dementia with parkinsonism-17) under the prion protein promoter, display NFT, cell loss, and memory impairment (Arendash et al., 2004; Lewis et al., 2000).

The biochemical basis for Aβ and tau toxic gain-of-function is still under exploration, but there is evidence that Aβ and tau toxicity are linked. The longstanding Amyloid Cascade Hypothesis postulates that Aβ induces tau hyperphosphorylation, though perhaps indirectly (Hardy and Allsop, 1991). Support for this hypothesis comes from mouse models combining amyloid and tau pathology. Crosses of Tg2576 AD mice with JNPL3 tau mice had enhanced tau pathology compared to JNPL3 mice (Lewis et al., 2001), whereas in 3xTg-AD mice (expressing APP^{Swe}, Presenilin 1 M146V, and Tau P301L), amyloid deposits precede neurofibrillary tangles (Oddo et al., 2003). In sum, both Aβ and tau contribute to AD pathology through toxic gain-of-function mechanisms. However, as current mouse models of AD do not recapitulate all features of AD including hallmarks such as progressive neuron loss (reviewed in (Spires and Hyman, 2005)), it is both reasonable and important to question whether toxic gain-of-function is the only process underlying AD phenotypes.

The complexity and diversity of AD etiology makes it difficult to identify phenotypes that are unambiguously the result of either APP or tau loss-of-function, but there are many putative functions of these proteins that, when lost during the disease course, might be ascribed to the observed symptomology (Table 1.2). The amyloidogenic APP cleavage pathway is favored over the non-amyloidogenic pathway in the AD state (Figure 1.3), which means that there may be insufficient sAPPα and AICD. sAPPα promotes proliferation of neural progenitors, facilitates neurite outgrowth, and is neuroprotective (reviewed in (Chasseigneaux and Allinquant, 2012)). Aβ peptides also appear to have

important physiological functions at low concentrations. For example $A\beta_{40}$ promotes neural stem cell proliferation and neurogenesis (Fonseca et al., 2013). Aβ monomers also stimulate neurite outgrowth (reviewed in (Chasseigneaux and Allinquant, 2012)). APP knockout mice exhibit gliosis (Zheng et al., 1995) and age-dependent memory impairments (Dawson et al., 1999; Muller et al., 1994) as seen in AD. Similarly, $Mapt^{-/-}$ mice share some features of mouse tauopathy models including axonal dystrophy and microtubule defects that can be reversed by the microtubule stabilizer, Epothiolone D (Zhang et al., 2012). Muscle weakness and hyperkinesis are also shared features of $Mapt^{-/-}$ mice and tauopathy models (Ikegami et al., 2000; Lei et al., 2014). It is noteworthy though, that AD-like cognitive deficits in $Mapt^{-/-}$ mice are controversial and may be dependent on mouse background strain (Ikegami et al., 2000; Lei et al., 2014; Ma et al., 2014). In fact, memory-impairing effects of a human APP transgene (with familial Aβ inducing mutations) were reduced in $Mapt^{+/-}$ mice and blocked in $Mapt^{-/-}$ mice (Roberson et al., 2007). Speculatively, this may be because tau increases the animals' sensitivity to excitotoxic insult (Roberson et al., 2007). To summarize, APP, Aβ, and tau all have functions in healthy brains that can be expected to be disrupted as a result of protein misfolding, and knockout mice lacking APP or tau display some (though importantly not all) symptoms of AD and other tauopathies. In sum, it is clear that Aβ and tau contribute to AD through toxic gain-of-function mechanisms, but studies from knockout mice suggest that loss of normal function of APP and tau may contribute to disease progression.

Both gain- and loss-of-function mechanisms are at play in prion-like diseases to varying degrees. A comparison of the extent of gain- versus loss-of-function in prion-like diseases is schematized in Figure 1.6.
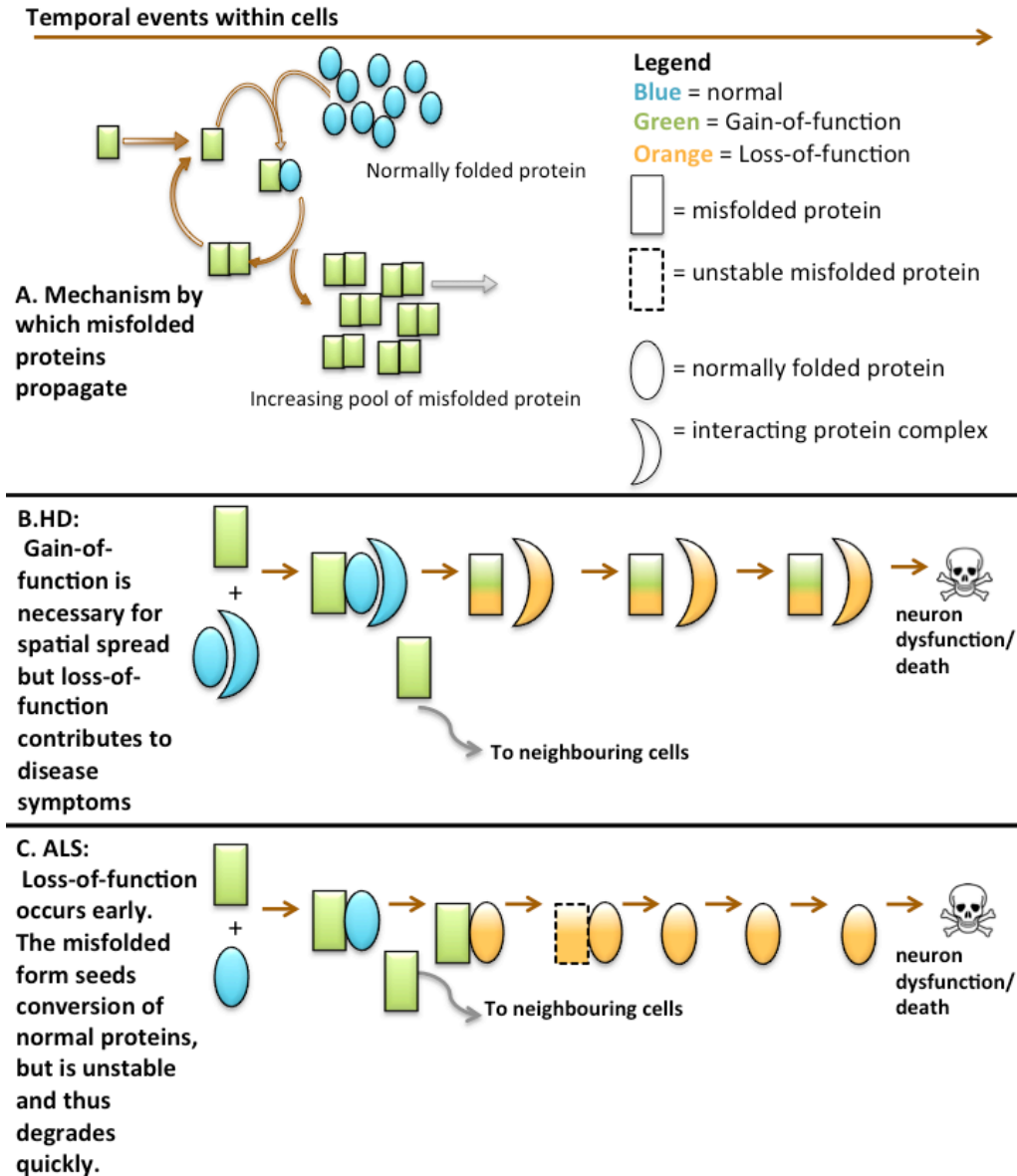
Figure 1.6. Both loss- and gain-of-function contribute to the etiology of prion-like diseases[8]

A. In prion-like diseases misfolded proteins seed the misfolding and/or aggregation of normal proteins and are required for spatial spread of the diseases. **B.** In HD, misfolded huntingtin associates with normally folded huntingtin and converts it to the misfolded form. Mutant huntingtin is unable to properly interact with other proteins such as PSD-95 and BDNF, thus neither mutant huntingtin nor huntingtin's interactors are able to perform their normal function (i.e., loss-of-function mechanisms are at work). Other disease phenotypes, however, can only be attributed to gain-of-toxic function. **C.** In ALS, misfolded SOD1 associates with normally folded SOD1 and converts it to the misfolded form. We hypothesize that since misfolded SOD1 is less stable than normally folded SOD1, misfolded SOD1 does not persist to cause damage inside the cell. Instead, loss of normally folded SOD1 has a strong influence on cell death and disease phenotypes at later temporal stages. Misfolded SOD1 also interacts with wildtype SOD1 producing loss-of-function phenotypes through dominant negative mechanisms.

1.3.2 Unpacking the evidence for loss-of-function in prion diseases

Gain-of-function is required but not sufficient for prion disease etiology: Evidence from classical prion disease studies

There exists strong consensus in the field that toxic gain-of-function is required for prion diseases, consistent with a large body of supporting experimental evidence (reviewed in (Poggiolini et al., 2013; Winklhofer et al., 2008)). Thus for prion diseases gain-of-function is accepted to be required—but is it sufficient? After considering the role of loss-of-function in other diseases, we suggest that protein loss-of-function is a causal contributor to prion disease pathology, rather than just a consequence. Prion diseases are slow and have multifaceted complex etiology, thus gain- and loss-of-function could be involved at different steps and in different brain regions (Figure 1.7). In this section, we consider how PrP^C levels correlate with disease progression and severity, and we later highlight potential physiological consequences of its loss relative to the symptoms observed during the course of prion disease.
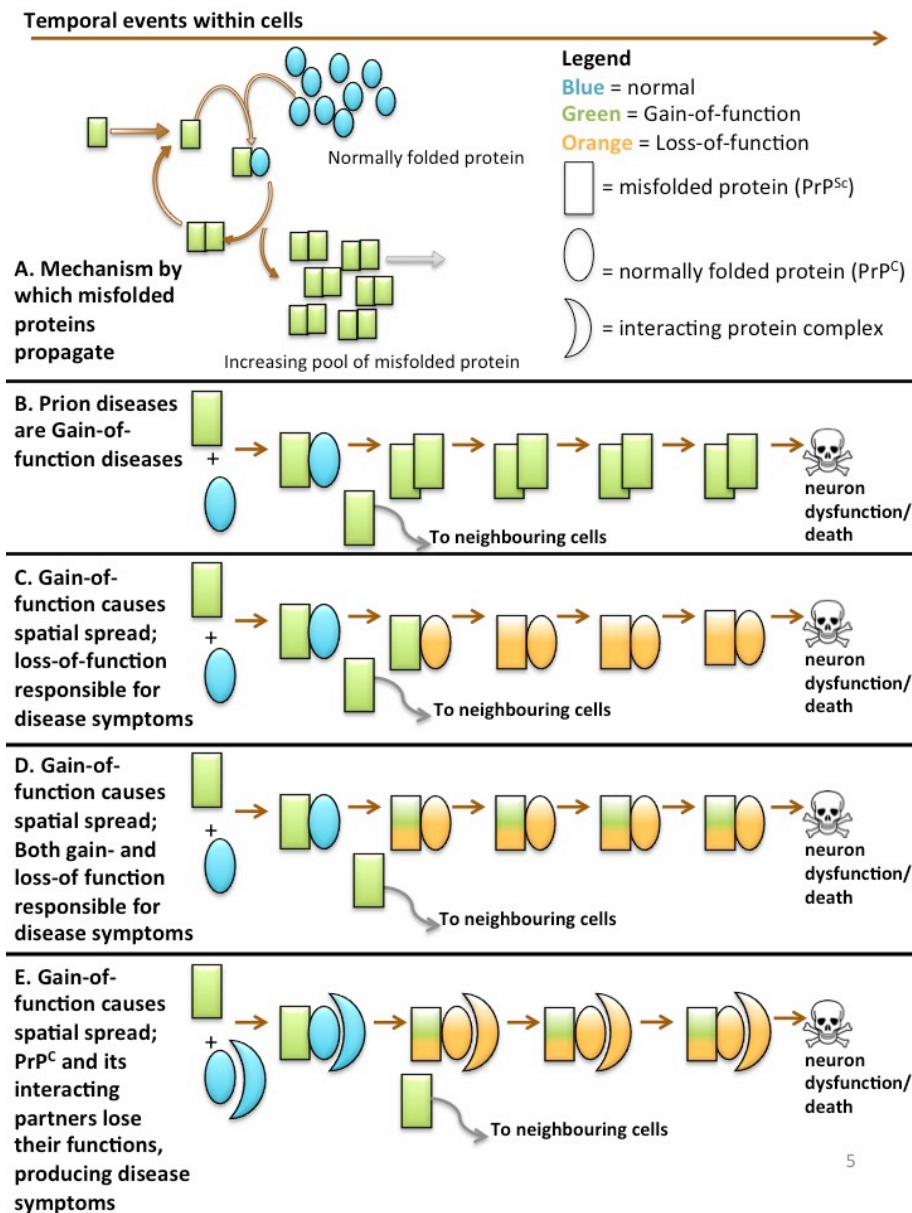
Figure 1.7. Simplified envisaged hypothetical events in prion disease (and related protein misfolding diseases) with respect to the role of protein gain-of-function (GOF) versus protein loss-of-function (LOF)[9]

---

[9] Reprinted from Journal of Alzheimer's Disease, Vol 54, Patricia L.A. Leighton and W.Ted Allison, Protein Misfolding in Prion and Prion-Like Diseases: Reconsidering a Required Role for Protein Loss-of-Function, Pages 3-29, Copyright (2016), with permission from IOS Press.

The publication is available at IOS Press through http://dx.doi.org/10.3233/JAD-160361

A. Simplified mechanism describing how misfolded proteins propagate. **B–E)** In each scenario we assume the process begins with a gain-of-function (GOF, green) event via the misfolded protein infecting a new cell (left side) and ends with cell death (right side). Normally functioning protein is represented in blue, whereas protein with some loss of function is represented in orange. The presented hypotheses (rows B–E) differ in the propensity for GOF to play a role, and whether any such role occurs throughout disease or early in disease. The two most extreme views are represented first, for emphasis that some mixture of GOF and LOF is likely. **B.** Prion disease etiology is solely via a toxic gain-of-function, and toxic misfolded prion protein kills cells. Newly misfolded protein goes on to nucleate additional events in adjacent cells (curved arrow). **C.** At the opposite extreme to schema B, Prion disease might be GOF only during spread of misfolded protein to an uninfected cell (either an adjacent cell or a cell in a distant tissue). Considering the biochemical stability of misfolded prion protein, this option may be unlikely. **D.** Hypothetically, misfolding of the prion protein may exert its effects through both GOF and LOF at different phases of disease, including the assumed GOF required for spread to a new cell inducing loss of function(s) both early and late in etiology. **E.** The reality is that these diseases are complex, and we conclude that both GOF and LOF are required for prion & prion-like disease progression. This conclusion sparks further questions including at which disease stages LOF plays a prominent role. Certainly protein-protein interactions are occurring amongst pools of proteins, in various states of oligomerization and with differential kinetics of protein turnover, thereby complicating the formation of testable hypotheses. PrP^{Sc} and PrP^{C} interact with each other in a complex environment of other proteins and macromolecules, and misfolding is reasonably expected to disrupt interacting proteins leading to toxic effects. Firstly, interacting proteins (complexes) may lose their own function when unable to interact normally with PrP^{C}. Further, accumulation of PrP^{Sc} is found to be coincident with an apparent degradation of PrP^{C} and as such interacting proteins would be expected to lose their function. If, for example, the functions of interacting proteins were neuroprotective, then cell death would be favored.

An interesting puzzle has recently emerged in the literature regarding the abundance of PrP^C and disease incubation period and severity. It was newly found that PrP^C is dramatically reduced in abundance during the preclinical disease stage, and this was suggested to occur through proteostatic mechanisms (Mays et al., 2014). Arguably, the decrease in PrP^C abundance might be viewed as a protective response undertaken by cells, as it extends the incubation time of the disease (Mays et al., 2014). At the same time, however, this response may sensitize cells to PrP^{Sc} by diminishing the neuroprotective properties of PrP^C. Regardless of its debated consequence, the observation that PrP^C is dramatically less abundant early in preclinical phases of prion disease starkly underscores the likelihood that PrP^C loss-of-function is a substantial and pervasive contributor to disease etiology.

Studies where PrP^C is knocked out or reduced during experimentally induced prion infection have produced mixed results, highlighting the need for further study into the contexts in which PrP^C is neuroprotective versus when it is instead a contributor to the disease course. On one hand, *Prnp* expression (Weissmann et al., 1994) and the presence of the GPI anchor (Chesebro et al., 2005) are requirements to infect mice with mouse prion strains, and halving the *Prnp* dosage (i.e., in *Prnp*$^{+/-}$ mice) is protective (Weissmann et al., 1994). On the other hand, murine PrP^C appears to be protective when prions from other species are present. Exemplifying the former*, Prnp*$^{+/-}$ mice had delayed onset of gliosis and spongiosis compared to wild type mice when infected with the Rocky Mountain Laboratory (RML) mouse adapted scrapie strain (Bueler et al., 1994). Suppression of *TgPrnp* expression also prevents CNS dysfunction, neuronal loss, vacuolation, and gliosis (Safar et al., 2005). Further, specific ablation of neuronal *TgPrnp* with a Cre-Lox system prevented neuronal loss, gliosis, and spongiosis despite accumulation of extraneuronal PrP^{Sc} (Mallucci et al., 2003). On the other hand, *Tg(HuPRNP)* mice with a *Prnp*$^{+/+}$ background were resistant to inoculum with human prions, but *Tg(HuPRNP)* mice with a *Prnp*$^{-/-}$ background were susceptible to prion disease (i.e., displayed clinical symptoms). Chimeric Tg (Mhu2M) mice with a *Prnp*$^{-/-}$ background were also more susceptible to prion infection (i.e., less time to symptom onset) than chimeric mice with a *Prnp*$^{+/+}$ background, but to a lesser extent. The authors hypothesized that the endogenous murine PrP^C had a greater affinity to the hypothetical

murine conversion cofactor, termed 'Protein X', than human or chimeric PrP^C, and thus hindered conversion of human or chimeric prions (by outcompeting the human or chimeric PrP^C for access to murine 'Protein X') (Telling et al., 1995). Interest in the 'Protein X' hypothesis has diminished because the past 20 years of research has failed to identify this accessory protein. Instead, PrP^C molecules encoded by different alleles are thought to compete for nascent prion seeds (Geoghegan et al., 2009). An alternate hypothesis to explain the phenomenon observed by Telling et al. (Telling et al., 1995) is that endogenous PrP^C has neuroprotective functions. Supporting this hypothesis, *Tg(MoPrnp P101L)* mice with a *Prnp* null background succumbed to disease faster than those with a murine $Prnp^{+/+}$ background and had more prion protein plaques and spongiform degeneration (Telling et al., 1996). *PRNP* P101L is a familial mutation in humans that underlies Gerstmann–Sträussler–Scheinker syndrome (GSS) and causes spontaneous misfolding of PrP^C into PrP^{Sc}. Additionally, when brain homogenate from sick *Tg(MoPrnp P101L)* mice were used to inoculate *Tg(MoPrnp-101L)/Prnp$^{-/-}$* and *Tg(MoPrnp-101L)/PrP$^{+/+}$* mice, the *Tg(MoPrnp-101L)/PrP$^{-/-}$* mice presented disease symptoms sooner than mice expressing *Prnp* (Telling et al., 1996). Overall these studies suggest that GPI-anchored PrP^C is a requirement for prion disease progression and reducing PrP expression slows disease. In some instances, however, if there is a sufficient 'species barrier' or 'strain barrier', other versions of PrP^C can be protective.

Further study is needed to ascertain when and where PrP^C is neuroprotective and when it becomes detrimental to cell/tissue health. It may be that PrP^C is protective early in, and prior to, the disease (when PrP^{Sc} levels are still relatively low), but that the presence of PrP^C accelerates disease at later stages. It is also possible that PrP^C is protective when expressed in some cell types and detrimental when expressed in other cell types. Regardless, reduced PrP^C abundance early in disease, accompanied by the myriad functions of PrP^C (reviewed immediately below) that are lost when PrP^C disappears and/or misfolds, lends some credence to the argument that loss-of- function may be a substantial contributor to prion disease progression. In the next section we consider the putative functions of PrP^C and how these functions may be disrupted during disease.

Putative functions of PrP^C may be lost during the course of prion disease infection

PrP^C has a number of putative functions (see Table 1.1) that are reasonably expected to be disrupted as a result of its decreased abundance early during disease, its conversion to PrP^{Sc}, and/or through dominant negative interactions between PrP^C and PrP^{Sc} in prion diseases. There is solid support for loss-of-function being a component of prion disease etiology because many prion disease symptoms can be mimicked by PrP^C loss-of-function (Table 1.4). Conversely, no disease symptom can be exclusively attributed to gain-of-function in transgenic overexpression models, as loss-of-function may also be occurring in these models. Thus it is difficult (if not impossible) to experimentally disentangle gain- from loss-of-function in transgenic overexpression models (Table 1.4). Efforts to study the normal physiology of PrP^C have typically been thwarted by inconsistency of phenotypes between different *Prnp*$^{-/-}$ mouse lines (Table 1.5, reviewed in (Striebel et al., 2013)). Some functions of PrP^C have been verified in other species including rats and zebrafish, and further research in these alternative animal models will help to establish which PrP^C functions are the most important/relevant to disease etiology. Currently, solid evidence exists for roles of PrP^C in neuroprotection and learning. While disparate lines of evidence support a role for PrP^C in neuroprotection, molecular mechanisms that underlie this outcome remain mysterious. Thus failure to acknowledge that we have much to learn about the role of PrP^C in normal physiology would severely limit progress on uncovering the pathophysiology of prion diseases and novel therapeutic strategies. Here we will examine what is known about the role of PrP in neuroprotection and learning.

Table 1.4. Disease symptoms observed in *Prnp* knockout animals[10]

	Loss-of-function?	Defects observed in:		
		KO or KD fish	KO mice/KO cell lines	Gain-of-function models
Neuroprotection from ischemia/traumatic brain injury	✓	TBD	Increased susceptibility to ischemia [1-2]	?
Neuroprotection against excitoxicity/seizures	✓	Increased susceptibility to PTZ convulsant [3]	Increased susceptibility to convulsants [4-7]	?
Regulation of NMDA receptor	✓	Altered NMDA receptor regulation [3]	Altered NMDA receptor regulation [8-11]	?
Metal homeostasis	✓	Preliminary/TBD	Altered distribution of iron, copper and zinc [12]	?
Cell Adhesion	✓	Disrupted cell adhesion in early development [13-15]	TBD	?
Synaptogenesis	✓	TBD	TBD	? Decreased Purkinje cell dendritic spine density during infection [16]
Adult Neurogenesis	✓	TBD	Reduced neural precursor proliferation [17]	? Prion-infected NSC have defective neuronal differentiation [18]
Learning	✓	Leighton *et al.* unpublished	Decline in spatial learning [19], age-dependent decline in learning [20-21]	?

TBD- To be determined

Table 1.4 References:

1 (Beraldo et al., 2013), 2 (McLennan et al., 2004), 3 (Fleisch et al., 2013), 4 (Carulla et al., 2015), 5 (Walz et al., 1999), 6 (Rangel et al., 2007), 7 (Carulla et al., 2011), 8

(Khosravani et al., 2008), 9 (Gasperini et al., 2015), 10 (You et al., 2012), 11 (Black et al., 2014), 12 (Pushie et al., 2011), 13 (Kaiser et al., 2012), 14 (Solis et al., 2013), 15 (Malaga-Trillo et al., 2009), 16 (Campeau et al., 2013), 17 (Steele et al., 2006), 18 (Relano-Gines et al., 2013), 19 (Criado et al., 2005), 20 (Schmitz et al., 2014a), 21 (Coitinho et al., 2003)

Table 1.5. Phenotypes of Prnp-/- mouse lines (modified from (Striebel et al., 2013))[11]

Prnp-/- Line	Genetic Background	Overt anatomical phenotypes	Seizure susceptibility/ learning deficits	Caveats
Edin 129/Ola [1]	129/Ola	No overt phenotype	Seizure susceptibility [2], Learning deficits [3]	-
Edin 129/Ola [4]	C57BL/10SnJ	None reported	Learning deficits [3]	Flanking genes[a]
ZrchI 129/Sv [5]	Various	No overt phenotype [5], Demyelinating polyneuropathy [6]	Seizure susceptibility [2, 7-10], Learning deficits [11-12]	Flanking genes[a]
Ngsk 129/Sv [13]	C57BL/6	No overt phenotype [13], demyelinating polyneuropathy [6]	Not tested	Increased Doppel Expression [14-15], Flanking genes[a]
Rikn 129/Ola [16]	C57BL/6	Tremor and ataxia in aged mice [16]	Not tested	Likely has increased Doppel Expression (not tested to our knowledge), Flanking genes[a]
ZrchII 129/Ola [17]	C57BL/6	Ataxia and Purkinje cell death [17]	Not tested	Increased Doppel Expression [17], Flanking genes[a]
Rcm0 129/Ola [18]	Unknown	Ataxia and purkinje cell death	Not tested	Increased Doppel Expression [14], Flanking genes[a]

[a] In the process of making these knockout mice, the embryonic stem cells transmitted both the *Prnp* null mutation as well as the alleles of the 129 background strain (i.e. 'flanking genes'). Hence when the mice were backcrossed into another strain (eg. C57BL), new generations of mice were not genetically identical to wild type C57BL mice (Striebel et al., 2013).

Table 1.5 References:

1 (Manson et al., 1994), 2 (Carulla et al., 2015), 3 (Criado et al., 2005), 4 (Chesebro et al., 2010), 5 (Bueler et al., 1992), 6 (Bremer et al., 2010), 7 (Ratte et al., 2011), 8 (Walz et al., 1999), 9 (Rangel et al., 2007), 10 (Carulla et al., 2011), 11 (Coitinho et al., 2003),

12 (Schmitz et al., 2014a), 13 (Sakaguchi et al., 1995), 14 (Moore et al., 1999), 15 (Li et al., 2000), 16 (Yokoyama et al., 2001), 17 (Rossi et al., 2001), 18 (Moore et al., 1995)

PrP^C regulates neurotransmission and provides protection from seizures

PrP^C promotes the survival of neurons in healthy brains by regulating neurotransmission, thus protecting against excitoxicity. PrP^C has been shown to regulate potassium currents in rat neurons, and this function is lost in PrP^C with a GSS mutation (insertion of 8 extra octarepeats) (Mercer et al., 2013). PrP^C also regulates NMDA receptors in brain slice cultures (Khosravani et al., 2008; Stys et al., 2012). Further, we have shown that zebrafish PrP2 (a zebrafish homlog of PrP^C) regulates NMDA receptors (Fleisch et al., 2013). Loss of normally folded PrP likely causes neuron death at some stages of prion disease courses because there is less PrP^C available to regulate neurotransmission.

PrP^C loss-of-function may also account for seizures and seizure-like symptoms in prion diseases, and support for this comes from PrP^C loss-of-function animal models that have increased susceptibility to convulsants. Seizures occur in 15% of patients with sporadic CJD and some patients with genetic prion diseases (~10% of patients with familial CJD, <10% of patients with GSS or FFI) (Wieser et al., 2006). Tremors also occur in some cases of BSE (Arai et al., 2009). Several studies have found that *Prnp* knockout mice are more susceptible to seizure-inducing drugs than wild type mice (Carulla et al., 2011; Carulla et al., 2015; Rangel et al., 2007; Walz et al., 1999). Controversy has existed regarding whether these seizures observed in *Prnp* knockout mice are a result of PrP^C loss-of-function or strain differences. A recent study, however, clarified this issue when the authors reported that increased seizure susceptibility in *Prnp* knockout mice exists when *Prnp* knockout mice are compared to wild type mice of the same strain (Carulla et al., 2015) (Table 1.5). Strikingly, we also found that the zebrafish homolog of PrP^C, PrP2, reduces the susceptibility of zebrafish larvae to pentylenetetrazole (PTZ)-induced seizures, pointing to an ancient and conserved (i.e., important) role of PrP^C in modulating seizures and neuronal activity (Fleisch et al., 2013).

PrP^C facilitates learning and memory

Cognitive deficits observed in prion disease patients may be due to the loss of normal PrP^C function. Prion disease patients (sporadic, iatrogenic, and familial CJD) have cognitive dysfunction beginning early in the presentation of disease. While the most

prevalent symptoms are executive dysfunction and language impairments, some patients have memory impairments that are related to visuospatial problems (Caine et al., 2015). $Prnp^{-/-}$ mice have learning deficits supporting a role for PrP^C loss-of-function in prion diseases (Coitinho et al., 2003; Criado et al., 2005; Schmitz et al., 2014a). $Prnp^{-/-}$ mice had reduced hippocampal dependent spatial learning compared to wild type mice (which was rescued by a neuron-specific human $PRNP$ transgene) (Criado et al., 2005), and aged $Prnp^{-/-}$ mice performed poorly in the novel object recognition (Schmitz et al., 2014a) and inhibitory avoidance tasks (Coitinho et al., 2003) compared to aged wild type mice. Aged rats treated with ▯-PrP^C antibody also performed poorly in an inhibitory avoidance test relative to aged rats treated with a control antibody (Coitinho et al., 2003). It is possible, however, that the ▯-PrP^C antibody induced a gain-of toxic function through PrP^C as some ▯-PrP^C antibodies induce toxicity and trigger the unfolded protein response (Herrmann et al., 2015). We have also found that loss of the prp2 paralog in zebrafish reduces the ability of aged zebrafish to recognize a novel object (Leighton et al., unpublished), supporting a conserved, ancient, and important role for PrP^C as a mediator of learning and memory.

Gain-of-function is required for initiation and spread of prion diseases, but loss-of-function is also an important disease contributor

In sum, while toxic gain-of-function is necessary to initiate and spread prion disease (as evidenced by lack of disease in $Prnp^{-/-}$ mice (Weissmann et al., 1994) and lack of infectivity in $Prnp^{-/-}$ tissue surrounding tissue grafts that express PrP^C (Brandner et al., 1996)), loss of PrP^C undoubtedly has detrimental effects for neuron health at some, if not all, stages of neurodegenerative disease. PrP^C levels are reduced through various mechanisms during the disease course (e.g., by conversion to PrP^{Sc} and by putative proteostatic mechanisms reducing its abundance (Mays et al., 2014)). Thus normal/healthy physiological processes are expected to be disrupted, including neuron survival signaling, regulation of neurotransmission, and synaptic plasticity underlying cognition. Many prion disease symptoms are observed in PrP loss-of-function animal models, and loss-of-function may be induced in gain-of-function animal models. We conclude that gain-of-function and subversion and/or partial loss of some functions occur

in concert in classical prion diseases. Future work is needed to determine *when* loss-of-function is most important for disease etiology because this will inform disease management strategies.

1.3.3 PrP^C influences the function and dysfunction of other proteins: a case study on the loss of PrP^C function during AD

PrP^C interacts with numerous CNS proteins that have keystone roles in neurodegenerative diseases, including APP and tau. Thus loss of PrP^C function may have a role in other diseases (e.g., AD, frontotemporal dementia, and PD). Likewise, loss of APP and tau function may impact classical prion disease course. Since AD and prion diseases have similar disease pathology and APP and PrP^C interact both physically and genetically (see below), we selected APP as a candidate for the case study below, as an exemplar of how loss of PrP^C might impact upon the normal physiology of other proteins, and the progression of other neurodegenerative diseases.

While the normal functions and molecular mechanisms of APP and PrP^C remain enigmatic (see sections "Complex roles for gain- and loss-of-function…" and "Putative functions of PrP^C…" above), numerous studies have demonstrated that APP and PrP^C have interacting roles in cell/organism physiology. It was recently established that PrP^C interacts biochemically with APP (Bai et al., 2008; Kaiser et al., 2012; Schmitt-Ulms et al., 2004; Schmitz et al., 2014b) and with Aβ (first reported in (Lauren et al., 2009)). It has been proposed that PrP^C may contribute to AD by acting as a receptor/mediator of Aβ toxicity (Lauren et al., 2009). One question that has been asked less often is whether these protein interactions have relevance for prion diseases. As PrP^C and APP interact, loss of normally folded PrP in prion diseases may disrupt normal physiology of APP and contribute to prion disease progression. Prion diseases and AD share many similarities (Table 1.6) and we postulate that studying interactions between APP and PrP^C will synergistically lead to insights on the mechanisms and novel therapies for both prion diseases and AD.

Table 1.6. Similarities between Alzheimer's disease and prion diseases[12]

Alzheimer's Disease (AD)	Prion diseases (prion diseases: BSE, CWD, CJD)
Protein misfolding → spreading amyloid plaques →neuron death → dementia	Protein misfolding → spreading amyloid plaques → neuron death → dementia
Experimentally transmissible [1-2]	Experimentally transmissible (reviewed in [3])
Sporadic & Familial [*APP, PS1, PRNP*, etc] (reviewed in [4-5])	Infectious, Sporadic & Familial [*PRNP, SPRN*] (reviewed in [3])
APP → Aβ plaques Tau →neurofibrillary tangles	PrP^C → PrP^{Sc} plaques
APP is transmembrane multidomain protein in lipid rafts [6], processed by endoproteolysis to release fragments (reviewed in [7])	PrP is GPI-anchored multidomain protein in lipid rafts [8], processed by endoproteolysis to release fragments (reviewed in [9])
APP's biological function is enigmatic	PrP^C's biological function is enigmatic
Homodimers of APP affect their processing towards pathogenesis [10]	Homodimers of PrP affect their aggregation towards pathogenesis [11]
APP−/− mouse is surprisingly normal [12-13]	*Prnp*−/− mouse is surprisingly normal [14-15]
Zebrafish with 2 copies: *appa* & *appb* [16]	Zebrafish with 2 copies: *prp1* & *prp2* [17]
Mammalian orthologues can replace zebrafish orthologues [18]	Mammalian orthologues can replace zebrafish prp1 orthologue [18]
Knockdown of *appa* or *appb* in zebrafish leads to a neurodevelopmental phenotype [18-19]	Knockdown of *prp1* or *prp2* in zebrafish leads to a neurodevelopmental phenotype [18, 20]

Table 1.6 References:

1 (Kane et al., 2000), 2 (Meyer-Luehmann et al., 2006), 3 (Prusiner, 1989), 4 (Van Cauwenberghe et al., 2016), 5 (Golanska et al., 2009), 6 (Parkin et al., 1999), 7 (Marotta et al., 1992), 8 (Stahl et al., 1987), 9 (Altmeppen et al., 2012), 10 (Kaden et al., 2008), 11 (Rambold et al., 2008), 12 (Zheng et al., 1995), 13 (Muller et al., 1994), 14 (Manson et al., 1994), 15 (Bueler et al., 1992), 16 (Musa et al., 2001), 17 (Cotto et al., 2005), 18 (Kaiser et al., 2012), 19 (Abramsson et al., 2013), 20 (Malaga-Trillo et al., 2009)

PrP^C has the potential to modulate AD pathogenesis and prion disease through regulation of APP metabolism and other underexplored mechanisms. PrP^C levels are reduced in sporadic AD patients (intriguingly reminiscent of reduced PrP^C early in prion disease) suggesting that loss of PrP^C could play a role in sporadic AD progression (Whitehouse et al., 2010; Whitehouse et al., 2013). PrP^C also inhibits β-secretase cleavage of wild type APP (Parkin et al., 2007; Schmitz et al., 2014b) such that loss of normally folded PrP may cause cells to favour the amyloidogenic pathway of APP cleavage. The PrP^C N1 cleavage product has also been reported to inhibit Aβ toxicity (Beland et al., 2014; Beland et al., 2012; Fluharty et al., 2013; Guillot-Sestier et al., 2012). It has been shown that prion infection can enhance Aβ$_{42}$ production in mouse models of AD (Baier et al., 2008; Morales et al., 2010), but a question that remains open is whether levels of Aβ peptides change during natural prion infection. Aβ oligomers can redistribute PrP^C to the cell surface, which may further propagate Aβ toxicity in AD or PrP^{Sc} toxicity in prion disease (Caetano et al., 2011). We previously found that zebrafish *appa* and *prp1* have a synergistic neuroprotective effect at the genetic level (Kaiser et al., 2012). Co-knockdown of zebrafish *appa* and *prp1* with morpholinos induces neuron death, but concerted knockdown of other zebrafish gene paralogs did not induce such effects. This effect is conserved since either mouse PrP^C or human APP rescues the phenotype (Kaiser et al., 2012). Thus a niche role for the interaction between mammalian APP and PrP^C was revealed, including modulating neuron survival (Kaiser et al., 2012). The molecular mechanisms behind this synergistic neuroprotection remain to be resolved, but APP and PrP^C clearly have important overlapping roles and ancient important interactions in normal CNS physiology.

We have highlighted several roles for PrP^C in modulating APP physiology and have noted that PrP^C abundance is reduced in some AD cases (Whitehouse et al., 2010; Whitehouse et al., 2013). Since APP and PrP^C interact (Kaiser et al., 2012), and because they have overlapping roles in the CNS (Kaiser et al., 2012), loss of PrP^C and its normal functions must be expected to influence AD progression (and loss of APP's normal functions may contribute at some stages of classical prion disease progression). The mechanisms underlying the interactions between AβPP and PrP^C remain enigmatic, and

further study in this area will importantly inform design of therapeutic strategies for both prion diseases and AD.

1.3.4 Future perspectives on prion and prion-like diseases

Experimental approaches that have been used to unravel loss- and gain-of-function in prion-like diseases

The historic approach that has been used to identify evidence of loss-of-protein-function in disease has been to examine how and to what extent knockout animals can phenocopy the disease state. As described in the sections above, loss-of-function phenotypes are relevant in prion-like diseases but are often subtle and difficult to untangle from the overt phenotypes that are induced by misfolded/aggregated proteins. An important addition to knockdown/knockout experimental approaches is to rescue the phenotypes by genetic complementation (i.e., transgene rescue, or better yet, conditional knock-in of the targeted gene). These types of experiments can also be used to determine whether mutant versions of a protein have lost their normal physiological functions. If the mutant form of a protein can rescue a loss-of- function phenotype, it means that the mutant form performs the same function as the wild type form but has an additional gain-of-function toxic mechanism. If the mutant form cannot rescue the phenotype, the theoretical interpretation is that the mutant form also loses its normal function. This result, however, is not definitive as it is difficult to prove that the negative result is due to loss-of mutant protein function. To date, very few studies of this type have been done for prion-like diseases (Table 1.7). An experiment in zebrafish suggests that the Swedish mutation renders APP unable to maintain its normal function in motor axon maintenance (Song and Pimplikar, 2012), though further experiments in this area are warranted. Similarly, it has been shown that mutant huntingtin can rescue embryonic lethality in *Htt*$^{-/-}$ mice (Cattaneo et al., 2005). Conditional knock-ins of mutant hungtintin at later developmental stages could be used to determine whether mutant hungtintin loses the neuroprotective functions of wild type huntingtin. Future research in this area would provide crucial insights into the progression of prion-like diseases.

Table 1.7. Rescue experiments can be used to determine whether mutant proteins retain their normal functions in prion-like disease[13]

Disease	Gene	Mutation	Rescue?
AD	*MAPT*	This has not been done to our knowledge	-N/A
	APP	-APPswe (K670N, M671L)	-Does not rescue convergent extension defects in zebrafish morphants [1] or motor axon deficits [2]
ALS	*SOD1*	This has not been done to our knowledge	-N/A
HD	*HTT*	-128 Poly-Q expansion	-Rescues embryonic lethality in ko mice (reviewed in [3])
PD	*SNCA*	This has not been done to our knowledge	-N/A

Table 1.7 References:

1 (Joshi et al., 2009), 2 (Song and Pimplikar, 2012), 3 (Cattaneo et al., 2005)

---

[13] Reprinted from Journal of Alzheimer's Disease, Vol 54, Patricia L.A. Leighton and W.Ted Allison, Protein Misfolding in Prion and Prion-Like Diseases: Reconsidering a Required Role for Protein Loss-of-Function, Pages 3-29, Copyright (2016), with permission from IOS Press.

The publication is available at IOS Press through http://dx.doi.org/10.3233/JAD-160361

How can we determine if and when PrP^C loss-of-function is important?

For injury or for many diseases outside of neurodegeneration, protein loss-of-function is a well-accepted disease mechanism, often associated with mutation (e.g., tumor suppressors mutated in cancers, or cystic fibrosis transmembrane conductance regulator (*CTFR*), which is mutated in cystic fibrosis). Here we have synthesized information from disparate diseases to argue that loss-of-function in template directed misfolding is prevalent and the norm rather than an exception. Prion disease is similar to HD in that the misfolded protein forms stable beta sheets and thus the toxic effects of the misfolded form are long lasting, masking the effects of PrP^C loss-of-function. To determine how PrP^C loss-of-function contributes to the disease it will be critical to identify subtle phenotypes in PrP^C null animals and determine whether these are phenocopied during prion infection. Part of this process will be to compare global gene expression in *Prnp* null mice to those with prion disease (a study of this nature has been done in the HD field (Jacobsen et al., 2011)). The genetic background in such studies would of course need to be carefully controlled. Assessing the ability of mutant PrP^C to rescue phenotypes in PrP^C null animals will also shed light on whether mutant PrP^C can perform its normal functions. Adding and removing PrP^C at different stages of experimentally induced prion disease could be used to determine when PrP^C loss-of-function is important for disease progression. We propose that expanding this approach by deploying transgenic variants of PrP^C that are seemingly inert to protein misfolding, such as rabbit PrP^C and human PrP G127V (Asante et al., 2015; Sarradin et al., 2015), would allow one to assess outcomes when PrP^C is not reduced in abundance or misfolded (i.e., the transgene would rescue the loss-of-function) and yet presumably would not be contributing to further gain-of-function etiology. A potential caveat of the proposed experiment is that expression of rabbit PrP^C may interfere with the gain-of-function conversion of PrP^C to its misfolded form and its associated toxicity, as has previously been the case when heterologous pools of PrP^C are present (Telling et al., 1995).

Implications for disease prevention and management

Misfolded PrP^{Sc} is an obvious therapeutic target in prion disease, and much effort has been put forth to enable such strategies, but PrP^C has also been proposed as a therapeutic

target for prion disease prophylaxis and treatment. Disruption of PrP^C through down-regulation or blocking interaction with PrP^{Sc} via antibodies or small molecules is proposed as a therapeutic strategy for prion diseases and AD. If PrP^C loss-of-function is an early disease mechanism, however, mitigation of treatment side effects will likely also require finding ways to normalize protective portions of PrP^C abundance or to target downstream pathways. Overall, further research is needed to understand the normal roles of PrP^C and prion-like proteins such as APP in healthy brains and their protective roles when AD or prion disease begins.

1.3.5 Concluding remarks on the contributions of loss-of-function to prion and prion-like diseases

Prion disease research has contributed much toward understanding progression of other neurodegenerative diseases. Here we 'turned the tables' to argue that strategies used to study prion-like diseases should now be applied to prion diseases to unravel the complexity of gain- versus loss-of PrP^C function in prion diseases. Our proposed strategies include: 1) Careful comparison between diseased animals and loss-of-function animal models to identify relevant phenotypes; 2) Genetic complementation to rescue phenotypes in *Prnp* null animals, and 3) Evaluation of whether mutant versions of PrP can adequately rescue phenotypes in *Prnp* null animals. We have also noted that there are many putative functions shared between PrP^C and its interaction partner, APP, which warrant continued investigation. Further research on the normal protective functions of both PrP^C and APP will be necessary to understand prion disease and AD etiology and to design novel and efficacious therapeutics.

1.4 Summary

Prion diseases and AD are devastating neurological diseases with tremendous societal and economic implications. As reviewed above, identifying contributions of protein loss-of-function to prion disease and AD pathology is a crucial step in the discovery of disease management strategies. As the physiological functions of PrP and APP in healthy individuals remain elusive, further research in this area is warranted. Herein, we contributed wholly unique genetic resources to the prion and AD fields (zebrafish *appa$^{-/-}$* mutants, *prp1$^{-/-}$* mutants, compound *prp1$^{-/-}$;prp2$^{-/-}$* mutants and compound *prp1$^{-/-}$;appa$^{-/-}$*

64

mutants) and used these tools to establish conserved and important biological roles for PrP^C and APP. In contrast to reports of severe phenotypes when either *prp1* or *prp2* are acutely knocked down (Kaiser et al., 2012; Malaga-Trillo et al., 2009; Nourizadeh-Lillabadi et al., 2010), zebrafish *prp1*$^{-/-}$ and compound *prp1*$^{-/-}$;*prp2*$^{-/-}$ mutants lack overt phenotypes and hence resemble mammalian *Prnp* knockouts. Further, *appa*$^{-/-}$ and compound *prp1*$^{-/-}$;*appa*$^{-/-}$ mutants also lacked overt phenotypes, but were slightly smaller than wild type fish at some developmental stages. This contrasted our previous work wherein severe developmental defects were observed in embryos when *appa* and *prp1* were transiently co-knocked down using morpholinos (Kaiser et al., 2012).

Previous reports that zebrafish *prnp* paralogs are expressed during early zebrafish development (Cotto et al., 2005; Malaga-Trillo et al., 2009) and that PrP^C participates in cell adhesion and neural outgrowth in primary neuronal cultures (Beraldo et al., 2011; Chen et al., 2003; Santuccione et al., 2005), prompted us to investigate contributions of prp1 and prp2 to zebrafish neural development. The zebrafish lateral line is an accessible neural system for studies of neural cell migration and cohesion, with neuromast structures that are homologous to the inner ear of mammals (Thomas et al., 2015). We thus examined neuromast deposition in zebrafish prion protein loss-of-function mutants in Chapter 4. We predicted that prp1 and prp2 would have redundant function in neuromast patterning, but instead we found that loss of prp1 reduced the number of posterior lateral line neuromasts, while loss of prp2 yielded an increase in the number of trunk neuromasts. Alternate hypotheses to explain these findings are 1) that prp1 and prp2 have sub-functionalized and participate at different stages of proneuromast development in the primordium or 2) prp1 and prp2 differentially regulate a hypothetical membrane receptor.

Further, we have clarified roles for PrP^C regulating neural excitability in vivo and in memory. One of the most debated putative functions of PrP^C to date has been a role in regulating neural excitability, with some studies reporting that *Prnp*$^{-/-}$ mice are more susceptible to seizure-inducing drugs and others refuting this (reviewed in (Carulla et al., 2015)). In Chapter 3, we demonstrate that PrP^C regulates neural activity in a disparate model organism, the zebrafish. Specifically, zebrafish paralogs of *Prnp* are protective against the convulsant pentylenetetrazole (PTZ). Inconsistent results have also been reported surrounding a role for PrP^C in learning and memory (for examples see (Rial et

al., 2009; Roesler et al., 1999; Schmitz et al., 2014a)). In Chapter 5, we demonstrate that *prp2$^{-/-}$* fish have age-dependent deficits in object recognition memory and cognitive appraisal. Overall, these results support ancient and conserved functions for PrP^C in regulating neural activity and in memory.

Additionally, in Chapter 2, we confirm that zebrafish *prp1* and *appa* interact, thus subversion of APP function in AD might disrupt some functions of PrP^C (described above), contributing to memory loss and other AD symptoms. Interestingly, acute (but not chronic) loss of *appa* in the context of PrP^C loss of function produces overt developmental deficits in zebrafish embryos. Mouse *Prnp* mRNA can rescue this phenotype, supporting the existence of a conserved interaction between APP and PrP^C.

Since most of the above studies were performed in young zebrafish larvae, rescue via microinjection of various mRNAs is now possible. Thus these paradigms, in combination with 'mRNA rescue' assays, will facilitate assignment of protein function to particular protein domains. Understanding what normal biological functions might be partially lost or subverted during prion diseases and AD and which proteins domains of PrP^C and APP mediate these functions will be informative for the design of AD and prion disease therapeutics.

Chapter 1 References

Prevalence and Monetary Costs of Dementia in Canada: Population Health Expert Panel. In: L. W. Chambers, et al., (Eds.). Alzheimer Society of Canada Toronto, Ontario, 2016, pp. 1-71.

Abramsson, A., et al., 2013. The zebrafish amyloid precursor protein-b is required for motor neuron guidance and synapse formation. Dev Biol. 381**,** 377-88.

Aguzzi, A., et al., 2007. Insights into prion strains and neurotoxicity. Nat Rev Mol Cell Biol. 8**,** 552-61.

Aguzzi, A., Rajendran, L., 2009. The transcellular spread of cytosolic amyloids, prions, and prionoids. Neuron. 64**,** 783-90.

Ahmed, Z., et al., 2014. A novel in vivo model of tau propagation with rapid and progressive neurofibrillary tangle pathology: the pattern of spread is determined by connectivity, not proximity. Acta Neuropathol. 127**,** 667-83.

Alonso, A. C., et al., 1994. Role of abnormally phosphorylated tau in the breakdown of microtubules in Alzheimer disease. Proc Natl Acad Sci U S A. 91**,** 5562-6.

Altmeppen, H. C., et al., 2012. Proteolytic processing of the prion protein in health and disease. Am J Neurodegener Dis. 1**,** 15-31.

Ambrose, C. M., et al., 1994. Structure and expression of the Huntington's disease gene: evidence against simple inactivation due to an expanded CAG repeat. Somat Cell Mol Genet. 20**,** 27-38.

Arai, S., et al., 2009. Brainstem auditory evoked potentials in experimentally-induced bovine spongiform encephalopathy. Res Vet Sci. 87**,** 111-4.

Arendash, G. W., et al., 2004. Multi-metric behavioral comparison of APPsw and P301L models for Alzheimer's disease: linkage of poorer cognitive performance to tau pathology in forebrain. Brain Res. 1012**,** 29-41.

Aula, P., et al., 1973. Partial trisomy 21. Clin Genet. 4**,** 241-51.

Ayers, J. I., et al., 2014. Experimental transmissibility of mutant SOD1 motor neuron disease. Acta Neuropathol. 128**,** 791-803.

Bai, Y., et al., 2008. The in Vivo brain interactome of the amyloid precursor protein. Mol Cell Proteomics. 7**,** 15-34.

Baier, M., et al., 2008. Prion infection of mice transgenic for human APPSwe: increased accumulation of cortical formic acid extractable Abeta(1-42) and rapid scrapie disease development. Int J Dev Neurosci. 26, 821-4.

Bayer, T. A., et al., 1999. It all sticks together--the APP-related family of proteins and Alzheimer's disease. Mol Psychiatry. 4, 524-8.

Beland, M., et al., 2014. Abeta induces its own prion protein N-terminal fragment (PrPN1)-mediated neutralization in amorphous aggregates. Neurobiol Aging. 35, 1537-48.

Beland, M., et al., 2012. PrP(C) homodimerization stimulates the production of PrPC cleaved fragments PrPN1 and PrPC1. J Neurosci. 32, 13255-63.

Beraldo, F. H., et al., 2011. Metabotropic glutamate receptors transduce signals for neurite outgrowth after binding of the prion protein to laminin gamma1 chain. FASEB J. 25, 265-79.

Beraldo, F. H., et al., 2013. Stress-inducible phosphoprotein 1 has unique cochaperone activity during development and regulates cellular response to ischemia via the prion protein. FASEB J. 27, 3594-607.

Bidhendi, E. E., et al., 2016. Two superoxide dismutase prion strains transmit amyotrophic lateral sclerosis-like disease. J Clin Invest. 126, 2249-53.

Birch, A. M., 2014. The contribution of astrocytes to Alzheimer's disease. Biochem Soc Trans. 42, 1316-20.

Black, S. A., et al., 2014. Cellular prion protein and NMDA receptor modulation: protecting against excitotoxicity. Front Cell Dev Biol. 2, 45.

Black, S. E., et al., 2010. Canadian Alzheimer's disease caregiver survey: baby-boomer caregivers and burden of care. Int J Geriatr Psychiatry. 25, 807-13.

Bodrikov, V., et al., 2011. Prion protein promotes growth cone development through reggie/flotillin-dependent N-cadherin trafficking. J Neurosci. 31, 18013-25.

Bolkan, B. J., Kretzschmar, D., 2014. Loss of Tau results in defects in photoreceptor development and progressive neuronal degeneration in Drosophila. Dev Neurobiol. 74, 1210-25.

Bolton, D. C., et al., 1982. Identification of a protein that purifies with the scrapie prion. Science. 218, 1309-11.

Bonaccorsi di Patti, M. C., et al., 2002. Analysis of Cu,ZnSOD conformational stability by differential scanning calorimetry. Methods Enzymol. 349**,** 49-61.

Borchelt, D. R., et al., 1994. Superoxide dismutase 1 with mutations linked to familial amyotrophic lateral sclerosis possesses significant activity. Proc Natl Acad Sci U S A. 91**,** 8292-6.

Bourdet, I., et al., 2015. The full-length form of the Drosophila amyloid precursor protein is involved in memory formation. J Neurosci. 35**,** 1043-51.

Brandner, S., et al., 1996. Normal host prion protein necessary for scrapie-induced neurotoxicity. Nature. 379**,** 339-43.

Bremer, J., et al., 2010. Axonal prion protein is required for peripheral myelin maintenance. Nat Neurosci. 13**,** 310-U9.

Broom, H. R., et al., 2015. Destabilization of the dimer interface is a common consequence of diverse ALS-associated mutations in metal free SOD1. Protein Sci. 24, 2081-2089.

Bruce, M., et al., 1994. Transmission of bovine spongiform encephalopathy and scrapie to mice: strain variation and the species barrier. Philos Trans R Soc Lond B Biol Sci. 343**,** 405-11.

Bruijn, L. I., et al., 1998. Aggregation and motor neuron toxicity of an ALS-linked SOD1 mutant independent from wild-type SOD1. Science. 281**,** 1851-4.

Brundin, P., et al., 2010. Prion-like transmission of protein aggregates in neurodegenerative diseases. Nat Rev Mol Cell Biol. 11**,** 301-7.

Budka, H., et al., 1995. Neuropathological diagnostic criteria for Creutzfeldt-Jakob disease (CJD) and other human spongiform encephalopathies (prion diseases). Brain Pathol. 5**,** 459-66.

Bueler, H., et al., 1992. Normal development and behaviour of mice lacking the neuronal cell-surface PrP protein. Nature. 356**,** 577-582.

Bueler, H., et al., 1994. High prion and PrPSc levels but delayed onset of disease in scrapie-inoculated mice heterozygous for a disrupted PrP gene. Mol Med. 1**,** 19-30.

Burns, C. S., et al., 2002. Molecular features of the copper binding sites in the octarepeat domain of the prion protein. Biochemistry. 41**,** 3991-4001.

Caetano, F. A., et al., 2011. Amyloid-beta oligomers increase the localization of prion protein at the cell surface. J Neurochem. 117, 538-53.

Caine, D., et al., 2015. The cognitive profile of prion disease: a prospective clinical and imaging study. Ann Clin Transl Neurol. 2, 548-58.

Calzolai, L., et al., 2005. Prion protein NMR structures of chickens, turtles, and frogs. Proc Natl Acad Sci U S A. 102, 651-5.

Campeau, J. L., et al., 2013. Early increase and late decrease of purkinje cell dendritic spine density in prion-infected organotypic mouse cerebellar cultures. PLoS One. 8, e81776.

Cao, X., Sudhof, T. C., 2001. A transcriptionally [correction of transcriptively] active complex of APP with Fe65 and histone acetyltransferase Tip60. Science. 293, 115-20.

Carulla, P., et al., 2011. Neuroprotective role of PrPC against kainate-induced epileptic seizures and cell death depends on the modulation of JNK3 activation by GluR6/7-PSD-95 binding. Mol Biol Cell. 22, 3041-54.

Carulla, P., et al., 2015. Involvement of PrP(C) in kainate-induced excitotoxicity in several mouse strains. Sci Rep. 5, 11971.

Cattaneo, E., et al., 2005. Normal huntingtin function: an alternative approach to Huntington's disease. Nat Rev Neurosci. 6, 919-30.

Chasseigneaux, S., Allinquant, B., 2012. Functions of Abeta, sAPPalpha and sAPPbeta : similarities and differences. J Neurochem. 120 Suppl 1, 99-108.

Chattopadhyay, M., et al., 2008. Initiation and elongation in fibrillation of ALS-linked superoxide dismutase. Proc Natl Acad Sci U S A. 105, 18663-8.

Chen, G., et al., 2000. A learning deficit related to age and beta-amyloid plaques in a mouse model of Alzheimer's disease. Nature. 408, 975-9.

Chen, S., et al., 2003. Prion protein as trans-interacting partner for neurons is involved in neurite outgrowth and neuronal survival. Mol Cell Neurosci. 22, 227-33.

Chesebro, B., et al., 2010. Fatal transmissible amyloid encephalopathy: a new type of prion disease associated with lack of prion protein membrane anchoring. PLoS Pathog. 6, e1000800.

Chesebro, B., et al., 2005. Anchorless prion protein results in infectious amyloid disease without clinical scrapie. Science (New York, N.Y.). 308, 1435-1439.

Chia, R., et al., 2010. Superoxide dismutase 1 and tgSOD1 mouse spinal cord seed fibrils, suggesting a propagative cell death mechanism in amyotrophic lateral sclerosis. PLoS One. 5, e10627.

Chishti, M. A., et al., 2001. Early-onset amyloid deposition and cognitive deficits in transgenic mice expressing a double mutant form of amyloid precursor protein 695. J Biol Chem. 276, 21562-21570.

Chung, E., et al., 2010. Anti-PrPC monoclonal antibody infusion as a novel treatment for cognitive deficits in an Alzheimer's disease model mouse. BMC Neurosci. 11, 130.

Clavaguera, F., et al., 2013. Brain homogenates from human tauopathies induce tau inclusions in mouse brain. Proc Natl Acad Sci U S A. 110, 9535-40.

Clavaguera, F., et al., 2009. Transmission and spreading of tauopathy in transgenic mouse brain. Nat Cell Biol. 11, 909-13.

Cohen, F. E., et al., 1994. Structural clues to prion replication. Science. 264, 530-1.

Coitinho, A. S., et al., 2003. Cellular prion protein ablation impairs behavior as a function of age. Neuroreport. 14, 1375-9.

Collins, S. J., et al., 2004. Transmissible spongiform encephalopathies. Lancet. 363, 51-61.

Come, J. H., et al., 1993. A kinetic model for amyloid formation in the prion diseases: importance of seeding. Proc Natl Acad Sci U S A. 90, 5959-63.

Conforti, P., et al., 2013. Lack of huntingtin promotes neural stem cells differentiation into glial cells while neurons expressing huntingtin with expanded polyglutamine tracts undergo cell death. Neurobiol Dis. 50, 160-70.

Costanzo, M., et al., 2013. Transfer of polyglutamine aggregates in neuronal cells occurs in tunneling nanotubes. J Cell Sci. 126, 3678-85.

Costanzo, M., Zurzolo, C., 2013. The cell biology of prion-like spread of protein aggregates: mechanisms and implication in neurodegeneration. Biochem J. 452, 1-17.

Cotto, E., et al., 2005. Molecular characterization, phylogenetic relationships, and developmental expression patterns of prion genes in zebrafish (Danio rerio). FEBS Journal. 272**,** 500.

Criado, J. R., et al., 2005. Mice devoid of prion protein have cognitive deficits that are rescued by reconstitution of PrP in neurons. Neurobiol Dis. 19**,** 255-65.

Daude, N., et al., 2012. Knockout of the prion protein (PrP)-like Sprn gene does not produce embryonic lethality in combination with PrP(C)-deficiency. Proc Natl Acad Sci U S A. 109**,** 9035-40.

Dawson, G. R., et al., 1999. Age-related cognitive deficits, impaired long-term potentiation and reduction in synaptic marker density in mice lacking the beta-amyloid precursor protein. Neuroscience. 90**,** 1-13.

Dawson, H. N., et al., 2001. Inhibition of neuronal maturation in primary hippocampal neurons from tau deficient mice. J Cell Sci. 114**,** 1179-87.

Diack, A. B., et al., 2014. Variant CJD. 18 years of research and surveillance. Prion. 8**,** 286-95.

Dragatsis, I., et al., 2000. Inactivation of Hdh in the brain and testis results in progressive neurodegeneration and sterility in mice. Nat Genet. 26**,** 300-6.

DuVal, M. G., et al., 2014. Growth differentiation factor 6 as a putative risk factor in neuromuscular degeneration. PLoS One. 9**,** e89183.

Fischer, L. R., et al., 2011. SOD1 targeted to the mitochondrial intermembrane space prevents motor neuropathy in the Sod1 knockout mouse. Brain. 134**,** 196-209.

Fischer, L. R., et al., 2012. Absence of SOD1 leads to oxidative stress in peripheral nerve and causes a progressive distal motor axonopathy. Exp Neurol. 233**,** 163-71.

Fleisch, V., et al., 2013. Targeted mutation of the gene encoding prion protein in zebrafish reveals a conserved role in neuron excitability. Neurobiol Dis. 55**,** 11-25.

Fluharty, B. R., et al., 2013. An N-terminal fragment of the prion protein binds to amyloid-beta oligomers and inhibits their neurotoxicity in vivo. J Biol Chem. 288**,** 7857-66.

Fonseca, M. B., et al., 2013. Amyloid beta peptides promote autophagy-dependent differentiation of mouse neural stem cells: Abeta-mediated neural differentiation. Mol Neurobiol. 48**,** 829-40.

Fraser, H., et al., 1992a. Transmission of bovine spongiform encephalopathy and scrapie to mice. J Gen Virol. 73 (Pt 8)**,** 1891-7.

Fraser, P. E., et al., 1992b. Fibril formation by primate, rodent, and Dutch-hemorrhagic analogues of Alzheimer amyloid beta-protein. Biochemistry. 31**,** 10716-23.

Frost, B., Diamond, M. I., 2010. Prion-like mechanisms in neurodegenerative diseases. Nat Rev Neurosci. 11**,** 155-9.

Fujio, K., et al., 2007. 14-3-3 proteins and protein phosphatases are not reduced in tau-deficient mice. Neuroreport. 18**,** 1049-52.

Gamblin, T. C., et al., 2003. Modeling tau polymerization in vitro: a review and synthesis. Biochemistry. 42**,** 15009-17.

Games, D., et al., 1995. Alzheimer-type neuropathology in transgenic mice overexpressing V717F beta-amyloid precursor protein. Nature. 373**,** 523-7.

Gasperini, L., et al., 2015. Prion protein and copper cooperatively protect neurons by modulating NMDA receptor through S-nitrosylation. Antioxid Redox Signal. 22**,** 772-84.

Gauthier, L. R., et al., 2004. Huntingtin controls neurotrophic support and survival of neurons by enhancing BDNF vesicular transport along microtubules. Cell. 118**,** 127-38.

Geoghegan, J. C., et al., 2009. Trans-dominant inhibition of prion propagation in vitro is not mediated by an accessory cofactor. PLoS Pathog. 5**,** e1000535.

Gerhard, G. S., et al., 2002. Life spans and senescent phenotypes in two strains of Zebrafish (Danio rerio). Exp Gerontol. 37**,** 1055-68.

Glenner, G. G., 2012. Reprint of "Alzheimer's disease: Initial report of the purification and characterization of a novel cerebrovascular amyloid protein". Biochem Biophys Res Commun. 425**,** 534-539.

Goate, A., et al., 1991. Segregation of a missense mutation in the amyloid precursor protein gene with familial Alzheimer's disease. Nature. 349**,** 704-706.

Goedert, M., et al., 2014. Prion-like mechanisms in the pathogenesis of tauopathies and synucleinopathies. Curr Neurol Neurosci Rep. 14, 495.

Goedert, M., et al., 1988. Cloning and sequencing of the cDNA encoding a core protein of the paired helical filament of Alzheimer disease: identification as the microtubule-associated protein tau. Proc Natl Acad Sci U S A. 85, 4051-5.

Golanska, E., et al., 2009. Earlier onset of Alzheimer's disease: risk polymorphisms within PRNP, PRND, CYP46, and APOE genes. J Alzheimers Dis. 17, 359-68.

Goldgaber, D., et al., 1987. Characterization and chromosomal localization of a cDNA encoding brain amyloid of Alzheimer's disease. Science. 235, 877-80.

Grad, L. I., Cashman, N. R., 2014. Prion-like activity of Cu/Zn superoxide dismutase: implications for amyotrophic lateral sclerosis. Prion. 8, 33-41.

Grad, L. I., et al., 2015. From molecule to molecule and cell to cell: Prion-like mechanisms in amyotrophic lateral sclerosis. Neurobiol Dis. 77, 257-65.

Grad, L. I., et al., 2011. Intermolecular transmission of superoxide dismutase 1 misfolding in living cells. Proc Natl Acad Sci U S A. 108, 16398-403.

Grad, L. I., et al., 2014a. Exosome-dependent and independent mechanisms are involved in prion-like transmission of propagated Cu/Zn superoxide dismutase misfolding. Prion. 8, 331-5.

Grad, L. I., et al., 2014b. Intercellular propagated misfolding of wild-type Cu/Zn superoxide dismutase occurs via exosome-dependent and -independent mechanisms. Proc Natl Acad Sci U S A. 111, 3620-5.

Graffmo, K. S., et al., 2013. Expression of wild-type human superoxide dismutase-1 in mice causes amyotrophic lateral sclerosis. Hum Mol Genet. 22, 51-60.

Gu, X., et al., 2015. N17 Modifies mutant Huntingtin nuclear pathogenesis and severity of disease in HD BAC transgenic mice. Neuron. 85, 726-41.

Guillot-Sestier, M. V., et al., 2009. The alpha-secretase-derived N-terminal product of cellular prion, N1, displays neuroprotective function in vitro and in vivo. J Biol Chem. 284, 35973-86.

Guillot-Sestier, M. V., et al., 2012. alpha-Secretase-derived fragment of cellular prion, N1, protects against monomeric and oligomeric amyloid beta (Abeta)-associated cell death. J Biol Chem. 287, 5021-32.

Gurney, M. E., et al., 1994. Motor neuron degeneration in mice that express a human Cu,Zn superoxide dismutase mutation. Science. 264**,** 1772-5.

Hall, G. F., Patuto, B. A., 2012. Is tau ready for admission to the prion club? Prion. 6**,** 223-33.

Harada, A., et al., 1994. Altered microtubule organization in small-calibre axons of mice lacking tau protein. Nature. 369**,** 488-91.

Haraguchi, T., et al., 1989. Asparagine-linked glycosylation of the scrapie and cellular prion proteins. Arch Biochem Biophys. 274**,** 1-13.

Hardy, J., 2006. A hundred years of Alzheimer's disease research. Neuron. 52**,** 3-13.

Hardy, J., Allsop, D., 1991. Amyloid Deposition as the Central Event in the Etiology of Alzheimers-Disease. Trends Pharmacol Sci. 12**,** 383.

Hay, B., et al., 1987a. Biogenesis and transmembrane orientation of the cellular isoform of the scrapie prion protein [published errratum appears in Mol Cell Biol 1987 May;7(5):2035]. Mol Cell Biol. 7**,** 914-20.

Hay, B., et al., 1987b. Evidence for a secretory form of the cellular prion protein. Biochemistry. 26**,** 8110-5.

Heber, S., et al., 2000. Mice with combined gene knock-outs reveal essential and partially redundant functions of amyloid precursor protein family members. J Neurosci. 20**,** 7951-7963.

Herms, J., et al., 2004. Cortical dysplasia resembling human type 2 lissencephaly in mice lacking all three APP family members. EMBO J. 23**,** 4106-15.

Herrmann, U. S., et al., 2015. Prion infections and anti-PrP antibodies trigger converging neurotoxic pathways. PLoS Pathog. 11**,** e1004662.

Hesse, L., et al., 1994. The beta A4 amyloid precursor protein binding to copper. FEBS Lett. 349**,** 109-16.

Hewitt, P. E., et al., 2006. Creutzfeldt-Jakob disease and blood transfusion: results of the UK Transfusion Medicine Epidemiological Review study. Vox Sang. 91**,** 221-30.

Hornshaw, M. P., et al., 1995. Copper binding to the N-terminal tandem repeat regions of mammalian and avian prion protein. Biochem Biophys Res Commun. 207**,** 621-629.

Horwich, A. L., Weissman, J. S., 1997. Deadly conformations--protein misfolding in prion disease. Cell. 89**,** 499-510.

Huang, Y., Mucke, L., 2012. Alzheimer mechanisms and therapeutic strategies. Cell. 148**,** 1204-22.

Huc-Brandt, S., et al., 2014. Zebrafish prion protein PrP2 controls collective migration process during lateral line sensory system development. PLoS One. 9**,** e113331.

Iba, M., et al., 2013. Synthetic tau fibrils mediate transmission of neurofibrillary tangles in a transgenic mouse model of Alzheimer's-like tauopathy. J Neurosci. 33**,** 1024-37.

Iba, M., et al., 2015. Tau pathology spread in PS19 tau transgenic mice following locus coeruleus (LC) injections of synthetic tau fibrils is determined by the LC's afferent and efferent connections. Acta Neuropathol. 130**,** 349-62.

Ikegami, S., et al., 2000. Muscle weakness, hyperactivity, and impairment in fear conditioning in tau-deficient mice. Neurosci Lett. 279**,** 129-32.

Irizarry, M. C., et al., 1997. Abeta deposition is associated with neuropil changes, but not with overt neuronal loss in the human amyloid precursor protein V717F (PDAPP) transgenic mouse. J Neurosci. 17**,** 7053-9.

Jacobsen, J. C., et al., 2011. HD CAG-correlated gene expression changes support a simple dominant gain of function. Hum Mol Genet. 20**,** 2846-60.

Jin, L. W., et al., 1994. Peptides containing the RERMS sequence of amyloid beta/A4 protein precursor bind cell surface and promote neurite extension. J Neurosci. 14**,** 5461-70.

Jonsson, P. A., et al., 2004. Minute quantities of misfolded mutant superoxide dismutase-1 cause amyotrophic lateral sclerosis. Brain. 127**,** 73-88.

Joshi, P., et al., 2009. Amyloid precursor protein is required for convergent-extension movements during Zebrafish development. Dev Biol. 335**,** 1-11.

Joyce, P. I., et al., 2011. SOD1 and TDP-43 animal models of amyotrophic lateral sclerosis: recent advances in understanding disease toward the development of clinical treatments. Mamm Genome. 22**,** 420-48.

Joyce, P. I., et al., 2015. A novel SOD1-ALS mutation separates central and peripheral effects of mutant SOD1 toxicity. Hum Mol Genet. 24**,** 1883-97.

Kaden, D., et al., 2008. Homophilic interactions of the amyloid precursor protein (APP) ectodomain are regulated by the loop region and affect beta-secretase cleavage of APP. J Biol Chem. 283**,** 7271-7279.

Kaiser, D., et al., 2012. Amyloid beta precursor protein and prion protein have a conserved interaction affecting cell adhesion and CNS development. PloS One. 7.

Kane, M. D., et al., 2000. Evidence for seeding of beta -amyloid by intracerebral infusion of Alzheimer brain extracts in beta -amyloid precursor protein-transgenic mice. J Neurosci. 20**,** 3606-11.

Kang, J., et al., 1987. The precursor of Alzheimer's disease amyloid A4 protein resembles a cell-surface receptor. Nature. 325**,** 733-6.

Karran, E., De Strooper, B., 2016. The amyloid cascade hypothesis: are we poised for success or failure? J Neurochem. 139, 237-252.

Kawas, C., et al., 2000. Age-specific incidence rates of Alzheimer's disease: the Baltimore Longitudinal Study of Aging. Neurology. 54**,** 2072-7.

Khare, S. D., et al., 2006. FALS mutations in Cu, Zn superoxide dismutase destabilize the dimer and increase dimer dissociation propensity: a large-scale thermodynamic analysis. Amyloid. 13**,** 226-35.

Khosravani, H., et al., 2008. Prion protein attenuates excitotoxicity by inhibiting NMDA receptors. J Cell Biol. 181**,** 551-565.

Kim, H. S., et al., 2003. C-terminal fragments of amyloid precursor protein exert neurotoxicity by inducing glycogen synthase kinase-3beta expression. FASEB J. 17**,** 1951-3.

Kimberly, W. T., et al., 2005. Physiological regulation of the beta-amyloid precursor protein signaling domain by c-Jun N-terminal kinase JNK3 during neuronal differentiation. J Neurosci. 25**,** 5533-43.

Kinoshita, A., et al., 2002. The gamma secretase-generated carboxyl-terminal domain of the amyloid precursor protein induces apoptosis via Tip60 in H4 cells. J Biol Chem. 277**,** 28530-6.

Kurt, T. D., Sigurdson, C. J., 2016. Cross-species transmission of CWD prions. Prion. 10**,** 83-91.

Kuznetsova, A., et al., 2014. Potential role of soil properties in the spread of CWD in western Canada. Prion. 8**,** 92-99.

Lansbury, P. T., Jr., Caughey, B., 1995. The chemistry of scrapie infection: implications of the 'ice 9' metaphor. Chem Biol. 2**,** 1-5.

Lasagna-Reeves, C. A., et al., 2010. Preparation and characterization of neurotoxic tau oligomers. Biochemistry. 49**,** 10039-41.

Lasagna-Reeves, C. A., et al., 2012. Alzheimer brain-derived tau oligomers propagate pathology from endogenous tau. Sci Rep. 2**,** 700.

Lauren, J., 2014. Cellular prion protein as a therapeutic target in Alzheimer's disease. J Alzheimers Dis. 38**,** 227-44.

Lauren, J., et al., 2009. Cellular prion protein mediates impairment of synaptic plasticity by amyloid-beta oligomers. Nature. 457**,** 1128-U84.

Le Roy, D. G., Klein, K. K., 2003. Apocalypse cow: the effect of BSE on Canada's beef industry. In Western Economics Forum (Vol. 2, No. 2, pp. 20-27). Western Agricultural Economics Association.

Leavitt, B. R., et al., 2001. Wild-type huntingtin reduces the cellular toxicity of mutant huntingtin in vivo. Am J Hum Genet. 68**,** 313-24.

Lei, P., et al., 2012. Tau deficiency induces parkinsonism with dementia by impairing APP-mediated iron export. Nat Med. 18**,** 291-5.

Lei, P., et al., 2014. Motor and cognitive deficits in aged tau knockout mice in two background strains. Mol Neurodegener. 9**,** 29.

Leiss, W., Nicol, A. M., 2006. A Tale of Two Food Risks: BSE and Farmed Salmon in Canada. J Risk Res. 9**,** 891-910.

Leissring, M. A., et al., 2002. A physiologic signaling role for the gamma -secretase-derived intracellular fragment of APP. Proc Natl Acad Sci U S A. 99**,** 4697-702.

Lewis, J., et al., 2001. Enhanced neurofibrillary degeneration in transgenic mice expressing mutant tau and APP. Science. 293**,** 1487-91.

Lewis, J., et al., 2000. Neurofibrillary tangles, amyotrophy and progressive motor disturbance in mice expressing mutant (P301L) tau protein. Nat Genet. 25**,** 402-5.

Li, A., et al., 2000. Identification of a novel gene encoding a PrP-like protein expressed as chimeric transcripts fused to PrP exon 1/2 in ataxic mouse line with a disrupted PrP gene. Cell Mol Neurobiol. 20, 553-67.

Lindberg, M. J., et al., 2002. Common denominator of Cu/Zn superoxide dismutase mutants associated with amyotrophic lateral sclerosis: decreased stability of the apo state. Proc Natl Acad Sci U S A. 99, 16607-12.

Luo, L., et al., 1992. Human amyloid precursor protein ameliorates behavioral deficit of flies deleted for Appl gene. Neuron. 9, 595-605.

Ma, Q. L., et al., 2014. Loss of MAP function leads to hippocampal synapse loss and deficits in the Morris Water Maze with aging. J Neurosci. 34, 7124-36.

Magara, F., et al., 1999. Genetic background changes the pattern of forebrain commissure defects in transgenic mice underexpressing the beta-amyloid-precursor protein. Proc Natl Acad Sci U S A. 96, 4656-61.

Malaga-Trillo, E., et al., 2009. Regulation of Embryonic Cell Adhesion by the Prion Protein. PloS Biology. 7, 576.

Mallm, J. P., et al., 2010. Generation of conditional null alleles for APP and APLP2. Genesis. 48, 200-6.

Mallucci, G., et al., 2003. Depleting neuronal PrP in prion infection prevents disease and reverses spongiosis. Science. 302, 871-4.

Manson, J. C., et al., 1994. 129/Ola mice carrying a null mutation in PrP that abolishes mRNA production are developmentally normal. Mol Neurobiol. 8, 121-7.

Marc, D., et al., 2007. Scavenger, transducer, RNA chaperone? What ligands of the prion protein teach us about its function. Cell Mol Life Sci. 64, 815-29.

Marciniuk, K., et al., 2013. Evidence for prion-like mechanisms in several neurodegenerative diseases: potential implications for immunotherapy. Clin Dev Immunol. 2013, 473706.

Marotta, C. A., et al., 1992. Molecular and cellular biology of Alzheimer amyloid. J Mol Neurosci. 3, 111-25.

Masters, C. L., et al., 1985a. Neuronal origin of a cerebral amyloid: neurofibrillary tangles of Alzheimer's disease contain the same protein as the amyloid of plaque cores and blood vessels. EMBO J. 4, 2757-63.

Masters, C. L., et al., 1985b. Amyloid plaque core protein in Alzheimer disease and Down syndrome. Proc Natl Acad Sci U S A. 82, 4245-9.

Maurer, K., et al., 1997. Auguste D and Alzheimer's disease. Lancet. 349, 1546-9.

Mays, C. E., et al., 2014. Prion disease tempo determined by host-dependent substrate reduction. J Clin Invest. 124, 847-58.

McCord, J. M., Fridovich, I., 1969. Superoxide dismutase. An enzymic function for erythrocuprein (hemocuprein). J Biol Chem. 244, 6049-55.

McDonald, A. J., et al., 2014. A new paradigm for enzymatic control of alpha-cleavage and beta-cleavage of the prion protein. J Biol Chem. 289, 803-13.

McGown, A., et al., 2013. Early interneuron dysfunction in ALS: insights from a mutant sod1 zebrafish model. Ann Neurol. 73, 246-58.

McLachlan, S. M., Yestrau, M., 2008. From the ground up: holistic management and grassroots rural adaptation to bovine spongiform encephalopathy across western Canada. Mitig Adapt Strat for Gl. 14, 299-316.

McLennan, N., et al., 2004. Prion protein accumulation and neuroprotection in hypoxic brain damage. Am J Pathol. 165, 227-235.

Mercer, R. C., et al., 2013. The prion protein modulates A-type K+ currents mediated by Kv4.2 complexes through dipeptidyl aminopeptidase-like protein 6. J Biol Chem. 288, 37241-55.

Meyer-Luehmann, M., et al., 2006. Exogenous induction of cerebral beta-amyloidogenesis is governed by agent and host. Science. 313, 1781-4.

Miesbauer, M., et al., 2006. Prion protein-related proteins from zebrafish are complex glycosylated and contain a glycosylphosphatidylinositol anchor. Biochem Biophys Res Commun. 341, 218-24.

Millhauser, G. L., 2007. Copper and the prion protein: Methods, structures, function, and disease. Annu Rev Phys Chem. 58, 299-320.

Mo, H., et al., 2001. Two different neurodegenerative diseases caused by proteins with similar structures. Proc Natl Acad Sci U S A. 98, 2352-7.

Moore, R. C., et al., 1999. Ataxia in prion protein (PrP)-deficient mice is associated with upregulation of the novel PrP-like protein doppel. J Mol Biol. 292, 797-817.

Moore, R. C., et al., 1995. Double replacement gene targeting for the production of a series of mouse strains with different prion protein gene alterations. Biotechnology (N Y). 13**,** 999-1004.

Morales, R., et al., 2015. Prion-like features of misfolded Abeta and tau aggregates. Virus Res. 207**,** 106-12.

Morales, R., et al., 2010. Molecular cross talk between misfolded proteins in animal models of Alzheimer's and prion diseases. J Neurosci. 30**,** 4528-35.

Muller, U., et al., 1994. Behavioral and anatomical deficits in mice homozygous for a modified beta-amyloid precursor protein gene. Cell. 79**,** 755-65.

Multhaup, G., et al., 1996. The amyloid precursor protein of Alzheimer's disease in the reduction of copper(II) to copper(I). Science. 271**,** 1406-9.

Musa, A., et al., 2001. Distinct expression patterns of two zebrafish homologues of the human APP gene during embryonic development. Dev Genes Evol. 211**,** 563.

Nakao, N., et al., 1995. Trophic and protective actions of brain-derived neurotrophic factor on striatal DARPP-32-containing neurons in vitro. Brain Res Dev Brain Res. 90**,** 92-101.

Ninomiya, H., et al., 1993. Amino acid sequence RERMS represents the active domain of amyloid beta/A4 protein precursor that promotes fibroblast growth. J Cell Biol. 121**,** 879-86.

Nishimoto, I., et al., 1993. Alzheimer amyloid protein precursor complexes with brain GTP-binding protein G(o). Nature. 362**,** 75-9.

Norton, W., Bally-Cuif, L., 2010. Adult zebrafish as a model organism for behavioural genetics. BMC Neurosci. 11**,** 90.

Nourizadeh-Lillabadi, R., et al., 2010. Early Embryonic Gene Expression Profiling of Zebrafish Prion Protein (Prp2) Morphants. PloS One. 5.

Novak, P., et al., 2011. Tauons and prions: infamous cousins? J Alzheimers Dis. 26**,** 413-30.

Nussbaum, J. M., et al., 2012. Prion-like behaviour and tau-dependent cytotoxicity of pyroglutamylated amyloid-beta. Nature. 485**,** 651-5.

Oddo, S., et al., 2003. Triple-transgenic model of Alzheimer's disease with plaques and tangles: intracellular Abeta and synaptic dysfunction. Neuron. 39**,** 409-21.

Oesch, B., et al., 1985. A cellular gene encodes scrapie PrP 27-30 protein. Cell. 40**,** 735-46.

Ohsawa, I., et al., 2001. Fibulin-1 binds the amino-terminal head of beta-amyloid precursor protein and modulates its physiological function. J Neurochem. 76**,** 1411-20.

Oueslati, A., et al., 2014. Protein Transmission, Seeding and Degradation: Key Steps for alpha-Synuclein Prion-Like Propagation. Exp Neurobiol. 23**,** 324-36.

Pan, K. M., et al., 1993. Conversion of alpha-helices into beta-sheets features in the formation of the scrapie prion proteins. Proc Natl Acad Sci U S A. 90**,** 10962-6.

Pantera, B., et al., 2009. PrPc activation induces neurite outgrowth and differentiation in PC12 cells: role for caveolin-1 in the signal transduction pathway. J Neurochem. 110**,** 194-207.

Panula, P., et al., 2010. The comparative neuroanatomy and neurochemistry of zebrafish CNS systems of relevance to human neuropsychiatric diseases. Neurobiol Dis. 40**,** 46-57.

Parkin, E. T., et al., 1999. Amyloid precursor protein, although partially detergent-insoluble in mouse cerebral cortex, behaves as an atypical lipid raft protein. Biochem J. 344**,** 23.

Parkin, E. T., et al., 2007. Cellular prion protein regulates beta-secretase cleavage of the Alzheimer's amyloid precursor protein. Proc Natl Acad Sci U S A. 104**,** 11062-11067.

Pearce, M. M., et al., 2015. Prion-like transmission of neuronal huntingtin aggregates to phagocytic glia in the Drosophila brain. Nat Commun. 6**,** 6768.

Peeraer, E., et al., 2015. Intracerebral injection of preformed synthetic tau fibrils initiates widespread tauopathy and neuronal loss in the brains of tau transgenic mice. Neurobiol Dis. 73**,** 83-95.

Poggiolini, I., et al., 2013. Prion protein misfolding, strains, and neurotoxicity: an update from studies on Mammalian prions. Int J Cell Biol. 2013**,** 910314.

Pokrishevsky, E., et al., 2012. Aberrant localization of FUS and TDP43 is associated with misfolding of SOD1 in amyotrophic lateral sclerosis. PLoS One. 7**,** e35050.

Prince, M., et al., 2013. The global prevalence of dementia: a systematic review and metaanalysis. Alzheimers Dement. 9**,** 63-75 e2.

Prudencio, M., et al., 2010. An examination of wild-type SOD1 in modulating the toxicity and aggregation of ALS-associated mutant SOD1. Hum Mol Genet. 19**,** 4774-89.

Prusiner, S., 1991. Molecular biology of prion diseases. Science. 252**,** 1515-1522.

Prusiner, S. B., 1982. Novel proteinaceous infectious particles cause scrapie. Science. 216**,** 136-44.

Prusiner, S. B., 1989. Scrapie prions. Annu Rev Microbiol. 43**,** 345-74.

Prusiner, S. B., et al., 1984. Purification and structural studies of a major scrapie prion protein. Cell. 38**,** 127-34.

Prusiner, S. B., et al., 1990. Transgenetic studies implicate interactions between homologous PrP isoforms in scrapie prion replication. Cell. 63**,** 673-86.

Pun, S., et al., 2006. Selective vulnerability and pruning of phasic motoneuron axons in motoneuron disease alleviated by CNTF. Nat Neurosci. 9**,** 408-19.

Pushie, M. J., et al., 2011. Prion protein expression level alters regional copper, iron and zinc content in the mouse brain. Metallomics. 3**,** 206-14.

Rakhit, R., et al., 2004. Monomeric Cu,Zn-superoxide dismutase is a common misfolding intermediate in the oxidation models of sporadic and familial amyotrophic lateral sclerosis. J Biol Chem. 279**,** 15499-504.

Rambold, A. S., et al., 2008. Stress-protective signalling of prion protein is corrupted by scrapie prions. EMBO J. 27**,** 1974-84.

Ramesh, T., et al., 2010. A genetic model of amyotrophic lateral sclerosis in zebrafish displays phenotypic hallmarks of motoneuron disease. Dis Model Mech. 3**,** 652-62.

Rangel, A., et al., 2007. Enhanced susceptibility of Prnp-deficient mice to kainate-induced seizures, neuronal apoptosis, and death: Role of AMPA/kainate receptors. J Neurosci Res. 85**,** 2741-55.

Ratte, S., et al., 2011. Threshold for epileptiform activity is elevated in prion knockout mice. Neuroscience. 179**,** 56-61.

Rauk, A., 2009. The chemistry of Alzheimer's disease. Chem Soc Rev. 38**,** 2698-715.

Reaume, A. G., et al., 1996. Motor neurons in Cu/Zn superoxide dismutase-deficient mice develop normally but exhibit enhanced cell death after axonal injury. Nat Genet. 13**,** 43-7.

Redler, R. L., Dokholyan, N. V., 2012. The complex molecular biology of amyotrophic lateral sclerosis (ALS). Prog Mol Biol Transl Sci. 107**,** 215-62.

Reinhard, C., et al., 2005. The amyloid-beta precursor protein: integrating structure with biological function. EMBO J. 24**,** 3996-4006.

Relano-Gines, A., et al., 2013. Prion replication occurs in endogenous adult neural stem cells and alters their neuronal fate: involvement of endogenous neural stem cells in prion diseases. PLoS Pathog. 9**,** e1003485.

Requena, J. R., Wille, H., 2014. The structure of the infectious prion protein: experimental data and molecular models. Prion. 8**,** 60-6.

Rial, D., et al., 2009. Cellular prion protein modulates age-related behavioral and neurochemical alterations in mice. Neuroscience. 164**,** 896-907.

Roberson, E. D., et al., 2007. Reducing endogenous tau ameliorates amyloid beta-induced deficits in an Alzheimer's disease mouse model. Science. 316**,** 750-4.

Rodriguez, F., et al., 2002a. Spatial memory and hippocampal pallium through vertebrate evolution: insights from reptiles and teleost fish. Brain Res Bull. 57**,** 499-503.

Rodriguez, J. A., et al., 2002b. Familial amyotrophic lateral sclerosis-associated mutations decrease the thermal stability of distinctly metallated species of human copper/zinc superoxide dismutase. J Biol Chem. 277**,** 15932-7.

Roesler, R., et al., 1999. Normal inhibitory avoidance learning and anxiety, but increased locomotor activity in mice devoid of PrP(C). Brain Res Mol Brain Res. 71**,** 349-53.

Rosenkranz, S. C., et al., 2013. Amyloid-precursor-protein-lowering small molecules for disease modifying therapy of Alzheimer's disease. PLoS One. 8**,** e82255.

Rossi, D., et al., 2001. Onset of ataxia and Purkinje cell loss in PrP null mice inversely correlated with Dpl level in brain. EMBO J. 20**,** 694-702.

Rothstein, J. D., et al., 1995. Selective loss of glial glutamate transporter GLT-1 in amyotrophic lateral sclerosis. Ann Neurol. 38**,** 73-84.

Saccon, R. A., et al., 2013. Is SOD1 loss of function involved in amyotrophic lateral sclerosis? Brain. 136, 2342-58.

Safar, J. G., et al., 2005. Prion clearance in bigenic mice. J Gen Virol. 86, 2913-23.

Sakaguchi, S., et al., 1995. Accumulation of proteinase K-resistant prion protein (PrP) is restricted by the expression level of normal PrP in mice inoculated with a mouse-adapted strain of the Creutzfeldt-Jakob disease agent. J Virol. 69, 7586-92.

Sakudo, A., et al., 2005. Octapeptide repeat region and N-terminal half of hydrophobic region of prion protein (PrP) mediate PrP-dependent activation of superoxide dismutase. Biochem Biophys Res Commun. 326, 600-6.

Santuccione, A., et al., 2005. Prion protein recruits its neuronal receptor NCAM to lipid rafts to activate p59fyn and to enhance neurite outgrowth. J Cell Biol. 169, 341-54.

Sarradin, P., et al., 2015. Transgenic Rabbits Expressing Ovine PrP Are Susceptible to Scrapie. PLoS Pathog. 11, e1005077.

Scheltens, P., et al., 2016. Alzheimer's disease. Lancet. 388, 505-17.

Schmitt-Ulms, G., et al., 2004. Time-controlled transcardiac perfusion cross-linking for the study of protein interactions in complex tissues. Nat Biotechnol. 22, 724-731.

Schmitz, M., et al., 2014a. Loss of Prion Protein Leads to Age-Dependent Behavioral Abnormalities and Changes in Cytoskeletal Protein Expression. Mol Neurobiol.

Schmitz, M., et al., 2014b. Impact of the cellular prion protein on amyloid-beta and 3PO-tau processing. J Alzheimers Dis. 38, 551-65.

Schwartz, P. J., et al., 1998. Effects of over- and under-expression of Cu,Zn-superoxide dismutase on the toxicity of glutamate analogs in transgenic mouse striatum. Brain Res. 789, 32-9.

Scott, A. C., et al., 1990. Bovine spongiform encephalopathy: detection and quantitation of fibrils, fibril protein (PrP) and vacuolation in brain. Vet Microbiol. 23, 295-304.

Scott, M., et al., 1989. Transgenic mice expressing hamster prion protein produce species-specific scrapie infectivity and amyloid plaques. Cell. 59, 847-57.

Selkoe, D. J., 2011. Resolving controversies on the path to Alzheimer's therapeutics. Nat Med. 17, 1060-5.

Sempou, E., et al., 2016. Activation of zebrafish Src family kinases by the prion protein is an amyloid-beta-sensitive signal that prevents the endocytosis and degradation of E-cadherin/beta-catenin complexes in vivo. Mol Neurodegener. 11, 18.

Shefner, J. M., et al., 1999. Mice lacking cytosolic copper/zinc superoxide dismutase display a distinctive motor axonopathy. Neurology. 53, 1239-46.

Small, D. H., et al., 1999. Neurite-outgrowth regulating functions of the amyloid protein precursor of Alzheimer's disease. J Alzheimers Dis. 1, 275-85.

Small, D. H., et al., 1994. A heparin-binding domain in the amyloid protein precursor of Alzheimer's disease is involved in the regulation of neurite outgrowth. J Neurosci. 14, 2117-27.

Soba, P., et al., 2005. Homo- and heterodimerization of APP family members promotes intercellular adhesion. Embo Journal. 24, 3624.

Solis, G. P., et al., 2013. Conserved roles of the prion protein domains on subcellular localization and cell-cell adhesion. PLoS One. 8, e70327.

Solomon, I. H., et al., 2010. Prion neurotoxicity: insights from prion protein mutants. Curr Issues Mol Biol. 12, 51-61.

Song, P., Pimplikar, S. W., 2012. Knockdown of amyloid precursor protein in zebrafish causes defects in motor axon outgrowth. PLoS One. 7, e34209.

Southwell, A. L., et al., 2013. A fully humanized transgenic mouse model of Huntington disease. Hum Mol Genet. 22, 18-34.

Spires, T. L., Hyman, B. T., 2005. Transgenic models of Alzheimer's disease: learning from animals. NeuroRx. 2, 423-37.

Stahl, N., et al., 1987. Scrapie prion protein contains a phosphatidylinositol glycolipid. Cell. 51, 229-40.

Stathopulos, P. B., et al., 2006. Calorimetric analysis of thermodynamic stability and aggregation for apo and holo amyotrophic lateral sclerosis-associated Gly-93 mutants of superoxide dismutase. J Biol Chem. 281, 6184-93.

Steele, A. D., et al., 2006. Prion protein (PrPc) positively regulates neural precursor proliferation during developmental and adult mammalian neurogenesis. Proc Natl Acad Sci U S A. 103, 3416-21.

Steele, A. D., et al., 2007. The prion protein knockout mouse: a phenotype under challenge. Prion. 1**,** 83-93.

Steinbach, J. P., et al., 1998. Hypersensitivity to seizures in beta-amyloid precursor protein deficient mice. Cell Death Differ. 5**,** 858-66.

Striebel, J. F., et al., 2013. Prion protein and susceptibility to kainate-induced seizures: genetic pitfalls in the use of PrP knockout mice. Prion. 7**,** 280-5.

Stys, P. K., et al., 2012. Copper-dependent regulation of NMDA receptors by cellular prion protein: implications for neurodegenerative disorders. J Physiol. 590**,** 1357-68.

Sun, Y., et al., 2001. Polyglutamine-expanded huntingtin promotes sensitization of N-methyl-D-aspartate receptors via post-synaptic density 95. J Biol Chem. 276**,** 24713-8.

Sunyach, C., et al., 2007. The C-terminal products of cellular prion protein processing, C1 and C2, exert distinct influence on p53-dependent staurosporine-induced caspase-3 activation. J Biol Chem. 282**,** 1956-63.

Takei, Y., et al., 2000. Defects in axonal elongation and neuronal migration in mice with disrupted tau and map1b genes. J Cell Biol. 150**,** 989-1000.

Tanzi, R. E., et al., 1988. Protease inhibitor domain encoded by an amyloid protein precursor mRNA associated with Alzheimer's disease. Nature. 331**,** 528-30.

Tarr, P. E., et al., 2002. Tyrosine phosphorylation of the beta-amyloid precursor protein cytoplasmic tail promotes interaction with Shc. J Biol Chem. 277**,** 16798-804.

Telling, G. C., et al., 1996. Interactions between wild-type and mutant prion proteins modulate neurodegeneration in transgenic mice. Genes Dev. 10**,** 1736-1750.

Telling, G. C., et al., 1995. Prion propagation in mice expressing human and chimeric PrP transgenes implicates the interaction of cellular PrP with another protein. Cell. 83**,** 79-90.

Thomas, E. D., et al., 2015. There and back again: development and regeneration of the zebrafish lateral line system. Wiley Interdiscip Rev Dev Biol. 4**,** 1-16.

Thomas, J. G., et al., 2013. Iatrogenic Creutzfeldt-Jakob disease via surgical instruments. J Clin Neurosci. 20**,** 1207-12.

Turk, E., et al., 1988. Purification and properties of the cellular and scrapie hamster prion proteins. Eur J Biochem. 176**,** 21-30.

Turner, B. J., Talbot, K., 2008. Transgenics, toxicity and therapeutics in rodent models of mutant SOD1-mediated familial ALS. Prog Neurobiol. 85**,** 94-134.

Urwin, P. J., et al., 2016. Creutzfeldt-Jakob disease and blood transfusion: updated results of the UK Transfusion Medicine Epidemiology Review Study. Vox Sang. 110**,** 310-6.

Van Cauwenberghe, C., et al., 2016. The genetic landscape of Alzheimer disease: clinical implications and perspectives. Genet Med. 18**,** 421-30.

van der Kant, R., Goldstein, L. S., 2015. Cellular Functions of the Amyloid Precursor Protein from Development to Dementia. Dev Cell. 32**,** 502-515.

Vázquez-Fernández, E., et al., 2016. The Structural Architecture of an Infectious Mammalian Prion Using Electron Cryomicroscopy. PLoS Pathog. 12**,** e1005835.

Walker, F. O., 2007. Huntington's disease. Lancet. 369**,** 218-28.

Walker, L. C., et al., 2013. Mechanisms of protein seeding in neurodegenerative diseases. JAMA Neurol. 70**,** 304-10.

Walsh, D. M., et al., 2002. Naturally secreted oligomers of amyloid beta protein potently inhibit hippocampal long-term potentiation in vivo. Nature. 416**,** 535-9.

Walsh, D. M., et al., 1997. Amyloid beta-protein fibrillogenesis. Detection of a protofibrillar intermediate. J Biol Chem. 272**,** 22364-72.

Walz, R., et al., 1999. Increased sensitivity to seizures in mice lacking cellular prion protein. Epilepsia. 40**,** 1679-1682.

Wang, P., et al., 2005. Defective neuromuscular synapses in mice lacking amyloid precursor protein (APP) and APP-Like protein 2. J Neurosci. 25**,** 1219-25.

Wang, Z., et al., 2009. Presynaptic and postsynaptic interaction of the amyloid precursor protein promotes peripheral and central synaptogenesis. J Neurosci. 29**,** 10788-801.

Ward, H. J., et al., 2006. Risk factors for variant Creutzfeldt-Jakob disease: a case-control study. Ann Neurol. 59**,** 111-20.

Watt, N. T., et al., 2012. Prion protein facilitates uptake of zinc into neuronal cells. Nat Commun. 3**,** 1134.

Watts, J. C., et al., 2014. Serial propagation of distinct strains of Abeta prions from Alzheimer's disease patients. Proc Natl Acad Sci U S A. 111, 10323-8.

Watts, J. C., Prusiner, S. B., 2014. Mouse models for studying the formation and propagation of prions. J Biol Chem. 289, 19841-9.

Weissmann, C., et al., 1994. Susceptibility to scrapie in mice is dependent on PrPC. Philos Trans R Soc Lond B Biol Sci. 343, 431-3.

Westergard, L., et al., 2011. A naturally occurring C-terminal fragment of the prion protein (PrP) delays disease and acts as a dominant-negative inhibitor of PrPSc formation. J Biol Chem. 286, 44234-42.

Whitehouse, I. J., et al., 2010. Prion Protein is Reduced in Aging and in Sporadic but not in Familial Alzheimer's Disease. J Alzheimers Dis. 22, 1023-1031.

Whitehouse, I. J., et al., 2013. Prion protein is decreased in Alzheimer's brain and inversely correlates with BACE1 activity, amyloid-beta levels and Braak stage. PLoS One. 8, e59554.

Wieser, H. G., et al., 2006. EEG in Creutzfeldt-Jakob disease. Clin Neurophysiol. 117, 935-51.

Will, R. G., et al., 1996. A new variant of Creutzfeldt-Jakob disease in the UK. Lancet. 347, 921-5.

Williams, E. S., Young, S., 1980. Chronic wasting disease of captive mule deer: a spongiform encephalopathy. J Wildl Dis. 16, 89-98.

Winklhofer, K. F., et al., 2008. The two faces of protein misfolding: gain- and loss-of-function in neurodegenerative diseases. EMBO J. 27, 336-49.

Wong, P. C., et al., 1995. An adverse property of a familial ALS-linked SOD1 mutation causes motor neuron disease characterized by vacuolar degeneration of mitochondria. Neuron. 14, 1105-16.

Wood, J. L., et al., 1997. Neuropathology of scrapie: a study of the distribution patterns of brain lesions in 222 cases of natural scrapie in sheep, 1982-1991. Vet Rec. 140, 167-74.

Yokoyama, T., et al., 2001. In vivo conversion of cellular prion protein to pathogenic isoforms, as monitored by conformation-specific antibodies. J Biol Chem. 276, 11265-71.

You, H., et al., 2012. Abeta neurotoxicity depends on interactions between copper ions, prion protein, and N-methyl-D-aspartate receptors. Proc Natl Acad Sci U S A. 109**,** 1737-42.

Young, R., et al., 2009. The prion or the related Shadoo protein is required for early mouse embryogenesis. FEBS Lett. 583**,** 3296-300.

Zahn, R., et al., 2000. NMR solution structure of the human prion protein. Proc Natl Acad Sci U S A. 97**,** 145-50.

Zanata, S. M., et al., 2002. Stress-inducible protein 1 is a cell surface ligand for cellular prion that triggers neuroprotection. EMBO J. 21**,** 3307-16.

Zeineddine, R., et al., 2015. SOD1 protein aggregates stimulate macropinocytosis in neurons to facilitate their propagation. Mol Neurodegener. 10**,** 57.

Zhang, B., et al., 2012. The microtubule-stabilizing agent, epothilone D, reduces axonal dysfunction, neurotoxicity, cognitive deficits, and Alzheimer-like pathology in an interventional study with aged tau transgenic mice. J Neurosci. 32**,** 3601-11.

Zheng, H., et al., 1995. beta-Amyloid precursor protein-deficient mice show reactive gliosis and decreased locomotor activity. Cell. 81**,** 525-31.

Zuccato, C., et al., 2001. Loss of huntingtin-mediated BDNF gene transcription in Huntington's disease. Science. 293**,** 493-8.

Chapter 2. Uncovering normal functions of APP and PrP by generating and characterizing zebrafish mutants[14]

---

[14] As mentioned in the Preface, Figure 2.15 and associated text have been previously published in:

Kaiser, D., et al., 2012. Amyloid beta precursor protein and prion protein have a
conserved interaction affecting cell adhesion and CNS development. PloS One. 7.

2.1 Summary

The normal biology of PrP^C and APP remain largely unexplored, despite years of intense study of the roles of their misfolded/aggregated forms in prion diseases and Alzheimer's disease, respectively. As some normal functions of these proteins are likely to be partially lost and/or subverted during the course of disease, understanding the normal physiology of these proteins will open up alternative therapeutic avenues for prion diseases and Alzheimer's disease. This chapter describes methods used to create and characterize genetic resources to study the normal physiology of PrP^C and APP, including tests of reagent specificity. Herein we generated zebrafish *prp1* and *appa* loss-of-function alleles as well as zebrafish compound *prp1$^{-/-}$; prp2$^{-/-}$* mutants and compound *prp1$^{-/-}$;appa$^{-/-}$* mutants. Zebrafish *prp1$^{-/-}$* and compound *prp1$^{-/-}$;prp2$^{-/-}$* mutants resemble mammalian *Prnp* knockouts insofar as they lack overt phenotypes, which surprisingly contrast reports of severe phenotypes when either *prp1* or *prp2* are transiently knocked down with morpholinos. Unexpectedly, *appa$^{-/-}$* and compound *prp1$^{-/-}$;appa$^{-/-}$* mutants also lacked overt phenotypes, but were smaller than wild type fish at some developmental stages. *prp1$^{-/-}$* mutants, however, were more sensitive to *appa* knockdown than wild type fish, and both *prp1* and mammalian *Prnp* mRNA could rescue this effect. Taken together, these results support a genetic interaction between *prp1* and *appa*, and they also support specificity of the mutant phenotypes.

2.2 Introduction

PrP loss-of-function is a likely contributor to prion disease progression, and loss of PrP and APP function are likely culprits in Alzheimer's disease (AD), thus it is important to understand their normal physiological functions to devise effective disease therapies. As reviewed in Chapter 1, there are many putative functions of PrP and APP but the molecular mechanisms underlying these functions and their *in vivo* relevance remain unresolved. Identification of normal *in vivo* functions of both PrP and APP has been thwarted by the lack of overt phenotypes in *Prnp* and *App* knockout mice (Bueler et al., 1992; Manson et al., 1994; Muller et al., 1994; Zheng et al., 1995), highlighting the need for alternative *in vivo* systems and methods. Zebrafish are emerging as genetically tractable disease models and can be used to complement studies performed in other

model organisms such as rats and mice (reviewed in (Lieschke and Currie, 2007)). Zebrafish are an attractive model organism because they reproduce in large numbers, have a sequenced and annotated genome and can be deployed in high throughput drug screens. Further, the overall brain structure and neurotransmitter systems are conserved between fish and mammals (Norton and Bally-Cuif, 2010; Panula et al., 2010; Rodriguez et al., 2002a). Here we used zebrafish as an alternative *in vivo* model to study the normal physiology of PrP and APP.

2.2.1 Zebrafish to uncover functions of PrP^C and APP

Previous studies in zebrafish have helped to uncover conserved *in vivo* functions of both APP and PrP. Both proteins have roles in development, which may be masked by gene compensation in mammals, as well as conserved neuroprotective functions. Transient knockdown of *prp1* with a high dose of *prp1* morpholino (MO) was found to arrest development during gastrulation (Malaga-Trillo et al., 2009), and at a lower dose caused developmental delay, CNS malformations and apoptosis (Kaiser et al., 2012). These phenotypes could be reversed through ectopic delivery of zebrafish and mammalian *Prnp* mRNA (Kaiser et al., 2012; Malaga-Trillo et al., 2009). Similarly, *prp2* morphants had differential expression of genes linked to apoptosis, neurogenesis and embryonic development (Nourizadeh-Lillabadi et al., 2010) and exhibited developmental deficits (Kaiser et al., 2012; Malaga-Trillo et al., 2009; Nourizadeh-Lillabadi et al., 2010). However, ectopic delivery of *prp2* mRNA could not rescue these developmental phenotypes (Kaiser et al., 2012; Malaga-Trillo et al., 2009), which means that the morpholino lacks specificity. Further, both of the zebrafish *APP* homologs (*appa* and *appb*) are upregulated in hypoxic conditions (Moussavi Nik et al., 2012), and *appa* is upregulated after chronic low-level domoic acid exposure (Hiolski et al., 2014), suggesting that *APP* is protective in conditions of stress. Transient acute knockdown of *appa* (Kaiser et al., 2012) and *appb* (Joshi et al., 2009; Kaiser et al., 2012; Song and Pimplikar, 2012) lead to CNS cell death (Kaiser et al., 2012) and developmental defects (rescued with various *APP* mRNAs (Joshi et al., 2009; Kaiser et al., 2012)), which were suggested to be due to defects in the convergent extension process (Joshi et al., 2009).

Zebrafish studies have also revealed that PrP and APP participate in cell adhesion *in vivo*. *Prp1* knockdown has revealed a role for *prp1* in mediating cell adhesion through E-

cadherin and Src kinases (Malaga-Trillo et al., 2009; Sempou et al., 2016; Solis et al., 2013). Using morpholino gene knockdown, we found that *prp1* and *appa* have synergistic roles in neuroprotection and cell adhesion (Kaiser et al., 2012). Transient loss of *appb* has produced neuromuscular deficits reminiscent to what was observed in conditional *APP* knockout mice and $APP^{-/-};APLP2^{-/-}$ mice (Wang et al., 2005; Wang et al., 2009). Specifically, loss of *appb* produced motor neuron defects that were rescued with zebrafish *appb* mRNA (Abramsson et al., 2013; Song and Pimplikar, 2012), including reduced neurite and growth cone size, disorganization of axon cytoskeletons (Song and Pimplikar, 2012), irregular patterning, and alteration in pre-and post-synaptic densities at neuromuscular junctions (Abramsson et al., 2013). Recently, it was found that *appb* is important for the development of Mauthner cells- the cells responsible for the characteristic C-bend escape response. Mauthner cells failed to develop on one or both sides of the body in *appb* morphants and this effect was partially rescued with *appb* mRNA. *Appb* morphants also had an increase in transcripts involved in Notch signalling (*notch 1a* and *her6*), and inhibition of Notch signalling partially restored Mauthner cell number (Banote et al., 2016). Taken together, these results suggest that *appb* participates in neurogenesis by negatively regulating Notch signalling.

While gene knockdown experiments described above have suggested several *in vivo* functions of APP and PrP, limitations of morpholino studies prompted us to consider alternative loss-of-function methods, outlined below. Morpholino knockdown is transient, with the timeframe of gene knockdown dependent on the morpholino, as well as the transcript and protein kinetics of the target. Thus it is only possible to study loss of function phenotypes for the first few days of development (Huang et al., 2012). Morpholinos may also have off-target effects that are often due to activation of the p53 cell death pathway. While this problem can be partially overcome by injecting *tp53* morpholino, it hinders the study of genes involved in the p53 pathway (Robu et al., 2007). A number of demanding control experiments are also required to confirm the efficacy and specificity of each injected morpholino (Eisen and Smith, 2008).

2.2.2 Reverse Genetic Techniques in Zebrafish

The pitfalls of morpholinos outlined above led us to consider reverse genetic tools that would enable us to produce heritable loss of gene function. Reverse genetic tools for

zebrafish began emerging in the early 2000s- first with TILLING (Targeting Induced Local Lesions IN Genomes) (Wienholds et al., 2002) and later with Tol 2 transposon mediated gene-trap screens (Kawakami et al., 2004). In TILLING, mutations are randomly introduced into a large population of zebrafish using chemical (ENU) mutagenesis, and mutations are identified in target genes using technologies such as NEXT generation sequencing. With Tol2 gene trapping, a marker (eg. GFP) is randomly introduced into the genome and sometimes integrates into the target gene causing loss of gene function (reviewed in (Huang et al., 2012)). These approaches are not practical for an average-sized zebrafish laboratory because large amounts of space and dedicated personnel are needed to screen for fish with desirable mutations. Targeted mutagenesis techniques in zebrafish, in which the mutation site is pre-selected rather than random, emerged in 2008 with the development and application of zinc finger nucleases (ZFNs) (Doyon et al., 2008; Meng et al., 2008), and the toolbox has expanded to include transcription activator-like effector nucleases (TALENs) (Huang et al., 2011; Sander et al., 2011) and most recently Clustered Regularly Interspaced Short Palindromic Repeats (CRISPRs) (Chang et al., 2013; Hwang et al., 2013). I used a TALEN mutagenesis approach because it had become an accessible gene-targeting technique for average-sized zebrafish laboratories by the midpoint of my PhD program and I had experienced difficulty with my earlier attempts to generate zebrafish mutants using ZFNs.

ZFNs and TALENs are similar in that they are both composed of a DNA binding domain fused to the cleavage domain of FokI (a restriction enzyme from *Flavobacterium okeanokoites*) (Kim et al., 1996; Miller et al., 2011; Porteus and Carroll, 2005), and they work as dimers to induce double stranded breaks in targeted DNA segments. Repair of breaks through the non-homologous end joining introduces small insertions and deletions, which lead to frameshifts and putative truncated proteins (Miller et al., 2011; Porteus and Carroll, 2005) and are stably inherited. ZFNs and TALENs differ in their binding domains. The binding domain of each member of a ZFN pair typically consists of three Cys_2His_2 zinc finger domains fused together, and each zinc finger interacts with a triplet of DNA. One drawback of zinc finger nucleases is that the individual fingers do not always function independently, thus binding efficiency is context dependent (i.e. binding efficiency varies based on neighbouring zinc fingers and neighbouring DNA

sequence). Thus it is necessary to empirically identify efficient zinc finger arrays, and not all DNA segments are amenable to efficient ZFN cleavage (Hurt et al., 2003). The binding domains of TALENs are derived from Transcription Activator-Like effectors of the *Xanthomonas* bacteria genus. In nature, these proteins cause disease in plants by mimicking plant transcription factors (Boch et al., 2009). The binding domain of a TALEN is composed of tandem repeats (~34 residues each) that individually recognize a single nucleotide. The last two residues in each repeat are variable (known as repeat variable diresidues or RVDs) and specify which nucleotide is recognized. Thus the number of repeats and the RVD make-up determines what DNA sequence is targeted (Bogdanove and Voytas, 2011). The modular nature of the TALEN binding domain makes it simpler to identify appropriate target sites for TALENs than it is to find target sites for ZFNs (Bogdanove and Voytas, 2011). There is also some evidence to suggest that TALENs have a higher mutagenesis rate (Chen et al., 2013) and have fewer off-target effects than ZFNs (Mussolino et al., 2011).

2.2.3 Aims and Hypotheses

Our aim herein was to deploy targeted mutagenesis to generate *prp1* mutants and compound *prp1/prp2* mutants, since others in the Allison lab had already generated a *prp2* mutant line (Fleisch et al., 2013), which we characterize further in Chapters 3-5. *Prp2* mutants lack overt phenotypes, which led us to speculate that some redundancy with *prp1* could be masking phenotypes. We also aimed to generate *appa* mutants since the function of *appa* remained largely unexplored and we had previously identified a specific genetic interaction between *appa* and *prp1* (Kaiser et al., 2012). We successfully generated multiple lines of *prp1*$^{-/-}$ and *appa*$^{-/-}$ fish with frameshift mutations, but mutating these genes did not produce overt phenotypes. The *prp1* alleles were designated University of Alberta (ua)5003 and ua5004 and had an 8bp deletion and a 19bp deletion, respectively. The *appa* alleles were designated ua5005 (8bp deletion), ua5006 (5bp deletion), ua5007 (5bp deletion) and ua5008 (1 bp insertion). We also did not observe the same phenotype in *appa*$^{ua5005/ua5005}$; *prp1*$^{ua5003/ua5003}$ fish as we had previously observed with co-knockdown of *appa* and *prp1* (Kaiser et al., 2012). We did find, however, that *prp1*$^{-/-}$ mutants are more sensitive to acute loss of *appa* (through morpholino gene knockdown) than *appa*$^{+/+}$ fish. Taken together, this data supports the hypothesis that a

specific genetic interaction exists between *appa* and *prp1,* and that gene compensatory mechanisms are occurring in *appa*^{-/-} and *prp1*^{-/-} fish.

2.3 Methods

2.3.1 Animal Ethics and Zebrafish Husbandry

Zebrafish were raised and maintained using protocols approved by the Animal Care & Use Committee: Biosciences at the University of Alberta, operating under the guidelines of the Canadian Council of Animal Care. The fish were raised and maintained within the University of Alberta fish facility at 28°C under a 14/10 light/dark cycle as previously described (Westerfield, 2000).

2.3.2 Targeted mutagenesis

Targeted mutagenesis was performed on the zebrafish *appa* gene (NCBI NC_007112, ZFIN ZDB-GENE-000616-13) and the *prp1* gene (Ensemble ENSDARG00000044048, ZFIN ZDB-GENE-041221-2) using TALENs. We previously generated and optimized ZFNs to target *prp1* (Pillay et al., 2013), but were unable to identify stably inherited *prp1* loss-of-function alleles using that method. The target sequences within *appa* and *prp1* genes are shown in Figure 2.1A and 2.1B, respectively, and a flowchart summarizing the steps involved in the targeted mutagenesis process is shown in Figure 2.1C. AB strain zebrafish were used unless otherwise noted. Wild type control fish were closely related to the mutant fish in the study, but were not siblings unless otherwise stated.

2.3.2a Production of TALEN plasmids

Custom TAL blocks[TM] and heterodimeric backbone plasmids were ordered from Transposagen (Lexington, KY, USA; http://www.transposagenbio.com). The backbone contains the first half site of the DNA binding domain, the sequence that recognizes the final base of the target site, and the FokI cleavage domain. The TAL blocks, which contain the remainder of the DNA binding domain, were assembled via Transposagen's FLASH build process. After digestion with BsmBI (NEB catalogue #R0580S, Ipswich, MA, USA), the vectors were purified using an Agencourt AMPure XP - PCR Purification kit (Beckman Coulter catalogue #A63880, Indianapolis, IN, USA). The custom TAL blocks[TM] of the forward TALENs were then ligated into the appropriate vectors (JDS 84

KKR heterodimer with HD to recognize the final guanine in the *appa* target sequence; JDS 82 KKR heterodimer with NN to recognize the final cytosine in the *prp1* target sequence) with T4 ligase (Invitrogen/ Thermo Fisher Scientific catalogue #15224-017, Waltham, MA, USA) and transformed them into Stbl3 cells (Invitrogen/Thermo Fisher Scientific catalogue #C7373-03, Waltham, MA,USA). Due to changes in Transposagen's manufacturing process, the *prp1* reverse and *appa* reverse TAL blocks^TM were provided by Transposagen as pre-ligated plasmids. Colony PCR was performed to screen for colonies with the correct number of repeats (Figure 2.2), and those yielding PCR products of the appropriate length were sequenced to ensure that they contained the correct TALEN sequence (see Table 2.1 for primer sequences, sequencing performed by the University of Alberta's Molecular Biology Service Unit). Clones with the full TALEN sequence were then prepared using a Plasmid Maxiprep kit (Qiagen catalogue #12163, Toronto, ON, Canada).

A. *appa* target site

Start codon

ATGCGGTCGAGGGAGCTCTTCATATTACTGATGGCCGTCGCGTCGACGCTCGCGGTGGAGGTAAGAAAACGA

M R S R E L F I L L M A V A S T L A V E

appa CDS

Forward TALEN | Cut site | Reverse TALEN

B. *prp1* target site

Start codon

ATGGGGGAGTTATGCAAACTTCTAGCCATCGTTTTTGGTTTTGATGGCAGTGTTACATTATAC

M G E L C K L L A I V L V L M A V L H Y T

prnprs1 CDS

Forward TALEN | Cut site | Reverse TALEN
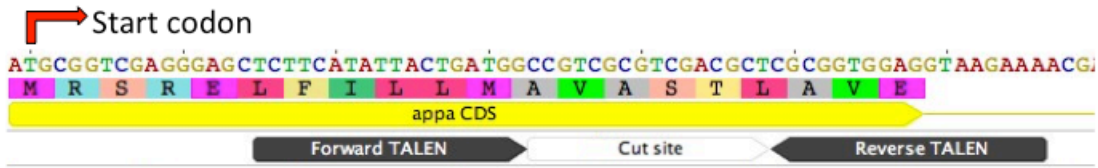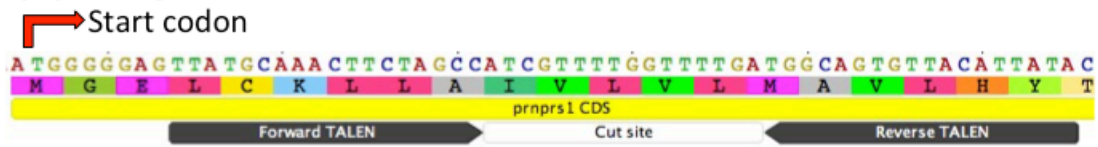
C. Overview of TALEN targetted mutagenesis

Prepare TALEN plasmids (Section 2.3.2a)

↓

Prepare TALEN mRNA and deliver mRNA to 1-cell stage zebrafish embryos (Section 2.3.2b)

↙   ↘

Screen F_0 generation embryos for somatic insertion/deletion mutations (Section 2.3.2c)

Grow up F_0 generation siblings and in-cross (Section 2.3.2c)

↓

Screen F_1 embryos to identify F_0 germline carriers (Section 2.3.2c)

↓

Grow up siblings of those F_1 fish that have in/del mutations (Section 2.3.2d)

↓

Screen F_1 fish fin-clips to identify heterozygous mutants; outcross mutants (Section 2.3.2d)

↓

Grow up, in-cross and genotype F_2 generation to obtain homozygous mutants (Section 2.3.3)

Figure 2.1. Regions near the translation start site of both *prp1* and *appa* were targeted using TALENs

A. TALEN forward and reverse binding sites for targeted mutagenesis of *appa* are shown relative to the translation start site. (red arrow). The red arrow indicates the translation start site. **B**. TALEN forward and reverse binding sites for targeted mutagenesis of *prp1* are shown relative to the translation start site. **C.** Flow-chart detailing the steps undertaken to generate stably inherited loss-of-function *appa* and *prp1* alleles.

A. Colony PCR: forward *appa* TALEN
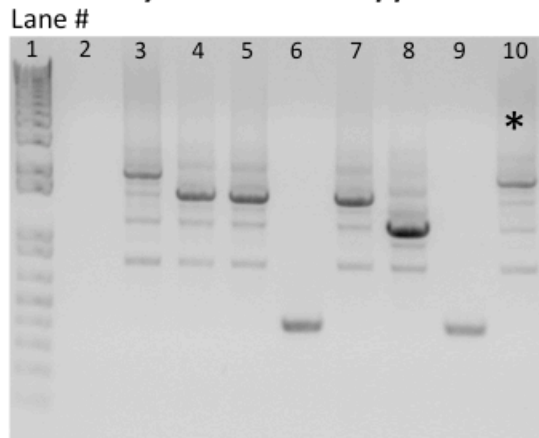
Lane #

B. Colony PCR: forward *prp1* TALEN
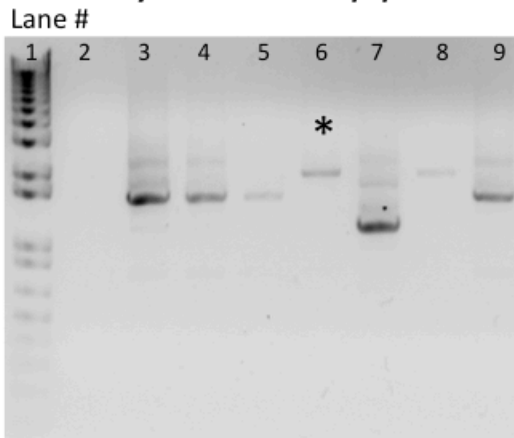
Lane #

C. Colony PCR: reverse *appa* and *prp1* TALENs
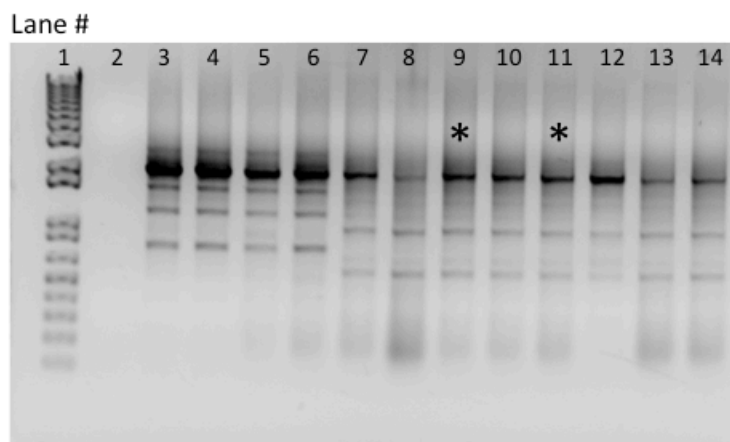
Lane #

Figure 2.2. Colony PCR for creating TALEN vectors

Constructs containing the correct insert yielded 2.1 kb PCR products (DNA ladder is shown in Lane 1 of each gel). A laddering effect was apparent in most cases because of the repetitive nature of the TALEN nucleotide sequence. **A.** *appa* forward TALEN PCR-products. The construct from lane 10, marked with an asterisk, was sequenced and found to contain the correct insert. **B.** *prp1* forward TALEN PCR-products. The construct used to produce the PCR product in lane 6, marked with an asterisk, was sequenced and found to contain the correct insert. **C.** *appa* reverse and *prp1* reverse TALEN PCR-products. The plasmids that yielded the bands in lanes 9 and 11 were sequenced and found to contain the correct inserts for the *appa* and *prp1* reverse TALENs, respectively.

Table 2.1. Primers used to engineer *prp1 and appa* TALENs

Assay	Primers
Colony PCR screening	Forward primer: 5'-AGT AAC AGC GGT AGA GGC AG-3' Reverse primer: 5'-TTA ATT CAA TAT ATT CAT GAG GCA C-3'
Sequencing	Forward primer: 5'-AGT AAC AGC GGT AGA GGC AG-3' Reverse primer 1: 5'-ATT GGG CTA CGA TGG ACT CC-3' Reverse primer 2: 5'-TTA ATT CAA TAT ATT CAT GAG GCA C-3'

2.3.2b Delivery of TALEN mRNA to zebrafish embryos

mRNA was synthesized from maxi-prepped plasmid DNA that had been linearized with Fast digest MssI (Thermo Fisher Scientific catalogue #FD1344, Waltham, MA, USA) and purified by ethanol precipitation. Briefly, 1 uL of 0.5 M EDTA pH 8, 2 uL 3M sodium acetate and 40 uL of 100% ethanol were added to the linearized plasmid and frozen overnight at -80°C. Linearized plasmid was then centrifuged for 15 minutes at 13 000 RPM at 4°C and the supernatant was removed. The pellet was then suspended in 6 µL of nuclease free water. mRNA was synthesized using the mMESSAGE mMachine T7 Ultra Kit (Invitrogen/Thermo Fisher Scientific catalogue #AM1345, Waltham, MA, USA) including the polyA tailing reaction as per manufacture's protocol. 100 pg each of *prp1* forward and reverse TALENs were injected into AB strain wild type zebrafish embryos, or 150 pg each of *appa* forward and reverse TALENs into the yolk of AB strain wild type zebrafish embryos or embryos homozygous for the *appa* is22gt allele ((Liao et al., 2012) Zfin ID: ZDB-ALT-120328-1). Fish with the *appa* is22gt allele have a gene trap insertion in intron 4 that disrupts splicing and causes an RFP coding sequence with a stop codon to be fused to the coding sequence for most of the N-terminus of appa (Liao et al., 2012). The is22gt allele is not expected to be a null allele because the N-terminus of the protein is present and some full-length transcript is produced (Liao et al., 2012); hence we sought to create fish with null alleles using TALENS. 25 pg of *egfp* mRNA was co-injected with the TALEN mRNA so that fish that were successfully injected could be identified and raised to adulthood. *egfp* mRNA was produced from pCS2+*egfp* by first linearizing the plasmid with Fast digest NotI (Thermo Fisher Scientific catalogue

#FD0593, Waltham, MA, USA) and then transcribing mRNA using the mMESSAGE MMachine SP6 Kit (Invitrogen/Thermo Fisher Scientific catalogue #AM1340, Waltham, MA, USA).

2.3.2c Detection of larvae with somatic and germline mutations in *prp1* and *appa*

The first step in our analyses of TALEN-effectiveness was determining whether TALENs induced somatic mutations in injected (F0 generation embryos). Siblings of successfully mutated F0 fish were grown to adulthood. F0 fish were then bred and pools of F1 generation embryos were screened for successful germline transmission of TALEN-induced mutations. For detection of both somatic and germline-transmitted mutations in embryos, genomic DNA was isolated from pools of test fish (injected F0 embryos for detection of somatic mutations, or offspring of F0 embryos for detection of germline-transmitted mutations) or un-injected wild type AB strain fish at either 24 hpf or 3 dpf using a protocol modified from (Meeker et al., 2007). Briefly, samples (pools of up to 20 embryos) were boiled for 15 minutes in 50 mM NaOH (5 uL/embryo), cooled on ice for 5 minutes and neutralized with 1 M Tris-HCl,pH 8 (0.5 uL/embryo). Genomic DNA was then diluted tenfold in sterile Milli-Q water prior to High Resolution Melt (HRM) analysis. Diluted genomic DNA was amplified using HRM primers (Table 2.2) and MeltDoctor™ HRM Master Mix (Thermo Fisher Scientific catalogue #4415440, Waltham, MA, USA). HRM data was generated using the Applied Biosystems 7500 Fast Real-Time PCR System with MeltDoctor™ HRM Master Mix. Data was then analyzed using the High ReSolution Melt (HRM) Software (Version 2.0, High ReSolution Melt, Thermo Fisher Scientific, Waltham, MA, USA).

Table 2.2. Primers for screening for TALEN mutations and genotyping *appa, prp1, and prp2* mutants

Assay	Gene	Primers
HRM Analysis	*prp1*	Forward: 5'-TGT TAG GAC CAA AAT GGG GGA G-3' Reverse: 5'-GAA CAG TCT TGC TTA CAG TGC C-3'
	Appa	Forward: 5'-GAA GCA TGC GGT CGA GGG AG-3' Reverse: 5'-TTT TCT TAC CTC CAC CGC GAG C-3'
RFLP Analysis	*Appa*	Forward: 5'-GAA GCA TGC GGT CGA GGG AG-3' Reverse: 5'-GCG TTT ACC ACC ACC GAC ACT C-3'
	prp2	Forward: 5'-TCC CCT GGA AAC TAT CCT CGC CAA C-3' Reverse: 5'-TGGGTTAGAGCCTGCTGGTGG-3'
Generate PCR Amplicon for Topo Cloning or Direct sequencing	*prp1*	Forward: 5'- AGC ATT CTC CAT TAG ACC TGT-3' Reverse 5'-CTG CTG GTT AGG GTA GCC TG-3'
	Appa	Forward: 5'-TGT TCT CCG TTT GCT CCT CC-3' Reverse: 5'-ATG TAA CGC TGA TGT AAC GCG G-3'
	prp2	Forward: 5'-ATG GGT CGC TTA ACA ATA CTA TTG-3' Reverse: 5'-CCA TTC ATG TTA CCG TCA GG-3'

    Upon identification of pools of genomic DNA with a distinct melt profiles (for example see Figure 2.4B) compared to un-injected wild type AB strain samples, those pools (and wild type control pools) were PCR-amplified with amplicon primers (Table 2.2) and cloned into the pCR2.1 Topo vector as per the instructions in the TOPO TA cloning kit (Invitrogen/Thermo Fisher Scientific catalogue #K4500-01, Waltham, MA, USA). Clones were dissolved in 25µL sterile Milli-Q water for HRM analysis, and a portion of each clone was streaked on agar plates for subsequent analysis. Clones with a different melt profile compared to control clones were mini-prepped with a Qiaprep Spin Miniprep Kit (Qiagen catalogue #27106, Toronto, ON, Canada) and submitted to the U of A's Molecular Biology Service Unit for sequencing.

2.3.2d Identification of adult F1 generation fish that are heterozygous for TALEN-induced mutations in *appa* or *prp1*

Siblings of F1 embryos that had germline transmitted TALEN mutations were grown to adulthood. These adult F1 fish were then screened to identify carriers of TALEN mutations. Fish were anaesthetized with 4.1% tricaine and a small piece of caudal fin was harvested. Genomic DNA extraction was performed as above, but with 15 uL of 50 mM NaOH and 1.5uL Tris-HCl per sample. DNA was diluted either twenty-fold or thirty-fold in sterile Milli-Q water prior to HRM analysis. A PCR product (primers shown in Table 2.2) containing the target site was amplified from genomic DNA and was cloned into the pCR2.1 Topo vector using a TOPO TA cloning kit (Invitrogen/ Thermo Fisher Scientific catalogue #K4500-01, Waltham, MA, USA). The construct was then mini-prepped with a Qiaprep Spin Miniprep kit (Qiagen catalogue #27106, Toronto, ON, Canada) and sequenced using a T7 primer sequence within the vector (5'-TAA TAC GAC TCA CTA TAG GG-3').

2.3.3 Genotyping

2.3.3a HRM to identify fish heterozygous for the ua5003 allele

Once stably inherited alleles had been identified (see Methods above and Results below), methods were developed for genotyping individual fish. Genomic DNA was amplified using HRM as described above. Sample melt curves are shown in Figure 2.3A. Genotyping via HRM was performed in a two-step process because genomic DNA from wild type and *prp1*$^{ua5003/ua5003}$ fish had overlapping melt profiles. Thus heterozygous individuals could be discriminated from homozygous individuals, but homozygous fish were not clearly mutant or wild type. In the second round of HRM, 0.5 uL of sample genomic DNA was spiked with 0.5 uL of known DNA (wild type or homozygous mutant) and diluted twenty-fold in sterile Milli-Q water. The accuracy of this method was confirmed by sequencing the area around the target site. Briefly, a 453 base pair region around the target site was amplified (Primers in Table 2.2). The amplicon was either cloned into pCR2.1, followed by sequencing of mini-prepped plasmid with a T7 vector specific primer (5'-TAA TAC GAC TCA CTA TAG GG-3') or the PCR-product was treated with Illustra ExoProstar (Sigma catalogue #US78210, St. Louis, MO, USA) as

specified in the manufacturer's instructions, and directly sequenced using the same primers used to generate the amplicon.

2.3.3b HRM to identify fish heterozygous for the ua5004 allele

One round of HRM (Primers listed in Table 2.2) was used to genotype fish for ua5004 using methods described above. Sample melt curves are shown in Figure 2.3B. As for the ua5003 allele (section immediately above), the validity of this method was verified via sequencing.

2.3.3c RFLP to detect fish heterozygous and homozygous for the ua5001 allele

For ease of genotyping fish with the *prp2*^*ua5001* allele previously isolated (Fleisch et al., 2013), an RFLP assay was developed. Genomic DNA was amplified using *prp2* RFLP primers (Table 2.2), and then digested with Fast Digest Mva I (Thermo Fisher Scientific, catalogue #FD0554, Waltham, MA, USA). As the ua5001 mutation disrupted the Mva I cut site, PCR products from mutant and wild type DNA produced different banding patterns on an Ethidium bromide agarose gel (wild type allele yields 3 bands with sizes of 21, 36 and 54 base pairs; ua5001 allele yields 2 bands with sizes of 36 and 71 base pairs; Figure 2.3C). The accuracy of this genotyping assay was confirmed by sequencing. Briefly, a 1039 base pair region around the target site was amplified (Primers in Table 2.2), and sequenced using the same primers used to generate the amplicon after treatment with Illustra ExoProstar (Sigma catalogue #US78210, St. Louis, MO, USA) to remove unincorporated nucleotides.

2.3.3d Restriction fragment length polymorphism (RFLP) to detect fish heterozygous and homozygous for the ua5005 allele of *appa*

Following identification/validation of the mutation present in the *appa*^*ua5005* allele, an RFLP assay was developed to ease genotyping. Genomic DNA was amplified using *appa* RFLP primers (Table 2.1), and then digested with Fast Digest Taq I (Thermo Fisher Scientific catalogue #FD0674, Waltham, MA, USA). As the ua5005 mutation disrupted the TaqI cut site, PCR products from mutant and wild type DNA produced different banding patterns on an Ethidium bromide agarose gel (wild type allele yields 4 bands with sizes of 12, 36, 102 and 255 nucleotides; ua5005 allele yields bands 3 bands with

sizes of 12, 102, and 283 nucleotides; Figure 2.3D). The accuracy of this genotyping assay was confirmed by sequencing. Briefly, a 461 base pair region around the target site was amplified (Primers in Table 2.2), and sequenced using the same primers used to generate the amplicon after treatment with Illustra ExoProstar (Sigma catalogue #US78210, St. Louis, MO, USA) to remove unincorporated nucleotides.
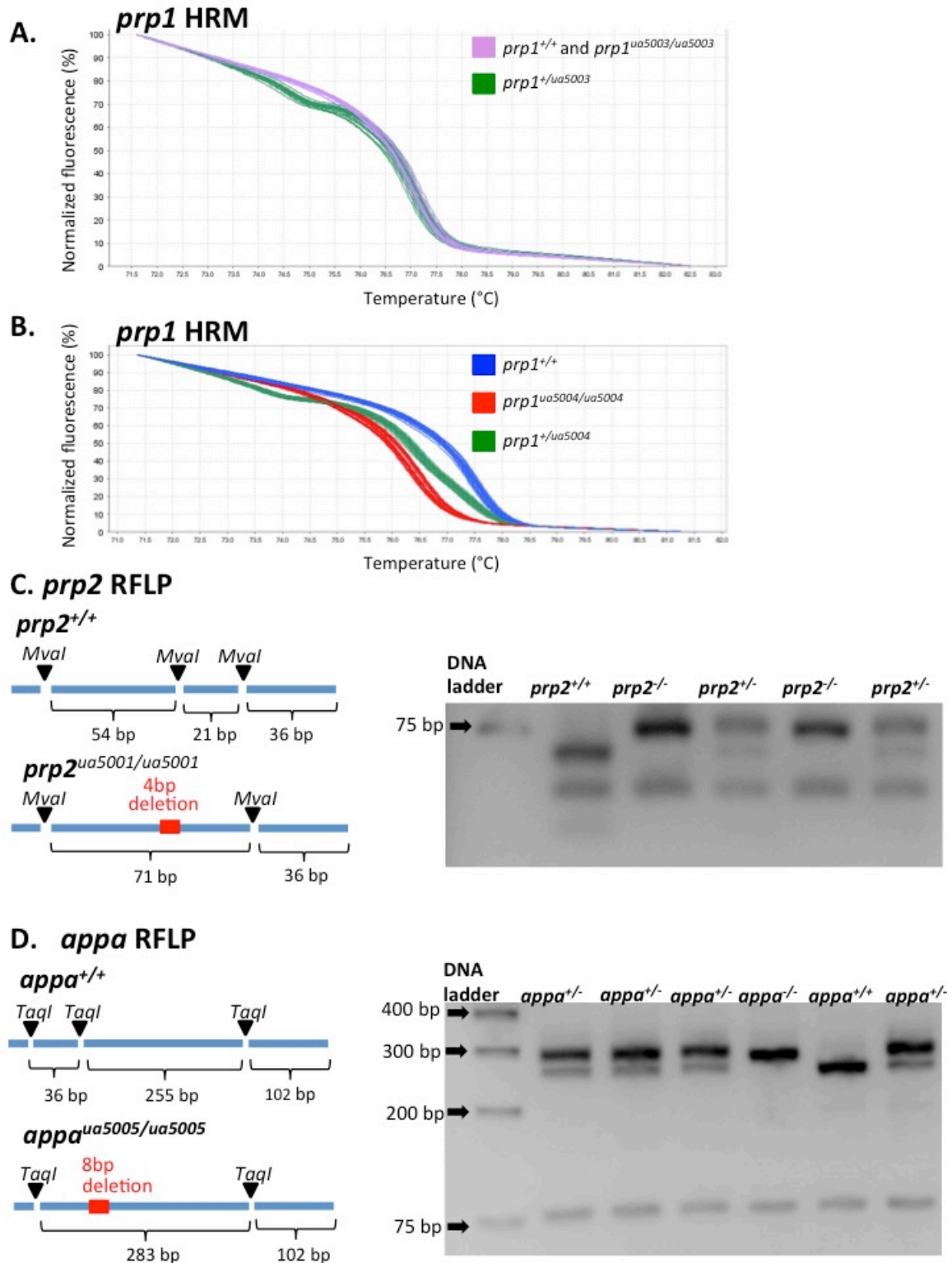
Figure 2.3. Genotyping assays for the *prp1 ua5003* and *ua5004* alleles, the *prp2 ua5001* allele and the *appa ua5005* allele

A. HRM analysis can be used to distinguish $prp1^{+/ua5003}$ fish (green curves) from fish that are either $prp1^{+/+}$ or $prp1^{ua5003/ua5003}$ (magenta curves), but it cannot distinguish the latter two homozygous states. One technical replicate each from three fish was excluded because they did not overlap with the other two replicates. Melt curves from 17 fish (3 technical replicates/fish) are shown here. **B.** $prp1^{+/+}$ fish (blue curves), $prp1^{+/ua5004}$ (green curves), and $prp1^{ua5004/ua5004}$ (red curves) each have unique HRM melt profiles. One technical replicate from one fish was excluded because it did not match the other two replicates. Melt curves from 20 fish (3 technical replicates/fish) are shown here. **C.** Restriction fragment length polymorphism (RFLP) to identify $prp2^{+/ua5001}$ and $prp2^{ua5001/ua5001}$ fish. Left panel: The restriction enzyme, *MvaI,* cuts the PCR product from a wild type template into 54 base pair (bp), 21 bp and 36 base pair fragments. The *prp2 ua5001* allele lacks one of the *MvaI* cut sites, so 71 bp and 36 bp bands are visible instead. Right panel: Example *prp2* PCR products cut with *MvaI* and separated on an agarose gel. **D.** RFLP to identify $appa^{+/ua5005}$ and $appa^{ua5005/ua5005}$ fish. Left panel: The restriction enzyme, *TaqI,* cuts the PCR product from a wild type template into 36 base pair (bp), 255 bp and 102 base pair fragments. The *appa ua5005* allele lacks one of the *TaqI* cut sites, so 283 bp and 102 bp bands are visible instead. Right panel: Example *appa* PCR products cut with *TaqI* and separated on an agarose gel.

2.3.4 Measurement of transcript abundance

2.3.4a. In situ hybridization to detect *appa*

2.3.4ai. Riboprobe production

Riboprobe was produced from a plasmid containing a 2069 base pair fragment of *appa* cDNA (NCBI Accession number JQ994487) that was cloned into the pCS2+ vector as described in (Kaiser et al., 2012). This plasmid was linearized with Fast Digest Hind III (Thermo Fisher Scientific catalogue #FD0504, Waltham, MA, USA) and purified using ethanol precipitation. Briefly, 1 uL of 0.5 M EDTA pH 8, 2 uL 3M sodium acetate and 40 uL of 100% ethanol were added to the linearized plasmid and frozen overnight at -80°C. Linearized plasmid was then centrifuged for 15 minutes at 13 000 RPM at 4°C and the supernatant was removed. The pellet was air dried, resuspended in 10 uL of 0.1 M Tris, (pH 8.5) and used to template production of DIG-labeled antisense riboprobe. To do this, 2 μL of DIG RNA labeling mix (Roche catalogue #11277073910, Basel, Switzerland), 2 μL of 10X transcription buffer (supplied with the T3 enzyme), 1 μL of RNase inhibitor (Roche catalogue # 03335399001, Basel, Switzerland), 2 μL of T3 RNA polymerase (Roche catalogue #11031171001, Basel, Switzerland) and 3 μL nuclease free water were added to the linearized *appa* plasmid DNA and incubated overnight at 37°C. Following this, 2 μL of 0.2M EDTA, 1 μL of glycogen, 2.5 μL of 4.0M LiCl and 75 μL of 100% ethanol were added, and the mixture was kept at -80°C overnight to precipitate the riboprobe. The mixture was centrifuged at 13 000 RPM for 15 minutes at 4°C. The pellet was then washed with 70% ethanol/ 30% diethyl pyrocarbonate (DEPC)-treated water and centrifuged at 13 000 RPM for 20 minutes. After removing the ethanol, the pellet was air dried for 5 minutes and resuspended in 25 μL of nuclease-free water. The riboprobe was quantified using a Nanodrop 2000 spectrophotometer (Thermo Scientific) and its quality and size were assessed by combining a sample of the probe with 2x RNA loading dye (Thermo Fisher Scientific catalogue #R0641, Waltham, MA, USA), heating it to 70°C, briefly cooling it on ice and running it on a 1% agarose gel. A one-third volume of RNAlater (Ambion/Thermo Fisher Scientific, catalogue #AM7021, Waltham, MA, USA) was added to the *appa* probe before storing it at -80°C.

2.3.4aii. Preparing larvae for in situ hybridization

3dpf larvae were fixed overnight in 4% paraformaldehyde (PFA) in phosphate buffer (pH 7.4) with 5% sucrose at 4°C. The PFA was then removed and the larvae were washed in 50% MeOH/50% diethyl pyrocarbonate (DEPC)-treated water for 5 minutes. Larvae were then rinsed with 100% MeOH for 1 minute and then incubated with 100% MeOH for 15 minutes at room temperature. Larvae were then stored in fresh 100% MeOH at -20°C. Larvae were re-hydrated by washing them into DEPC-treated water with 0.1% tween. Larvae were first washed for 5 minutes in 75% MeOH/ 25% DEPC-treated water with 0.1% tween, then for 5 minutes in 50% MeOH/ 50% DEPC-treated water with 0.1% tween, then for 5 minutes in 25% MeOH/ 75% DEPC-treated water and finally for 5 minutes in DEPC-treated water with 0.1% tween. Larvae were permeabilized by treatment with -20°C acetone for 7 minutes, rinsed for 5 minutes in DEPC-treated phosphate buffered saline (PBS) with 0.1% tween, and treated with 10ug/mL proteinase K for 30 minutes at room temperature. Larvae were then rinsed with DEPC-treated 1xPBS with 0.1% tween and re-fixed in 4% PFA in phosphate buffer (pH 7.4) with 5% sucrose for 20 minutes at room temperature. After this, larvae were washed three times in DEPC-treated 1x PBS with 0.1% tween. Larvae were then incubated at 60°C for at least 2 hours in Hauptmann's hybridization solution (50% formamide, saline sodium citrate (750 mM NaCl, 75 mM trisodium citrate, pH 7), 50μg/mL heparin, 5mg/ml Torula yeast RNA, and 0.1% Tween) that had been pre-warmed to 60°C.

2.3.4aiii. Hybridization and post-hybridization washes

The larvae were hybridized in 1 μg/mL of *appa* probe in Hauptmann's hybridization solution for 2 nights (approximately 40 hours) at 60°C. Larvae were then washed two times, 30 minutes each in 50% formamide/ 2x saline sodium citrate (SSC; 300 mM NaCl, 30 mM trisodium citrate, pH 7) at 60°C. Fish were then washed for 15 minutes in 2x SSC and two times, 30 minutes each in 0.2x SSC (30 mM NaCl, 3 mM trisodium citrate) at 60 °C.

2.3.4aiv. Probe detection

Larvae were blocked for 2-3 hours in 2% RMB blocker (Blocking reagent; Sigma/Roche catalogue #11096176001, St. Louis, MO, USA) in 1x Maleate (100 mM

maleic acid, 150 mM NaCl, pH 7.5) with 1% DMSO and 0.1% Tween. Larvae were then incubated overnight in 1:5000 α-DIG-Alkaline phosphatase antigen binding fragments (Roche catalogue #11093274910, Basel, Switzerland) in 2% RMB blocker in 1x Maleate with 1% DMSO and 0.1% tween. The antibody was then removed and the larvae were washed four times (30 minutes each) with 1x Maleate with 1% DMSO and 0.1% tween. They were subsequently incubated for 15 minutes in fresh alkaline phosphatase buffer (pH 9.5; 100 mM Tris-HCl, 100 mM NaCl, 50 mM MgCl2) with 0.1% tween and developed in alkaline phosphatase buffer containing 0.225% NBT and 0.175% BCIP (Roche catalogue #s11383213001 and 11383221001, Basel, Switzerland) for approximately 30 minutes. Fish were then washed for 30 minutes in alkaline phosphatase wash buffer (pH 7.5;154 mM NaCl, 11 mM Tris/ HCl, 1 mM EDTA) with 0.1% tween, fixed in 4% PFA with 5% sucrose, and washed 3x in PBS with 0.1% Tween20 (PBST). For visualization, the larvae were gradually washed into 70% glycerol/PBST (first transferred to 30% glycerol, then to 50% glycerol and finally to 70% glycerol). Larvae were imaged and photographed with a Leica M165 FC dissecting microscope and a Leica DFC 400 camera.

2.3.4b. qPCR to detect *appa* and *prp1*

qPCR to detect *appa* and *prp1*. Experiments were performed in compliance with the MIQE guidelines (Minimum Information for Publication of Quantitative Real-Time PCR Experiments) (Bustin et al., 2009). RNA samples for comparing *prp1* transcript abundance in *prp1$^{ua5003/ua5003}$* mutants versus *prp1* transcript abundance in wild type fish were obtained from pools of larvae at 71-73 hpf (hours post-fertilization; each biological replicate represents 15-20 larvae) that had been stored in RNAlater (Ambion/Thermo Fisher Scientific, catalogue #AM7021, Waltham, MA, USA). RNA samples for comparing *prp1* transcript abundance in *prp1$^{ua5004/ua5004}$* mutants versus *prp1* transcript abundance in wild type fish were obtained from pools of larvae treated with 20 mM pentylenetetrazole (PTZ) at 3dpf (days post-fertilization) as described in Chapter 3 (each biological replicate represents 5 larvae). RNA samples for comparing *appa* transcript abundance in *appa$^{ua5005/ua5005}$* mutants versus *appa* transcript abundance in wild type fish obtained from pools of 2dpf larvae (each biological replicate represents 5 larvae) or from adult zebrafish brains (1 brain/biological replicate). Total RNA was extracted from pools

of embryos using the RNeasy Kit (Qiagen catalogue #74104,Toronto, ON, Canada) and from adult zebrafish brains using the RNeasy Lipid Tissue Mini Kit (Qiagen catalogue #74804, Toronto, ON, Canada) as outlined in the manufacturer's protocols. The samples were homogenized in the appropriate lysis buffer (Buffer RLT for larvae, QIAzol for adult brain) with a rotor stator homogenizer (VWR catalogue #47747-370, Radnor, PA, USA), and on-column DNA digestion was performed using Qiagen DNase I (Qiagen catalogue #79254, Toronto, ON, Canada). RNA quantity was determined using a Nanodrop 2000 spectrophotometer (Thermo Scientific). All of the samples had ribosomal RNA profiles with strong 28S and 18S bands and RNA integrity numbers of at least 7/10 as determined using an Agilent RNA 6000 NanoChip and Agilent 2100 Bioanalyzer. cDNA was then generated using a qScript Supermix kit (Quanta BioSciences catalogue #95048-100, Beverly, MA, USA).

qPCR was performed using a 7500 Real-Time PCR system (ABI Applied Biosystems). Primers were designed using Primer Express (Version 3.0, Primer Express, Thermo Fisher Scientific, Waltham, MA, USA) and previously verified with standard curves and melt curves (Fleisch et al., 2013). qPCR reactions were performed with 3 technical replicates of each biological replicate. Each reaction contained 5 μL Dynamite Master Mix (prepared and supplied by Molecular Biology Service Unit, University of Alberta. The mix included SYBR Green and platinum Taq hot start enzyme), 2.5 μL of pre-mixed primer working stocks (final concentrations of the *β-actin*, *appa*, and *prp1* primers were 800 nM, 800nM and 200 nM, respectively) and 2.5 μL cDNA for a total volume of 10 μL. After an initial denaturation step (2 min at 95 °C), cycling consisted of 40 cycles of 95 °C for 15 s followed by 60 °C for 1 min. One cycle for melting dissociation curve analysis followed these 40 cycles and consisted of 95 °C for 15 s, 60 °C for 1 min, 95 °C for 15 s, and finally 60 °C for 1 min. Data analysis was performed using 7500 Software for 7500 and 7500 Fast Real Time PCR Systems version 2.0.1 (AB Applied Biosystems) with auto CT calling. Transcript abundance was normalized to *β-actin* levels. Relative fold change in transcript abundance was statistically analyzed on the resulting RQ values.

2.3.5 Length measurements of mutant larvae

2dpf larvae were fixed overnight in 4% paraformaldehyde (PFA) in phosphate buffer (pH 7.4) with 5% sucrose at 4°C. Larvae were then rinsed several times with 1xPBS and imaged and photographed with a Leica M165 FC dissecting microscope and a Leica DFC 400 camera. 7dpf larvae were euthanized in MS222, mounted in 5% methyl cellulose and imaged with a Leica DFC 400 camera. The scale bar feature in the Leica software was then used to measure the length of each fish from the forebrain to the tip of the caudal fin.

2.3.6 Production of mRNAs

To test for dominant effects, *appa* mRNA and *appb* mRNA matching the predicted variants following splice block MO injection were ordered as custom minigenes (Integrated DNA Technologies, San Diego, CA) and cloned into pCS2+ using engineered restriction sites. In the case of *appa*, this included exons 1 and 2, along with intron 2-3 (= 279 bp CDS, denoted 'appa-i2'). In the base of appb, this included exons 1-3 along with intron 3-4 (= 538 bp CDS, denoted '*appb-i3*'). The intronic sequences cloned were the 5' portion up to and including the first endogenous in-frame stop codon. The minigene and pCS2+ plasmids were digested with fast digest EcoRI and fast digest XhoI (Thermo Fisher Scientific, catalogue #FD0275 and #FD0695, Waltham, MA, USA) and the insert was ligated into pCS2+ with T4 DNA ligase (Invitrogen/Thermo Fisher Scientific catalogue #10004917, Waltham, MA, USA). The sequence of the insert was verified using an SP6 primer (sequence within the pCS2+ vector, 5'-TACGATTTAGGTGACACTATAG-3'). The plasmid was linearized with FastDigest Not I (Thermo Fisher Scientific, catalogue #FD0593, Waltham, MA, USA), purified by ethanol precipitation as described in section 2.3.2b, and mRNA was synthesized using an mMessage mMachine SP6 kit (Ambion/Thermo Fisher Scientific catalogue #AM1340, Waltham, MA, USA). For 'rescue' experiments zebrafish *prp1* (NCBI accession number JQ994489) was cloned into the pCS2+ vector as previously described (Kaiser et al., 2012). Mouse *Prnp* cDNA (NCBI accession NM_011170) was cloned into the pCS2+ vector. Following linearization with FastDigest Not I (Thermo Fisher Scientific, catalogue #FD0593, Waltham, MA, USA), mRNA was transcribed from these plasmids *in vitro* using an mMessage SP6 kit (Ambion/Thermo Fisher Scientific catalogue

#AM1340, Waltham, MA, USA) and mRNA concentration was determined using a NanoDrop 2000 spectrophotometer (Thermo Scientific). mRNA quality was assessed by examining the results of an mRNA Nano Assay with an Agilent 2100 Bioanalyzer and mRNA with virtual bands of the appropriate size were used for experiments.

2.3.7 Microinjection of zebrafish embryos with morpholinos and mRNA

Morpholino injections. Previously published *appa* and *appb* splice blocking morpholinos (Kaiser et al., 2012) (APPa_SB 5' -TAG TGT TGC TTC ACC TCC TGG CAG T -3'; ZDB-MRPHLNO-130125-1; APPb_SB 5'-59 CAC ACA CAT ACA TAC CCA GGC AAC G- 3'; ZDB-MRPHLNO-130125-3) were used to disrupt splicing at the exon 2-intron 2 boundary of *appa* mRNA and the exon3-intron3 boundary of *appb* mRNA, respectively, thereby disrupting protein production by the introduction of premature STOP codons. A standard control morpholino from Gene Tools LLC (5'- CCT CTT ACC TCA GTT ACA ATT TAT A- 3'; Philomath, OR, USA) was used as a negative control. Unless otherwise specified, a standard zebrafish *tp53* morpholino from Gene Tools (5'- GCG CCA TTG CTT TGC AAG AAT TG- 3'; ZDB-MRPHLNO-070126-7) was included in the injection solution to counter possible morpholino off-target effects (Langheinrich et al., 2002).

We also performed experiments with a previously published *prp1* translation blocking morpholino (Malaga-Trillo et al., 2009) (Prp1_TBb 5'-TGA GCA GAG AGT GCT GCG GGA GAG A-3'), but later discovered that this sequence was incorrect (i.e. the morpholino sequence was the same sense as the *prp1* 5'UTR instead of antisense). The correct sequence (Prp1_TBm 5'- TCTCTCCCGCAGCACTCTCTGCTCA-3'; **ZFIN ID:** ZDB-MRPHLNO-100423-4) was published in (Sempou et al., 2016). At the time of writing, we were in the process of determining an appropriate morpholino dosage by injecting   the   new   morpholino   sequence   (Prp1_TBm   5'-TCTCTCCCGCAGCACTCTCTGCTCA-3'; **ZFIN ID:** ZDB-MRPHLNO-100423-4) into both wild type AB strain zebrafish embryos and the *prp1*$^{-/-}$ embryos that we engineered herein.

Injection solutions were prepared by combining 1.0 uL of 0.1M KCl, 2.5 uL of 0.25% dextran ruby red, 3 uL of 10 mg/mL *tp53* morpholino stock, the appropriate volume of gene-specific morpholino, the appropriate volume of 'rescue' mRNA (where applicable)

and nuclease free water up to a total volume of 10 uL. In experiments where *tp53* morpholino was not included, nuclease free water replaced it in the injection solution. The injection volume was calibrated to 1 nL by injecting into mineral oil to assess volume, assessed using an ocular micrometer, immediately prior to injections. Zebrafish embryos at the 1-2 cell stage were injected with 1 nL of gene-specific or standard control morpholino delivered into the yolk. The embryos were subsequently screened for dextran labeling.

2.3.7 Screening embryos for morpholino and mRNA-induced phenotypes

The morning following injections, dead embryos were removed and fresh embryo growth medium (E3 medium) was applied to the surviving embryos. Embryos (approximately 24 hpf) were then dechorionated with a 10-minute treatment with 10-mg/mL pronase at 28.5°C. Embryos were then washed 3-4 times with embryo medium and screened for dextran labeling (marker of successfully injected embryos) using a Leica M165 FC dissecting microscope. Embryos that were successfully labeled with dextran were then visually scored using a Leica M165 FC dissecting microscope by a blinded observer. Embryos were scored based on their size relative to un-injected wild type fish embryos that were collected on the same day (using an ocular micrometer as a guide), body morphology and extent of opaque, 'necrotic-like' tissue (lack of transparency typical of normal embryos; See Figure 2.16A). Embryos were assigned a score of 0 if they were similar in size and transparency to un-injected wild type fish and had no obvious defects in body morphology. Embryos that were slightly smaller and/or slightly more opaque than un-injected wild type fish were assigned a score of 1. Embryos with a truncated body axis (tip of caudal fin tapered at or slightly past the end of the yolk sac extension) and had an opaque appearance were assigned a score of 2. Finally, fish with a deformed head (or absence of discernable head), very truncated body axis (not extending much past the yolk sac) and opaque appearance were assigned a score of 3.

2.3.8 Western blots

Brains were dissected from adult *prp2^{ua5001/ua5001}* fish and wild type AB-strain fish and stored at -80°C. Brains were then lysed in Tris cell lysis buffer (pH 7.4; 50 mM Tris, 0.5% sodium deoxycholate, 0.5% Triton) with 1:200 protease inhibitor cocktail (EMD Millipore/VWR catalogue #CA80053-852, Darmstadt, Germany) and homogenized with

a rotor stator homogenizer (VWR catalogue #47747-370, Radnor, PA, USA). Tissue was then broken up with a 26G ½ needle and samples were centrifuged for 5 minutes at 900g. Total protein in the supernatant was quantified using BioRad Protein Assay Dye (BioRad catalogue #5000006, Hercules, CA, USA). Lysates were diluted with 2X SDS loading dye (12.5 mM Tris, 2% glycerol, 0.4% SDS, 0.2% β-mercaptoethanol, 0.1% bromophenol blue). Samples (30μg of total protein) were loaded into a 12 % SDS-PAGE gel to separate the proteins, and then proteins were transferred to a membrane. Membranes were blocked in 5% milk in Tris buffered saline (pH 7.5-8) with 0.1% tween (TBST). The membranes were then probed with an □-human APP antibody clone 22C11 (Millipore MAB348SP, Darmstadt, Germany) that has been previously shown to bind both appa and appb (Kaiser et al., 2012) at a 1:2000 dilution in TBST with 5% milk. The α-APP antibody was then detected using 1:5000 goat α-mouse HRP (Jackson Immunoresearch catalogue #115-035-003, West Grove, PA, USA) in TBST with 5% milk, and developed with Enhanced Chemiluminescence western blot substrate (Pierce/Thermo Fisher Scientific catalogue #32106, Waltham, MA, USA). The blot was then re-probed with α-β-Actin antibody (Sigma catalogue #A2066, St. Louis, MO, USA) at a 1:500 dilution in TBST with 5% milk, and detection was performed using 1:5000 goat α-Rabbit HRP (Jackson Immunoresearch catalogue #111-035-144, West Grove, PA, USA) in TBST with 5% milk. The intensity of the bands was measured using ImageJ (National Institutes of Health, Bethesda, MD, USA) and the ratio of APP to β-actin for each biological replicate (1 brain/replicate) was calculated.

2.3.9 Statistical Analysis

All statistics were performed using GraphPad Prism Software (Version 6, GraphPad, San Diego, CA). Prior to performing pairwise comparisons between groups, the F-test was used to assess variance. If variance within groups was not statistically significant, pairwise comparisons were performed using paired t-tests. If variance was statistically different, Mann-Whitney U-tests were performed instead. For multiple group comparisons, groups were assessed for variance and normal distribution using the Brown Forsythe and Bartlett's tests. If variance was not significant, data was analyzed using One-Way Anova's, and if variance was significant, data was analyzed using a Kruskal

Wallis test. qPCR data was analyzed by performing statistics on the RQ values. For graphical presentation, data was normalized to the wild type samples and plotted as a percentage.

2.4 Results

2.4.1 *prp1* TALENs induced somatic mutations in *prp1*

To ensure that our TALENs were capable of producing mutations *in vivo*, we first analyzed somatic cutting in embryos injected with the *prp1* TALEN reagents. To do this, we injected 1-2 cell stage zebrafish embryos and extracted genomic DNA when they reached at least 24 hpf. We then performed HRM on genomic DNA from pools of 20 injected embryos or uninjected controls. 3/3 pools of TALEN-injected embryos had different melt profiles than the controls. Genomic DNA from these pools were then PCR-amplified and cloned into the pCR2.1 Topo vector. We then performed HRM analysis on 12 of these clones and identified 2 clones (17%) that had different melt profiles than clones containing a wild type *prp1* fragment. Sequencing revealed that the first clone contained a 1 base pair deletion and the second contained a 6 base pair deletion (Figure 2.4A).

A. Somatic mutations in *prp1*

1 bp deletion
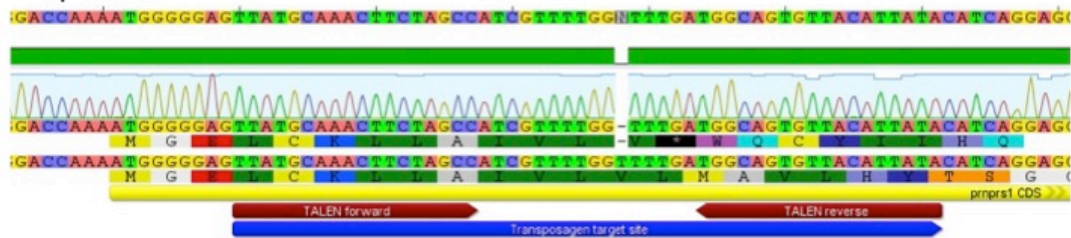
6 bp deletion

B. Germline mutations in *prp1*

- prp1+/+
- prp1+/+ outlier
- prp1 with 6 bp deletion
- prp1 with polymorphism upstream of prp1 target site
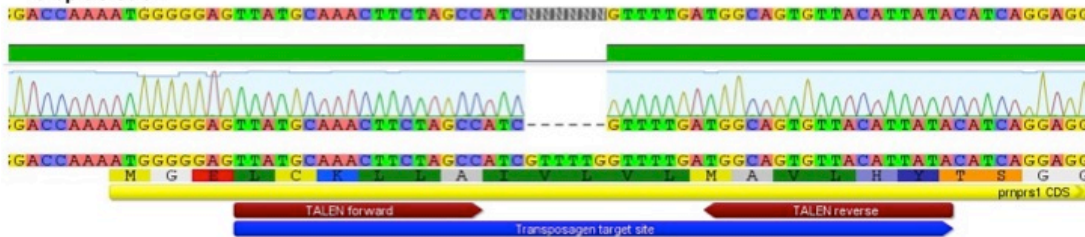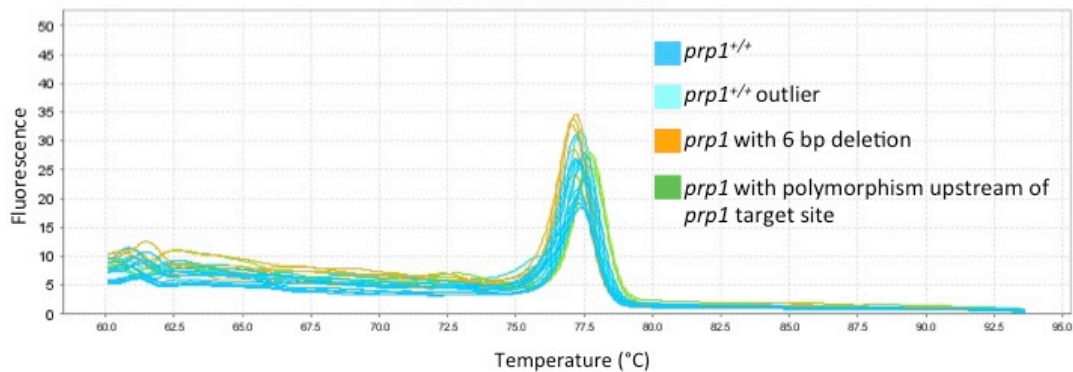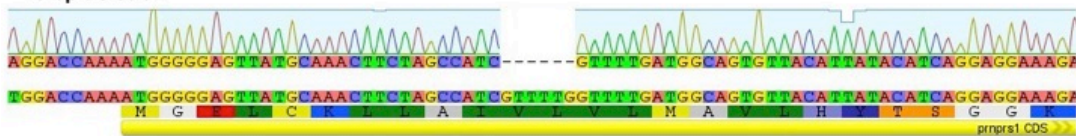
6 bp deletion

Figure 2.4. We identified somatic in-del mutations in *prp1* TALEN injected embryos and found that TALEN-induced mutations were transmitted through the germline
A. Somatic mutations induced in *prp1* by TALENs. The 1 bp deletion is a frameshift mutation, while the 6 bp deletion is not. **B.** We raised injected (F_0) fish to adulthood and genotyped pools of F_1 generation fish (Topo-clones). This informed us that the F_0 parents

were carriers of a 6-bp deletion allele of *prp1*. Unfortunately, in this case the mutation is not predicted to produce a disrupted gene product, as would be expected via frameshift.

2.4.2 *prp1* TALENs induce germline mutations in *prp1*

Some of the *prp1* TALEN injected fish were raised to adulthood and in-crossed to assess germline transmission of *prp1* mutations. Genomic DNA was extracted from pools of 10 F1 generation fish and assessed by HRM analysis. Genomic DNA from 5/15 pairs of F0 generation fish showed interesting melt profiles compared to controls and were PCR amplified and cloned into the pCR2.1 Topo vector. 63 clones were screened using HRM and those with a different melt profile the controls were sequenced (Sample melt profiles shown in Figure 2.4B) 4/63 clones (6%) had 6-bp deletions (For sample see Figure 2.4B) and 3/63 clones (4%) had base pair substitutions. These interesting clones originated from 3 pairs of fish, and sibling fish from these crosses were raised to adulthood and genotyped.

2.4.3 Identification of fish heterozygous for the *prp1* ua5003 and ua5004 frameshift alleles

48 adults injected with *prp1* TALENS as above were fin-clipped and screened for *prp1* mutations. To analyze the first 25 fish, we amplified genomic DNA from finclips and sequenced the PCR products. The traces from a few of these fish appeared heterozygous, thus we cloned the corresponding PCR products into the pCR2.1 Topo vector and sequenced 4 clones from each fish. Clones from 4 male fish had the same in-frame mutation (6-bp deletion). To analyze the next 39 fish, we pre-screened genomic DNA from fin clips using HRM. We used genomic DNA from F1 fish that were known to have 6-bp deletions as a positive control in the HRM analysis. Two males and 3 females had different melting profiles that the controls. Genomic DNA from these fish was amplified, cloned into pCr2.1, and clones were sequenced. One female had an in-frame mutation (6 bp deletion), one male had an 8 bp deletion and an I10T missense mutation (designated as allele ua5003, Figure 2.5A) 3 females and 1 male had a 19 bp deletion (designated as allele ua5004, Figure 2.5A). "ua" in our allele names is the identifier assigned by ZFin.org, the Zebrafish Model Organism Database, to denote "University of Alberta". These frameshift alleles are predicted to produce truncated, nonsense proteins (Figure 2.5B).

A. Two stably inherited *prp1* frameshift alleles were identified.

prp1 ua5003 allele (8 bp deletion + missense mutation)

prp1 ua5004 allele (19bp deletion)
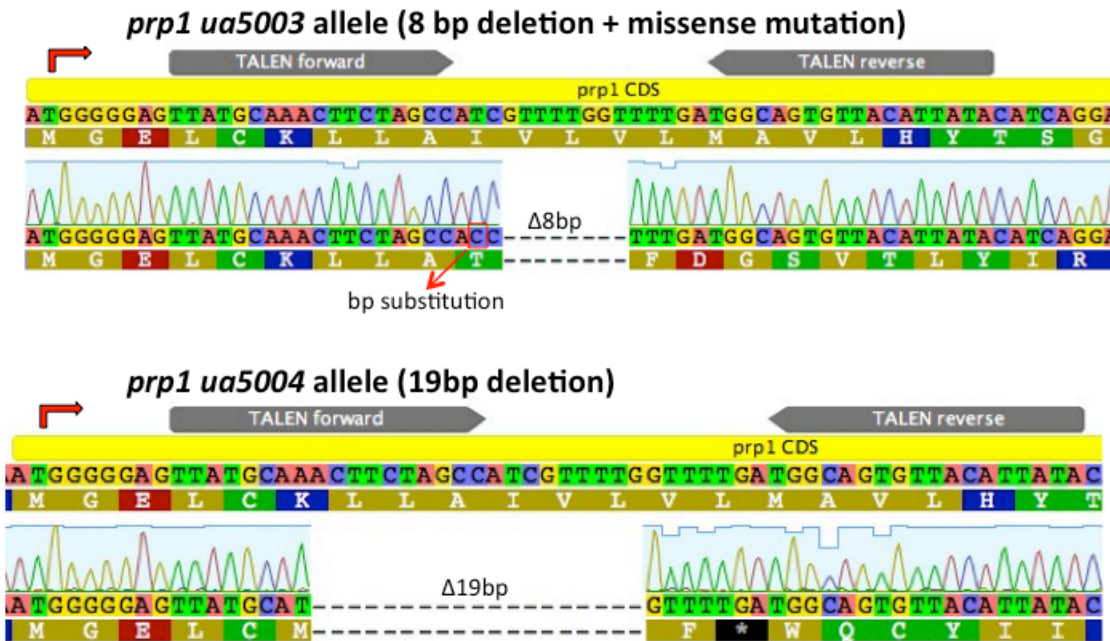
B. TALEN-induced frameshift mutations in *prp1* are predicted to produce nonsense proteins.

Prp1 Wild-type

Predicted proteins resulting from frame-shift in mutant *prp1* alleles

ua5003 allele — Missense 36 a.a. — Stop

ua5004 allele — Missense 2 a.a. — Stop

Figure 2.5. Two stable lines of *prp1*^{-/-} fish were established

A. Fish with the ua5003 allele have an 8-bp deletion and fish with the ua5004 allele have a 19-bp deletion. **B.** Schematic of the Prp1 protein. The protein has a signal peptide, repetitive region, hydrophobic domain and a GPI anchor. Putative proteins from the ua5003 allele and ua5004 allele have a small piece of signal peptide, followed by nonsense sequence and early stop codons.

2.4.4 $prp1^{ua5003/ua5003}$ and $prp1^{ua5004/ua5004}$ mutants have no overt phenotype, except being slightly smaller than $prp1^{+/+}$ at larval stages

We bred fish with the *prp1 ua5003* and *ua5004* alleles to homozygosity and observed no overt phenotypes at larval or adult stages in zygotic mutants (zygotic mutants have maternally provided mRNA from the egg cell). Fish with the *ua5003* allele are shown in Figure 2.6 A-B. To test the hypothesis that maternally provided *prp1* mRNA is enough to mask early developmental phenotypes, we raised maternal zygotic mutants for the *prp1 ua5003* and *ua5004* alleles (i.e. fish that do not have maternally provided *prp1* mRNA from the egg cell). Again, we observed no overt phenotypes (Figure 2.6 C-D, F-G), except that $prp1^{-/-}$ maternal zygotic mutants with the *ua5003* and *ua5004* alleles were, respectively, approximately 3% and 2.5% shorter than $prp1^{+/+}$ fish at 50 hpf (Figure 2.6E; $p<0.05$). Thus reduced body size is a consistent phenotype across two independent disruptions of *prp1*, but its biological significance (if any) remains to be determined.
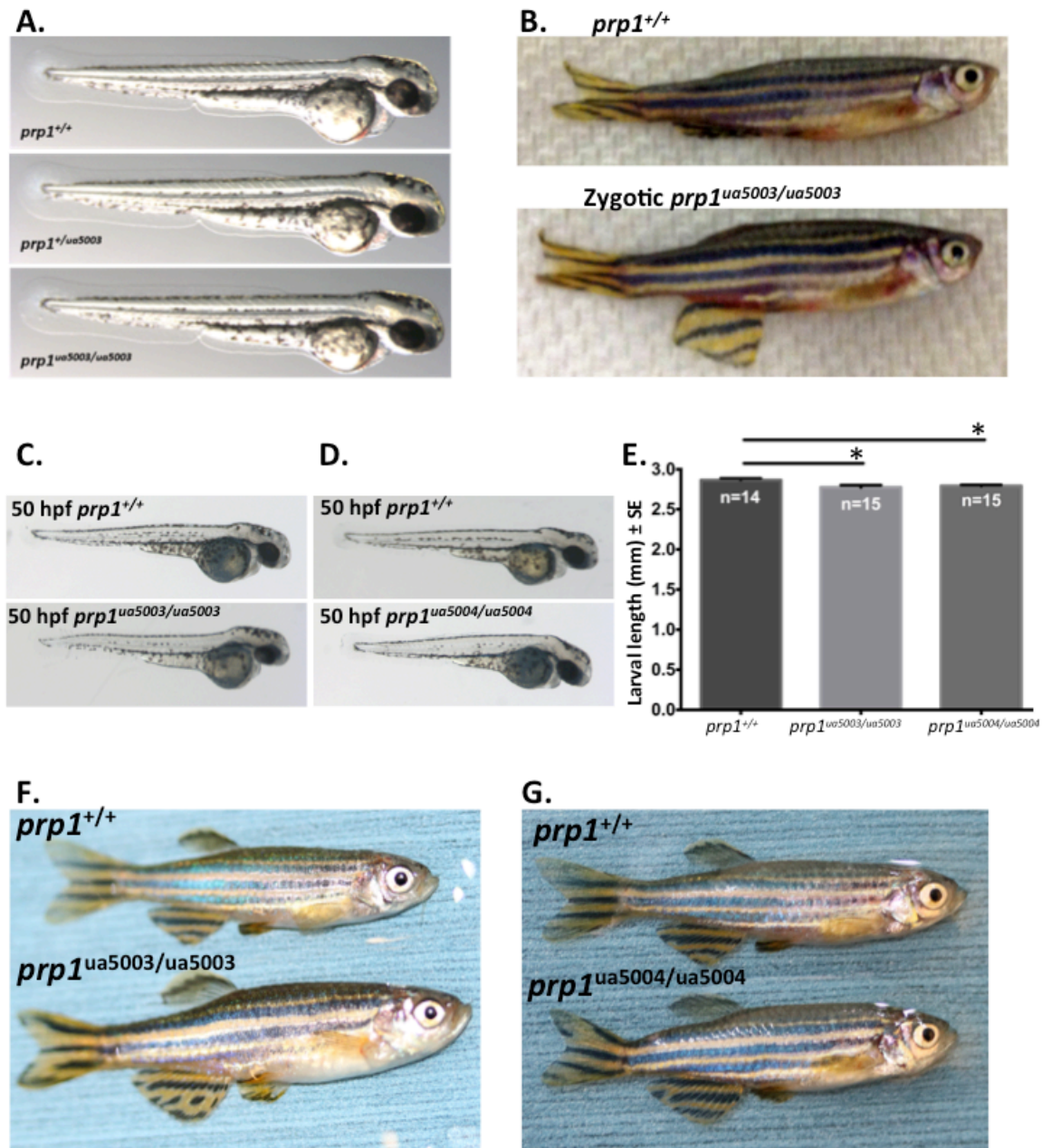
Figure 2.6. *prp1^{ua5003/ua5003}* and *prp1^{ua5004/ua5004}* fish have no overt phenotypes but are slightly smaller than wild type as larvae

A. 2dpf *prp1^{+/ua5003}* and zygotic *prp1^{ua5003/ua5003}* larvae have no overt phenotypes. **B.** Zygotic *prp1^{ua5003/ua5003}* adult survive to adulthood and are similar in appearance to adult wild-type fish. Maternal zygotic *prp1^{ua5003/ua5003}* larvae (**C.**) and maternal zygotic *prp1^{ua5004/ua5004}* larvae (**D.**) are similar in appearance to wild type larvae at 50 hpf. **E.** The mean lengths of maternal zygotic *prp1^{ua5003/ua5003}* larvae and maternal zygotic

prp1^{ua5004/ua5004} larvae are reduced by 3% and 2.5%, respectively, compared to *prp1^{+/+}* larvae at 50hpf. * $p < 0.05$ with the Kruskal Wallis test. n refers to the number of fish. Maternal zygotic *prp1^{ua5003/ua5003}* fish **(F.)** and maternal zygotic *prp1^{ua5004/ua5004}* fish **(G.)** survive to adulthood and have no overt phenotypes compared to wild type fish.

2.4.5 Maternal zygotic *prp1*$^{-/-}$ fish have reduced *prp1* transcript abundance

Since we did not observe overt phenotypes in our *prp1* mutants, we tested the alternate hypothesis that the *prp1* alleles were not null alleles. We found that *prp1* transcript abundance was reduced in 3dpf maternal zygotic *prp1*$^{ua5003/ua5003}$ fish to levels that were 9.46% of wild type (Figure 2.7A, p=0.0027). Further, levels of *prp1* transcript abundance were reduced in PTZ-treated 3dpf maternal zygotic *prp1*$^{ua5004/ua5004}$ larvae to levels that were 36.71% of those observed in PTZ-treated wild type larvae (Figure 2.7B, p=0.0043). This analysis should be repeated in untreated *prp1*$^{ua5004/ua5004}$ larvae and wild type larvae because treatment with PTZ may influence *prp1* transcription and/or kinetics of its degradation. Overall, however, it appears that *prp1* transcript levels are reduced in fish with the *prp1 ua5003* and *ua5004* alleles- perhaps through nonsense mediated decay. Nonsense mediated decay is an RNA surveillance mechanism that degrades mRNAs harbouring nonsense and frameshift mutations (Culbertson, 1999). These results support the hypothesis that the *prp1 ua5003* and *ua5004* alleles are null alleles.

2.4.6 Maternal zygotic *prp1*$^{ua5003/ua5003}$; *prp2*$^{ua5001/ua5001}$ fish have no overt phenotypes

As neither *prp1*$^{-/-}$ mutants (described above) nor *prp2*$^{-/-}$ mutants (Fleisch et al., 2013) exhibited overt phenotypes in larval or adult stages, we hypothesized that *prp1* and *prp2* have redundant functions in zebrafish development. We therefore created compound *prp1*$^{ua5003/ua5003}$;prp2$^{ua5001/ua5001}$ mutants. These fish did not have overt phenotypes, compared to wild type fish at larval (50 hpf, Figure 2.8A) or adult (Figure 2.8C) stages. Loss of *prp2* also appeared to rescue the size reduction relative to wild type fish that had been observed in *prp1*$^{-/-}$ larvae since compound *prp1*$^{ua5003/ua5003}$; prp2$^{ua5001/ua5001}$ mutants were instead approximately 2% longer than wild type fish at 50 hpf (Figure 2.8B, p=0.0123).
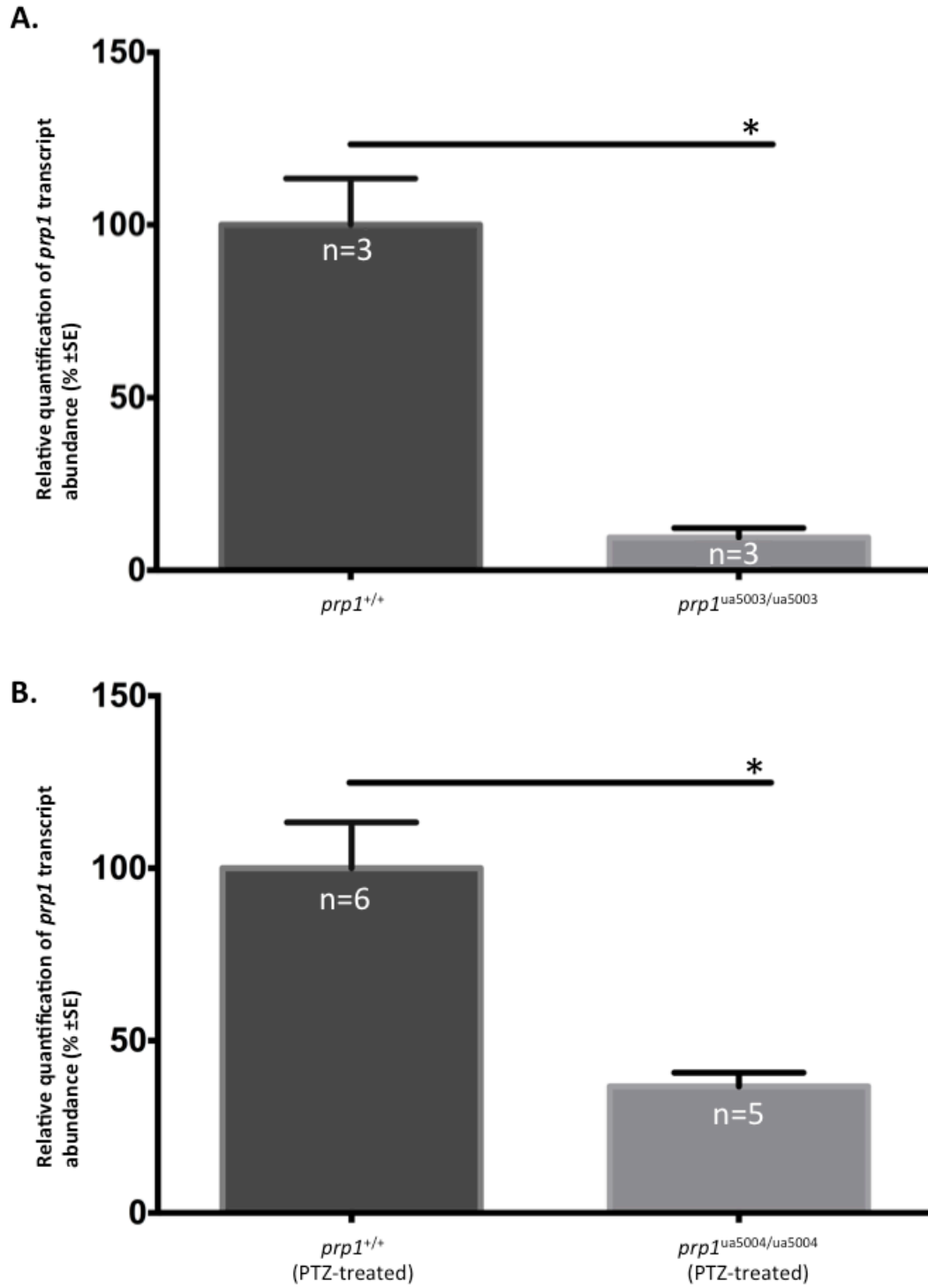
Figure 2.7. *prp1* transcript abundance is reduced in *prp1*^{-/-} mutants likely due to nonsense mediated decay

A. *prp1* transcript abundance was reduced   by approximately 10-fold in 3dpf *prp1^{ua5003/ua5003}* larvae compared to 3dpf wild type larvae. Data is normalized to the wild type fish. * p=0.0027 with the unpaired t-test. n refers to the number of biological replicates (15-20 larvae/biological replicate). **B.** *prp1* transcript abundance was reduced by approximately 2.7-fold in PTZ-treated 3dpf *prp1^{ua5004/ua5004}* larvae compared to 3dpf PTZ-treated wild type larvae. Data is re-plotted in Figure 3.8D. Here the data is normalized to the PTZ-treated wild type fish. *p=0.0043 with the Mann Whitney U test. n refers to the number of biological replicates (5 larvae/biological replicate).
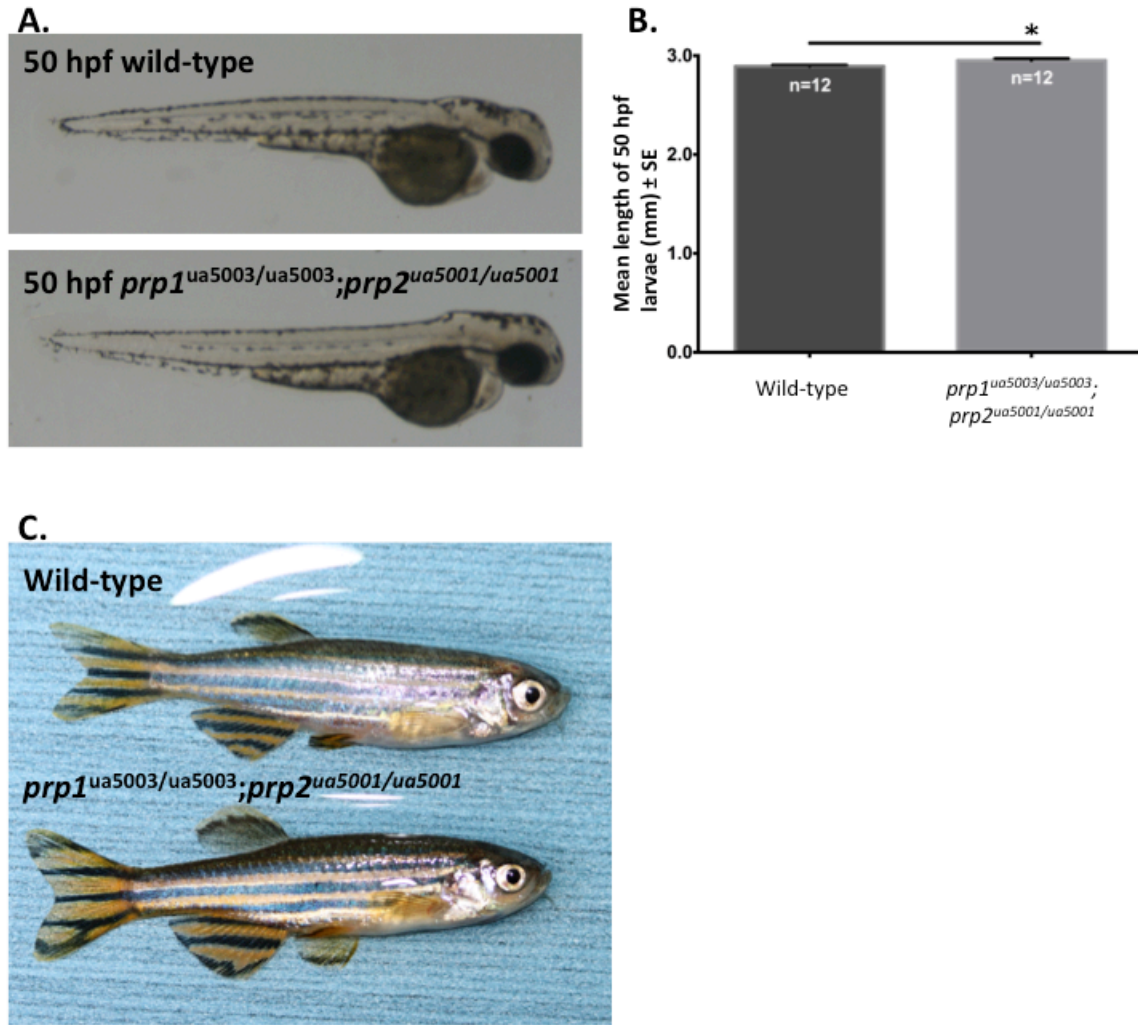
Figure 2.8. Maternal zygotic *prp1*[ua5003/ua5003]; *prp2*[ua5001/ua5001] fish have no overt phenotypes

A. Maternal zygotic compound *prp1*[ua5003/ua5003]; *prp2*[ua5001/ua5001] mutants (bottom) have no overt phenotypes compared to wild type fish (top) at 50 hpf. **B.** The *prp1*[ua5003/ua5003];*prp2*[ua5001/ua5001] mutants have a mean length that is increased by approximately 2% compared to wild type fish. * p=0.0123 with the unpaired t-test. n refers to the number of fish. **C.** Maternal zygotic compound *prp1*[ua5003/ua5003]; *prp2*[ua5001/ua5001] mutants (bottom) survive to adulthood and have no overt phenotypes compared to wild type fish (top).

2.4.7 *appa* TALENs induce somatic mutations in *appa*

We first screened for mutations in somatic tissues of embryos injected with the *appa* TALENs to ensure that the TALENs were capable of producing mutations *in vivo*. We performed HRM on genomic DNA from pools of 20 injected embryos or uninjected controls. 3/3 pools of TALEN-injected embryos had different melt profiles than the controls (For sample HRM trace see Figure 2.9A). Genomic DNA from these pools were then PCR-amplified and cloned into the pCR2.1 Topo vector. We then performed HRM analysis on 36 of these clones and identified 4 clones (11%) that had different melt profiles than clones containing a wild type *appa* fragment. Sequencing revealed that one clone had a 12 bp deletion and the other clones had 8 bp deletions (Figure 2.9B).

2.4.8 *appa* TALENs induce germline mutations in the *appa* gene of wild type zebrafish

Some of the *appa*-TALEN injected fish were raised to adulthood and in-crossed to assess germline transmission of *appa* mutations. Genomic DNA was extracted from pools of 10 F1 generation fish and assessed by HRM analysis. Genomic DNA from 5/29 (11 pairs + 7 outcrossed) F0 generation fish showed interesting melt profiles compared to the controls and were PCR amplified and cloned into the pCR2.1 Topo vector. 56 clones were picked into sterile water and screened using HRM and those with a different melt profile from the controls were sequenced (For sample traces see Figure 2.9C). 7/56 clones (12.5%) had deletions (3- 8bp deletions, 3 5-bp deletions, and 1-12 bp deletion) and 2/56 clones (3.6%) had base pair substitutions. Sample sequencing traces are shown in Figure 2.9C.

2.4.9 Identification of fish heterozygous for the *appa*^{ua5005} frameshift allele

To identify adult fish with stably inherited loss-of-function mutations in *appa*, genomic DNA from fin clips of 17 fish were pre-screened using HRM. One female had a different melt profile than the controls. Genomic DNA from this fish was amplified, cloned into pCr2.1, and clones were sequenced. The fish had an 8 bp deletion (designated as allele *ua5005*, Figure 2.10A). This allele is predicted to produce a nonsense protein due to generation of a premature stop codon (Figure 2.10B).

A. Somatic mutations in *appa*
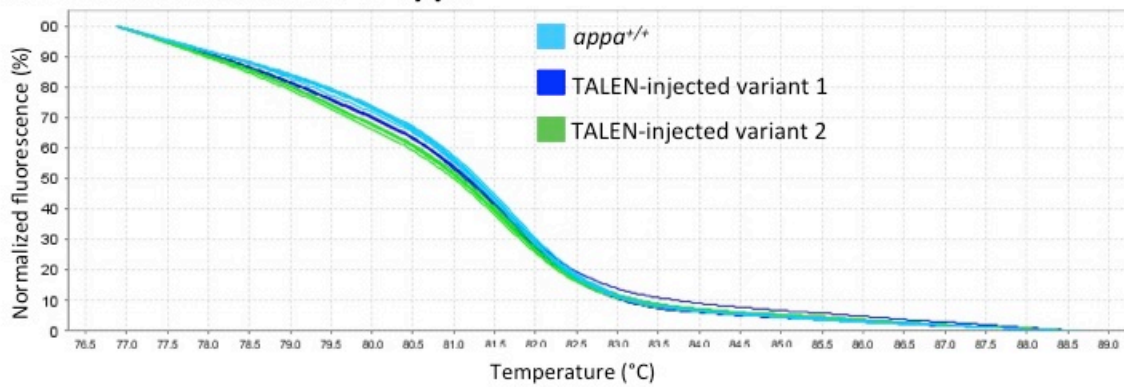
B. Somatic mutations in *appa*
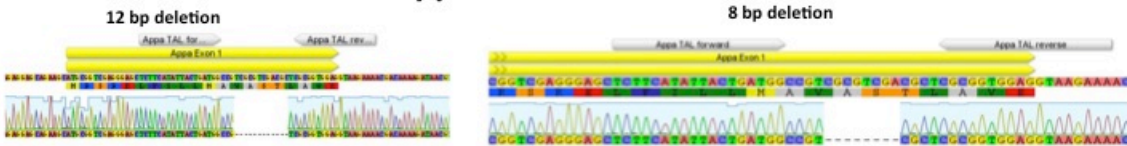
C. Germline mutations in *appa*
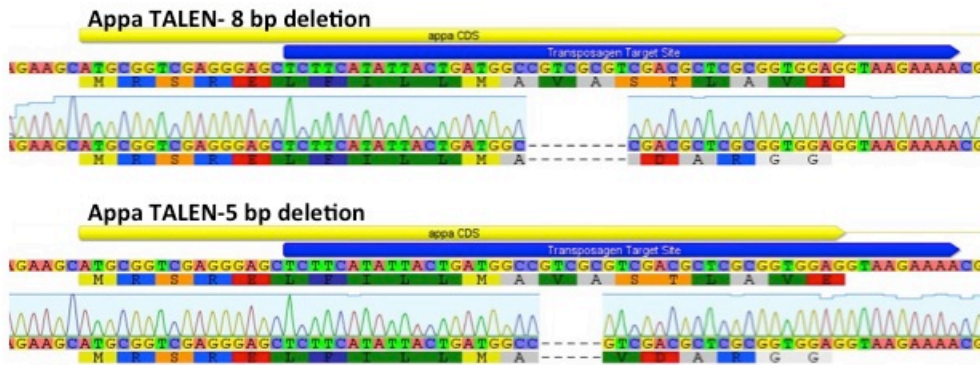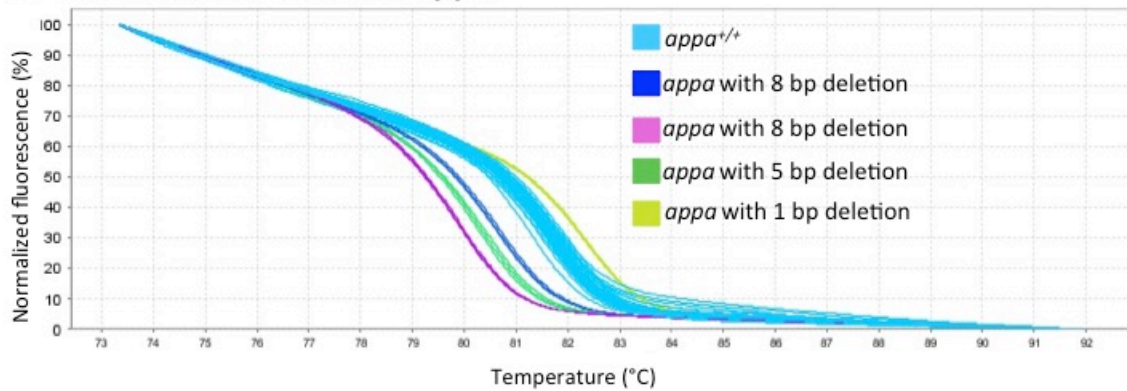
Figure 2.9. TALENs induced somatic and germline mutations in *appa*.

A. Pooled genomic DNA isolated from injected (F1) embryos produced melt curves that differed from pooled genomic DNA from wild type embryos. **B.** Genomic DNA from panel A. was Topo-cloned. After screening individual clones with HRM, variant clones were sequenced. A sample 12-bp deletion and 8-bp deletion of *appa* are shown. **C.** Results from an HRM plate showing germline mutations in *appa*. Colonies with melt profiles that appeared different from wild type were sequenced, revealing clones with 8 bp and 5 bp deletions.

A. One stably inherited *appa* frameshift allele was identified on a wild-type AB strain background.

appa ua5005 allele (8bp deletion)

Forward TALEN

Reverse TALEN

appa CDS

ATGCGGTCGAGGGAGCTCTTCATATTACTGATGGCCGTCGCGTCGACGCTCGCGGTGGAGGTAAGAAAACGACAA
M R S R E L F I L L M A V A S T L A V E V R K R Q

ATGCGGTCGAGGGAGCTCTTCATATTACTGATGGCCGTCG--------CTCGCGGTGGAGGTAAGAAAACGACAA
M R S R E L F I L L M A V --------A R G G G K K T T

Δ8bp
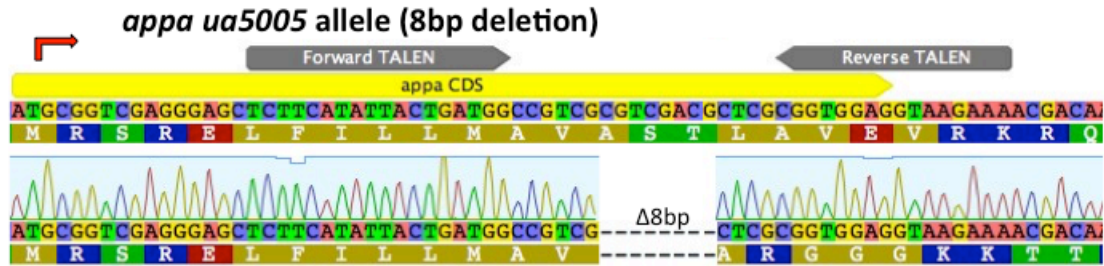
B. *appa ua5005* allele is predicted to produce a truncated nonsense protein

Appa

S | | Aβ | AICD

Predicted protein resulting from frame-shift in *appa ua5005* allele

50 a.a. stop

Figure 2.10. One line of *appa⁻ᐟ⁻* fish was established on a wild type AB-strain background.

A. Fish with the *appa* ua5005 allele have an 8-bp deletion that produces a frameshift. **B.** Schematic of the appa protein. The putative protein product from the *ua5005 allele* has a small piece of signal peptide, followed by nonsense sequence and early stop codons.

2.4.10 Zygotic and maternal zygotic *appa*$^{ua5005/ua5005}$ fish have no overt phenotypes

We bred fish with the *appa ua5005* allele to homozygosity and observed no overt phenotypes in zygotic mutants at larval or adult stages. To test the hypothesis that maternally provided *appa* mRNA is enough to mask early developmental phenotypes, we raised maternal zygotic *appa*$^{ua5005/ua5005}$ mutants. Again, we observed no overt phenotypes at larval or adult stages (Figure 2.11), but they were approximately 8% shorter than wild type at 7dpf (Figure 2.11c, p<0.0001).

2.4.11 Compound maternal zygotic *prp1*$^{ua5003/ua5003}$;*appa*$^{ua5005/ua5005}$ fish have no overt phenotypes but are slightly shorter than wild type at some developmental stages

We had previously observed a genetic interaction between *prp1* and *appa* when both were transiently knocked down using morpholinos (Kaiser et al., 2012), thus we generated compound *prp1*$^{ua5003/ua5003}$;*appa*$^{ua5005/ua5005}$ to determine whether this could be recapitulated in double mutants. Surprisingly, compound maternal zygotic *prp1*$^{ua5003/ua5003}$;*appa*$^{ua5005/ua5005}$ mutants had no overt phenotypes at 50 hpf or at adult stages (Figure 2.12 A,C). Compound maternal zygotic *prp1*$^{ua5003/ua5003}$;*appa*$^{ua5005/ua5005}$ mutants, however, were slightly shorter (by approximately 4%) than wild type larvae at 50 hpf (Figure 2.12B, p=0.0385).
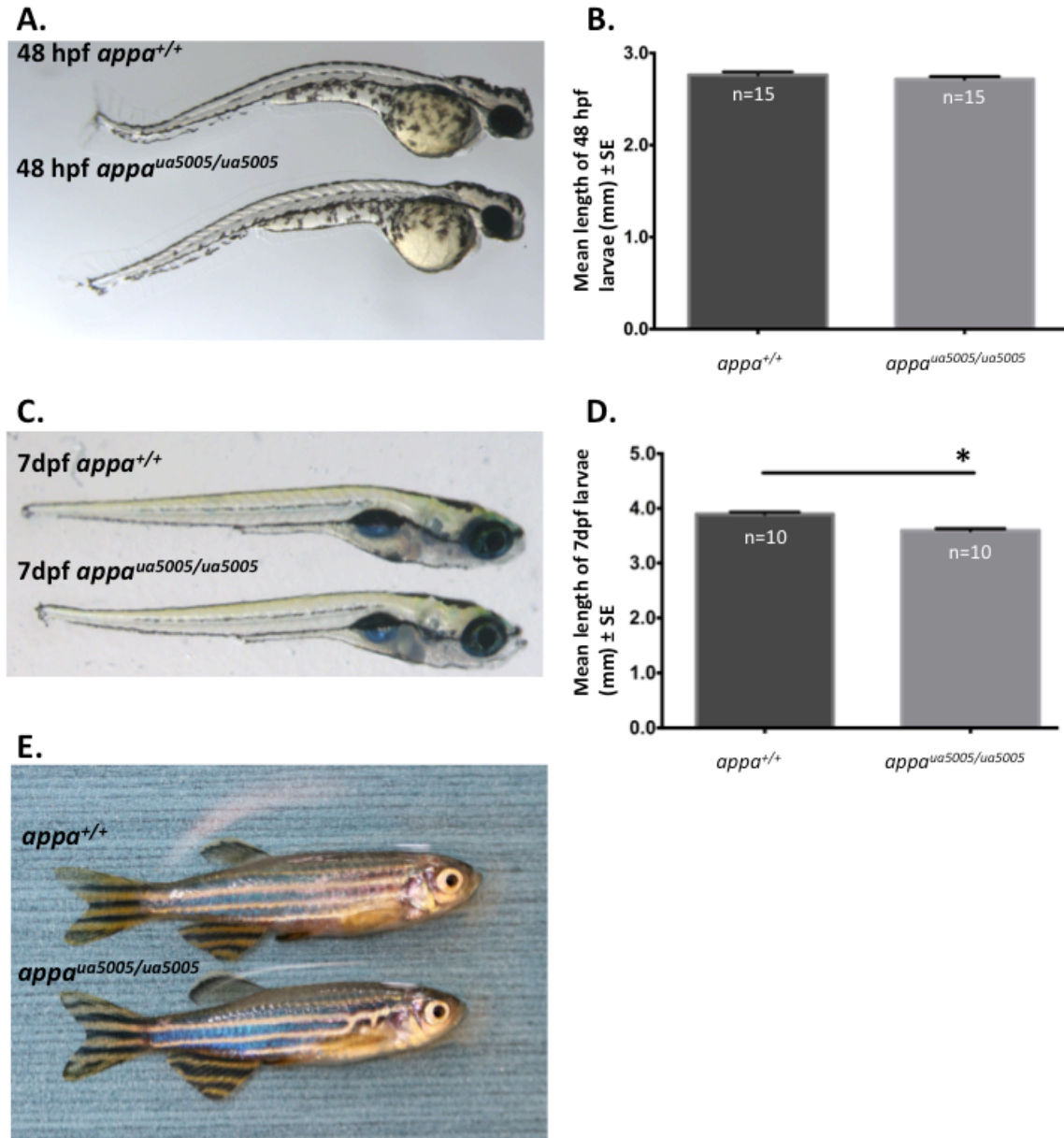
Figure 2.11. Maternal zygotic *appa^ua5005/ua5005* fish have no overt phenotypes, but are slightly smaller than wild type fish at some developmental stages

A-B. Maternal zygotic *appa^ua5005/ua5005* larvae have no overt phenotypes and display no significant differences in size relative to wild type larvae at 48 hpf with the unpaired t-test. n refers to the number of fish. **C-D.** Maternal zygotic *appa^ua5005/ua5005* larvae have no overt phenotypes at 7dpf but are approximately 8% shorter than wild type larvae. *p<0.0001 with the unpaired t-test. n refers to the number of fish. **E.** Maternal zygotic *appa^ua5005/ua5005* fish survive to adulthood and display no overt phenotypes.
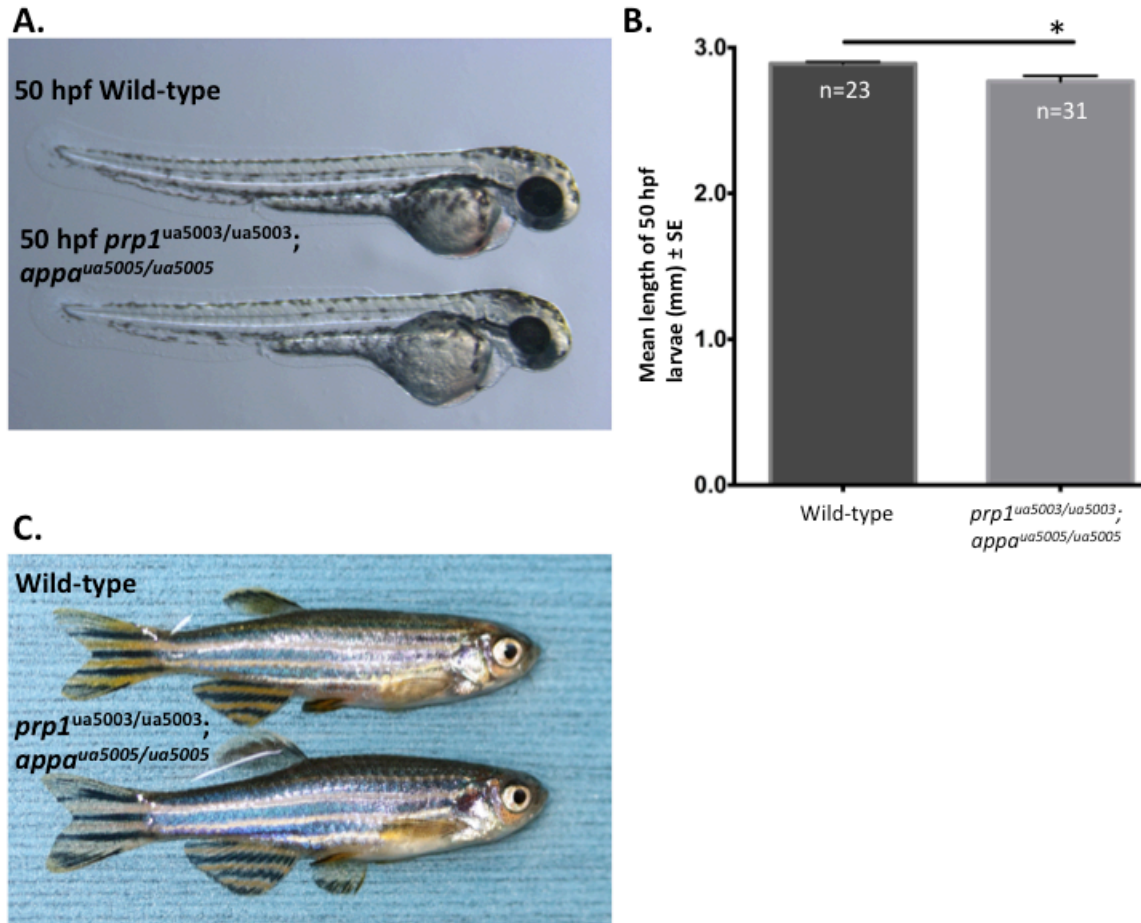
Figure 2.12. Compound _prp1^ua5003/ua5003_; _appa^ua5005/ua5005_ fish have no overt phenotypes, but are slightly smaller than wild type fish as larvae

A. Maternal zygotic compound _prp1^ua5003/ua5003_; _appa^ua5005/ua5005_ mutants (bottom) have no overt phenotypes compared to wild type fish (top) at 50 hpf. **B.** The _prp1^ua5003/ua5003_;_appa^ua5005/ua5005_ mutants have a mean length that is decreased by approximately 4% at 50 hpf compared to wild type larvae. * p=0.0385 with the Mann-Whitney U-test. n refers to the number of fish. **C.** Maternal zygotic compound _prp1^ua5003/ua5003_; _appa^ua5005/ua5005_ mutants (bottom) survive to adulthood and have no overt phenotypes compared to wild type fish (top).

2.4.12 *appa* TALEN mutants exhibit disrupted transcript and protein abundance

Since *appa*^{ua5005/ua5005} and compound *prp1*^{ua5003/ua5003};*appa*^{ua5005/ua5005} lacked overt phenotypes, we sought to test the hypothesis that we had indeed generated null alleles. To confirm that the TALENs we used would disrupt production of appa protein, we injected our *appa* TALENs into fish that were homozygous for the *appa is22gt* allele (Liao et al., 2012). The gene trap in this allele disrupts splicing, causing an RFP coding sequence with a stop codon to be fused to the coding sequence for most of the N-terminus of appa (Liao et al., 2012). As the TALEN target site is upstream of the gene-trap (within Exon 1), TALEN-induced frameshift mutations are expected to introduce premature stop codons and thereby prevent translation of the RFP coding sequence (within Intron 4; Figure 2.13A). We raised TALEN-injected fish to adulthood and performed incrosses. We then screened for F1 larvae with reduced levels or absence of RFP using a Leica M165 FC dissecting microscope. A larva with reduced red fluorescence was found to be heterozygous for a TALEN-induced frameshift mutation, while a larva with no red fluorescence was found to have two different TALEN-induced frameshift mutations (Figure 2.13B). We grew other F1 larvae with reduced or no red fluorescence to adulthood and genotyped them by taking caudal fin samples. To do this, we amplified a portion of *appa* surrounding the target site, cloned them into the pCR.2.1 Topo vector and submitted plasmid to the U of A's Molecular Biology Service Unit for sequencing. From this group of fish, we identified adult fish with the *appa ua5006*, *ua5007* and *ua5008* alleles (Figure 14). In addition, we found that F2 generation fish from these parents had markedly reduced *appa* transcript abundance at 3dpf (as observed by in situ hybridization), presumably through nonsense mediated decay (Figure 2.13C). *appa* transcript abundance was also reduced in 3dpf *appa*^{ua5005/ua5005} maternal zygotic larvae (Figure 2.13D), in 2 dpf *appa*^{ua5005/ua5005} maternal zygotic larvae (Figure 2.13E, ~18.5 fold reduction, p=0.0043) and in the brains of adult maternal zygotic *appa*^{ua5005/ua5005} fish relative to wild type (Figure 2.13E, ~13-fold reduction).
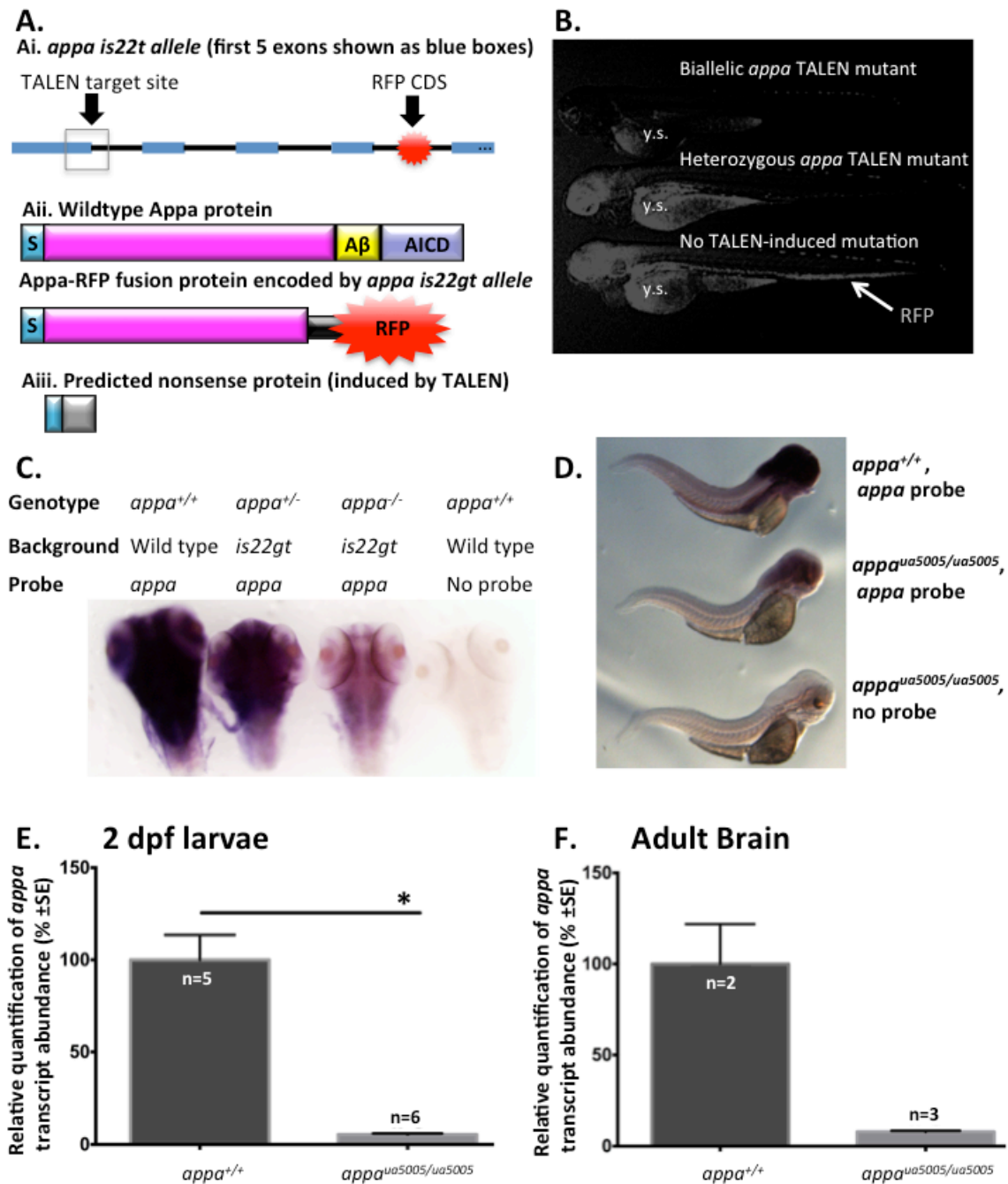
Figure 2.13. Reduced levels of appa-RFP fusion protein and *appa* transcript abundance in *appa* mutants.

A. Schematic of the protein products produced by loss-of-function *appa* alleles. **Ai.** The *is22gt* allele (Liao et al., 2012) contains a Tol2 insertion of the RFP coding sequence (red star) and splice acceptor site within intron 4, downstream of the TALEN-target site (grey

box). Exons are presented as blue boxes and introns are presented as black lines. **Aii.** The *is22gt* allele produces a truncated appa protein fused to RFP. **Aiii.** Frame-shift alleles created by *appa* TALENs are predicted to produce truncated Appa proteins that lack the RFP-fusion. **B.** RFP levels were reduced in offspring of TALEN injected-is22gt allele fish that also had TALEN-induced mutations in one or both copies. There is some auto-fluorescence in the yolk sac (y.s.). **C.** In situ hybridization revealed that 3dpf *appa*$^{+/-}$ larvae had reduced *appa* transcript abundance compared to 3dpf AB strain *appa*$^{+/+}$ larvae, and *appa* transcript abundance in 3dpf zygotic *appa*$^{-/-}$ fish was even further reduced. The *appa* mutant fish had an is22gt background and were sorted into heterozygous (*appa*$^{+/-}$) or homozygous (*appa*$^{-/-}$) groups based on RFP abundance as described in panel B. **D.** *appa* transcript levels were reduced in 3dpf *appa*$^{ua5005/ua5005}$ larvae, as shown by in situ hybridization. **E.** *appa* transcript abundance was reduced by approximately 18.5-fold in 2dpf maternal zygotic *appa*$^{ua5005/ua5005}$ fish compared to *appa* transcript abundance in 2dpf wild type fish.

 *p=0.0043 with the Mann-Whitney U-test. **F.** *appa* transcript abundance was reduced by approximately 13-fold in the brains of adult *appa*$^{ua5005/ua5005}$ fish compared to *appa* transcript abundance in brains from wild type fish. Statistics were not performed because the sample size from the wild type fish was too small (one replicate was an outlier and hence removed). n refers to the number of biological replicates (1 brain/replicate).

Three stably inherited *appa* frameshift alleles were identified in fish with the *is22gt* background

A. *appa ua5006* allele (5 bp deletion)
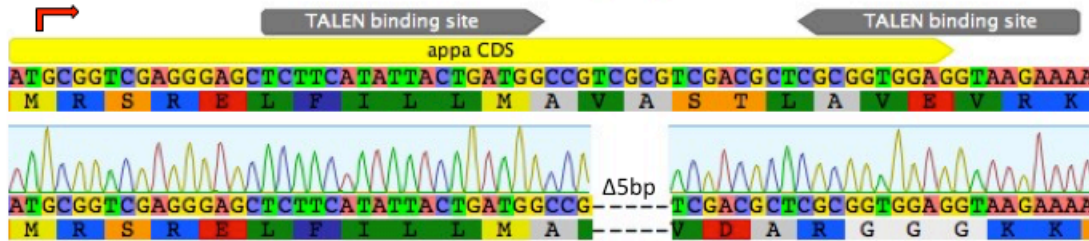
B. *appa ua5007* allele (5 bp deletion)
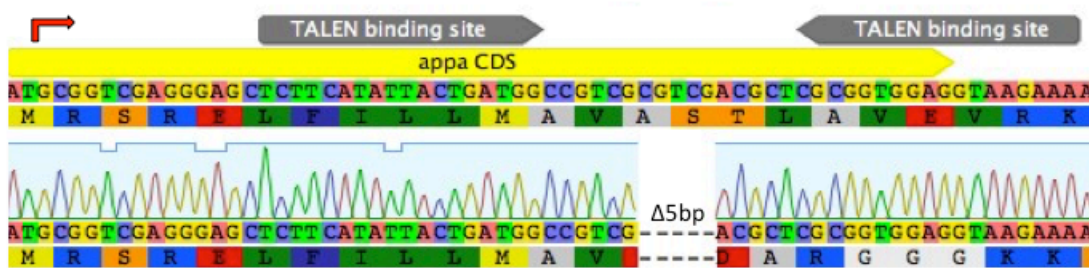
C. *appa ua5008* allele (1 bp insertion)
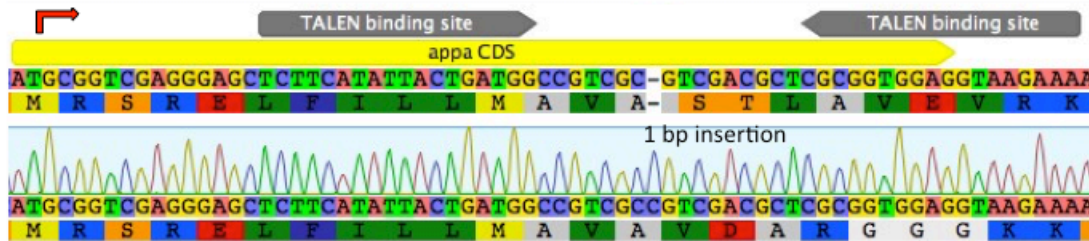
Figure 2.14. We generated multiple frameshift alleles with an is22gt background
We injected *appa* TALENs into fish that were homozygous for the *is22gt* allele (Liao et al., 2012) creating **A.** the *ua5006 appa* allele, **B.** the *ua5007 appa* allele and **C.** the *ua5008 appa* allele.

2.4.13 Why do mutants and morphants have different phenotypes?

Given that we had previously found a genetic interaction between *appa* and *prp1* via concerted injection of morpholinos (Kaiser et al., 2012), it was surprising that *appa*$^{ua5005/ua5005}$; *prp1*$^{ua5003/ua5003}$ fish displayed no overt phenotypes (Figure 2.12). In this section we address the following alternative hypotheses for these discrepancies: 1) our mutant alleles are not null; and 2) one or both morpholinos have non-specific effects.

2.4.13a. Alternative hypothesis 1-Null alleles were not generated

We partially addressed whether these alleles are null in sections above. We found that fish with the *ua5003* and *ua5004* alleles exhibit reduced *prp1* transcript abundance, and that fish with the *ua5005* allele have reduced abundance of *appa* transcripts (Figures 2.7 and 2.13, respectively); presumably through nonsense-mediated decay. It remains possible, however, that these alleles produce alternatively spliced products that escape detection by our qPCR assays. Attempts to confirm reduced protein abundance using custom rabbit α-PrP1 antibodies from GenScript's SC1649 PolyExpress Gold package (GenScript, Piscataway, NJ, USA) are not yet informative. Western blots and IHC are currently being optimized.

2.4.13b. Alternative hypothesis 2- Morpholinos used had non-specific effects

We have performed a number of experiments both herein and in our previous publication (Kaiser et al., 2012) to confirm the specificity of the *appa* and *prp1* morpholinos (Table 2.3). Among other hypotheses for our *appa* (and *appb*) morpholino results, we tested the hypothesis that pre-mRNA left behind as a result of the splice blocking morpholinos have dominant effects. As suggested by reviewers of our manuscript, we synthesized *appa* mRNA retaining intron 2 and *appb* mRNA retaining intron 3, and microinjected them into zebrafish embryos. These mRNAs did not produce toxic effects at the doses we injected (Figure 2.15, (Kaiser et al., 2012)). The design of these experiments is inherently flawed, however, because this lack of a phenotype could be the physiologically relevant answer or the result of technical failure (e.g. failure of mRNA delivery). Further, toxicity would be expected at some high dose, but such a dose may not be a physiologically relevant.

Table 2.3. Summary of experiments supporting *appa* and *prp1* morpholino specificity and a genetic interaction between *appa* and *prp1*

	Experiment	Gene targeted with Morpholino (MO)	
		Appa	*prp1*
MO co-knockdown	Multiple MOs produce same phenotype (p53 MO included)	Yes[1]	Only used 1 MO
	Partial rescue with cognate mRNA	Yes[1]	Yes[1]
	Cognate mutant mRNA (ie. mRNA with engineered stop codons) *does not* rescue	Yes[1]	Not tried
	Splicing is disrupted (for splice blocking MOs)	Yes[1]	N/A
	Reduction in protein product	Yes[1]	Yes[2]
	Mammalian homologs rescue	Yes (Human APP)[1]	Yes (Mouse *Prnp*)[1]
	mRNAs envisaged following splice blocking *do not* produce a phenotype	Yes (Figure 2.15A)[1]	N/A
	Paralog *does not* rescue co-knockdown phenotype[3]	Yes[1]	Yes[1]
	Related gene(s) *do not* rescue	Not done	Yes[1] (*sprn* ie. *Shadoo 1*)
MO into cognate	MOs *do not* produce a phenotype in cognate mutants (p53 MO included)	No (Figure 2.16B)	To be determined
	MOs produce a lesser phenotype in cognate mutants than wild type fish (p53 excluded)	Yes (Figure 2.16C)	To be determined
MO into mutant	*appa* MO into *prp1*^{-/-} mutant:		
	Same phenotype with multiple lines	Yes (Figures 2.17 and 2.18)	N/A
	Rescue with *prp1* mRNA	Yes (Figure 2.18B)	
	Mutant *prp1* mRNA *does not* rescue	Not tried	
	prp2 mRNA *does not* rescue	In progress	
	mouse *Prnp* mRNA rescues	Yes (Figure 2.18)	
	prp1 MO into *appa*^{-/-} mutant:		
	Same phenotype with multiple lines	N/A	Not tried
	Rescue with *appa* mRNA		?
	Mutant *appa* mRNA *does not* rescue		Not tried
	appb mRNA *does not* rescue		Not tried
	Mammalian APP rescues		Not tried

[1](Kaiser et al., 2012)

[2](Malaga-Trillo et al., 2009)

[3]*appb* mRNA, however, rescues knockdown of *appa* alone (Kaiser et al., 2012)
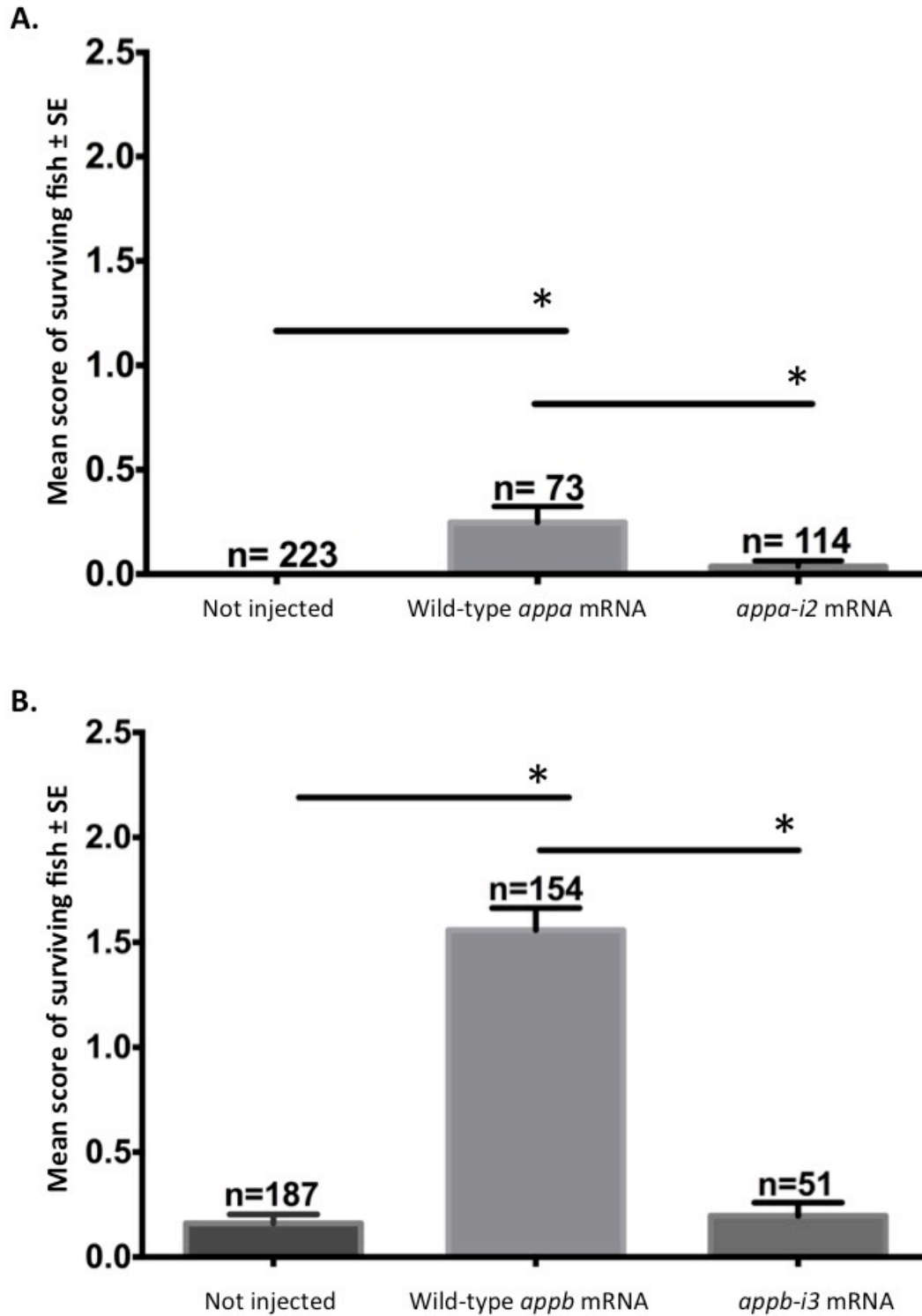
Figure 2.15. mRNAs with retained introns in *appa* and *appb* (following application of splice blocking morpholinos) do not produce dominant effects

Splice blocking morpholinos lead to mRNA with inappropriately retained introns, which contain STOP codons. Such mRNA is predicted to encode truncated proteins. While the altered mRNAs are likely to be degraded, the kinetics of this process are unknown. Thus we tested potential dominant effects of the predicted protein products by injecting mRNA with the retained introns of *appa* and *appb* into 1-2 cell stage embryos. **A.** No dominant effects were observed when 57.1pg *appa* mRNA containing the first 2 exons of *appa* plus intron 2 (*appa-i2*) was injected. Phenotypes observed in *appa-i2* mRNA-injected fish were not significantly different than those observed in un-injected embryos and milder than those observed in embryos injected with control mRNA (411.2 pg of full-length *appa* mRNA). **B.** No dominant effects were observed when *appb* mRNA containing the first 3 exons of *appb* mRNA plus intron 3 (865.1 pg *appb-i3*) was injected. Phenotypes observed in *appb-i3* mRNA-injected fish were not significantly different than those observed in un-injected embryos and milder than those observed in embryos injected with control mRNA (full-length *appb* mRNA). * $p<0.05$ with the Kruskal Wallis test. n refers to the number of embryos. Data is re-plotted from Supplemental Figure 6 in (Kaiser et al., 2012).

We further tested *appa* morpholino specificity by microinjecting our *appa* splice blocking morpholino into our *appa*$^{ua5005/ua5005}$ mutants. We found that various doses of the *appa* splice blocking morpholino produces phenotypes in *appa*$^{ua5005/ua5005}$ mutants that are comparable to what is observed in wild type fish (Figure 2.16 A-B). When *tp53* morpholino was removed from the injection solution, however, the *appa* morpholino-induced phenotype was not as penetrant in *appa*$^{-/-}$ fish as in wild type fish (Figure 2.16C, $p<0.05$) and phenotypes in *appa*$^{-/-}$ fish were in a range typical of un-injected wild type fish (Figure 2.16C). This may mean that the *appa*$^{ua5005/ua5005}$ mutants were generally sensitive to morpholino injections. In support of this hypothesis, the *appa*$^{ua5005/ua5005}$ mutants were more strongly (though not significantly) affected by the 1- ng dose of standard control morpholino than *appa*$^{+/+}$ fish (Figure 2.16B). In sum, it appears that the *appa* splice block morpholino is specific. At the time of writing, we were in the process of testing the specificity of a previously published *prp1* translation block morpholino (ZFIN ID: ZDB-MRPHLNO-100423-4; (Sempou et al., 2016)) by comparing its effects in *prp1*$^{-/-}$ embryos versus wild type embryos.
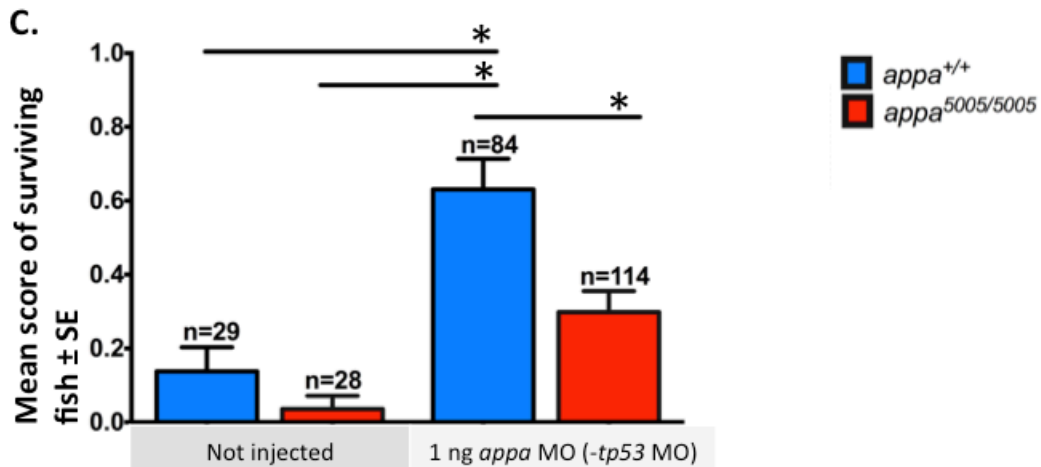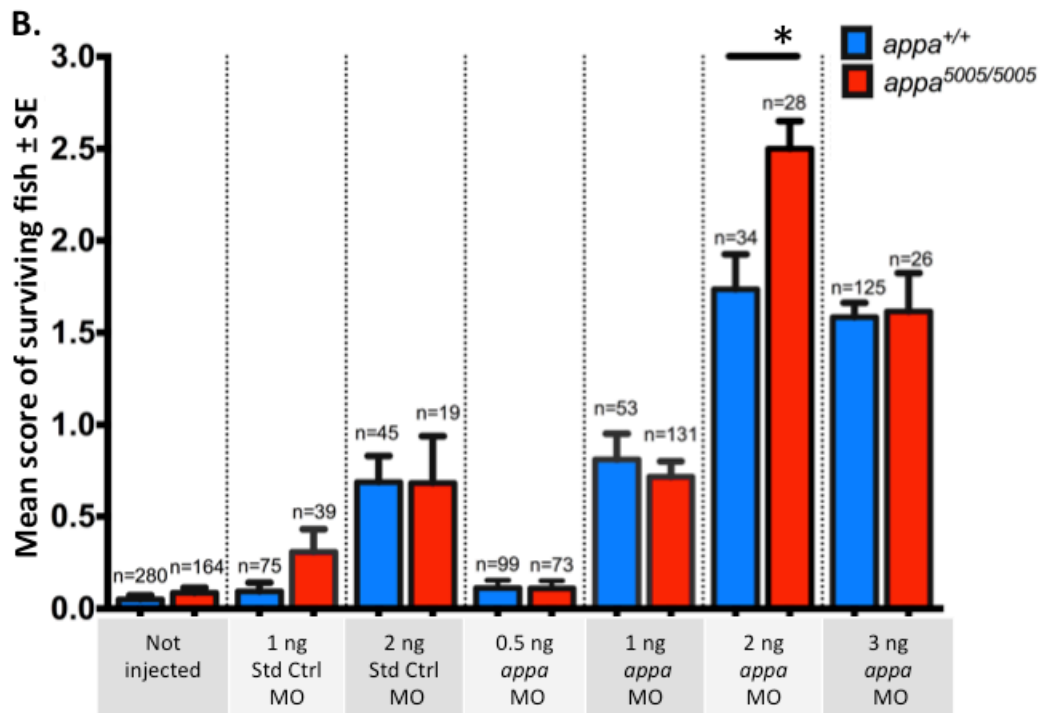
Figure 2.16. *appa* **morpholino produces milder phenotypes in** *appa*^{-/-} **mutants than in wild type embryos when injected alone, but not when co-injected with** *tp53* **morpholino**

A. *appa* splice block morpholino produced phenotypes in wild type and *appa*$^{ua5005/ua5005}$ embryos including a shorter body axis and a necrotic-like appearance in the CNS. Individual fish were assessed a score from 0-3 (3 being the most severe) based on their overall appearance. **B.** The mean scores were not significantly different between *appa*$^{ua5005/ua5005}$ embryos and *appa*$^{+/+}$ fish that were un-injected, treated with 1 or 2 ng of Std control morpholino, or treated with 0.5 ng, 1ng or 3 ng of *appa* morpholino as measured using unpaired t-tests. With 2 ng of *appa* morpholino, the mean score of the *appa*$^{ua5005/ua5005}$ mutants was significantly higher (ie. the severity of the phenotypes greater) than in *appa*$^{+/+}$ fish. *p=0.0033 with unpaired t-test. **C.** When *tp53* morpholino was not included in the injection solution, 1 ng of *appa* MO produced a mean score in wild type fish that was significantly greater (ie. The mean phenotype was more severe) than that produced in *appa*$^{ua5005/ua5005}$ fish injected with 1 ng of *appa* MO or in un-injected wild type fish. There was no significant difference in phenotypes observed between un-injected wild type or *appa*$^{ua5005/ua5005}$ and *appa*$^{ua5005/ua5005}$ embryos injected with *appa* MO. *p<0.05 with the Kruskal Wallis test. This argues in favour of *appa* MO specificity. n represents the number of fish.

2.4.14 *prp1* and *appa* specifically interact when *appa* is acutely knocked down

It is possible that selection pressure on successive generations of heterozygous and homozygous mutants of *appa* or *prp1* fish favoured compound *prp1^{ua5003/ua5003}; appa^{ua5005/ua5005}* fish that acquired compensatory genetic mechanisms to accommodate loss of these gene products. We sought to test the hypothesis that acute loss of *appa* would synergize with chronic loss of *prp1* in fish with mutant *prp1* alleles. We found that acute loss of *appa*, through the delivery of subeffective doses of *appa* morpholino, synergized with the *prp1* ua5004 allele to produce fish with morphological phenotypes that were more severe than when *appa* morpholino was delivered to wild type embryos (Figure 2.17, p<0.01). Phenotypes induced by the *appa* morpholino were partially suppressed in *prp1^{ua5004/ua5004}* fish treated with mouse *Prnp* mRNA compared to those observed in *prp1^{ua5004/ua5004}* fish treated with control mRNA (mouse *Prnp* mRNA with an early stop codon; Figure 2.18A, p<0.05). Similarly phenotypes induced by the *appa* morpholino in *prp1^{ua5003/ua5003}* fish treated with either mouse *Prnp* mRNA or *prp1* were partially suppressed (i.e. a partial rescue effect was observed) compared to those observed in fish treated with mouse *Prnp* mRNA with an early stop codon (Figure 2.18 B, p<0.05). Taken together, these results support the hypothesis that *appa* and *prp1* synergize in a protective role during early zebrafish development. These results also support specificity of the mutant phenotypes. Finally, this further suggests mammalian *Prnp,* in the context of *appa* knockdown, can functionally replace zebrafish *prp1*.
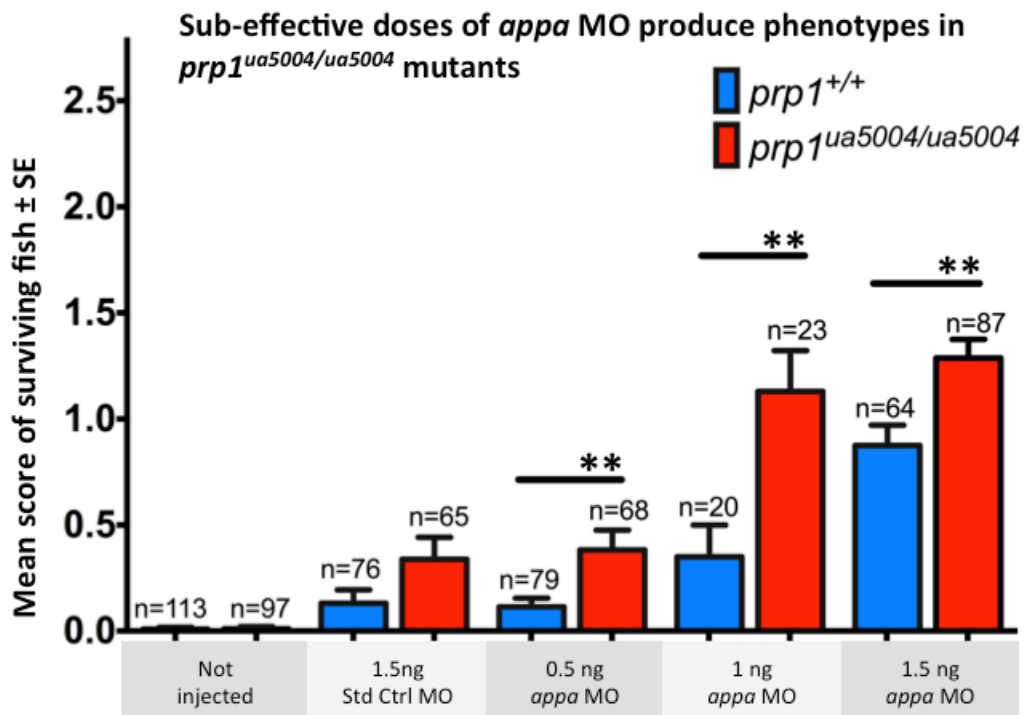
Figure 2.17. Acute loss of *appa* produces more severe developmental deficits in *prp1^{-/-}* mutants than in wild type embryos

appa MO induces a phenotype in *prp1^{ua5004/ua5004}* fish. 0.5 ng, 1 ng and 1.5 ng doses of *appa* splice blocking MO induce phenotypes that are significantly more severe in maternal zygotic *prp1^{ua5004/ua5004}* embryos than in wild type embryos. The *prp1^{ua5004/ua5004}* embryos were also more affected by 1.5 ng of standard control morpholino (Std Ctrl MO), but this did not reach statistical significance. **p<0.01 with the Mann-Whitney U-test. n refers to the number of fish. Fish were scored using the scoring criteria outlined in Figure 2.16A.
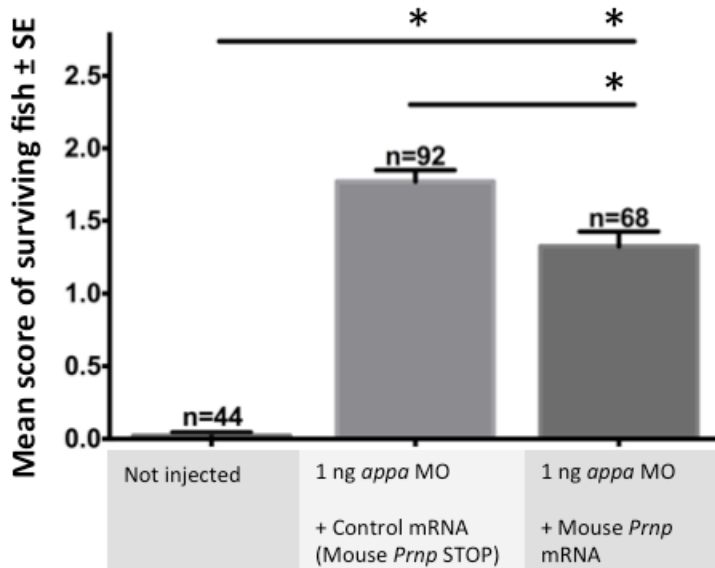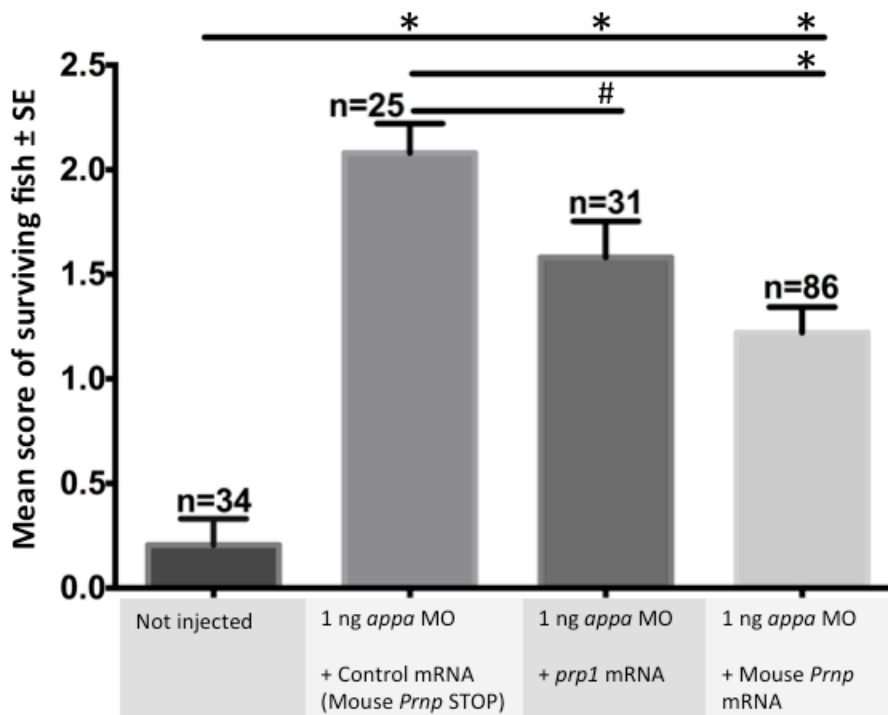
Figure 2.18. Mouse *Prnp* mRNA and *prp1* mRNA can partially rescue developmental defects observed in *prp1*^{-/-} fish treated with *appa* morpholino

A. Mouse *Prnp* mRNA partially rescues *appa* morpholino induced phenotypes in *prp1$^{ua5004/ua5004}$* mutants. *p<0.05 with Kruskal Wallis test. n refers to the number of fish. **B.** *prp1* mRNA and mouse *Prnp* mRNA partially rescue *appa* morpholino induced phenotypes in *prp1$^{ua5003/ua5003}$* mutants. *p<0.05 with Kruskal Wallis test. #p<0.05 with Mann-Whitney test. Fish were scored using the scoring criteria outlined in Figure 2.16A.

2.4.15 *prp2* does not appear to influence levels of zebrafish APP paralogs in the brain or to interact with *appb*

Since *prp1* and *appa* were found to have a specific genetic interaction, we speculated that *prp2* might also interact with the zebrafish APP paralogs. We first hypothesized that *prp2* would affect levels of zebrafish APP in the brain. The mouse α-human APP antibody clone 22C11 has previously been shown to recognize both appa and appb (Kaiser et al., 2012), so we used the same antibody here. We found that levels of zebrafish APPs were not statistically significant between brains of adult *prp2$^{ua5001/ua5001}$* mutants and the brains of wild type fish (Figure 2.19A). We also found that 2.5 ng of *appb* splice blocking morpholino produced phenotypes of similar magnitude in *prp2$^{ua5001/ua5001}$* embryos as those observed in wild type embryos (Figure 2.19B). It remains possible, however, that a difference might be observed between genotypes with a lower dose of *appb* morpholino.

A. Loss of Prp2 in adult zebrafish did not affect APP levels in the brain.
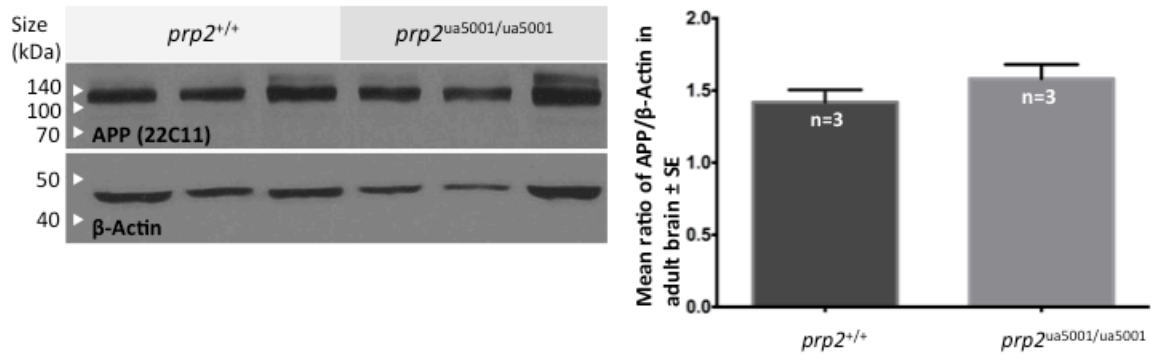
B. *appb* MO has similar effects in *prp2^{ua5001/ua5001}* fish as in wild type fish
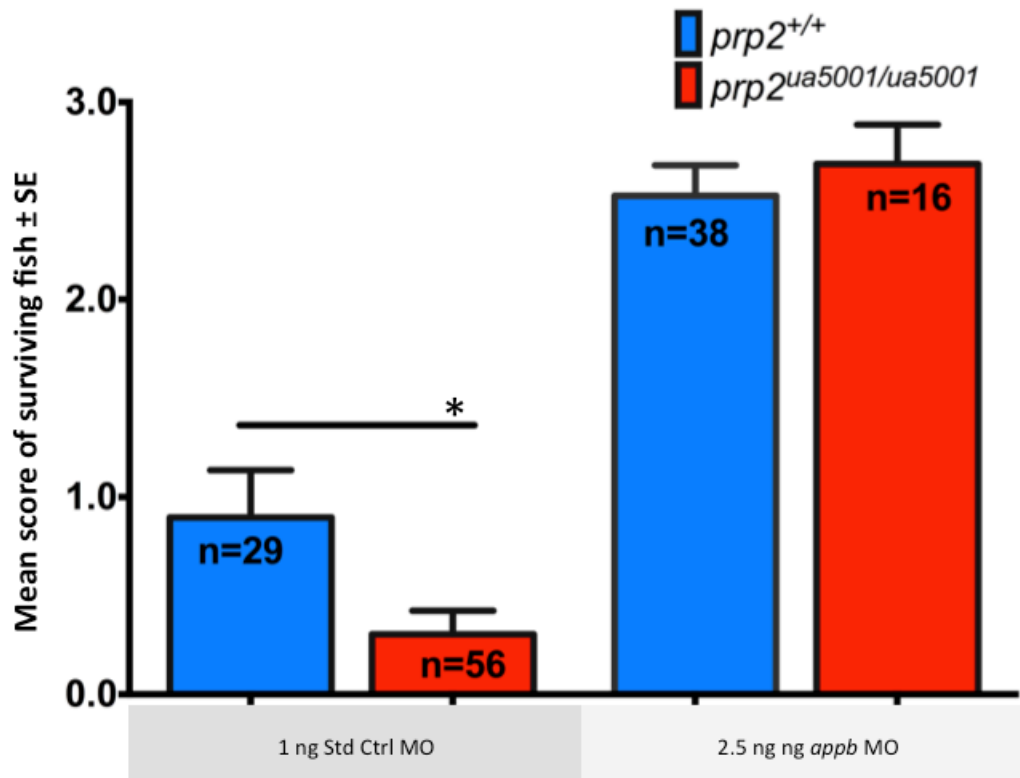
Figure 2.19. The *prp2* ua5001 allele does not appear to affect levels of zebrafish APP in adult zebrafish brains, nor synergize with acute loss of appb in zebrafish larvae

A. Western blots using the α-APP antibody clone 22C11 did not reveal a significant difference in appa and appb levels in the brains of maternal zygotic *prp2^{ua5001/ua5001}* mutants compared to those in wild type zebrafish brains with the Mann-Whitney U-test.

B. The *appb* morpholino (2.5 ng dose) did not produce significant differences in phenotype severity in *prp2*$^{ua5001/ua5001}$ embryos compared to those observed in wild type embryos (as measured with the Mann-Whitney U-test). Phenotypes observed in *prp2*$^{ua5001/ua5001}$ larvae treated with standard control morpholino (Std Ctrl MO) were slightly less severe than those observed in wild type larvae. *p= 0.0163 with the Mann-Whitney U-test.

2.5 Discussion

The overall objective of this chapter was to generate and characterize genetic resources (zebrafish *prnp* and *app* loss-of-function mutants) that could be used to study the normal physiological functions of PrP^C and APP and to identify genetic interactions between the zebrafish *prnp* and *app* paralogs. Here, we successfully used TALENs to engineer multiple lines of fish that have frameshift mutations in *appa* and *prp1*. We also generated compound maternal zygotic *prp1$^{-/-}$;prp2$^{-/-}$* fish and compound maternal zygotic *appa$^{-/-}$;prp1$^{-/-}$* fish. All of the mutant lines generated, including the compound mutants, survived to adulthood without noticeable deficits. However, *prp1$^{-/-}$* mutants were sensitive to acute loss of *appa*, supporting a genetic interaction between *appa* and *prp1*. A summary of the known interactions between zebrafish *prnp* and *app* paralogs, and those yet to be investigated are outlined in Table 2.4. The loss-of-function mutants generated herein will be used to study normal molecular functions of PrP^C and APP, which may be partially lost or subverted during prion diseases and AD.

The lack of overt phenotypes in zebrafish *prnp* and *appa* mutants is in line with what has been observed in *Prnp* knockout mice, goats and cattle (Bueler et al., 1992; Manson et al., 1994; Richt et al., 2007; Yu et al., 2009), in goats with a naturally occurring *Prnp* null allele (Benestad et al., 2012) and in *APP* knockout mice (Muller et al., 1994; Zheng et al., 1995), but differs from the developmental defects and CNS cell death found in *prp1* morphants, *appa* morphants, and when *prp1* and *appa* are knocked-down simultaneously (Kaiser et al., 2012; Malaga-Trillo et al., 2009). The differences between the morphants and mutants could be because 1) we have not created null alleles, 2) the mutant alleles are linked to other protective factors, 3) the morpholinos have off-target effects, 4) gene compensatory mechanisms exist in the mutants, and 5) a combination of these alternatives. In the next sections we consider these alternatives in turn.

Table 2.4. Summary of interactions between zebrafish *prnp* and *app* paralogs

	prp1 morphant	*prp2* morphant[3]	*appa* morphant	*appb* morphant	*prp1* mutant	*prp2* mutant	*appa* mutant
prp1 morphant							
prp2 morphant	?						
appa morphant	✔[1]	?					
appb morphant	×[1]	?	✔[1]				
prp1 mutant	?	?	✔	?			
prp2 mutant	?	?	?	×	×		
appa mutant	?	?	×*	?	×	? -Not with *appa* is22gt allele	
appb mutant[2]	?	?	?	?	?	?	?

Legend
✔ Synergize to produce overt phenotypes
✗ Do not synergize to produce overt phenotypes
? Not tested

[1](Kaiser et al., 2012)
[2]*appb* mutants have not been generated yet
[3]*prp2* morpholinos available prior to 2014 produced off-target effects (Fleisch et al., 2013; Malaga-Trillo et al., 2009; Nourizadeh-Lillabadi et al., 2010)
*Depends whether *tp53* MO is co-injected with *appa* MO (see Figure 2.16)

While we show here that *prp1* and *appa* have reduced transcript abundance, likely due to nonsense mediated decay (Culbertson, 1999), and that TALENs reduced levels of an appa-RFP fusion protein (Liao et al., 2012), we have not yet shown definitively that we have created null alleles. While deemed very unlikely, it remains theoretically possible that the *appa* mutant alleles caused a disruption in splicing such as exon skipping (Kok et al., 2015) or that the *appa* and/or *prp1* mutants begin translation at downstream translation initiation sites (Law and Sargent, 2014), or some other unknown mechanism to produce functional proteins despite the mutations we have engineered. Others in the lab are currently testing custom antibodies to determine whether we have reduced/abolished prp1 and appa protein levels in our mutant lines.

It is possible that one (or more) of the mutant alleles is on the same chromosome as protective alleles of other genes. If this were the case, an alternative combination of *prp1* and *prp2* loss-of-function alleles (or an alternative combination of *appa* and *prp1* alleles) would be expected to produce an overt phenotype. To address this hypothesis, we crossed fish with the *prp1 ua5004* allele with fish carrying the *prp2 ua5001* allele, thus reproducing the gene product disruptions of the double $prp1^{ua5003/ua5003};prp2^{ua5001/ua5001}$ mutants with an alternate *prp1* allele. If maternal zygotic $prp1^{ua5004/ua5004};prp2^{ua5001/ua5001}$ fish also display no overt phenotype, it is unlikely that the *prp1 ua5003* allele is linked to some unexpected and unlikely combination of neuroprotective factors in our compound mutants. Indeed, maternal zygotic $prp1^{ua5004/ua5004};prp2^{ua5001/ua5001}$ fish have been raised to adulthood and display no overt phenotypes, thus it is unlikely that the *prp1 ua5003* allele is linked to a protective allele of a second gene. We also crossed fish with the *prp1 ua5004* allele with fish carrying the *appa ua5007* allele, thus reproducing the gene product disruptions in $prp1^{ua5003/ua5003};appa^{ua5005/ua5005}$ compound mutants above with two independent alleles. If maternal zygotic $prp1^{ua5004/ua5004};appa^{ua5007/ua5007}$ fish also display no overt phenotype, it is unlikely that the *appa ua5005* alleles in the first set of $prp1^{-/-};appa^{-/-}$ compound mutants are linked to an unexpected protective allele. At the time of writing, others in the lab were in the process of genotyping a mixed clutch of adult fish to identify compound heterozygous $prp1^{+/ua5004};appa^{+/ua5007}$ mutants. To further test this, other independent methods to disrupt these proteins were also used, including use of morpholino knockdown of *appa* into *prp1* mutants and *vice versa*. The outcomes,

described below, are not consistent with the hypothesis that our mutant alleles are individually linked to protective factors.

While we have demonstrated specificity of the *appa* and *prp1* morpholinos herein and previously (Kaiser et al., 2012), some dose dependent off-target toxicity may exist. Rescue of a morphant phenotype with cognate mRNA is an important control to test for morpholino specificity (Bedell et al., 2011). We previously *partially* rescued our *prp1* morpholino and *appa* morpholino induced phenotypes using cognate mRNA and homologous mammalian mRNA. *appa* mRNA harbouring stop codons did not rescue the observed phenotype. We also found that a second *appa* morpholino produced the same phenotypes (Kaiser et al., 2012). Further, *appa* mRNA could rescue the *appa* and *prp1* co-knockdown, but *appb* mRNA could not (though this mRNA was able to rescue phenotypes in other gene knockdown combinations), further supporting specificity of the methods. mRNA rescue experiments in past efforts thus were thorough (thousands of embryos phenotyped in dozens of mRNA + MO rescue combinations) (Kaiser et al., 2012), and strongly supportive of MO specificity. Here, we further challenged the argument for morpholino specificity. We microinjected *appa* morpholino into its cognate mutant. Unexpectedly, we found that the *appa* morpholino produced a similar phenotype in *appa* mutants as in wild type fish. This tentatively suggests that the morpholino produce at least some off-target effects at a 1 ng dose. Without *tp53* morpholino, however, the morpholino produced phenotypes that were more penetrant in wild type fish than in their cognate mutants. Thus the apparent off-target effects observed in the *prp1*^{-/-} mutants are partly due to their sensitivity to *tp53* knockdown. Since *appa* and *prp1* were previously shown to be neuroprotective (Kaiser et al., 2012), it could be that loss of appa and prp1 sensitizes the embryos to other insults including loss of p53. An alternative explanation for the *appa* MO producing phenotypes in its cognate mutant is that the *appa* ua5005 allele is not a complete null, in which case the phenotypes observed might be caused through MO acting solely on its target transcript. Finally it is possible, though unlikely, that the *appa* MO acts on the frameshift *appa* mutant allele to produce an unusual protein product – i.e. the combination of intron inclusion and frameshift could produce a non-sense peptide with toxic effects. This would be difficult to test because delivery of mRNA with the retained intron and frameshift would be expected to produce

toxicity at some high dose and absence of a phenotype at a lower dose is not interpretable.

Chronic loss of gene function through gene editing approaches may induce compensatory mechanisms that are not induced during acute loss of the same gene. Other groups have found discrepancies between morpholino and mutant phenotypes (for examples see (Kok et al., 2015; Rossi et al., 2015)), and similar discrepancies have been found between mouse gene knockouts and siRNA knockdown (for examples see (Daude et al., 2012; Smart and Riley, 2013)). Recently, knockdown of *egfl7* using an alternative gene knockdown method, CRISPR interference (CRISPRi), was found to produce the same vascular defect phenotype in zebrafish as an *egfl7* morpholino and this phenotype was not observed in zebrafish *egfl7* loss-of function mutants (Rossi et al., 2015). CRISPRi is a variation on CRISPR/CAS9 gene editing technology. Bacteria and archaea naturally possess CRISPR systems in which CRISPR RNAs form a complex with Cas proteins to degrade complementary sequences of foreign viral and plasmid DNA (Mali et al., 2013). In CRISPR-Cas9 gene editing engineered guide RNA (gRNA) directs Cas 9 to a specific sequence where Cas9 then makes a double stranded break in the DNA (Wei et al., 2013). CRISPRi is a variation on the original CRISPR-Cas9 system that replaces Cas9 with a catalytically inactive version, dead Cas 9 (Qi et al., 2013). In zebrafish, dead Cas 9 blocks transcription of a gene when the gRNA targets the non-template strand (Rossi et al., 2015). Rossi *et al.* 2015 found that genes with similar function to *egfl7* were upregulated in *egfl7* mutants, but not in fish treated with an *egfl7* morpholino or *egfl7* CRISPRi (Rossi et al., 2015). In sum, this experience with *egfl7* supported the notion that engineering mutants (and subsequently breeding them to homozygosity) unavoidably leads to selection for individuals that are able to thrive in absence of the target gene product.

Since *appa*$^{-/-}$;*prp1*$^{-/-}$ mutants did not recapitulate the developmental phenotype we observed through co-knockdown of of *appa* and *prp1*, we set out to test the hypothesis that *prp1* is protective when *appa* is acutely knocked down (ie. when there is no opportunity for gene compensation due to selection pressure). We found that *prp1* mutants were more sensitive to acute loss of *appa* than wild type fish and this effect could be rescued with *prp1* mRNA and mouse *Prnp* mRNA. It will be important to

determine whether *appa* mutants are more sensitive to *prp1* knockdown than wild type fish. Taken together, these results support the hypothesis that gene compensation is occurring in the *prp1*$^{-/-}$ mutants.

Compound maternal zygotic *prp1*$^{-/-}$;*prp2*$^{-/-}$ zebrafish mutants also did not display overt phenotypes, which is surprising in light of the developmental defects that are observed when *prp1* is acutely knocked down (Kaiser et al., 2012; Malaga-Trillo et al., 2009). Others in the lab are now searching for molecular phenotypes in these mutants via RNA-sequencing (RNA-Seq). The RNA-Seq data has provided independent confirmation that *prp1* and *prp2* transcript levels are reduced in compound *prp1*$^{ua5003/ua003}$;*prp2*$^{ua5001/ua5001}$ mutants (Pollock et al., unpublished). Transcript abundance of *appa*, *appb* and the APP family member, *amyloid beta (A4) precursor-like protein 2* (*aplp2*) were unchanged in *prp1*$^{ua5003/ua5003}$;*prp2*$^{ua5001/ua5001}$ mutants compared to wild type larvae in the RNA Seq data, but this awaits verification via qPCR (Pollock et al., unpublished).

In the future it will also be interesting to test whether *prp2* mutants are more sensitive to acute loss of *prp1* than wild type fish, and whether *prp1* mutants are more sensitive to acute loss of *prp2* than wild type fish. The latter could be tested using the new *prp2* morpholinos described in (Huc-Brandt et al., 2014) that appear to lack the off-target effects produced by previous *prp2* morpholinos.(Fleisch et al., 2013; Malaga-Trillo et al., 2009; Nourizadeh-Lillabadi et al., 2010).

The new *appa*$^{-/-}$ mutants, *prp1*$^{-/-}$ mutants, compound *prp1*$^{-/-}$;*prp2*$^{-/-}$ mutants and compound *prp1*$^{-/-}$;*appa*$^{-/-}$ mutants we have generated herein will be used to uncover *in vivo* functions of APP and PrP. Further investigation of mouse *APP* and *Prnp* knockouts has unveiled subtle phenotypes (examples include alterations in circadian rhythm and disrupted myelination in *Prnp*$^{-/-}$ mice (Bremer et al., 2010; Tobler et al., 1996)), and both *APP* and *Prnp* knockout mice are more sensitive to insults such as seizure inducing drugs or hypoxic conditions (Beraldo et al., 2013; Carulla et al., 2011; Carulla et al., 2015; McLennan et al., 2004; Rangel et al., 2007; Steinbach et al., 1998; Walz et al., 1999). We discuss roles for zebrafish Prp in protecting against seizure susceptibility and in memory in Chapters 3 and 5, respectively. One of the main advantages of creating our mutant zebrafish alleles is that they will serve as a backdrop and wholly unique resource to study the normal role of APP and PrP, including mammalian homologs. We will attempt to

rescue further loss of function phenotypes that we identify in our mutants (such as the neural development phenotypes, which are discussed in Chapter 4) using mammalian *APP* and *Prnp* mRNA. We will then be able to dissect the roles of particular protein domains and residues by attempting to rescue these phenotypes with mutated mammalian *APP* and *Prnp* mRNA.

Chapter 2 References

Abramsson, A., et al., 2013. The zebrafish amyloid precursor protein-b is required for motor neuron guidance and synapse formation. Dev Biol. 381**,** 377-88.

Banote, R. K., et al., 2016. beta-Amyloid precursor protein-b is essential for Mauthner cell development in the zebrafish in a Notch-dependent manner. Dev Biol. 413**,** 26-38.

Bedell, V. M., et al., 2011. Lessons from morpholino-based screening in zebrafish. Brief Funct Genomics. 10**,** 181-8.

Beraldo, F. H., et al., 2013. Stress-inducible phosphoprotein 1 has unique cochaperone activity during development and regulates cellular response to ischemia via the prion protein. FASEB J. 27**,** 3594-607.

Boch, J., et al., 2009. Breaking the code of DNA binding specificity of TAL-type III effectors. Science. 326**,** 1509-12.

Bogdanove, A. J., Voytas, D. F., 2011. TAL effectors: customizable proteins for DNA targeting. Science. 333**,** 1843-6.

Bremer, J., et al., 2010. Axonal prion protein is required for peripheral myelin maintenance. Nat Neurosci. 13**,** 310-8.

Bueler, H., et al., 1992. Normal development and behaviour of mice lacking the neuronal cell-surface PrP protein. Nature. 356**,** 577-582.

Bustin, S. A., et al., 2009. The MIQE guidelines: minimum information for publication of quantitative real-time PCR experiments. Clin Chem. 55**,** 611-22.

Carulla, P., et al., 2011. Neuroprotective role of PrPC against kainate-induced epileptic seizures and cell death depends on the modulation of JNK3 activation by GluR6/7-PSD-95 binding. Mol Biol Cell. 22**,** 3041-54.

Carulla, P., et al., 2015. Involvement of PrP(C) in kainate-induced excitotoxicity in several mouse strains. Sci Rep. 5**,** 11971.

Chang, N., et al., 2013. Genome editing with RNA-guided Cas9 nuclease in zebrafish embryos. Cell Res. 23**,** 465-72.

Chen, S., et al., 2013. A large-scale in vivo analysis reveals that TALENs are significantly more mutagenic than ZFNs generated using context-dependent assembly. Nucleic Acids Res. 41**,** 2769-78.

Culbertson, M. R., 1999. RNA surveillance. Unforeseen consequences for gene expression, inherited genetic disorders and cancer. Trends Genet. 15**,** 74-80.

Daude, N., et al., 2012. Knockout of the prion protein (PrP)-like Sprn gene does not produce embryonic lethality in combination with PrP(C)-deficiency. Proc Natl Acad Sci U S A. 109**,** 9035-40.

Doyon, Y., et al., 2008. Heritable targeted gene disruption in zebrafish using designed zinc-finger nucleases. Nat Biotechnol. 26**,** 702-8.

Eisen, J. S., Smith, J. C., 2008. Controlling morpholino experiments: don't stop making antisense. Development. 135**,** 1735-43.

Fleisch, V., et al., 2013. Targeted mutation of the gene encoding prion protein in zebrafish reveals a conserved role in neuron excitability. Neurobiol Dis. 55**,** 11-25.

Hiolski, E. M., et al., 2014. Chronic low-level domoic acid exposure alters gene transcription and impairs mitochondrial function in the CNS. Aquat Toxicol. 155**,** 151-9.

Huang, P., et al., 2011. Heritable gene targeting in zebrafish using customized TALENs. Nat Biotechnol. 29**,** 699-700.

Huang, P., et al., 2012. Reverse genetic approaches in zebrafish. J Genet Genomics. 39**,** 421-33.

Huc-Brandt, S., et al., 2014. Zebrafish prion protein PrP2 controls collective migration process during lateral line sensory system development. PLoS One. 9**,** e113331.

Hurt, J. A., et al., 2003. Highly specific zinc finger proteins obtained by directed domain shuffling and cell-based selection. Proc Natl Acad Sci U S A. 100**,** 12271-6.

Hwang, W. Y., et al., 2013. Efficient genome editing in zebrafish using a CRISPR-Cas system. Nat Biotechnol. 31**,** 227-9.

Joshi, P., et al., 2009. Amyloid precursor protein is required for convergent-extension movements during Zebrafish development. Dev Biol. 335**,** 1-11.

Kaiser, D., et al., 2012. Amyloid beta precursor protein and prion protein have a conserved interaction affecting cell adhesion and CNS development. PloS One. 7.

Kawakami, K., et al., 2004. A transposon-mediated gene trap approach identifies developmentally regulated genes in zebrafish. Dev Cell. 7**,** 133-44.

Kim, Y. G., et al., 1996. Hybrid restriction enzymes: zinc finger fusions to Fok I cleavage domain. Proc Natl Acad Sci U S A. 93, 1156-60.

Kok, F. O., et al., 2015. Reverse genetic screening reveals poor correlation between morpholino-induced and mutant phenotypes in zebrafish. Dev Cell. 32, 97-108.

Langheinrich, U., et al., 2002. Zebrafish as a model organism for the identification and characterization of drugs and genes affecting p53 signaling. Curr Biol. 12, 2023-8.

Law, S. H., Sargent, T. D., 2014. The serine-threonine protein kinase PAK4 is dispensable in zebrafish: identification of a morpholino-generated pseudophenotype. PLoS One. 9, e100268.

Liao, H. K., et al., 2012. Tol2 gene trap integrations in the zebrafish amyloid precursor protein genes appa and aplp2 reveal accumulation of secreted APP at the embryonic veins. Dev Dyn. 241, 415-425.

Lieschke, G. J., Currie, P. D., 2007. Animal models of human disease: zebrafish swim into view. Nat Rev Genet. 8, 353-67.

Malaga-Trillo, E., et al., 2009. Regulation of Embryonic Cell Adhesion by the Prion Protein. PloS Biology. 7, 576-590.

Mali, P., et al., 2013. RNA-guided human genome engineering via Cas9. Science. 339, 823-6.

Manson, J. C., et al., 1994. 129/Ola mice carrying a null mutation in PrP that abolishes mRNA production are developmentally normal. Mol Neurobiol. 8, 121-7.

McLennan, N., et al., 2004. Prion protein accumulation and neuroprotection in hypoxic brain damage. Am J Pathol. 165, 227-235.

Meeker, N. D., et al., 2007. Method for isolation of PCR-ready genomic DNA from zebrafish tissues. Biotechniques. 43, 610.

Meng, X., et al., 2008. Targeted gene inactivation in zebrafish using engineered zinc-finger nucleases. Nat Biotechnol. 26, 695-701.

Miller, J. C., et al., 2011. A TALE nuclease architecture for efficient genome editing. Nat Biotechnol. 29, 143-8.

Moussavi Nik, S. H., et al., 2012. The BACE1-PSEN-AbetaPP regulatory axis has an ancient role in response to low oxygen/oxidative stress. J Alzheimers Dis. 28**,** 515-30.

Muller, U., et al., 1994. Behavioral and anatomical deficits in mice homozygous for a modified beta-amyloid precursor protein gene. Cell. 79**,** 755-65.

Mussolino, C., et al., 2011. A novel TALE nuclease scaffold enables high genome editing activity in combination with low toxicity. Nucleic Acids Res. 39**,** 9283-93.

Norton, W., Bally-Cuif, L., 2010. Adult zebrafish as a model organism for behavioural genetics. BMC Neurosci. 11**,** 90.

Nourizadeh-Lillabadi, R., et al., 2010. Early Embryonic Gene Expression Profiling of Zebrafish Prion Protein (Prp2) Morphants. PloS One. 5.

Panula, P., et al., 2010. The comparative neuroanatomy and neurochemistry of zebrafish CNS systems of relevance to human neuropsychiatric diseases. Neurobiol Dis. 40**,** 46-57.

Pillay, L. M., et al., 2013. Evaluating the Mutagenic Activity of Targeted Endonucleases Containing a Sharkey FokI Cleavage Domain Variant in Zebrafish. Zebrafish. 10, 353-64.

Porteus, M. H., Carroll, D., 2005. Gene targeting using zinc finger nucleases. Nat Biotechnol. 23**,** 967-73.

Qi, L. S., et al., 2013. Repurposing CRISPR as an RNA-guided platform for sequence-specific control of gene expression. Cell. 152**,** 1173-83.

Rangel, A., et al., 2007. Enhanced susceptibility of Prnp-deficient mice to kainate-induced seizures, neuronal apoptosis, and death: Role of AMPA/kainate receptors. J Neurosci Res. 85**,** 2741-55.

Richt, J. A., et al., 2007. Production of cattle lacking prion protein. Nat Biotechnol. 25**,** 132-8.

Robu, M. E., et al., 2007. p53 activation by knockdown technologies. PloS Genetics. 3**,** 787-801.

Rodriguez, F., et al., 2002. Spatial memory and hippocampal pallium through vertebrate evolution: insights from reptiles and teleost fish. Brain Res Bull. 57**,** 499-503.

Rossi, A., et al., 2015. Genetic compensation induced by deleterious mutations but not gene knockdowns. Nature. 524, 230-3.

Sander, J. D., et al., 2011. Targeted gene disruption in somatic zebrafish cells using engineered TALENs. Nat Biotechnol. 29, 697-8.

Sempou, E., et al., 2016. Activation of zebrafish Src family kinases by the prion protein is an amyloid-beta-sensitive signal that prevents the endocytosis and degradation of E-cadherin/beta-catenin complexes in vivo. Mol Neurodegener. 11, 18.

Smart, N., Riley, P. R., 2013. Thymosin beta4 in vascular development response to research commentary. Circ Res. 112, e29-30.

Solis, G. P., et al., 2013. Conserved roles of the prion protein domains on subcellular localization and cell-cell adhesion. PLoS One. 8, e70327.

Song, P., Pimplikar, S. W., 2012. Knockdown of amyloid precursor protein in zebrafish causes defects in motor axon outgrowth. PLoS One. 7, e34209.

Steinbach, J. P., et al., 1998. Hypersensitivity to seizures in beta-amyloid precursor protein deficient mice. Cell Death Differ. 5, 858-66.

Tobler, I., et al., 1996. Altered circadian activity rhythms and sleep in mice devoid of prion protein. Nature. 380, 639-42.

Walz, R., et al., 1999. Increased sensitivity to seizures in mice lacking cellular prion protein. Epilepsia. 40, 1679-1682.

Wang, P., et al., 2005. Defective neuromuscular synapses in mice lacking amyloid precursor protein (APP) and APP-Like protein 2. J Neurosci. 25, 1219-25.

Wang, Z. L., et al., 2009. Presynaptic and Postsynaptic Interaction of the Amyloid Precursor Protein Promotes Peripheral and Central Synaptogenesis. J Neurosci. 29, 10788.

Wei, C., et al., 2013. TALEN or Cas9 - Rapid, Efficient and Specific Choices for Genome Modifications. J Genet Genomics. 40, 281-9.

Westerfield, M., 2000. The Zebrafish Book. A Guide for the Laboratory Use of Zebrafish (Danio rerio). University of Oregon Press, Eugene, OR.

Wienholds, E., et al., 2002. Target-selected inactivation of the zebrafish rag1 gene. Science. 297, 99-102.

Yu, G., et al., 2009. Generation of goats lacking prion protein. Mol Reprod Dev. 76, 3.

Zheng, H., et al., 1995. beta-Amyloid precursor protein-deficient mice show reactive gliosis and decreased locomotor activity. Cell. 81**,** 525-31.

Chapter 3. PrP^C has an ancient conserved role in regulating neural activity[15]

3.1 Summary

Neuroprotection is one of many roles that have been attributed to PrP^C in healthy brains, and disruption of these neuroprotective functions likely contributes to neuron degeneration in prion diseases and Alzheimer's disease (AD), as discussed in Chapter 1. It is important, therefore, to uncover the molecular mechanisms underlying PrP^C's neuroprotective functions to develop effective therapies. Here we sought to develop a zebrafish paradigm to study PrP^C's role in protecting against convulsant-induced seizures. We found that zebrafish prp2 (one of the two zebrafish paralogs of PrP^C) protects against induced seizure-like behaviour. Further, $prp2^{-/-}$ larvae, $prp1^{-/-}$ larvae, and compound $prp1^{-/-};prp2^{-/-}$ larvae had increased expression of the immediate early gene, *c-fos,* compared to wild type fish when exposed to the convulsant, PTZ; indirectly suggesting that *prp1* and *prp2* have redundant roles in suppressing neural activity. Further, it appears that PrP^C has a conserved role in regulating neural activity because mouse *Prnp* rescued PTZ-induced *c-fos* expression in $prp1^{-/-};prp2^{-/-}$ larvae. Future studies will use this zebrafish paradigm to determine which residues of PrP^C mediate this protective function and to screen for therapeutic candidates for prion disease and AD.

3.2 Introduction

While PrP^C has many putative functions, one of its most consistently reported roles is neuroprotection, loosely defined as the protection of neurons from dysfunction or death (reviewed in (Steele et al., 2007)). PrP^C protects against ischemia and convulsant induced-seizures (Carulla et al., 2011; Carulla et al., 2015; McLennan et al., 2004; Rangel et al., 2007; Sakurai-Yamashita et al., 2005; Shyu et al., 2005; Walz et al., 1999; Weise et al., 2006), but the molecular mechanisms underlying these protective effects, including elucidating which domains of PrP^C are involved, require further investigation. PrP^C may mediate neuroprotection through various mechanisms by interacting with multiple ligands. For example, it has been demonstrated that PrP^C prevents apoptosis (Chiarini et al., 2002), likely through its interaction with stress-inducible protein 1 (Sti1) (Zanata et al., 2002). Another possibility is that PrP^C mediates neuroprotection by regulating neuron activity. PrP^C has been shown to regulate NMDA receptors in mouse brain slices through its interaction with copper ions (Khosravani et al., 2008; You et al.,

2012), and loss of *prp2* (one of two *Prnp* parologs in zebrafish) was found to alter the decay kinetics of NMDA receptors in zebrafish larvae (Fleisch et al., 2013). Phenotypes observed in mice transgenically expressing N-terminal deletion mutants of PrP[C] led to the broad hypothesis that PrP[C] initiates neuroprotection through its interaction with yet-to-be identified ligands. Mice transgenically expressing murine PrP[C] lacking residues 32-121 or 32-134 (PrPΔ32-121 and PrPΔ32-134, respectively) exhibit ataxia and neuron degeneration, which can be reversed with one copy of wild type PrP[C] (Flechsig et al., 2003; Shmerling et al., 1998); while murine PrPΔ94-134 and PrPΔ105-125 cause lethality that can be rescued with higher gene doses of wild type *Prnp* (Baumann et al., 2007; Li et al., 2007). *Prnp*^{-/-} mice expressing the PrPΔ32-134 transgene also display myelination and axon defects (Radovanovic et al., 2005). Because smaller deletions (Δ32-80, Δ32-93 and Δ32-106) did not produce the ataxic and neuronal degeneration phenotypes, it was suggested that PrP[C] residues between 106 and 134 might mediate neurotrophic signalling through interaction with a ligand. Truncated proteins PrPΔ32-121 and PrPΔ32-134 might still bind to the ligand but be unable to initiate neurotrophic signalling (Shmerling et al., 1998). *In vivo* disruptions of protein function resulting from amino acid changes or larger domain changes can be assayed with relative ease by delivering control and modified mRNAs to one-cell stage zebrafish embryos, and zebrafish larvae are amenable to high throughput drug screens (reviewed in (Lieschke and Currie, 2007)). We therefore sought to develop a paradigm to assay PrP[C]'s protective functions in zebrafish. Since assays to assess seizure susceptibility are well established in zebrafish larvae (Baraban et al., 2007; Baraban et al., 2005), we aimed to test the hypothesis that PrP[C]'s function in suppressing convulsant-induced seizures is conserved between fish and mammals.

The convulsant pentylenetetrazole (PTZ) reliably induces seizure-like behaviour in zebrafish larvae, and electrophysiological and molecular indicators of seizures, comparable to those in mammalian seizure models, are observed in PTZ-treated larval zebrafish (Baraban et al., 2007; Baraban et al., 2005; Baxendale et al., 2012). Three stages of seizure-like activity are elicited in PTZ-treated larvae in a dose-dependent manner (2.5 mM induces Type I and Type II seizures, 5 mM induces Stage III seizures in some fish). Stage I seizures are characterized by a marked increase in activity compared

to that observed in untreated larvae. Larvae undergoing Stage II seizures display a rapid circling pattern of movement, while those undergoing Stage III seizures display clonus-like convulsions and fall onto their sides (Baraban et al., 2005). Further, electrophysiological recordings revealed epileptiform discharges in larvae exposed to a high dose (15 mM) of PTZ (Baraban et al., 2005). Finally, PTZ-treated zebrafish larvae upregulate expression of immediate-early genes including *c-fos*, bHLH-PAS-domain-containing transcription factor (*npas4*) and brain-derived neurotrophic factor (*bdnf*), and expression of *c-fos* in PTZ-treated fish was suppressed with the anti-epilectic drug, sodium valproate (Baxendale et al., 2012). These genes are involved in neuron survival, neurite growth and synaptic development (Greer and Greenberg, 2008). Since these genes are regulated by neuronal activity, they can be deployed as markers of neural activity (Baxendale et al., 2012). We deployed PTZ-induced seizure-like activity and *c-fos* expression in larvae zebrafish to study the role of PrP^C in neuroprotection.

We hypothesized that *prp2* modulates convulsant-induced activity in zebrafish larvae, and that *prp2* and *prp1* have redundant and conserved roles in modulating convulsant-induced neural activity. Indeed we found that *prp2$^{-/-}$* larvae were more susceptible to PTZ-induced seizure-like behaviour. Further, *prp2$^{-/-}$, prp1$^{-/-}$* and compound *prp1$^{-/-}$;prp2$^{-/-}$* larvae had increased expression of the immediate early gene, *c-fos,* compared to wild type fish when exposed to PTZ. This indirectly suggests that *prp1* and *prp2* have redundant roles in suppressing neural activity. Further, mouse *Prnp* appeared to rescue PTZ-induced *c-fos* expression in *prp1$^{-/-}$;prp2$^{-/-}$* larvae in one trial, suggesting that PrP^C has a conserved role in regulating neural activity.

3.3 Methods

3.3.1 Animal ethics and zebrafish husbandry

Zebrafish were raised and maintained using protocols approved by the Animal Care & Use Committee: Biosciences at the University of Alberta, operating under the guidelines of the Canadian Council of Animal Care. The fish were raised and maintained within the University of Alberta fish facility at 28°C under a 14/10 light/dark cycle as previously described (Westerfield, 2000). The *prp2$^{ua5001/ua5001}$* mutants, generated in (Fleisch et al., 2013), and the *prp1$^{ua5003/ua5003}$* , *prp1$^{ua5004/ua5004}$* and compound *prp1$^{ua5003/ua5003}$;*

prp2^{ua5001/ua5001} mutants, generated as described in Chapter 2, were maintained on an AB background. Closely related (though not siblings unless otherwise stated) wild type AB strain zebrafish were used as controls. Larvae used for *in situ* hybridization and qPCR experiments were treated with 1-phenol-2-thiourea (PTU) at approximately 24 hpf (or 8-10 hpf for fish used for the in situ hybridization experiment) to prevent formation of melanin pigment.

3.3.2 Behavioural analysis of PTZ-induced seizures

Established assays for measuring stage I and II seizures were performed (Baraban et al., 2007; Baraban et al., 2005). Behavioral tracking software quantified the movement of zebrafish larvae arrayed in a 96-well plate. 3 dpf zebrafish larvae were acclimatized in their typical embryonic growth media (E3 medium) for 30 min and subsequently subjected to 2.5 mM PTZ for 30 min. This dose has previously been shown to produce Stage I and Stage II Stage seizures in larval zebrafish (defined in section 3.2 (Baraban et al., 2005)). Swimming behavior during both acclimation and PTZ exposure was monitored. Fish were monitored individually in single wells of a 96 well, flat bottom plate containing 100 or 200 μL of fluid. The plate was placed on a light box with an overhead video recording and tracking system. Motion was captured at 30 frames per second using a high-resolution camera (SX-920C-HR; Matco Canada, St. Laurent, QC) connected to a video capture card (Picolo H.264; Euresys, San Juan Capistrano, CA) in a PC running EthoVision® XT7 software (Noldus, Wageningen, Netherlands), as described previously (Bhinder and Tierney, 2012). Researchers were blinded to fish genotype throughout the behavioral assessment. After tracking the fish movement, raw data (30 data points/second/ fish) was exported to Microsoft Excel to calculate swimming speed and then transformed into 10 s time bins. The average velocity, excluding data points generated when the fish were out of view from the camera, was calculated during two time periods consisting of the final 15 min of the acclimation period, and minutes 5–20 following PTZ addition. Movement following addition of convulsant (2.5 mM PTZ) was normalized to the movement of the larva during an acclimation period prior to addition of convulsant.

3.3.3 Production and delivery of mRNA for rescue experiments

Zebrafish *prp1* and *prp2* (NCBI accession numbers JQ994489 and JQ994490, respectively) were cloned into the pCS2+ vector as previously described (Kaiser et al., 2012). Mouse *Prnp* cDNA (NCBI accession NM_011170) was cloned into the pCS2+ vector. A QuikChange Lightning Site-Directed Mutagenesis Kit (Stratagene/Agilent catalogue #210518, Santa Clara, CA, USA) was used to introduce a stop codon at the 8th codon (T to A substitution at position 23) in pCS2+ zebrafish *prp2* and at the 16th codon (G to A substitution at position 48) in pCS2+ *mouse Prnp*. Site-directed mutagenesis was also used to create a 1 base pair deletion in pCS2-*prp1* and an 8 base pair deletion in pMe-*prp2* (equivalent to the ua5001 mutation). Primers used for site directed mutagenesis are shown in Table 3.1. *egpf* and *mcherry* were obtained as 3' Gateway entry clones and cloned into the pCS2+ destination vector using LR Clonase II (Invitrogen/Thermo Fisher Scientific catalogue #11791101, Waltham, MA, USA). Following linearization with FastDigest Not I (Thermo Fisher Scientific, catalogue #FD0593, Waltham, MA, USA), mRNA was transcribed from these plasmids *in vitro* using an mMessage SP6 kit (Ambion/ Thermo Fisher Scientific catalogue #AM1340, Waltham, MA, USA) and mRNA concentration was determined using a NanoDrop spectrophotometer.

Table 3.1. Site directed mutagenesis primers use to modify template plasmids for mRNA synthesis

Plasmid	Mutated Codon	Forward primer	Reverse primer
pCS2+ Mouse *Prnp* stop	Codon16 (G→A)	5'CTCTTTGTGACTATGTG AACTGATGTCGGCCTCTG-3'	5'CAGAGGCCGACATCAGTTC ACATAGTCACAAAGAG-3'
pCS2+ *prp2* stop	Codon 8 (T→A)	5'GATGGGTCGCTTAACAA TACTATAGCTCTGTCTGGC-3'	5'GCCAGACAGAGCTATAGTA TTGTTAAGCGACCCATC-3'
pCS2+ *prp1*stop	Codon 5 ΔT	5'GGACCAAAATGGGGGA GTTAGCAAACTTCTAGCC ATCG-3'	5'CGATGGCTAGAAGTTTGCTA ACTCCCCCATTTTGGTCC-3'
pCS2+ *prp2 ua5001*	Codon 92 Δ8bp	5'AGAATCCACCTCCCTCC CTGCTGGAGGTGGGTA-3'	5'TACCCACCTCCAGCAGGGA GGGAGGTGGATTCT-3'

For rescue of the PTZ-induced behavioural phenotypes, microinjection solutions were prepared with the appropriate volume of 'rescue' or control mRNA, 0.0625 % Dextran, KCl (to a final concentration of 0.01mM), and nuclease free water. For rescue of PTZ-induced expression of *c-fos*, microinjection solutions were prepared with the appropriate volume of 'rescue' or control mRNA, 25 pg of *mCherry* mRNA (for use in qPCR) or *egfp* mRNA (for use in *in situ* hybridization), KCl (to a final concentration of 0.01mM), phenol red (to a final concentration of 0.0125-0.0625%) and nuclease free water. The injection volume was calibrated to 1 nL using an ocular micrometer immediately prior to injections. Fish were screened for the appropriate marker (Dextran, egfp mRNA or mCherry mRNA) at 24 hpf and again immediately before drug treatments to screen for individuals that were successfully injected.

3.3.4 Inducing *c-fos* expression with PTZ for in situ hybridization experiments

Larvae (2dpf) were dechorionated using 1 mg/mL pronase and rinsed three times with E3 embryo media prior to drug treatment. Deformed/developmentally delayed fish were removed. Fish injected with mRNA were sorted for *egfp* fluorescence and those with comparable levels of *egfp* between treatments were selected for analysis. Fish were then treated with 20 mM PTZ or vehicle (E3 medium) for 90 minutes at room temperature in a well-lit room. After PTZ treatment, fish were rinsed several times with E3 medium and then fixed overnight in 4% (PFA) in phosphate buffer (pH 7.4) with 5% sucrose. Fish were then washed in 50% methanol/DEPC-treated water for 5 minutes, rinsed in 100% MeOH and stored in 100% MeOH at -20° C until being re-hydrated for *in situ* hybridization.

3.3.5 *c-fos* in situ hybridization

Probe production: RNA was extracted from wild type zebrafish larvae using an RNeasy Mini Kit (Qiagen catalogue #74104, Toronto, ON, Canada). A 602 base pair cDNA product was then produced from wild type zebrafish larvae using a Qiagen LongRange 2-Step RT-PCR kit (Qiagen catalogue #205920, Toronto, ON, Canada). For the initial PCR reaction, primers from a previous publication (deCarvalho et al., 2013) were used: Forward: 5'-TCTCCTCTGTGGCGCCCTCC-3'; Reverse 5'GTCTGGAACCGAGCGAGCCG-3'. In the second step of the synthesis, the enzyme

mix was replaced with recombinant Taq (Invitrogen/ Thermo Fisher Scientific catalogue #10342-020, Waltham, MA, USA) as the enzyme provided in the kit removes 3' poly-A overhangs that are required for Topo cloning. The cDNA product was then cloned into the pCr2.1 Topo vector (Invitrogen) and sequenced to verify the insert orientation in the plasmids. The resulting plasmid was linearized with FastDigest KpnI (ThermoFisher Scientific catalogue #FD0524, Waltham, MA, USA), purified by ethanol precipitation as outlined in Chapter 2 and used to template production of DIG-labeled riboprobe with T7 RNA polymerase (Roche/Sigma catalogue #10881775001, St. Louis, MO, USA) as described in Chapter 2, except larger volumes of each reagent were added to facilitate production of a larger batch of probe (25 uL linearized *c-fos* plasmid DNA, 10 uL DIG RNA labeling mix, 10 uL of 10x transcription buffer, 1 uL RNase inhibitor, 44 μL of nuclease free water and 10 uL of T7 RNA polymerase). The probe was then precipitated by adding 10 μL of 0.2M EDTA, 5 μL of glycogen, 12.5 μL of 4.0M LiCl and 380 μL of 100% ethanol to the mixture and purified as described in Chapter 2.

In situ hybridization, labeling of the riboprobe with α-DIG alkaline phosphatase and detection with nitroblue tetrazolium and 5-Bromo-4-chloro-3-indoyl phosphate (NBT/BCIP) was performed on 2dpf larvae as described in Chapter 2.

3.3.6 Semi-quantitative scoring of *c-fos* labeled with DIG riboprobe

Following detection of the *c-fos* riboprobe, fish were imaged using a Leica M165 FC dissecting microscope and visually scored for intensity of NBT/BCIP staining by a blinded observer. Scoring criteria are shown in Figure 3.6B. Images were collected using a Leica DFC 400 camera.

3.3.7 PTZ treatment for qPCR

2dpf larvae were dechorionated at least one hour prior to PTZ treatment using 1 mg/mL pronase and rinsed three times with E3 embryo media prior to drug treatment (3dpf fish did not require dechorionation). Deformed/developmentally delayed fish were removed and fish that had been injected with mRNA were sorted for *mCherry* mRNA expression and returned to the incubator. Fish were taken out of the incubator into a well-lit room for at least 30 minutes prior to PTZ-exposure. Fish were then treated with PTZ at room temperature in the light. Fish were treated with various doses of PTZ for either 30

or 90 minutes. Immediately following drug treatment, 5 larvae per biological replicate were transferred to an Eppendorf microfuge tube. PTZ or E3 medium was then removed and replaced with RNAlater (Ambion/Thermo Fisher Scientific, catalogue #AM7021, Waltham, MA, USA). Samples were then stored at 4 °C until RNA extraction.

3.3.8 Determining relative transcript abundance using RT-qPCR

Experiments were performed as described in Chapter 2. qPCR was performed on pools of larvae (each biological replicate represents 5 larvae) treated with PTZ or vehicle (E3 medium). Total RNA was extracted from pools of embryos and quality was assessed using an Agilent RNA 6000 NanoChip and Agilent 2100 Bioanalyzer as described in Chapter 2. Sample bioanalyzer traces are shown in Figure 3.1A. cDNA synthesis and quantitative PCR were performed as described in Chapter 2. Transcript abundance for *c-fos* and *prp1* were assessed relative to *β-actin*. *Prp1* and *β-actin* primers were designed using Primer Express 3.0 and previously verified with melt curves (Fleisch et al., 2013). The *c-fos* qPCR primers (forward: 5'-GCAAAGACCTCCAACAAGAGA-3'; reverse: 5'- TTTCGCAGCAGCCATCTT-3') span intron 2-3 of the *c-fos* gene (PMID Gene ID: 394198; ZFIN ID: ZDB-GENE-031222-4) and produce a 102 bp product from cDNA. Melt curves were used to confirm *c-fos* primer specificity. The presence of a single peak indicated that there was a single product for each primer set and no primer dimers (Figure 3.1B). The *c-fos* and *β-actin* primers were used at a final concentration of 800 nM, and the final concentration of the *prp1* primers was 200 nM.

A.

	Ladder	Wild type			prp2−/−			prp1−/−; prp2−/−			prp1−/−		
		— Bioanalyzer Results											
		RIN Number											
		9.5	9.2	9.0	9.2	9.0	9.7	9.6	9.0	9.1	9.4	9.3	9.5

B.

C.
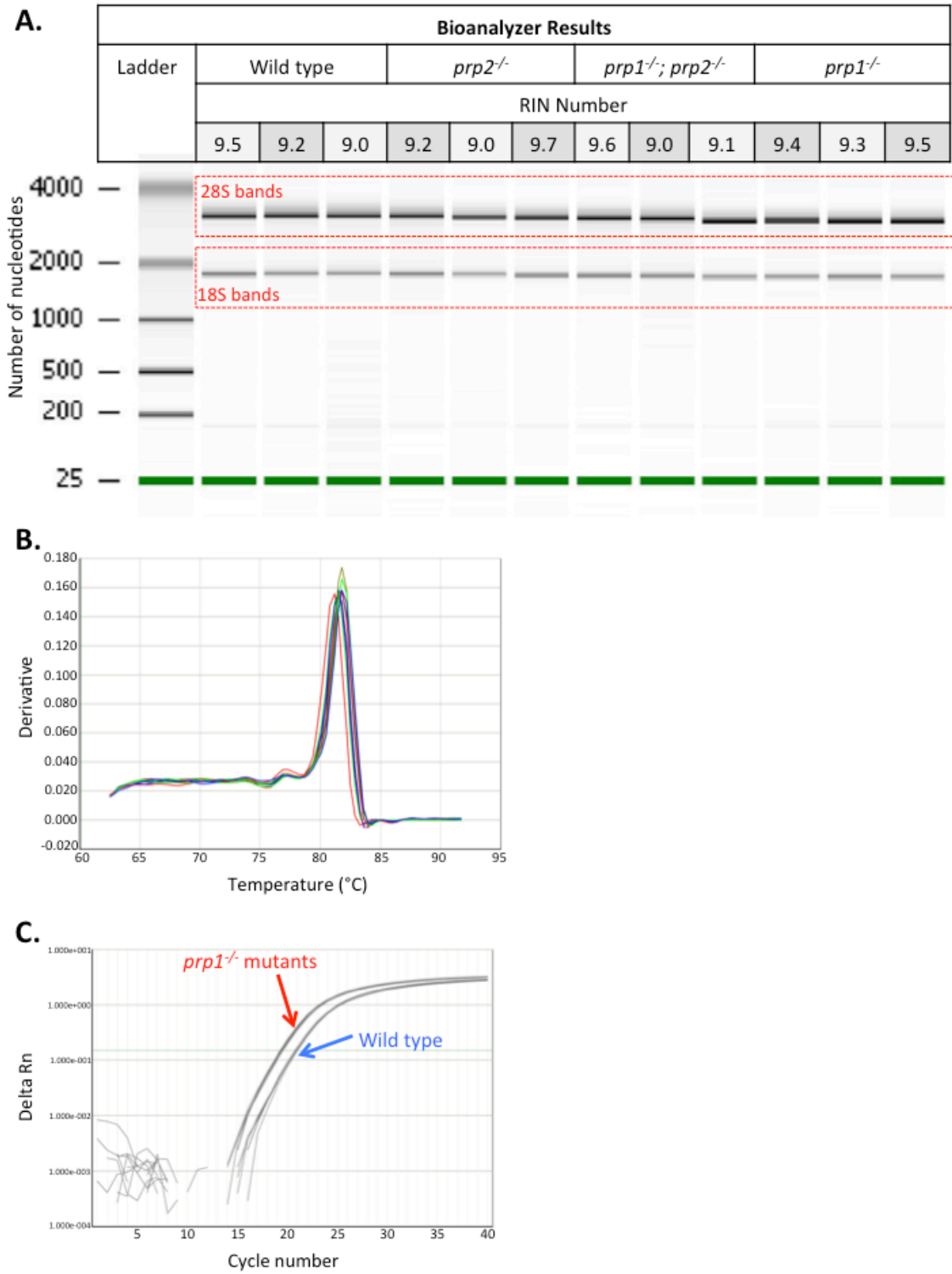
Figure 3.1. Quality assessment of total RNA samples and qPCR analysis of *c-fos* transcript abundance

A. Example bioanalyzer traces, including RNA integrity numbers (RIN) scored out of 10, show that the total RNA extracted from larvae of all genotypes tested were of high quality. The bands represent the 18S and 28S ribosomal RNA. **B.** Example melt dissociation curves used to assess the qPCR reaction integrity for the *c-fos* primers. Presence of a single large peak means that the primers are specific and that the sample is not contaminated with genomic DNA. Samples depicted are from wild type fish treated with PTZ. **C.** Example raw data (used to generate Figure 3.8) presented as sigmoidal plots show an increase in PTZ-induced *c-fos* transcript abundance in 3dpf *prp1*$^{ua5004/ua5004}$ larvae (traces indicated by red arrow) compared to 3dpf wild type fish (traces indicated by blue arrow).

3.3.9 Statistics

All statistics, except previously published behavioural results presented in Figure 3.2, were performed using GraphPad Prism Software (Version 6, GraphPad, San Diego, CA). Data was assessed for variance using the F-test prior to application of unpaired t-tests. If variance was significantly different, a Mann-Whitney U test was performed instead. Data was assessed for variance and normal distribution using the Brown-Forsythe's test and Barlett's test prior to application of a one-way ANOVA. If variance was significantly different between groups, a Kruskal Wallis test was performed instead. For the results presented in Figure 3.2, Mann-Whitney and Kruskal Wallis tests (with Tukey post-hoc pairwise tests) were performed using Systat Software (Version 12, Systat, San Jose, CA).

3.4 Results

3.4.1 Disruption of *prp2* enhances susceptibility to drug-induced seizures in zebrafish larvae

To characterize the role of *prp2* with respect to neuron function, we assayed if *prp2* loss-of-function leads to increased seizure susceptibility, as has been observed in $Prnp^{-/-}$ mice (Carulla et al., 2011; Rangel et al., 2007; Walz et al., 1999). Zebrafish have often been used in assays of seizure induction and sensitization, enabling testing of pharmacological and/or genetic interventions. We deployed an assay that has been established as a sensitive proxy of seizures (Baraban et al., 2007; Teng et al., 2010): hyperactivity measured as increased total movement of zebrafish larvae following addition of the convulsant PTZ. Examples of the method and tracking of fish movement are shown in Figure 3.2.

Our primary analysis focused on assessing fish movement during PTZ application, which was normalized to the levels of fish movement prior to PTZ application. The latter can account for inter-individual variability in baseline activity, which can be substantial in larval zebrafish (Shamchuk and Tierney, 2012). Movement representing Stage I and Stage II seizures was increased by about 50% in 5dpf homozygous mutants compared to wild type fish (p<0.001, Figure 3.2C), indicating that prp2 plays a role in modulating neuron excitability and seizures. Amongst the 5dpf fish, the wild type fish, $prp2^{+/ua5001}$

and zygotic *prp2$^{ua5001/ua5001}$* were siblings, while the maternal zygotic *prp2$^{ua5001/ua5001}$* fish were closely related. *Prp2$^{+/ua5001}$* fish were noted to have responses to PTZ that were approximately midway between the wild type and *prp2$^{ua5001/ua5001}$* fish, though this difference was not statistically significant from either genotype (Figure 3.2C). Similarly, the average velocity after versus before the addition of 2.5 mM PTZ was greater for 3 dpf *prp2$^{ua5001/ua5001}$* mutants compared to wild type controls (Figure 3.2D, p<0.05). In sum, *prp2$^{ua5001/ua5001}$* fish are susceptible to hyperactivity by PTZ to a greater extent compared to wild type controls.

Further analysis was warranted, however, because changes to this after-PTZ/before-PTZ ratio could represent both increased movement of mutants following PTZ or decreased movement of mutants prior to PTZ exposure. Indeed both effects were observed in the 5dpf fish from Figure 3.2C, depending on whether maternal mRNA was present during development. Larvae lacking maternal contribution (denoted as 'maternal zygotic' mutants, resulting from breeding *prp2$^{ua5001/ua5001}$* fish) had baseline movement levels that were reduced by about four times compared to wild type fish (Figure 3.3A, p<0.05; also see velocities and velocity ratios of individual fish in Figure 3.4A), along with the previously mentioned increased activity following PTZ (Figure 3.2C, p< 0.001). These were in distinct contrast to larvae with maternal deposition of *prp2* mRNA (zygotic mutants, resulting from breeding *prp2$^{ua5001/+}$* fish), where the significant increase in movement with PTZ was observed (Figure 3.3A, ratio 1.4, p < 0.001, n = 6) despite mean velocity prior to PTZ being comparable to wild type and heterozygous fish (Figure 3.3A). Therefore decreased baseline movement cannot by itself account for the increased ratio of PTZ-induced activity. Maternal zygotic mutants at 3dpf also had reduced baseline movement (Figure 3.3B, p<0.001; see also velocities of individual fish in Figure 3.4B). Decreased baseline movement is unto itself a phenotype of interest in the maternal zygotic *prp2$^{-/-}$* zebrafish.

Overall, *prp2$^{-/-}$* zebrafish have greater susceptibility to the convulsant compared to wild type fish. No difference was noted regarding induction of increased movement by PTZ when comparing maternal zygotic and zygotic mutant fish, suggesting that maternal contributions of *prp2* mRNA were inert towards the PTZ-induced seizure-like phenotype.

Similar results from *Prnp*$^{-/-}$ mice (reviewed in (Carulla et al., 2015)) suggest that PrP^C has a deeply conserved role in modulating neuron excitability.
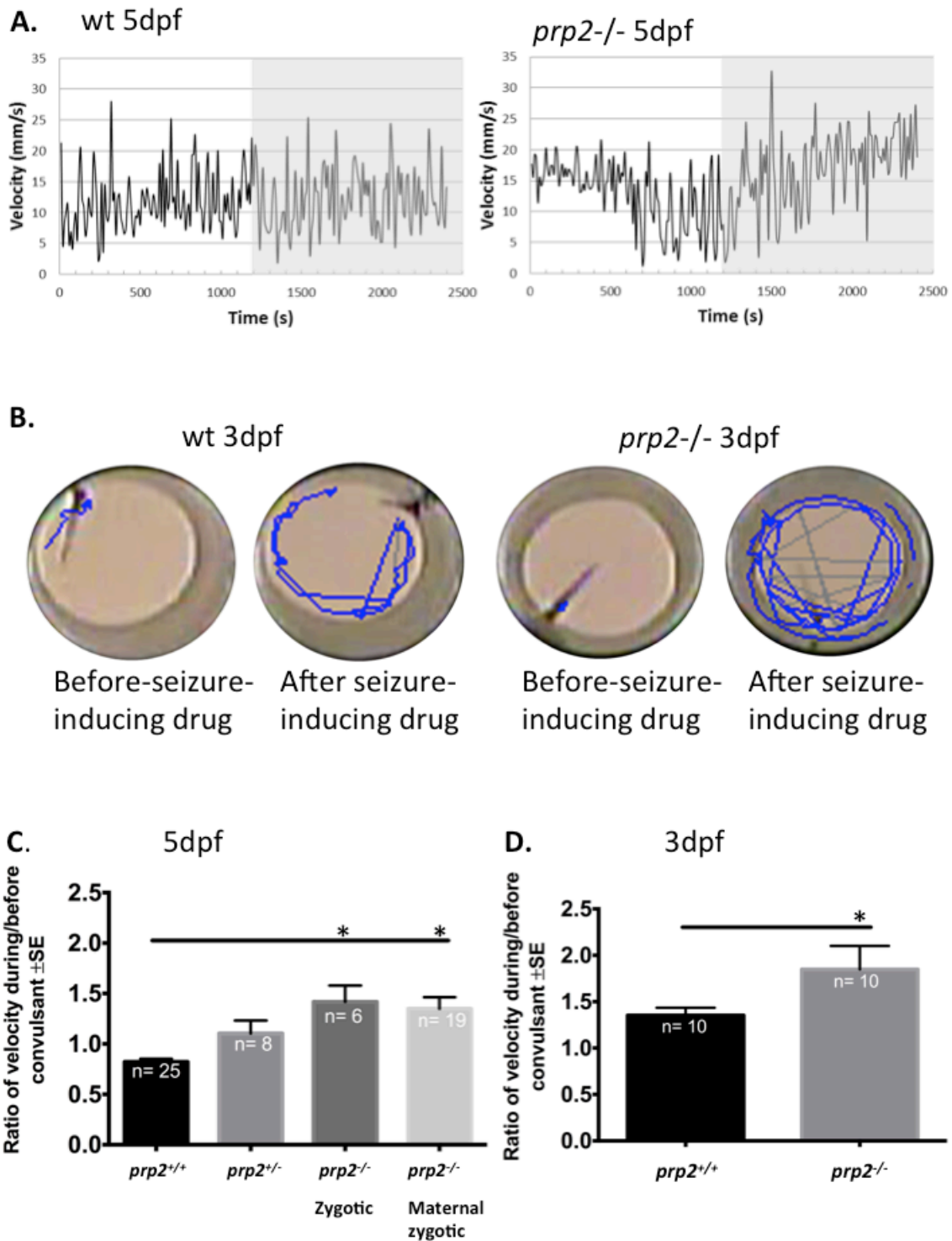
Figure 3.2. *prp2* disruption in zebrafish increases seizure-like activity upon exposure to the convulsant, PTZ[16]

---

[16] Panels A-B Reprinted from Neurobiology of Disease, Vol 55, Valerie C. Fleisch, P.L.

The convulsant pentylenetetrazole (PTZ, 2.5 mM) increases hyperactivity to a greater extent in *prp2*^{-/-} larval fish compared to wild type sibling fish. **A.** The seizure analysis method involved collecting data traces from video recordings of fish before and after PTZ application, examples of which are shown from individual 5 days post-fertilization (dpf) larvae. The movement of each fish was tracked over 20 min, with bath application of PTZ beginning at 1200 s (shaded area). **B.** Video stills of individual larvae, with blue lines depicting motion paths of 3 dpf *prp2*[ua5001/ua5001] and *prp2*^{+/+} fish, over a 5 second duration, either before or during PTZ exposure. Behavior of larvae was monitored in 96-well plates (individual wells shown here, e.g. in 3rd well fish is oriented towards southwest and moved little). Fish of both genotypes exhibited stage I to stage II seizures upon PTZ exposure (defined previously ((Baraban et al., 2007; Baraban et al., 2005)) as a general increase in activity and 'whirlpool' swimming patterns, respectively. **C.** Quantifying movement velocity as a proxy of seizure-like hyperactivity shows that 5dpf *prp2*^{-/-} fish (both zygotic and maternal zygotic) respond to the PTZ with greater magnitude compared to 5dpf *prp2*^{+/+} fish. Data are presented as a ratio of velocity during/before PTZ treatment. *$p < 0.001$ compared to wild type *prp2*^{+/+}, determined with Kruskal–Wallis one-way ANOVA and Tukey post hoc pair-wise tests. Raw data is presented in Figure 3.4A. **D.** Ratio of the average velocities of of 3 dpf *prp2*^{-/-} and *prp2*^{+/+} fish during versus before treatment with 2.5 mM PTZ. *$p = 0.016$ with the Mann Whitney U-test. Raw data is presented in Figure 3.4B. n refers to the number of fish.
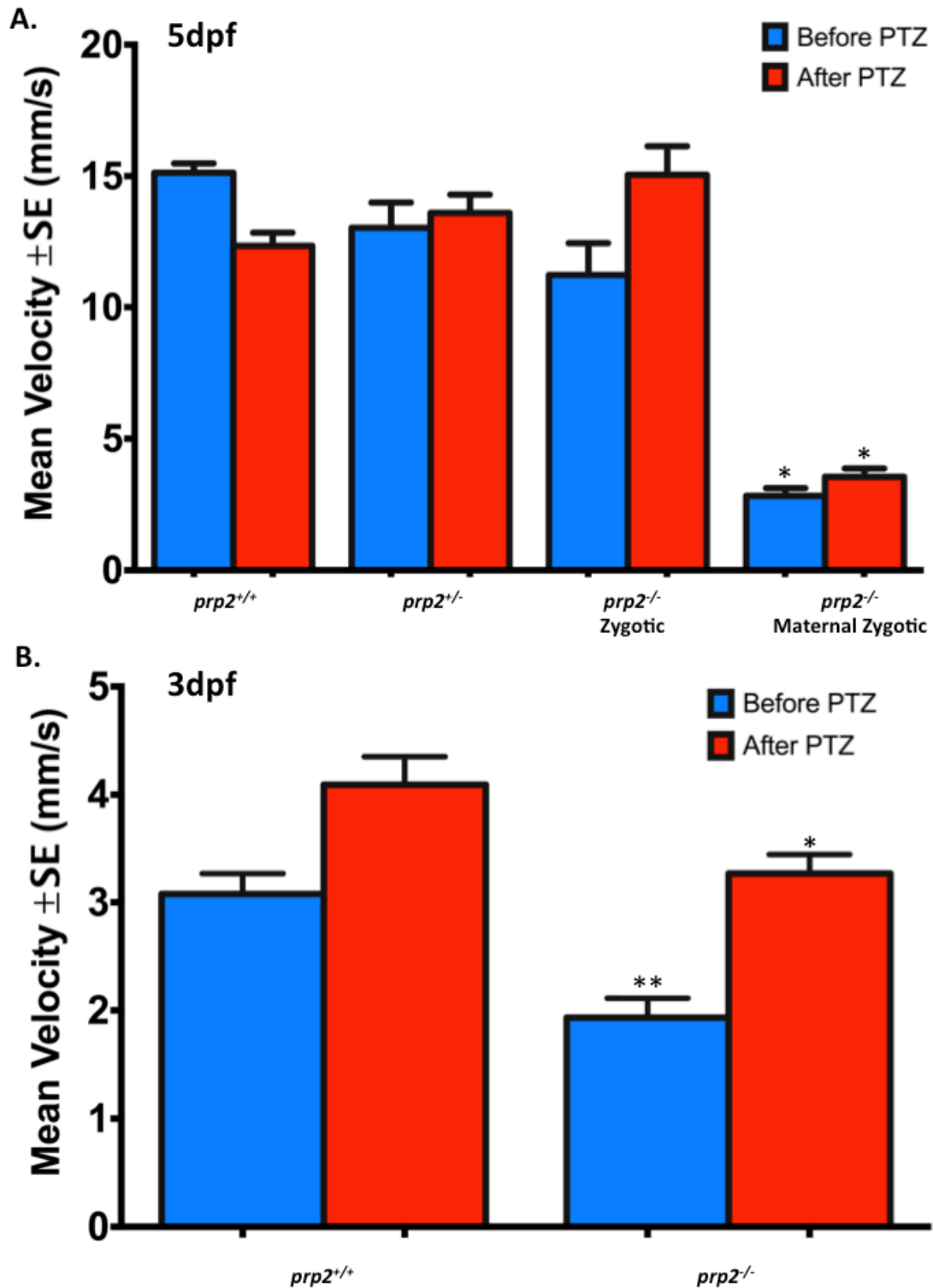
Figure 3.3. *prp2*$^{-/-}$ **mutants without maternally provided** *prp2* **mRNA have reduced velocities compared to** *prp2*$^{+/+}$ **fish both before and after treatment with PTZ**

A. 5dpf maternal zygotic *prp2*$^{-/-}$ mutants have a significantly reduced velocity before PTZ treatment compared to 5dpf *prp2*$^{+/+}$ or *prp2*$^{+/-}$ fish. After PTZ treatment, maternal zygotic *prp2*$^{-/-}$ mutants still have a reduced velocity compared to 5dpf PTZ- treated *prp2*$^{+/+}$ fish, *prp2*$^{+/-}$ fish, and zygotic *prp2*$^{-/-}$ mutants. *$p<0.05$ with Kruskal Wallis Test. **B.** 3dpf maternal zygotic *prp2*$^{-/-}$ mutants have a reduced velocity compared to 3dpf *prp2*$^{+/+}$ fish both before and after treatment with PTZ. *$p=0.0232$, ** $p=0.0005$ with the Mann-Whitney U test. n refers to the number of fish.
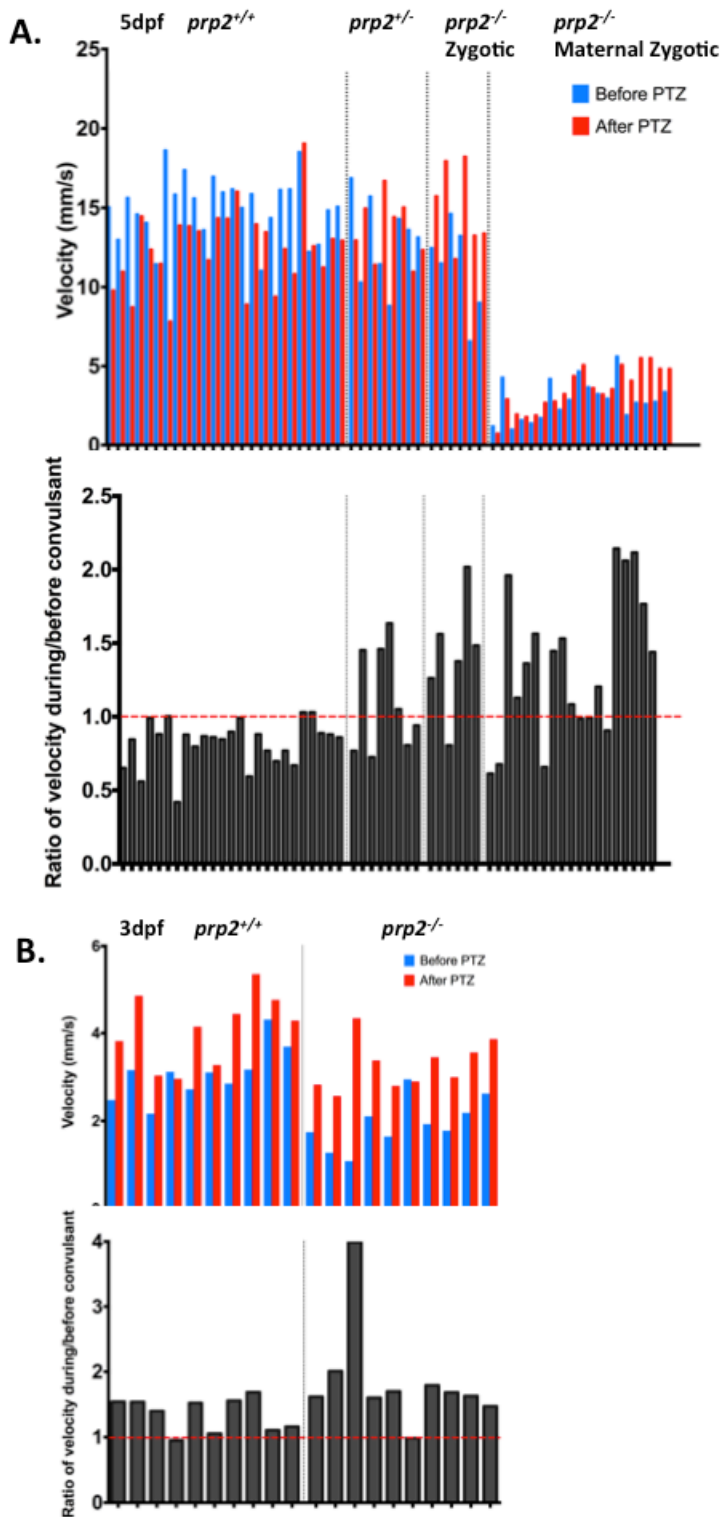
Figure 3.4. Raw data demonstrating that *prp2⁻/⁻* mutants, regardless of maternal *prp2* contribution, have an increased activity ratio after/before PTZ treatment

A. Raw velocity values used for analysis shown in Figure 3.2C, wherein each pair of blue and red bars represents the activity of an individual 5dpf fish before and after application of the convulsant PTZ, respectively. The graph underneath represents the ratios of these values for each individual fish as grey bars. Wild type and heterozygous fish have similar activity levels, but $prp2^{-/-}$ fish have a greater proportional response to PTZ regardless of maternal contributions of $prp2$ (grey bars), even though maternal zygotic $prp2^{-/-}$ mutants (lacking maternal $prp2$ mRNA) have lower levels of activity overall (both before and after PTZ). **B.** Raw velocity values used for analysis in Figure 3.2D, wherein each pair of blue and red bars represents the activity of an individual 3 dpf fish before and after application of the convulsant PTZ. $prp2^{-/-}$ fish had reduced velocities both before and after PTZ treatment than $prp2^{+/+}$ fish. The graph underneath represents the ratios of these values as grey bars. The $prp2^{-/-}$ fish showed a greater proportional change in velocity after versus before PTZ treatment than the $prp2^{+/+}$ fish.

3.4.2 *prp2* mRNA increased baseline activity of *prp2⁻/⁻* fish towards wild type levels at some doses, but did not rescue the drug-induced seizure-like activity

The gold standard for confirming that a phenotype observed in a loss-of-function mutant is due to loss of the target gene is through successful 'rescue' of the organism from the phenotype (i.e. the phenotype is reversed when the gene product is reintroduced to the organism). Gene rescue experiments also open up opportunities to assess how altered versions of protein (e.g. due to a missense mutation) affect its function. Lack of rescue in these experiments, however, must be considered as un-interpretable because this result may be biologically relevant (i.e. the mutated protein has lost its function) or due to technical confounds. One technical confound to consider in mRNA 'rescue' experiments is that ectopically expressed mRNA may not be expressed at appropriate levels or at the correct time in the cell type(s) of interest to properly recapitulate its normal function. Nevertheless, we next attempted to rescue the PTZ-induced seizure-like activity and reduced baseline activity in 3dpf *prp2^{ua5001/ua5001}* larvae using *prp2* mRNA. Ectopic delivery of *prp2* mRNA (400 pg and 800 pg) did not suppress the PTZ-induced increase in velocity in 3dpf *prp2^{ua5001/ua5001}* mutants compared to the activity observed in 3dpf *prp2⁻/⁻* mutants receiving control mRNA (Figure 3.5A). *prp2* mRNA at the 400 pg dose, however, increased the mean baseline velocity of the 3 dpf *prp2^{ua5001/ua5001}* larvae towards that observed in 3dpf wild type fish; yet the mean velocity of *prp2^{ua5001/ua5001}* fish treated with 400 pg of *prp2* mRNA was not statistically increased compared to *prp2^{ua5001/ua5001}* fish treated with 400 pg of control mRNA (Figure 3.5B).

The overall reduced velocity in 3dpf *prp2^{ua5001/ua5001}* fish treated with 800 pg of *prp2* mRNA (and in fish treated with 400 pg of control mRNA) compared to that of the un-injected fish in Figure 3.3B suggests that the injection process is a confound. For example, it may cause developmental delay. Reduced activity in injected fish produced by developmental delay may mask 'rescue' by the re-introduced *prp2* gene product. Alternatively, the injected *prp2* mRNA is not expressed at an appropriate abundance at the correct time(s) in development or at the correct location(s) to suppress PTZ-induced seizure-like activity in 3dpf fish. In sum, convincing rescue of the PTZ-induced activity phenotype in *prp2⁻/⁻* mutants has yet to be observed via measures of movement in behavioural tracking software.
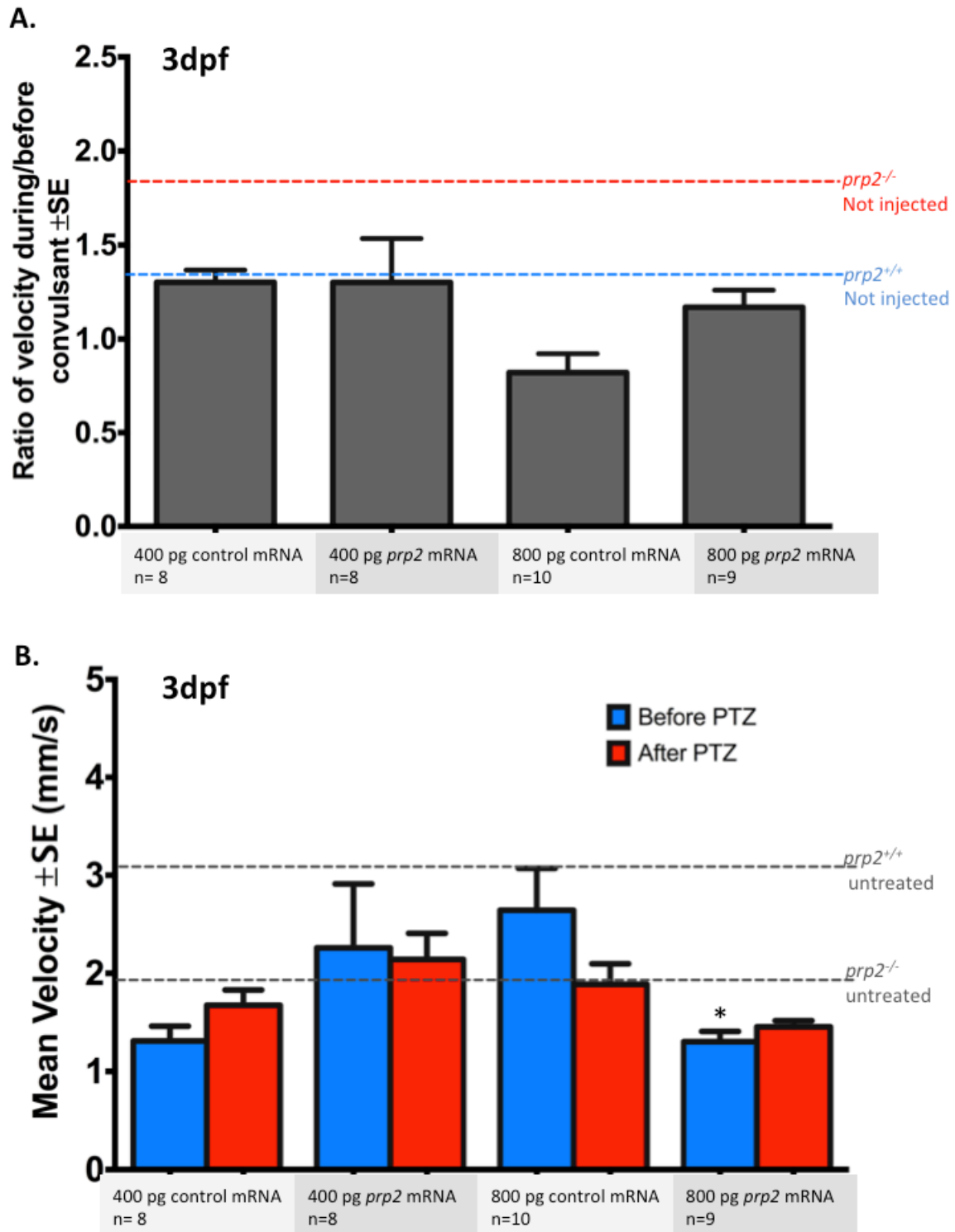
Figure 3.5. Ectopic delivery of *prp2* mRNA did not suppress seizure-like activity in 3dpf *prp2*^{-/-} mutants

A. *prp2* mRNA (400 pg and 800 pg doses) did not significantly reduce the PTZ-induced activity in 3dpf *prp2*$^{-/-}$ fish compared to the PTZ-induced activity in 3dpf *prp2*$^{-/-}$ fish receiving equivalent doses of control mRNA (*prp2* mRNA with the ua5001 allele). *prp2*$^{-/-}$ fish injected with either *prp2* mRNA or control mRNA had reduced PTZ-induced activity compared to *prp2*$^{-/-}$ fish that were not injected, but similar activity to wild type un-injected fish. The dashed red and blue lines indicates the mean ratio of velocity after/before PTZ of *prp2*$^{-/-}$ mutants and *prp2*$^{+/+}$ fish, respectively, that were reported in Figure 3.2D. **B.** 400 pg of *prp2* mRNA increased the velocity of the 3dpf *prp2*$^{-/-}$ fish (before PTZ) towards what was observed in untreated 3dpf *prp2*$^{+/+}$ fish in Figure 3.3B. There was no statistically significant difference, however, between the velocities of fish treated with 400 pg of *prp2* mRNA versus 400 pg of control mRNA (*prp2* mRNA with the ua5001 allele). 800 pg of *prp2* mRNA reduced the velocity of the 3dpf *prp2*$^{-/-}$ fish compared to the velocity of 3dpf *prp2*$^{-/-}$ fish treated with control mRNA. *p = 0.0057 with the Mann-Whitney U test. The dashed grey lines indicate the velocities of untreated 3dpf *prp2*$^{+/+}$ and *prp2*$^{-/-}$ fish reported in Figure 3.3B. n refers to the number of fish.

3.4.3 Disruption of zebrafish *prp2* increases expression of the immediate early gene, *c-fos*

As we were unable to rescue the PTZ-induced behavioural phenotype described above using *prp2* mRNA, we elected to search for a phenotype at a younger age that would be more amenable to mRNA rescue and moved away from behavioural experiments so that we could perform experiments in higher throughput. We chose to look for a molecular marker of enhanced seizure susceptibility to independently assess the increased susceptibility to seizures that we had found with behavioural assays. *c-fos* is an immediate early response gene representing neuron activity, and PTZ has been shown to induce its expression in zebrafish (Baxendale et al., 2012). We therefore performed *in situ* hybridization with a *c-fos* riboprobe to determine whether there was a difference in *c-fos* expression pattern and/or abundance in 2dpf $prp2^{ua5001/ua5001}$ versus wild type fish treated with PTZ. PTZ-induced *c-fos* expression was observed in the skeletal muscles as well as in the brains and spinal cords of both 2dpf wild type and 2dpf $prp2^{ua5001/ua5001}$ mutants (Figure 3.6A). Analysis using a semi-quantitative scoring system revealed a statistically significant increase in *c-fos* expression in PTZ- treated (20 mM PTZ for 90 minutes) 2dpf $prp2^{ua5001/ua5001}$ larvae compared to PTZ-treated wild type larvae (Figure 3.6B-C, p<0.05).

We next asked whether re-introduction of *prp2* mRNA could suppress *c-fos* expression in PTZ-treated (20 mM PTZ for 90 minutes) 2dpf $prp2^{ua5001/ua5001}$ mutants. *c-fos* expression was indeed significantly reduced in PTZ-treated 2dpf $prp2^{ua5001/ua5001}$ mutants injected with 200 pg *prp2* mRNA compared to PTZ-treated 2dpf $prp2^{ua5001/ua5001}$ mutants injected with 200 pg control (*prp2* with ua5001 mutant allele) mRNA (Figure 3.6C, p<0.01). There was, however, also a significant reduction in *c-fos* levels in PTZ-treated $prp2^{ua5001/ua5001}$ fish that were injected with control *prp2* mRNA, compared to PTZ-treated $prp2^{ua5001/ua5001}$ fish that were not injected (Figure 3.6C, p<0.05). Thus suppression of *c-fos* expression observed in the PTZ-treated $prp2^{ua5001/ua5001}$ mutants injected with *prp2* mRNA versus un-injected mutants may be partially due to developmental delay. In sum, based on these semi-quantitative measures, it appears that *prp2* may suppress PTZ-induced *c-fos* expression.
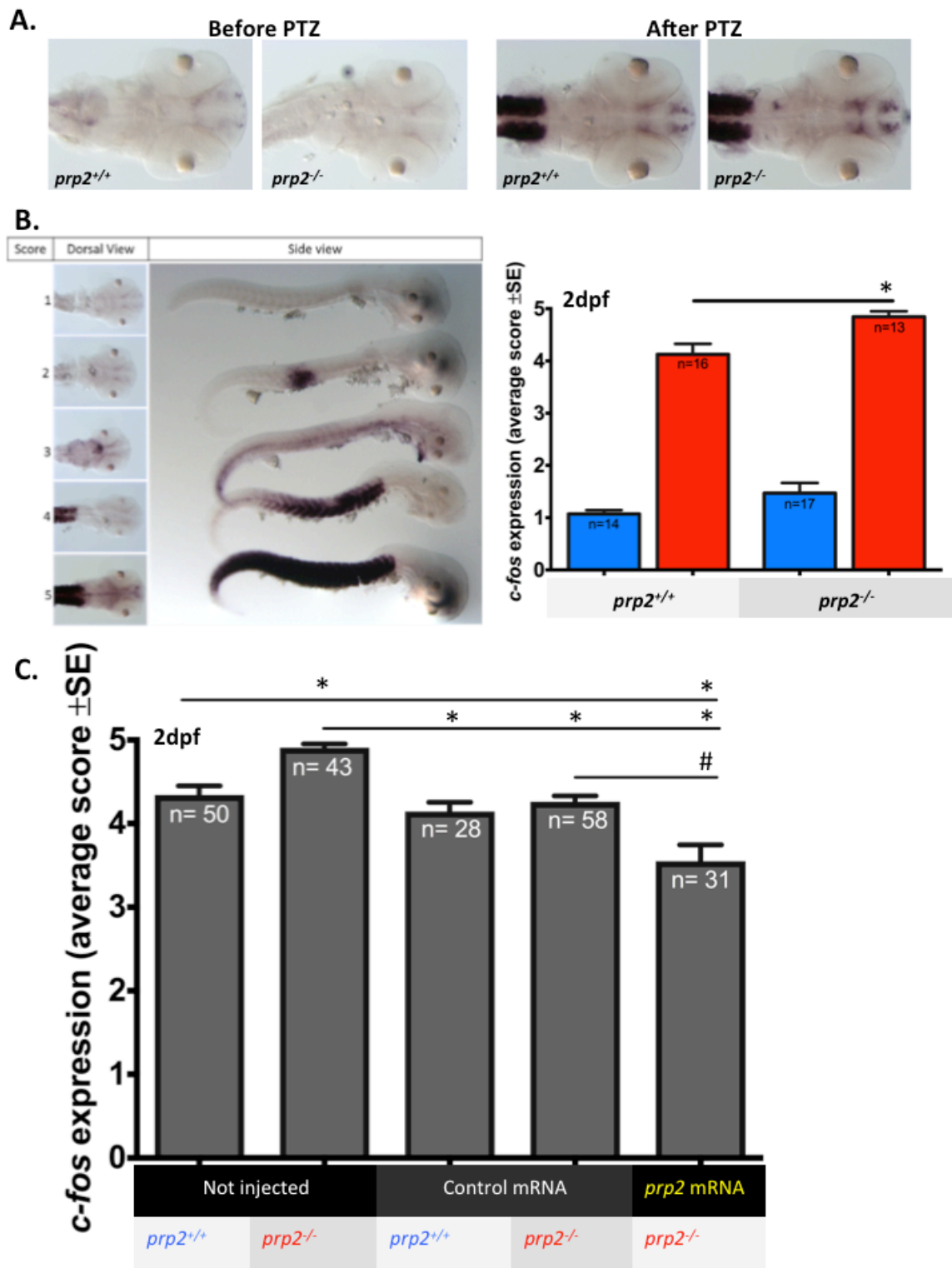
Figure 3.6. Zebrafish *prp2* appears to suppress expression of the immediate early gene, *c-fos* in PTZ-treated larvae

A. Representative images of PTZ-induced *c-fos* expression in skeletal muscles, spinal cords, and brains of both 2dpf $prp2^{+/+}$ and $prp2^{ua5001/ua5001}$ larvae. **B.** PTZ-induced increase in *c-fos* expression in 2 dpf zebrafish larvae was revealed using *in situ* hybridization. **Left panel:** Semi-quantitative scoring criteria used to assess *c-fos* expression intensity in PTZ-treated 2 dpf $prp2^{ua5001/ua5001}$ mutants relative to *c-fos* expression in PTZ-treated $prp2^{+/+}$ fish. **Right panel:** PTZ-treated 2dpf $prp2^{ua5001/ua5001}$ mutants had an increase in *c-fos* expression intensity compared to PTZ-treated 2dpf $prp2^{+/+}$ fish. Values were obtained using the *in situ* scoring criteria. * $p = 0.008$ with Mann Whitney U-Test. **C.** Ectopic overexpression of *prp2* mRNA (200 pg) reduced *c-fos* expression intensity in 2dpf PTZ-treated $prp2^{ua5001/ua5001}$ fish compared to *c-fos* expression observed in 2dpf PTZ-treated $prp2^{ua5001/ua5001}$ fish with overexpression of control mRNA (*prp2* with the ua5001 allele; # $p=0.0009$ with Mann-Whitney U-Test). Injection of either *prp2* mRNA or control mRNA, however, suppressed *c-fos* expression in PTZ-treated $prp2^{ua5001/ua5001}$ fish compared to *c-fos* levels in PTZ-treated $prp2^{ua5001/ua5001}$ fish that were not injected. As in (A), un-injected PTZ-treated 2dpf $prp2^{ua5001/ua5001}$ mutants had an increase in *c-fos* transcript abundance compared to PTZ-treated 2dpf $prp2^{+/+}$ fish. *$p<0.05$ with Kruskal Wallis test. n refers to the number of fish.

3.4.4 *prp2* and *prp1* have redundant, and possibly conserved, functions in suppressing *c-fos* expression

As the *in situ* hybridization is a semi-quantitative method, we next turned to qPCR to quantify changes in *c-fos* abundance in PTZ-treated zebrafish prion protein mutants ($prp2^{ua5001/ua5001}$, $prp1^{ua5004/ua5004}$ and compound $prp1^{ua5003/ua5003}$; $prp2^{ua5001/ua5001}$ mutants) compared to PTZ-treated wild type fish. Our first set of experiments was performed on 2dpf larvae because we predicted that it would be possible to rescue any observed phenotypes in $prp1^{-/-}$ or $prp2^{-/-}$ mutants with cognate mRNA at this age (i.e. mRNA injected at the one-cell stage was expected to still be present in the system by 2dpf). To determine an appropriate PTZ dose to use in our experiments, we treated 2dpf wild type and 2dpf $prp2^{-/-}$ mutants with 5mM, 10mM, 20mM, 40mM and 80 mM PTZ for 90 minutes. *c-fos* expression levels were consistently increased in 2dpf $prp2^{-/-}$ mutants compared to 2dpf wild type fish at the 20mM dose; therefore we chose to use this dose in subsequent experiments. There was also a clearer increase in *c-fos* expression levels in both $prp1^{-/-}$ and $prp2^{-/-}$ mutants compared to wild type when treated with 20mM PTZ for 90 minutes, compared to the same treatment for 30 minutes; therefore we treated fish for 90 minutes in subsequent experiments.

Upon treatment with 20 mM PTZ for 90 minutes, 2dpf $prp2^{ua5001/ua5001}$, $prp1^{ua5004/ua5004}$ and compound $prp1^{ua5003/ua5003}$;$prp2^{ua5001/ua5001}$ mutants expressed increased *c-fos* levels (115%, 144.5%, and 146%, respectively) compared to those in 2dpf PTZ-treated wild type fish, but these changes were not statistically significant (Figure 3.7A). With the same PTZ treatment at 3dpf, $prp2^{ua5001/ua5001}$, $prp1^{ua5004}$ and compound $prp1^{ua5003/ua5003}$;$prp2^{ua5001/ua5001}$ mutants also expressed increased *c-fos* levels (179%, 185%, and 133%, respectively) compared to those in 3dpf PTZ-treated wild type fish, though only levels in $prp1^{ua5004/ua5004}$ fish reached statistical significance (Figure 3.8A, $p<0.05$).

We next asked whether suppression of PTZ-induced *c-fos* expression is a conserved function of PrP^C, and attempted to answer this question by ectopically expressing mouse *Prnp* mRNA. Since mRNA rescue experiments are predicted to be more effective at younger ages due to time-dependent degradation of the injected mRNA, we sought to rescue the increase in *c-fos* expression in PTZ-treated (20 mM for 90 minutes) 2dpf

prp1$^{ua5003/ua5003}$*; prp2*$^{ua5001/ua5001}$ mutants. In our first rescue attempt, *c-fos* expression was suppressed in PTZ-treated *prp1*$^{ua5003/ua5003}$*; prp2*$^{ua5001/ua5001}$ mutants injected with 100 pg of mouse *Prnp* mRNA compared to those injected with 100 pg of control mRNA (mouse *Prnp* mRNA with a premature stop codon), though this was not statistically significant (Figure 3.7B). In subsequent trials, we did not observe this rescue effect. *c-fos* levels in PTZ-treated wild type fish, however, were also variable between trials leading us to speculate that other factors such as inter-trial variations in ambient light or noise levels were confounding the results of the rescue experiment. It is also unclear whether mouse PrP^C was present in the larvae at similar levels between trials. In the future, qPCR will be performed to assess levels of mouse *Prnp* in the fish alongside qPCR assessing *c-fos* abundance. In sum, *prp1* and *prp2* have redundant functions in suppressing PTZ-induced *c-fos* expression and mammalian PrP^C may have a similar function.
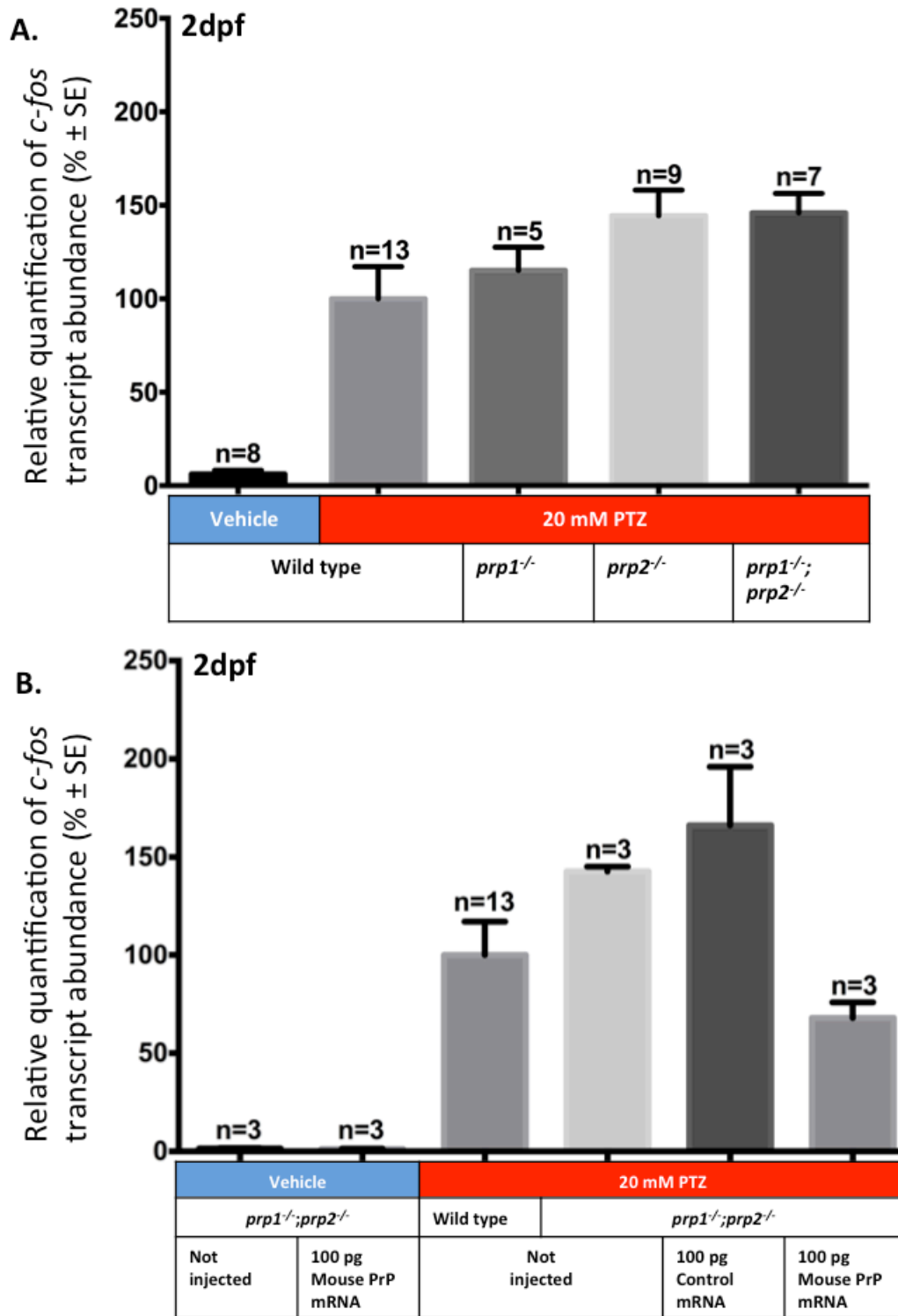
Figure 3.7. Prp1 and Prp2 appear to suppress PTZ-induced increase in *c-fos* expression in 2dpf larvae, and this may be a conserved function of PrP^C

A. 2dpf maternal zygotic *prp1*$^{ua5004/ua5004}$, *prp2*$^{ua5001/ua5001}$, and compound *prp1*$^{ua5003/ua5003}$; *prp2*$^{ua5001/ua5001}$ mutants show a trend towards increased *c-fos* expression compared to 2dpf wild type fish upon stimulation with 20 mM PTZ for 90 minutes, but were not statistically significant with the Kruskal Wallis test. **B.** Mouse *Prnp* mRNA suppressed the PTZ-induced *c-fos* induction in 2 dpf *prp1*$^{ua5003/ua5003}$; *prp2*$^{ua5001/ua5001}$ compared to *c-fos* abundance measured in 2-dpf *prp1*$^{ua5003/ua5003}$; *prp2*$^{ua5001/ua5001}$ mutants treated with control mRNA (Mouse *Prnp* with an engineered stop codon) or un-injected 2-dpf *prp1*$^{ua5003/ua5003}$; *prp2*$^{ua5001/ua5001}$ mutants. This suppression did not reach statistical significance with the Kruskal Wallis test. Fish were treated with 20 mM PTZ for 90 minutes as in (A). *c-fos* abundance in PTZ-treated, un-injected wild type fish is replotted from (A) for comparison. Data is normalized to the average *c-fos* abundance measured in 2dpf PTZ treated wild type fish. n refers to the number of biological replicates (5 larvae/biological replicate).

3.4.5 *Prp1 mRNA* may suppress PTZ-induced *c-fos* expression in 3dpf *prp1*$^{-/-}$ mutants

Because PTZ induced greater increases in *c-fos* levels in 3dpf *prp2*$^{ua5001/ua5001}$, *prp1*^{ua5004} and compound *prp1*$^{ua5003/ua5003}$;*prp2*$^{ua5001/ua5001}$ mutants compared to at 2dpf (Figure 3.8B), we next asked whether cognate mRNA could suppress *c-fos* expression in 3dpf mutants. As a starting point, we hypothesized that *prp1* mRNA would suppress *c-fos* expression in 3dpf *prp1*$^{ua5004/ua5004}$ mutants. In our first experiment, we compared the effect of 10 mM PTZ treatment for 90 minutes on 3dpf *prp1*$^{ua5004/ua5004}$ mutants injected with 0.2 fmol (117.5 pg) *prp1* mRNA versus those injected with 0.2 fmol (66.7pg) of *egfp* mRNA (doses were adjusted so that an equivalent number of mRNA molecules would be injected into *prp1* mRNA-treated and *egfp* mRNA-treated embryos). While the *prp1* mRNA suppressed (though not significantly) *c-fos* expression in PTZ-treated *prp1*$^{ua5004/ua5004}$ fish compared to PTZ-treated *prp1*$^{ua5004/ua5004}$ fish that were not injected, *egfp* mRNA produced even greater *c-fos* reduction (Figure 3.8C). This suggested that *egfp* mRNA or the injection process itself reduced *c-fos* expression, perhaps through developmental delay. In the next experiment, we used *prp1* mRNA with an early stop codon as control mRNA and assessed levels of *prp1* mRNA at the termination of PTZ-treatment to determine how much injected mRNA was present at this time. *prp1*$^{ua5004/ua5004}$ fish injected with 0.2 fmol (117.5pg) and 1 fmol (587.5pg) of *prp1* mRNA had 1485% and 2932%, respectively, of the *prp1* mRNA levels in *prp1*$^{ua5004/ua5004}$ fish that were not injected. Compared to PTZ-treated *prp1*$^{ua5004/ua5004}$ fish not injected with mRNA, those injected with either dose of *prp1* mRNA had reduced *c-fos* levels, though more trials will be needed to determine whether this reduction is statistically significant (Figure 3.8D). Since 0.2 fmol *prp1* mRNA with a premature stop codon also reduced *c-fos* levels, the injection process itself apparently influences *c-fos* levels. This may be due to developmental delay, since PTZ-treated, un-injected *prp1*$^{ua5004/ua5004}$ mutants express less *c-fos* at 2dpf compared to at 3dpf. At the 1fmol dose, *prp1* mRNA produced toxic effects including heart edema and spine curvature in siblings of the fish analyzed for qPCR. Therefore, 0.2 fmol of *prp1* mRNA will be used in future trials. Overall, further experimentation is needed to assess whether ectopically expressed *prp1* mRNA suppresses PTZ-induced *c-fos* expression.
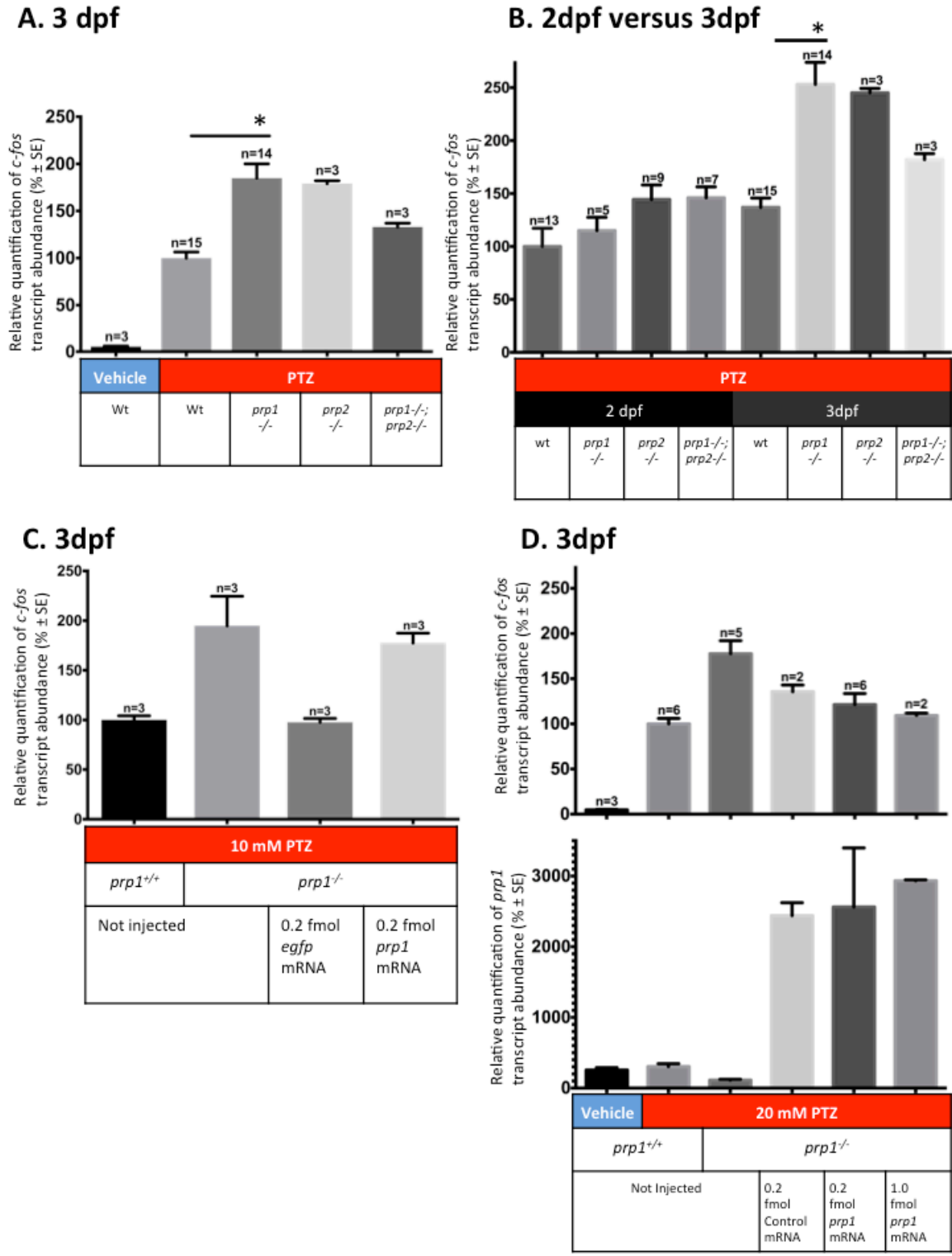
Figure 3.8. Extent of PTZ induction of *c-fos* expression in zebrafish PrP mutants is greater in 3dpf larvae than in 2dpf larvae, and *prp1* mRNA may suppress PTZ-induced *c-fos* expression

A. PTZ treatment (20 mM for 90 minutes) induced significantly more *c-fos* expression in 3dpf $prp1^{ua5004/ua5004}$ fish than in 3dpf wild type fish (*p<0.05 with the Kruskal Wallis test). There was also an increase, though not statistically significant, in PTZ-induced *c-fos* expression in 3dpf $prp2^{ua5001/ua5001}$ and 3dpf $prp1^{ua5003/ua5003}$;$prp2^{ua5001/ua5001}$ mutants compared to 3dpf wild type fish. Data is normalized to the average *c-fos* abundance measured in 3dpf PTZ-treated wild type fish. **B.** *c-fos* expression was increased in PTZ-treated 3dpf zebrafish prion protein mutants compared to PTZ-treated 2dpf prion proteins mutants. Data is replotted from Figures 2A and 3A and normalized to the average *c-fos* abundance measured in 2dpf PTZ-treated wild type fish. **C.** Injection of 0.2 fmol *prp1* mRNA suppressed (though not significantly) *c-fos* expression induced by 90 minutes of 10 mM PTZ treatment in 3dpf $prp1^{ua5004/ua5004}$ fish compared to *c-fos* induction in 3dpf $prp1^{ua5004/ua5004}$ fish that were treated with PTZ but not injected. Control mRNA (0.2 fmol egfp mRNA), however, suppressed *c-fos* expression more than the *prp1* mRNA. **D.** Top panel: Injection of 0.2 fmol *prp1* mRNA reduced (though not significantly) PTZ-induced *c-fos* expression in 3dpf $prp1^{ua5004/ua5004}$ fish compared to *c-fos* induction in 3dpf $prp1^{ua5004/ua5004}$ fish that were treated with PTZ but not injected. *C-fos* suppression also appeared to be greater in 3 dpf $prp1^{ua5004/ua5004}$ fish injected with 0.2 fmol *prp1* mRNA and 1 fmol *prp1* mRNA than in 3dpf $prp1^{ua5004/ua5004}$ fish injected with 0.2 fmol control mRNA (*prp1* mRNA with an early stop codon). Injection of either *prp1* or control mRNA, however, reduced *c-fos* expression compared to that observed in $prp1^{ua5004/ua5004}$ mutants that were not injected. At time of writing the sample sizes were not large enough for statistical analysis. Data is normalized to un-injected 3dpf wild type fish treated with PTZ. Bottom panel: *prp1* and control mRNA were detected at high levels in $prp1^{ua5004/ua5004}$ mutants that were injected. Data is normalized to *prp1* levels in un-injected 3dpf $prp1^{ua5004/ua5004}$ fish treated with PTZ. n refers to the number of biological replicates (5 larvae/biological replicate).

3.5 Discussion

Here we have shown that endogenous zebrafish *prp2* protects zebrafish larvae against PTZ-induced seizure-like behaviour, and we have indirectly shown (by measuring *c-fos* abundance) that endogenous *prp1* and *prp2* have redundant roles in regulating neural activity. PTZ's increased effect on *c-fos* expression in 3dpf prion protein mutants compared to 2dpf mutants is likely due to a greater abundance of mature neurons by 3dpf. The reduced *c-fos* abundance in 3dpf PTZ-treated compound *prp1*$^{-/-}$; *prp2*$^{-/-}$ fish compared to that observed in PTZ-treated single *prp1*$^{-/-}$ and *prp2*$^{-/-}$ mutants is predicted to be due to induction of alternate biological pathways. RNA sequencing comparing single *prp1*$^{-/-}$ and *prp2*$^{-/-}$ mutants to compound *prp1*$^{-/-}$; *prp2*$^{-/-}$ fish will be the first step towards testing this prediction.

We were unable to definitively demonstrate suppression of the PTZ-induced *c-fos* expression by injecting cognate mRNA into the prion protein mutants, and were unable to rescue the behavioral phenotype in PTZ-treated *prp2*$^{-/-}$ larvae. Notably, in some cases, injection of control mRNA produced a different result in PTZ-treated fish than what was observed in PTZ-treated fish that were not injected (i.e. reduced velocity or reduced *c-fos* expression compared to un-injected fish), and is probably related to developmental delay. The ~2500-fold increase in *prp1* mRNA levels in *prp1*$^{-/-}$ mutants injected with *prp1* mRNA at 3dpf compared to wild type levels argues against the hypothesis that the injected mRNA is degraded by this time in larval development. Ectopically expressed mRNA may also lack efficacy because it is not restricted to the activated neurons, and may also explain why maternally provided *prp2* mRNA was unable to protect against PTZ-induced seizures in 5dpf larvae. In the future it may be possible to induce cognate prion protein expression specifically in neurons of *prp1*$^{-/-}$ and *prp2*$^{-/-}$ mutants through Cre-Lox transgene technology (Hans et al., 2009) prior to PTZ application.

We have preliminarily demonstrated that protection against drug-induced seizures is a conserved function of PrP^C by slightly suppressing *c-fos* expression in 2dpf compound *prp1*$^{-/-}$; *prp2*$^{-/-}$ fish with mouse *Prnp* mRNA. Since *c-fos* was significantly increased in PTZ-treated 3dpf *prp1*$^{-/-}$ fish compared to PTZ-treated wild type fish, it is possible that a more convincing 'rescue' effect with mouse *Prnp* mRNA could be achieved in these fish than what was observed in 2dpf *prp1*$^{-/-}$; *prp2*$^{-/-}$ fish.

Limitations in using *c-fos* abundance as a measure of neural activity are that it is an indirect measure, it is not cell type specific, and it is sensitive to other environmental factors (and hence can be variable). For example, odorants change *c-fos* expression in the rat olfactory bulb (Montag-Sallaz and Buonviso, 2002), and light has been shown to induce *c-fos* expression in the rat suprachiasmatic nuclei and in the adult zebrafish brain (Moore and Whitmore, 2014; Rea, 1989). Expression of *c-fos* in the adult zebrafish brain also displays circadian rhythmicity (Moore and Whitmore, 2014). For these reasons, we suspect that ambient light conditions may have been a source of variability in our experiments. Intracellular calcium concentrations change transiently in concert with neural activity- hence calcium reporters represent an alternative tool to abundance of immediate early genes for measuring neural activity.

A photoactivatable calcium protein, Calcium-Modulated Photoactivatable Ratiometric Integrator (CaMPARI), has recently been developed and has been used to directly measure neuronal activation in zebrafish larvae (Fosque et al., 2015). Two conditions must be present for conversion of CaMPARI from green to red fluorescence: presence of intracellular calcium, and stimulation with a violet light. CaMPARI can also be targeted to specific cell types under the control of cell-specific promoters such as the *ELAV like neuron-specific RNA binding protein 3* (*elavl3*) promoter (Fosque et al., 2015). Others in the lab are breeding CaMPARI transgenes into the *prp1*$^{-/-}$, *prp2*$^{-/-}$ and compound *prp1*$^{-/-}$; *prp2*$^{-/-}$ mutants, and are using CaMPARI to measure neural activity in PTZ-treated fish. If increases in neural activity in PTZ-treated prion protein mutants compared to PTZ-treated wild type fish can be verified with CaMPARI, it will then be possible to directly measure whether injecting cognate mRNA or mammalian mRNA suppresses neural activity. From there, it will be possible to query which regions of the PrP^C molecule are protective against drug-induced seizures by attempting to suppress neuronal activity in PTZ-treated fish with modified *Prnp* mRNA. For example, residues between 106-121 in mouse PrP^C could be modified since this region of the protein has previously been shown to be protective (Shmerling et al., 1998). PrP^C residues 23-29 were also recently shown to mediate myelin homeostasis through interaction with the G-protein coupled receptor, Adgrg6 (Kuffer et al., 2016). Thus it will be interesting to test the hypothesis that these residues participate in neuroprotection.

In summary, we have shown that *prp2* is protective against PTZ-induced seizure-like activity and that endogenous *prp1* and *prp2* suppress *c-fos* levels in PTZ-treated larvae. Protection against neural hyperexcitability has been a putative function of PrP^C that has received much attention by the prion and AD fields, as loss of this function is likely to contribute to disease phenotypes (eg. seizures). Resolving the issue has been difficult due to inconsistent reports on whether *Prnp* knockout mice have enhanced susceptibility to convulsants (reviewed in (Carulla et al., 2015; Striebel et al., 2013)). Here we have found that PrP^C is regulates neural activity in a more basal vertebrate species- the zebrafish. Hence it appears that PrP^C has an ancient and conserved role in regulating neural activity. Future work (eg. using CaMPARI) will be needed to confirm that cognate mRNA and mouse *Prnp* mRNA can suppress neuronal activation in *prp1$^{-/-}$*, *prp2$^{-/-}$* and compound *prp1$^{-/-}$*; *prp2$^{-/-}$* mutants and thus act as rescues. Once this is completed, this zebrafish neural activity regulation paradigm can be used to identify which PrP^C residues mediate this type of neuroprotection, and it can also be used in high throughput screens to identify potential therapeutics for prion diseases and AD.

Chapter 3 References

Baraban, S., et al., 2007. A large-scale mutagenesis screen to identify seizure-resistant zebrafish. Epilepsia. 48**,** 1151-1157.

Baraban, S. C., et al., 2005. Pentylenetetrazole induced changes in zebrafish behavior, neural activity and c-FoS expression. Neuroscience. 131**,** 759-768.

Baumann, F., et al., 2007. Lethal recessive myelin toxicity of prion protein lacking its central domain. EMBO J. 26**,** 538-47.

Baxendale, S., et al., 2012. Identification of compounds with anti-convulsant properties in a zebrafish model of epileptic seizures. Dis Model Mech. 5**,** 773-84.

Bhinder, G., Tierney, K. B., 2012. Olfactory-Evoked Activity Assay for Larval Zebrafish. Zebrafish Protocols for Neurobehavioral Research. 66**,** 71-84.

Carulla, P., et al., 2011. Neuroprotective role of PrPC against kainate-induced epileptic seizures and cell death depends on the modulation of JNK3 activation by GluR6/7-PSD-95 binding. Mol Biol Cell. 22**,** 3041-54.

Carulla, P., et al., 2015. Involvement of PrP(C) in kainate-induced excitotoxicity in several mouse strains. Sci Rep. 5**,** 11971.

Chiarini, L. B., et al., 2002. Cellular prion protein transduces neuroprotective signals. EMBO J. 21**,** 3317-26.

deCarvalho, T. N., et al., 2013. Aversive cues fail to activate fos expression in the asymmetric olfactory-habenula pathway of zebrafish. Front Neural Circuits. 7**,** 98.

Flechsig, E., et al., 2003. Expression of truncated PrP targeted to Purkinje cells of PrP knockout mice causes Purkinje cell death and ataxia. EMBO J. 22**,** 3095-101.

Fleisch, V., et al., 2013. Targeted mutation of the gene encoding prion protein in zebrafish reveals a conserved role in neuron excitability. Neurobiol Dis. 55**,** 11-25.

Fosque, B. F., et al., 2015. Neural circuits. Labeling of active neural circuits in vivo with designed calcium integrators. Science. 347**,** 755-60.

Greer, P. L., Greenberg, M. E., 2008. From synapse to nucleus: calcium-dependent gene transcription in the control of synapse development and function. Neuron. 59**,** 846-60.

Hans, S., et al., 2009. Temporally-controlled site-specific recombination in zebrafish. PLoS One. 4, e4640.

Kaiser, D., et al., 2012. Amyloid beta precursor protein and prion protein have a conserved interaction affecting cell adhesion and CNS development. PloS One. 7.

Khosravani, H., et al., 2008. Prion protein attenuates excitotoxicity by inhibiting NMDA receptors. J Cell Biol. 181, 551-565.

Kuffer, A., et al., 2016. The prion protein is an agonistic ligand of the G protein-coupled receptor Adgrg6. Nature. 536, 464-8.

Li, A., et al., 2007. Neonatal lethality in transgenic mice expressing prion protein with a deletion of residues 105-125. EMBO J. 26, 548-58.

Lieschke, G. J., Currie, P. D., 2007. Animal models of human disease: zebrafish swim into view. Nat Rev Genet. 8, 353-67.

McLennan, N., et al., 2004. Prion protein accumulation and neuroprotection in hypoxic brain damage. Am J Pathol. 165, 227-235.

Montag-Sallaz, M., Buonviso, N., 2002. Altered odor-induced expression of c-fos and arg 3.1 immediate early genes in the olfactory system after familiarization with an odor. J Neurobiol. 52, 61-72.

Moore, H. A., Whitmore, D., 2014. Circadian rhythmicity and light sensitivity of the zebrafish brain. PLoS One. 9, e86176.

Radovanovic, I., et al., 2005. Truncated prion protein and Doppel are myelinotoxic in the absence of oligodendrocytic PrPC. J Neurosci. 25, 4879-88.

Rangel, A., et al., 2007. Enhanced susceptibility of Prnp-deficient mice to kainate-induced seizures, neuronal apoptosis, and death: Role of AMPA/kainate receptors. J Neurosci Res. 85, 2741-55.

Rea, M. A., 1989. Light increases Fos-related protein immunoreactivity in the rat suprachiasmatic nuclei. Brain Res Bull. 23, 577-81.

Sakurai-Yamashita, Y., et al., 2005. Female-specific neuroprotection against transient brain ischemia observed in mice devoid of prion protein is abolished by ectopic expression of prion protein-like protein. Neuroscience. 136, 281-7.

Shamchuk, A. L., Tierney, K. B., 2012. Phenotyping stimulus evoked responses in larval zebrafish. Behaviour. 149, 1177-1203.

Shmerling, D., et al., 1998. Expression of amino-terminally truncated PrP in the mouse leading to ataxia and specific cerebellar lesions. Cell. 93**,** 203-14.

Shyu, W. C., et al., 2005. Overexpression of PrPC by adenovirus-mediated gene targeting reduces ischemic injury in a stroke rat model. J Neurosci. 25**,** 8967-77.

Steele, A. D., et al., 2007. The prion protein knockout mouse: a phenotype under challenge. Prion. 1**,** 83-93.

Striebel, J. F., et al., 2013. Prion protein and susceptibility to kainate-induced seizures: genetic pitfalls in the use of PrP knockout mice. Prion. 7**,** 280-5.

Teng, Y., et al., 2010. Knockdown of zebrafish Lgi1a results in abnormal development, brain defects and a seizure-like behavioral phenotype. Hum Mol Genet. 19**,** 4409-20.

Walz, R., et al., 1999. Increased sensitivity to seizures in mice lacking cellular prion protein. Epilepsia. 40**,** 1679-1682.

Weise, J., et al., 2006. Deletion of cellular prion protein results in reduced Akt activation, enhanced postischemic caspase-3 activation, and exacerbation of ischemic brain injury. Stroke. 37**,** 1296-300.

Westerfield, M., 2000. The Zebrafish Book. A Guide for the Laboratory Use of Zebrafish (Danio rerio). University of Oregon Press, Eugene, OR.

You, H., et al., 2012. Abeta neurotoxicity depends on interactions between copper ions, prion protein, and N-methyl-D-aspartate receptors. Proc Natl Acad Sci U S A. 109**,** 1737-42.

Zanata, S. M., et al., 2002. Stress-inducible protein 1 is a cell surface ligand for cellular prion that triggers neuroprotection. EMBO J. 21**,** 3307-16.

Chapter 4. PrP^C has a role in development of the zebrafish posterior lateral line[17]

---

[17] As outlined in the preface, a portion of Chapter 4 (Figure 4.3A) has been published in: Huc-Brandt, S., et al., 2014. Zebrafish prion protein PrP2 controls collective migration process during lateral line sensory system development. PLoS One. 9, e113331.

4.1 Summary

Misfolded forms of the Cellular Prion Protein (PrP^C) and Amyloid Precursor Protein (APP) are implicated in neurodegenerative disorders, but the functions of these proteins in healthy brains remain elusive. There is evidence to suggest, however, that both proteins participate in neural cell adhesion. Here we used the zebrafish lateral line, a mechanosensory system in fish that possesses hair cells homologous to those found in the inner ear of mammals, as a tractable model to investigate the roles of zebrafish PrP^C and APP homologs in neural cell development and adhesion. As *prp2* morphants had previously been shown to affect deposition pattern and adhesion of lateral line organs (neuromasts), we hypothesized that *prp1* would have roles redundant with those of *prp2* in lateral line development. We found that both *prp1* and *prp2* are involved in neuromast patterning in the lateral line, but they appear to have opposing functions. Given that *prp1* and *appa* interact in other capacities during zebrafish development, we also predicted that zebrafish prion proteins and appa would interact in lateral line patterning. While *appa* loss-of-function did not appear to influence the overall neuromast patterning defects in *prp1*$^{-/-}$ or *prp2*$^{-/-}$ mutant larvae, it is possible that it induces subtler effects on the structure of deposited neuromasts such as the localization of adherens junction proteins. Further investigation of the mechanisms underlying lateral line patterning defects in zebrafish prion protein mutants may uncover signalling pathways of relevance to neural cell adhesion and maintenance in mammals, which may be disrupted in prion diseases and Alzheimer's disease (AD).

4.2 Introduction

While the normal functions of PrP^C are not well characterized, it is known to interact with numerous extracellular matrix and cell surface proteins including laminin (Graner et al., 2000) and NCAM (Schmitt-Ulms et al., 2001; Watts et al., 2009). Further investigation of these interactions revealed participation of PrP^C in processes such as neuritogenesis and neurite outgrowth (Beraldo et al., 2011; Santuccione et al., 2005). Recently, it was also found that PrP^C is involved in polysialyation of NCAM during epithelial-to-mesenchymal transitions (Mehrabian et al., 2015). Further, PrP^C interacts with APP (Kaiser et al., 2012; Schmitz et al., 2014b), which is also involved in neural

development (reviewed in (Nicolas and Hassan, 2014)). Zebrafish homologs of *PRNP* and *APP* (*appa* and *prp1*) were shown to interact in mediating cell adhesion and neuroprotection in early stage zebrafish embryos (Kaiser et al., 2012), but their contributions to nervous system development have not been thoroughly explored. Further, *prp2*, *appa* and *appb* are expressed within the zebrafish lateral line ganglion (Cotto et al., 2005; Huc-Brandt et al., 2014; Malaga-Trillo et al., 2009; Musa et al., 2001). Given the expression pattern of these genes and the finding that zebrafish *prp2* morphants have lateral line defects (Huc-Brandt et al., 2014), we sought to confirm the role of *prp2* in lateral line development using *prp2^{ua5001/ua5001}* mutants, and to investigate potential contributions of *prp1* and *appa* to lateral line development.

The zebrafish lateral line mechanosensory system is a tractable system for studying nervous system development and collective cell migration (Thomas et al., 2015). Lateral lines are mechanosensory systems found in aquatic vertebrates that allow these animals to detect water movements. Neuromasts are the sensory organs of the lateral line and consist of mechanosensory hair cells, homologous to those found in the inner ear of mammals, surrounded by support cells (reviewed in (Ma and Raible, 2009)). Aquatic vertebrates use sensory information from the lateral line to detect the motions of predators and prey and to orient their bodies towards water currents (Dijkgraaf, 1963). The lateral line is made up of two major systems: the anterior lateral line and the posterior lateral line (PLL). The anterior lateral line includes the neuromasts of the head, jaw and operculum with their associated sensory neurons, while the posterior lateral line includes the neuromasts of the trunk and tail and associated sensory neurons (Ghysen and Dambly-Chaudiere, 2007). The development of the PLL is described in Figure 4.1.
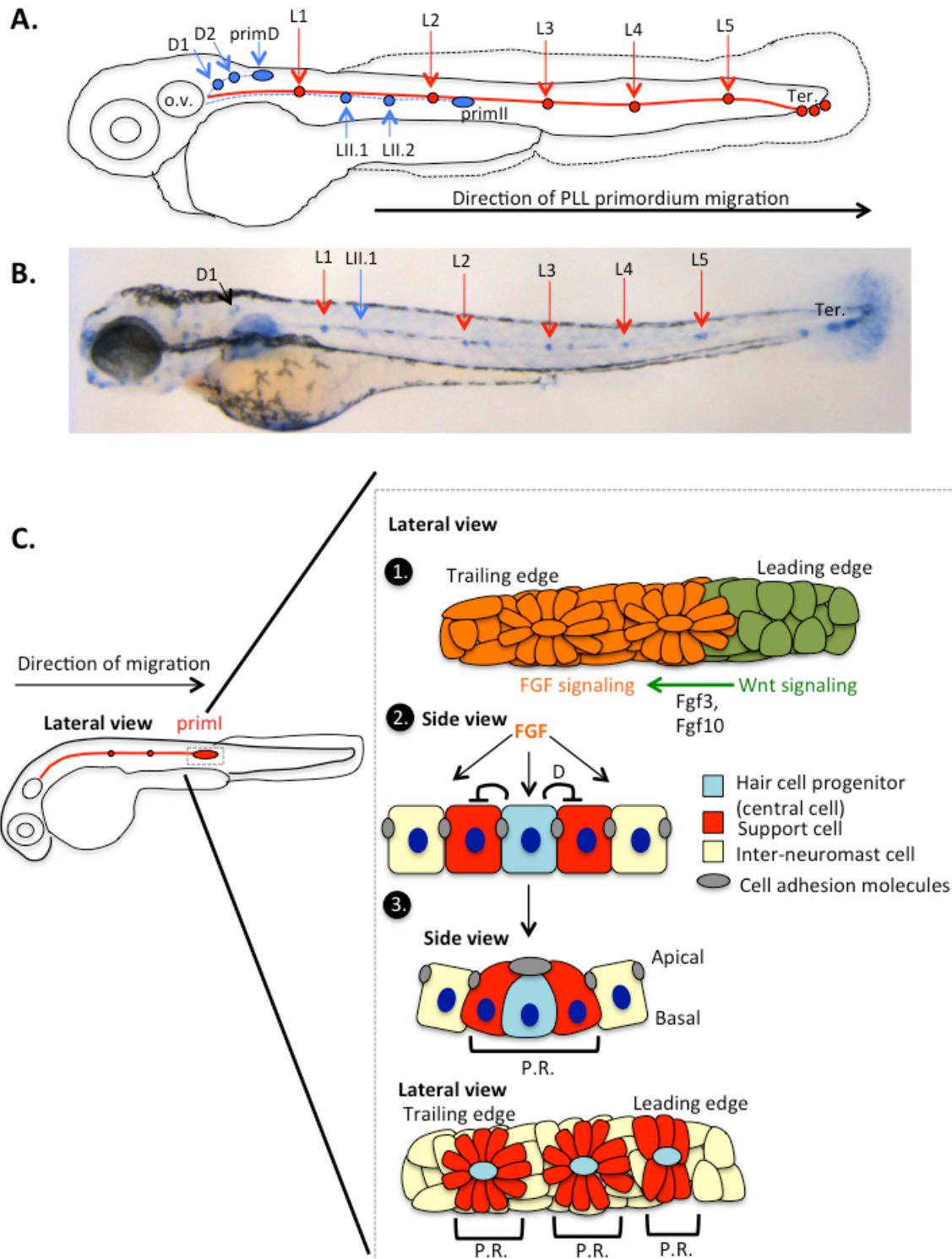
Figure 4.1. The posterior lateral line (PLL) is an accessible and well-characterized tissue to study neural cell cohesion and patterning

A. Schematic of the development of the zebrafish PLL. The fish depicted here is 48 hours post fertilization (hpf). At this stage of development, Prim I (solid red line; the first PLL system to form) has already completed its migration. It originated as a placode posterior to the otic vesicle (o.v., similar to the ear in mammals). During its migration towards the tail (from left to right in this diagram), it deposited 5 lateral posterior lateral line (L-PLL) trunk proneuromasts (L1-L5) and a stream of interneuromast cells on each side of the body. At about 40 hpf, PrimI reached the tip of the tail to produce 2-3 terminal neuromasts (Ter.). At the same time (~40 hpf), a second primordium (dashed blue line) formed near the otic vesicle. This primordium split to form the dorsal primoridum (prim D), which has deposited the first two dorsal neuromasts here (D1 and D2); and a secondary lateral PLL (prim II), which has begun following the migration path of primI and has deposited the first two secondary neuromasts (LII.1 and LII.2)(Dambly-Chaudiere et al., 2007). **B.** This sample image of a 72hpf wild type fish depicts the primary neuromasts and the first neuromast arising from the primII primordium. The alkaline phosphatase stain is not as dark in the LII.1 neuromast (blue arrow) as it is in the primary neuromasts (red arrows). Unlabeled neuromasts in the head region are part of the anterior lateral line. **C.** Signaling events in the primordium determine cell fate and regulate neuromast deposition. The fish shown on the left is approximately 30 hpf and the grey box demarks the primordium, which is enlarged on the right. **Part 1.** Wnt signaling in the leading edge of the primordium leads to production of Fgf3 and FgF10, which activate and maintain FGF signaling in the trailing edge. **Part 2.** Fgf signaling induces expression of *atoh1a* (marker of hair cell fate) and *deltaA*. Delta A (D) produced by hair cell progenitors prevents neighbouring cells from adopting a hair cell fate by restricting *atoh1a* expression. Meanwhile, FGF signaling causes neighbouring cells to adopt an epithelial cell fate. **Part 3.** Epithelial cells in contact with the hair cell progenitor are fated to become support cells of the neuromast. These support cells form apical clusters of cell adhesion molecules (including actin and ZO1). This process is at least partially mediated by Lgl1 and Lgl2. Since the adhesive forces among proneuromast rosette cells (hair cell progenitor and its associated support cells, P.R.) are stronger than those between proneuromast rosette cells and interneuromast cells, the rosette proneuromast cells will separate from the primordium as their migration velocity is reduced. The

212

bottom panel depicts a lateral view of 3 proneuromast rosettes (P.R.). The one on the far right is still forming, while the one left will be deposited next.

A summary of PLL anatomy in 30 hpf and 48 hpf larvae are shown in Figure 4.1C and Figure 4.1A, respectively. The primary PLL primordium (prim I, Figure 4.1C) originates posterior to the otic vesicle and deposits proneuromasts at regular intervals as it migrates towards the tail (reviewed in (Ghysen and Dambly-Chaudiere, 2007)). By 42 hpf, the primary PLL primordium has deposited 5-6 proneuromasts along the body axis (trunk neuromasts) and fragmented to form 2-3 neuromasts at the tip of the tail. By 48 hpf the cells in the proneuromasts have differentiated, producing mature neuromast organs ((Gompel et al., 2001); Figure 4.1A).

Considering the observations that *prp2* alters PLL development (Huc-Brandt et al., 2014), the known pathways of PLL development are worthy of consideration because they might hold clues into PrP[C] function. The migrating primordium is divided into two major zones. The leading zone is characterized by expression of genes involved in canonical Wnt (Wnt/β-catenin) signalling and proliferating cells, while the trailing zone is characterized by genes involved in FGF signalling and cells organized into rosettes that stabilize to form the proneuromasts (reviewed in (Thomas et al., 2015), Figure 4.1C Part 1). Wnt signalling in the leading zone induces production of fgf3 and fgf10a, which activate FGF signalling in the trailing zone. Wnt signalling also induces *sef* expression, which inhibits FGF activity in the leading zone. Similarly, FGF signalling induces production of dkk1b, which inhibits Wnt signalling in the trailing zone (Aman and Piotrowski, 2008). FGF signalling is responsible for the formation of proneuromast rosettes (Lecaudey et al., 2008), and contributes to cell fate determination of the rosette cells (Matsuda and Chitnis, 2010). FGF signalling induces expression of *atoh1a* and *deltaA*, a Notch ligand (Matsuda and Chitnis, 2010). Atoh1a induces production of atp2b1a, which exports calcium and is required for formation of hair cell specific structures including stereocilia and kinocilia (Go et al., 2010). Delta A restricts *atoh1a* expression to a central hair cell progenitor, which later differentiates to form the first hair cell of the rosette ((Matsuda and Chitnis, 2010), Figure 4.1C Part 2). This hair cell progenitor expresses *fgf10*, which maintains FGF signalling in neighbouring cells (Matsuda and Chitnis, 2010). FGF signalling causes the surrounding cells to adopt epithelial cell fate (Lecaudey et al., 2008) and stabilizes the rosette ((Matsuda and Chitnis, 2010), Figure 4.1C Part 2). Cells in contact with hair cell progenitors form apical

clusters of ZO1 and actin and remain a cohesive rosette unit during migration; whereas cells not in contact with a hair cell progenitor do not form apical cell junctions and become interneuromast cells ((Hava et al., 2009), Figure 4.1C Part 3).

Tight control of signalling events in the rosette is required for proper neuromast formation. *Ahoh1a* and *atp2b1* morphants have a reduced number of neuromasts and reduced number of hair cells in the L2 and L3 neuromasts (Go et al., 2010). Expansion of *atoh1a* expression into neighbouring cells causes them to become hair cell precursors and reduces cohesion among rosette cells, likely by disrupting expression of cell adhesion molecules (Matsuda and Chitnis, 2010). In fact, reduction in E-cadherin levels has been observed in *mib1* mutants, which have markedly reduced Notch signaling and an expanded *atoh1a* expression domain (Matsuda and Chitnis, 2010).

Morpholino knockdown of *prp2* by our collaborators was shown to produce lateral line defects. Specifically, morphants had a shortened PLL nerve, a reduced number of neuromasts and a reduced number of hair cells/neuromast. The change in neuromast number was likely due to a lack of cohesion within the neuromast rosettes, as clustering of actin and □-catenin at the apical side of rosette was reduced (Huc-Brandt et al., 2014). From there, we hypothesized that prp1 and prp2 have redundant roles in neuromast patterning in the zebrafish lateral line, and that zebrafish prion proteins interact with appa in this role. Instead, we found that $prp1^{-/-}$ fish had a reduced number of PLL trunk neuromasts (opposite to the phenotype observed in $prp2^{-/-}$ mutants). Intriguingly, combined loss of *prp1* and *prp2* yielded fish with a comparable number of trunk neuromasts as wild type fish, suggesting that Prp1 and Prp2 have opposing/competing roles in signalling pathway(s) underlying neuromast patterning. Loss of *appa* did not appear to modify the phenotypes observed in either $prp1^{-/-}$ or $prp2^{-/-}$ fish.

4.3 Methods

4.3.1 Fish lines/strains

Zebrafish of the AB strain were used as the wild type fish in this study unless otherwise noted. These wild type fish were closely related to the mutant fish used in the study. The previously published $prp2^{ua5001}$ allele (Fleisch et al., 2013) and $prp1^{ua5003}$, $prp1^{ua5004}$, and $appa^{ua5005}$ alleles (described in Chapter 2) were maintained on an AB

background. *Is22gt* larvae (Zfin ID: ZDB-ALT-120328-1) on an AB/Wik background were kindly provided by Maura McGrail's lab and bred to homozygosity (Liao et al., 2012). The *is22gt* allele was later crossed into the *prp2 ua5001* line. The *appa*^{ua5006} and *appa*^{ua5007} alleles were generated on an *is22gt* background using TALENs as described in Chapter 2. Tg(*clndb:gfp*) larvae (Tg *(-8.0cldnb:Ly-EGFP*, Zfin ID: ZDB-ALT-060919-2; referred to herein as *clndb:gfp*) (Haas and Gilmour, 2006) were kindly provided by Pierre Drapeau and were bred to the *prp1 ua5004*, *prp1 ua5003,* and *prp2 ua5001* mutant lines upon reaching adulthood.

4.3.2 Alkaline Phosphatase staining

Neuromasts are rich in endogenous alkaline phosphatase and staining for this allows for their observation. Zebrafish larvae were fixed in 4% paraformaldehyde (PFA) in phosphate buffer (pH 7.4) with 5% sucrose for 3–3.5 hours at room temperature. They were subsequently washed 4x in phosphate buffered saline (PBS; pH 7.4) with 0.1% tween (PBST) and then for 15 minutes in fresh alkaline phosphatase buffer (pH 9.5; 100 mM Tris-HCl, 100 mM NaCl, 50 mM MgCl2) with 0.1% tween. They were developed in alkaline phosphatase buffer containing 0.225% NBT and 0.175% BCIP (Roche catalogue #s11383213001 and 11383221001, Basel, Switzerland) for approximately 10 minutes. Fish were then washed for 30 minutes in alkaline phosphatase wash buffer (pH 7.5;154 mM NaCl, 11 mM Tris/ HCl, 1 mM EDTA) with 0.1% tween, fixed in 4% PFA with 5% sucrose, and washed 3x in PBST. Some fish were counterstained with Phalloidin 488 or 555 (Invitrogen Molecular Probes, catalogue #sA12379 and A34055, Eugene OR, USA) prior to imaging. For this, fish were incubated in PBS with 2% Triton X100 for 2 hrs. Phalloidin 488 was diluted twenty-fold in PBS with 2% Triton X 100 and left overnight at 4°C. Fish were then washed 3x 20 minutes in PBS with 2% triton and then washed into PBS with 0.1% tween. Wholemounts were transferred to a PBST/glycerol mixture and imaged with a Leica M165 FC dissecting microscope and Leica DFC 400 camera.

4.3.3 Analysis of neuromast number and position

Trunk neuromasts of the PLL were visualized by NBT/BCIP staining, or by detection of GFP fluorescence in *Tg*(*clndb:gfp*) using a Leica M165 FC dissecting microscope. An observer, who was blinded to the genotype of the fish, counted the

number of neuromasts. In some analyses, we examined neuromast number with respect to somite number. In some fish 3dpf fish, we noticed lighter stained neuromasts between the L1 and L2 neuromasts. These were likely neuromasts of the secondary posterior lateral line system (Figure 1). We considered these to be part of the secondary posteror lateral line system, and excluded them from our counts if they were ≤ 5 somite lengths posterior to the L1 neuromasts.

4.3.4 Fm43fx staining and β-catenin IHC

Fish were bathed in 3μM FM 1-43 Fx to label activated hair cells (i.e. hair cells undergoing mechanotransduction) (Invitrogen Molecular Probes, catalogue # F35355, Eugene OR, USA) in E3 medium/0.366% DMSO for 45 seconds. Fish were then rinsed 3x with E3 medium and euthanized using MS222. Fish were then fixed overnight in 4% PFA in phosphate buffer (pH 7.4) with 5% sucrose. Fish were first washed 3x 20 minutes in 0.1 M phosphate buffer with 5% sucrose, followed by a 5 minute wash in Milli-Q water with 1% Tween 20. Fish were then treated with chilled acetone for 7 minutes, and washed again for 5 minutes in Milli-Q water with 1% Tween 20. Fish were blocked for 1 hour in 10% natural goat serum (Thermo Fisher Scientific catalogue# 16210-064, Waltham MA, USA) in 1X PBS^{3+} (PBS containing 1% DMSO, 1% Tween 20 and 1% Triton). Fish were incubated with β-catenin primary antibody (Sigma catalogue #C2206, St. Louis, MO, USA) at a 1:1000 dilution overnight at 4°C in 2% natural goat serum in PBS^{3+}. Fish were rinsed with PBS^{3+} and then washed 2x 30 minutes with PBS^{3+} before the application of 1:1000 donkey α-Rabbit Alexa Fluor 555 secondary antibody (Invitrogen Molecular Probes, catalogue # A31572, Eugene OR, USA) in 2% natural goat serum in PBS^{3+}. Following an overnight incubation at 4°C, fish were washed 3x 30 minutes each in PBS^{3+} and treated for 1 hour with 1:5000 642/661 Topro 3 Iodide (Invitrogen Molecular Probes, catalogue #T3605, Eugene OR, USA). Fish were then washed several times with PBS^{3+} and 3x 5 minutes in 1xPBS. Fish were then embedded in 1% low melting point agarose (Sigma catalogue # A4018, St. Louis, MO, USA) on a cover slip and placed into depression slides. Wholemounts were imaged with a Zeiss LSM 700 Confocal Miscoscope with a Zeiss Axio Observer.Z1 and ZEN 2010 Software (version 6.0, Carl Zeiss MicroImaging, Oberkochen). Images were then processed using Imaris x64 (version 7.6.5, Bitplane Scientific Software, Badenerstrasse) and hair cells

were counted manually.

4.3.5 Genotyping

When larvae were from a mixed clutch, genomic DNA was extracted to genotype single larvae following analysis of neuromast number/positioning using 15 uL of 50 mM NaOH and 1.5 uL of 1 M Tris/HCl (pH 8) as described in Chapter 2. *prp1* mutants were genotyped using the RFLP described in Chapter 2, while *appa ua5005* mutants were genotyped using the RFLP described in Chapter 2. *ua5006* and *ua5007* alleles were generated by injecting maternal zygotic *appa*[is22gt/is22gt] larvae with TALENs against *appa* (Chapter 2). The *appa*[ua5006/ua5007] were offspring from an *appa*[is22gt/ua5006] x *appa*[is22gt/ua5007] cross and were genotyped based on the lack of RFP fluorescence, which is present in fish carrying the *is22gt* allele.

4.3.6 Statistics

Data were analyzed using GraphPad Prism Software (Version 6, GraphPad, San Diego, CA). Data were assessed for variance using the F-test prior to application of unpaired t-tests. If variance was significantly different, a Mann-Whitney test was performed instead. Data were assessed for variance and normal distribution using the Brown-Forsythe's test and Barlett's test prior to application of a one-way ANOVA. If variance was significantly different between groups, a Kruskal Wallis test was performed instead.

4.4 Results

4.4.1 Loss of *prp1* reduces the number of neuromasts in the developing zebrafish posterior lateral line

PrP[C] has previously been shown to contribute to neurite outgrowth (Beraldo et al., 2011; Pantera et al., 2009; Santuccione et al., 2005), and transient disruption of the zebrafish *prp2* paralog with morpholinos was found to affect posterior lateral line (PLL) primordium migration and neuromast number (Huc-Brandt et al., 2014). We therefore studied the role of the zebrafish *prp1* paralog in neuromast organization. As the alkaline phosphatase enzyme accumulates in mature neuromasts (Dambly-Chaudiere et al., 2007), we deployed an established alkaline phosphatase staining protocol (Villablanca et al.,

2006) to examine neuromast number and position in our $prp1^{ua5004/ua5004}$ mutants. Wild type fish typically have 5 primary trunk neuromasts and 2-3 terminal neuromasts at the tip of the tail arising from the primI primordium ((Ghysen and Dambly-Chaudiere, 2007); Figure 4.1). In some cases, the 6th primary neuromast is deposited before the primoridum reaches the tip of the tail (Gompel et al., 2001). We focused our analysis on the trunk neuromasts after finding that the terminal neuromasts of wild type fish were not reliably labeled with the alkaline phosphatase stain. 2dpf maternal zygotic $prp1^{ua5004/ua5004}$ mutants had fewer trunk neuromasts than age-matched wild type AB strain zebrafish (Figure 4.2 A-B, p<0.05). To verify this phenotype, we crossed our *prp1 ua5004* allele into the *Tg*(*clndb:gfp*) line. In this line, GFP labels the cell membranes of all PLL cells including those of the neuromasts, the interneuromast cells, and the migrating primordium (Haas and Gilmour, 2006). The trunk neuromast number was reduced in 50 hpf *Clnb:gfp*-labeled zygotic $prp1^{ua5004/ua5004}$ fish and $prp1^{+/ua5004}$ fish compared to closely related, age-matched *Clnb:gfp*-labeled $prp1^{+/+}$ fish (Figure 4.2 C-D, p<0.05). The difference in neuromast number between wild type clnb:gfp fish compared to non-transgenic wild type fish stained with alkaline phosphatase is likely due to the labeling method. Both mature and immature neuromast express *gfp* mRNA under the clnb promoter, whereas mature neuromasts produce more alkaline phosphatase; hence are more likely to be detected (Dambly-Chaudiere et al., 2007). To ensure that the observed phenotype was not due to developmental delay, neuromast number in 3dpf larvae were also examined. Again, trunk neuromast number was reduced in $prp1^{ua5004/ua5004}$ larvae compared to age-matched wild type AB strain larvae (Figure 4.3C, p<0.05), as assessed through alkaline phosphatase labeling. Upon counter-staining the fish with the actin stain, phalloidin, to more easily visualize the somites, it was found that the L1 neuromast was deposited more posterior (near somites 7-8) in 20% of the $prp1^{ua5004/ua5004}$ fish compared to the wild type fish examined, wherein the L1 neuromast was deposited near somites 5-6 (although 7% of wild type fish examined on a different day had L1 positioned near somites 7-8 as well; data not shown). In sum, these data support that Prp1 is required for normal development of the zebrafish PLL.
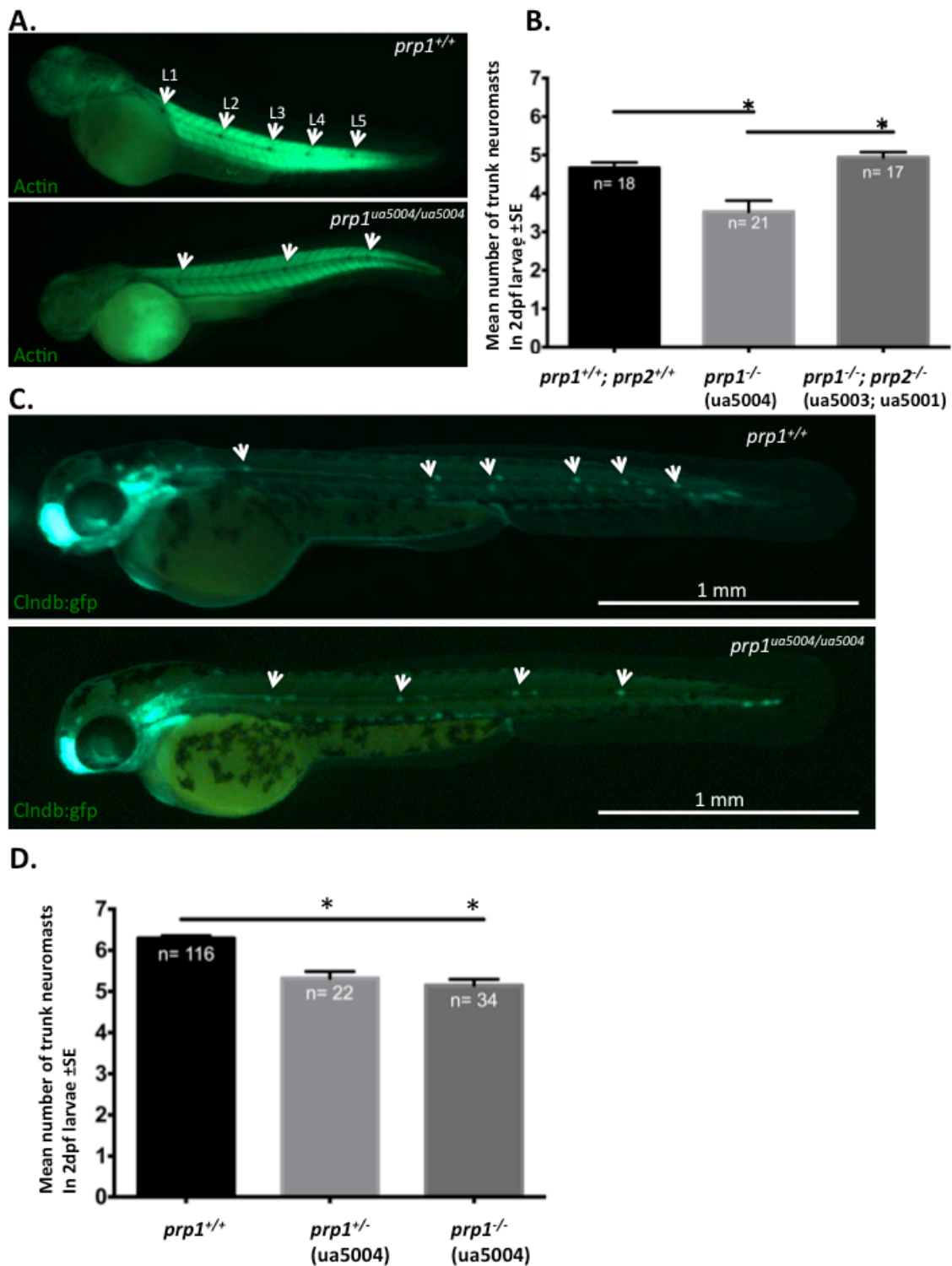
Figure 4.2. *prp1^{ua5004/ua5004}* **larvae have a reduced number of prim I trunk neuromasts compared to *prp1^{+/+}* larvae at 2dpf**

A. 2dpf wild type AB strain (*prp1^{+/+}*) zebrafish larvae (top) has 5 trunk neuromasts, while

a 2dpf maternal zygotic $prp1^{ua5004/ua5004}$ larvae (bottom) has 3 trunk neuromasts. Neuromasts are visualized by endogenous alkaline phosphatase labeling and larvae are counterstained with phalloidin 488. **B.** Quantification of the number of neuromasts through labeling of endogenous alkaline phosphatase revealed a reduction in trunk neuromast number in maternal zygotic $prp1^{ua5004/ua5004}$ mutants compared to wild type ($prp1^{+/+}$) fish. The number of neuromasts in compound maternal zygotic $prp1^{ua5003/ua5003}$; $prp2^{ua5001/ua5001}$ mutants is not statistically different compared to wild type fish. *$p<0.05$ with Kruskal-Wallis test. **C.** A 2dpf clnb:gfp $prp1^{+/+}$ larvae (top) has 6 trunk neuromasts, while a 2dpf maternal zygotic clnb:gfp $prp1^{ua5004/ua5004}$ mutant (bottom) has 4 trunk neuromasts. **D.** Quantification of the number of neuromasts in Clnb:gfp fish revealed a reduction in trunk neuromast number in both 2dpf $prp1^{+/ua5004}$ fish and 2dpf maternal zygotic $prp1^{ua5004/ua5004}$ fish compared to 2dpf Clnb:gfp $prp1^{+/+}$ larvae. *$p<0.05$ with one-way ANOVA. Sample sizes (n) refers to the number of fish.
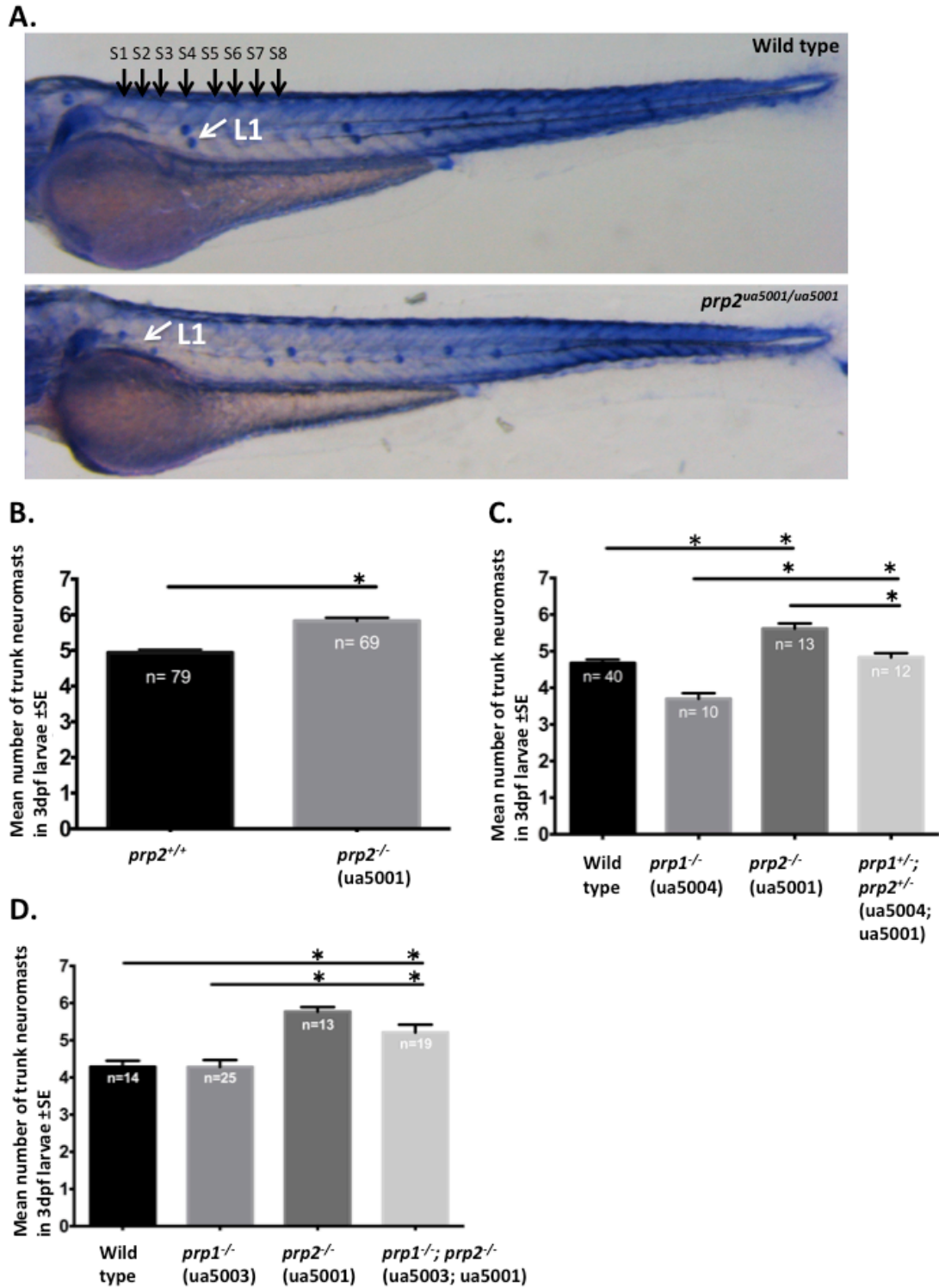
Figure 4.3. PrimI trunk neuromast number and position are altered in zebrafish *prnp* mutants[18]

---

[18] Panel A is modified/adapted from Huc-Brandt, S., et al., 2014. Zebrafish prion protein

A. In a representative 3dpf wild type AB strain (*prp2*$^{+/+}$) fish (top) the L1 neuromast was deposited at the boundary of the 5th and 6th somites, whereas in a representative 3 dpf maternal zygotic *prp2*$^{ua5001/ua5001}$ fish, the L1 neuromast was prematurely deposited at the boundary of the 1st and 2nd somites (bottom). Image was previously published in (Huc-Brandt et al., 2014). Endogenous alkaline phosphatase labeling was used to visualize the neuromasts. S, somite. Somites are numbered from anterior to posterior. **B.** Quantification of the number of trunk prim I neuromasts in 3dpf larvae revealed an increase in neuromast number in maternal zygotic *prp2*$^{ua5001/ua5001}$ mutants compared to wild type AB strain larvae. Both groups include offspring from 4 sets of parents (4 clutches/genotype). *$p<0.0001$ with unpaired t-test. n refers to the number of fish. **C.** A reduction in neuromast number in maternal zygotic *prp1*$^{ua5004/ua5004}$ mutants and an increase in neuromast number in maternal zygotic *prp2*$^{ua5001/ua5001}$ mutants compared to wild type AB strain larvae was observed. Combined loss of *prp1* and *prp2* in compound heterozygous *prp1*$^{+/ua5004}$; *prp2*$^{+/ua5001}$ fish reverted this phenotype. The wild type group includes offspring from 5 independent sets of parents (clutches), while each of the other groups include offspring from 2 independent sets of parents (clutches). *prp2*$^{ua5001/ua5001}$ fish were from a separate day of experiments than the other mutant groups and wild type fish were pooled from both experimental days (2 clutches from one day and 3 from the second day). A subset of the wild type and *prp2*$^{ua5001/ua5001}$ are re-plotted from part B. * $p<0.05$ with one-way ANOVA. **D.** Again, a significant increase in neuromast number was observed in 3dpf maternal zygotic *prp2*$^{ua5001/ua5001}$ larvae compared to age-matched wild type larvae. Unexpectedly, 3dpf maternal zygotic *prp1*$^{ua5003/ua5003}$ larvae had approximately the same number of neuromasts as wild type larvae. Combined loss of *prp1* and *prp2* reduced the number of neuromasts in *prp1*$^{ua5003/ua5003}$;*prp2*$^{ua5001/ua5001}$ mutants towards wild type levels, though not significantly. *$p<0.05$ with the Kruskal Wallis test.

---

n refers to the number of fish. Endogenous alkaline phosphatase labeling was used to visualize the neuromasts.

4.4.2 Loss of *prp2* increases the number of neuromasts in the developing zebrafish posterior lateral line

We hypothesized that *prp1* and *prp2* have redundant roles in PLL development, thus we expected that loss of *prp2* would also disrupt PLL neuromast deposition. As neuromast patterning was previously found to be disrupted in *prp2* morphants (Huc-Brandt et al., 2014), we examined neuromast position and number in maternal zygotic *prp2*$^{ua5001/ua5001}$ mutants. As reported in Huc-Brandt et al. (2014), the L1 neuromast was deposited prematurely (near somites 1-3) in 92% of maternal zygotic *prp2*$^{ua5001/ua5001}$ mutants. In wild type fish, the L1 neuromast was typically found near somites 5-6, with a range between the 3rd-8th somites. Representative images are shown in Figure 4.3A and were published previously in (Huc-Brandt et al., 2014). Additionally, the maternal zygotic *prp2*$^{ua5001/ua5001}$ mutants had extra primI trunk neuromasts at 3dpf compared to age-matched wild type AB strain (*prp2*$^{+/+}$) fish (Figure 4.3B, p<0.0001). Four clutches of fish from each genotype were included in the analysis. Comparing this data with that of the previous section, an unexpected contrast emerges: *prp1* promotes neuromast formation and/or deposition, whereas *prp2* restricts the number of neuromasts in the PLL.

4.4.3 Combined loss of *prp1* and *prp2* restores the number of posterior lateral line neuromasts to wild type levels

Considering the opposite effects of loss of *prp1* compared to loss of *prp2* on neuromast abundance reported above, we next examined whether an interaction between *prp1* and *prp2* might exist in neuromast number and patterning. For this experiment, fish (including a subset of fish in Figure 4.2B) were counterstained with the actin stain, phalloidin, to facilitate visualization of the somites. Somites are regularly spaced in developing zebrafish embryos, thus we assessed neuromast position relative to its closest somite (Figure 4.3A). Partial loss of both *prp1* and *prp2* in 3dpf compound *prp1*$^{+/ua5004}$; *prp2*$^{+/ua5001}$ fish restored the neuromast number to the range found in age-matched wild type AB strain (*prp1*$^{+/+}$; *prp2*$^{+/+}$ fish) (Figure 4.3C). The compound *prp1*$^{+/ua5004}$; *prp2*$^{+/ua5001}$ fish had significantly more prim I trunk neuromasts than maternal zygotic *prp1*$^{ua5004/ua5004}$ mutants and significantly fewer prim I trunk neuromasts than maternal zygotic *prp2*$^{ua5001/ua5001}$ mutants (Figure 4.3C, p<0.05). Additionally, the L1 neuromasts in

prp1^{+/ua5004}; *prp2*^{+/ua5001} mutants were positioned near somites 4-6, matching the pattern seen in wild type AB strain zebrafish. We next asked whether this apparent rescue of the *prp1*^{-/-} and *prp2*^{-/-} mutant phenotypes in *prp1*^{+/ua5004}; *prp2*^{+/ua5001} mutants might be due to gene linkage of a protective factor. To rule out the possibility that the *prp1 ua5004* allele was linked to a protective factor, we assessed neuromast number in compound *prnp* mutants with a second *prp1* allele. 2dpf maternal zygotic *prp1*^{ua5003/ua5003}; *prp2*^{ua5001/ua5001} fish also had trunk neuromast numbers comparable to those observed in age-matched wild type AB strain fish (Figure 4.2B). Unexpectedly, when we compared the number of neuromasts in 3dpf maternal zygotic *prp1*^{ua5003/ua5003} to age-matched wild type larvae, we found approximately the same number of neuromasts in both genotypes (Figure 4.3D). This may be partially because the neuromast number in wild type fish in this clutch was slightly reduced compared to the number in other wild type clutches examined in this study. Nevertheless the neuromast number in 3dpf compound *prp1*^{ua5003/ua5003};*prp2*^{ua5001/ua5001} larvae was still reduced (though not significantly) relative to the number of neuromasts in 3dpf *prp2*^{ua5001/ua5001} fish (Figure 4.3D). Overall concerted loss of *prp1* and *prp2* in *prp1*^{-/-};*prp2*^{-/-} double mutants reverted the phenotypes observed in single *prp1*^{-/-} and *prp2*^{-/-} mutants.

4.4.4 Some *appa* loss-of-function alleles reduce the number of neuromasts in the posterior lateral line

As APP has also been shown to be involved in neurodevelopment (reviewed in (Nicolas and Hassan, 2014)), and *appa* is expressed in the PLL (Musa et al., 2001) we next asked whether *appa* has a role in neuromast organization within the PLL. We first examined neuromast number in fish with the *appa is22gt* allele, an allele with partial loss of *appa* function. These fish have an RFP gene trap insertion within intron 4 of *appa*, which leads to production a truncated appa protein fused to RFP. The splice machinery at the gene-trap site isn't completely efficient, however, leading to production of a small amount of full-length *appa* transcript (Liao et al., 2012). Maternal zygotic *appa*^{is22gt/is22g} fish had significantly fewer trunk neuromasts at 3dpf compared to age matched wild type (*appa*^{+/+}) zebrafish (Figure 4.4A, p=0.0011).
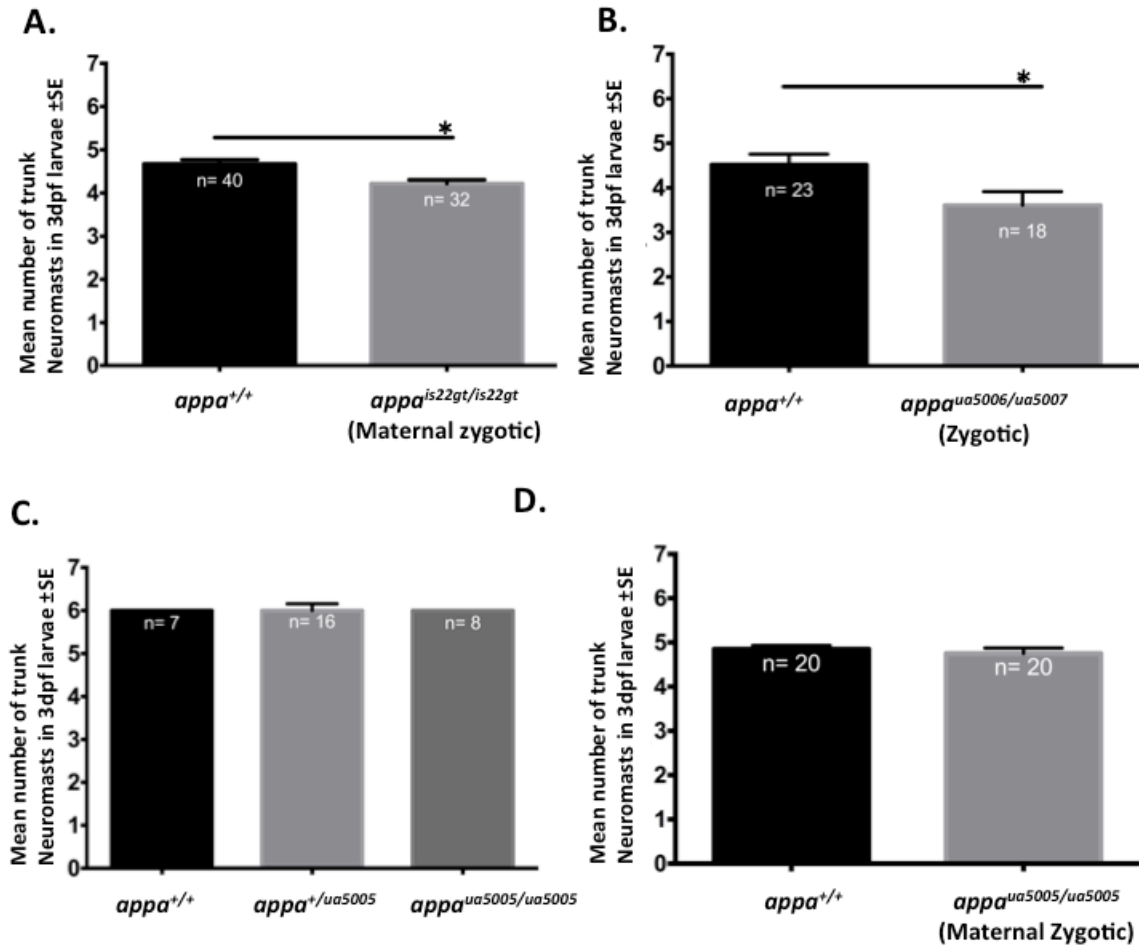
Figure 4.4. The number of Prim I trunk neuromasts is reduced in fish with some loss-of-function *appa* alleles

A. Quantification of the number of trunk prim I neuromasts in 3dpf larvae revealed a reduction in neuromast number in maternal zygotic *appa*[is22gt/is22gt] fish (Liao et al., 2012) compared to wild type AB strain (*appa*^{+/+}) larvae. Both groups of fish were pooled from two separate experimental days and represent offspring from 4 independent sets of parents (4 clutches/genotype). *p=0.0011 with unpaired t-test. Endogenous alkaline phosphatase labeling was used to visualize the neuromasts. **B.** Quantification of the number of trunk prim I neuromasts in 3dpf larvae revealed a reduction in neuromast number in zygotic *appa*[ua5006/ua5007] fish compared to wild type AB strain (*appa*^{+/+}) larvae. One clutch of fish is represented/genotype. *p=0.0205 with unpaired t-test. n refers to the number of fish. Endogenous alkaline phosphatase labeling was used to visualize the neuromasts. **C.** Quantification of the number of trunk neuromasts in 3dpf larvae did not

reveal a difference in neuromast number between zygotic $appa^{ua5005/ua5005}$ fish and either $appa^{+/ua5005}$ or $appa^{+/+}$ siblings. It is possible that secondary neuromasts were counted in this dataset because it was collected before we became aware of the potential confound that secondary neuromasts appear during day 3 of development. Endogenous alkaline phosphatase labeling was used to visualize the neuromasts. **D.** Quantification of prim I trunk neuromasts in 3dpf larvae did not reveal a difference in neuromast number between wild type AB strain ($appa^{+/+}$) fish and maternal zygotic $appa^{ua5005/ua5005}$ mutants. Two clutches of fish are represented/genotype. n refers to the number of fish. Endogenous alkaline phosphatase labeling was used to visualize the neuromasts.

We next examined the affect of frameshift *appa* alleles (predicted to be null due to premature stop codons) on neuromast number. We first examined the affect of *appa* alleles generated on the *is22gt* background. Zygotic *appa*$^{ua5006/ua5007}$ fish had a reduced number of trunk neuromasts at 3dpf compared to age-matched wild type (*appa*$^{+/+}$) AB strain zebrafish (Figure 4.4B, p =0.0205). In contrast, 3dpf fish with the *appa ua5005* frame-shift allele (generated on a wild type AB background) did not have a difference in neuromast number compared to control fish. Neither *appa*$^{+/ua5005}$ nor zygotic *appa*$^{ua5005/ua5005}$ fish had a difference in trunk neuromast number compared to *appa*$^{ua5005/ua5005}$ fish (Figure 4.4C). Further, maternal zygotic *appa*$^{ua5005/ua5005}$ did not display a difference in neuromast number compared to age-matched wild type (*appa*$^{+/+}$) AB strain zebrafish (Figure 4.4D). It is possible that differences between the data sets are due to strain differences as the *appa*^{is22gt} fish had a mixed AB/Wik background. In sum, whether *appa* plays a role in the deposition of lateral line neuromasts remains ambiguous.

4.4.5 Loss of *appa* does not synergize with loss of zebrafish *prnps* to exert a significant effect on PLL neuromast number

As we previously showed that acute knockdown of *prp1* and *appa* reveal interacting roles in early development, including in cell adhesion processes (Kaiser et al., 2012), we next asked whether zebrafish *prnps* and *appa* have additive affects in PLL development. We found no significant difference in the number of primI trunk neuromasts in compound 3dpf maternal zygotic *appa*$^{is22gt/is22gt}$;*prp2*$^{ua5001/ua5001}$ mutants compared to age-matched *prp2*$^{ua5001/ua5001}$ mutants (Figure 4.5A). Further, while the number of neuromasts was significantly reduced in *prp1*$^{ua5003/ua5003}$;*appa*$^{ua5005/ua5005}$ fish relative to wild type fish and *prp1*$^{ua5003/ua5003}$ fish (Figure 4.5B, p<0.05), it was not significantly different from that observed in *appa*$^{ua5005/ua5005}$ fish. Thus an additive effect of concerted loss of *appa* and *prp1* on neuromast number was not demonstrated. Overall our crosses of *prnp* and *appa* mutants did not reveal a convincing interaction between *appa* and *prnps* on neuromast number.
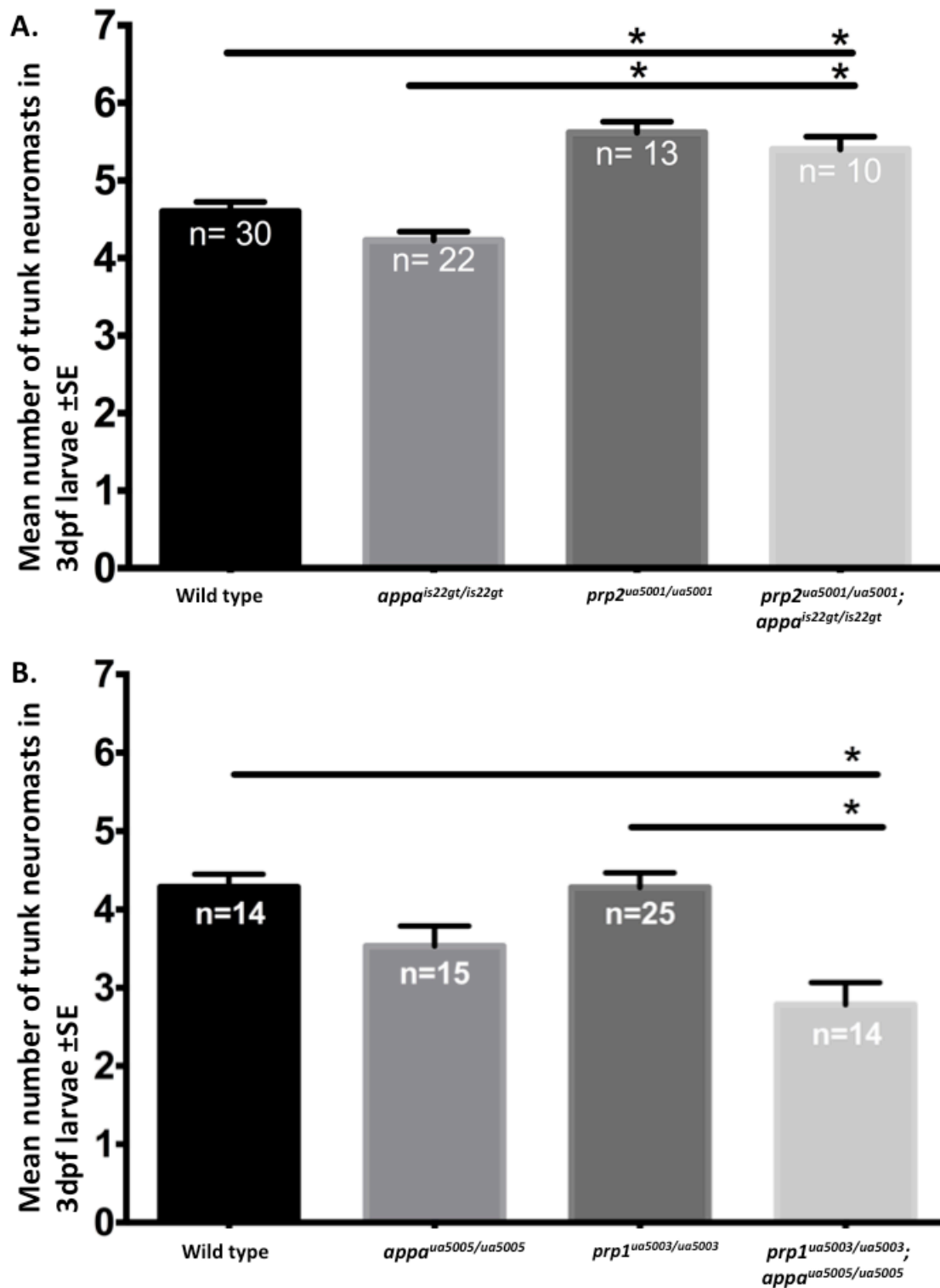
Figure 4.5. Loss of *appa* does not appear to synergize with loss of *prp2* or *prp1* in double mutants

A. Quantification of the number of prim I trunk neuromasts in 3dpf larvae did not reveal

a difference in neuromast number between maternal zygotic $prp2^{ua5001/ua5001}$ mutants and maternal zygotic compound $prp2^{ua5001/ua5001}$; $appa^{is22gt/is22gt}$ fish. Both groups had an increase in neuromast number compared to 3dpf wild type AB strain ($prp2^{+/+};appa^{+/+}$) and $appa^{is22gt/is22gt}$ zebrafish. The wild type group includes offspring from 3 sets of independent parents, the $prp2^{ua5001/ua5001}$ and $appa^{is22gt/is22gt}$ groups include offspring from 2 independent sets of parents, and the $prp2^{ua5001/ua5001}$; $appa^{is22gt/is22gt}$ group includes offspring from 1 set of parents. *p<0.05 with one-way ANOVA. **B.** Quantification of the number of prim I trunk neuromasts in 3dpf larvae did not reveal a significant difference in neuromast number between maternal zygotic $appa^{ua5005/ua5005}$ mutants and maternal zygotic $prp1^{ua5003/ua5003}$;$appa^{ua5005/ua5005}$ fish. Compound $prp1^{ua5003/ua5003}$;$appa^{ua5005/ua5005}$ fish did, however, have a significant reduction in neuromast number compared to wild type fish and single $prp1^{ua5003/ua5003}$ fish. *p<0.05 with one-way ANOVA. Wild type and $prp1^{ua5003/ua5003}$ data is replotted from Figure 4.2D. Endogenous alkaline phosphatase was used to visualize the neuromasts. n refers to the number of fish.

4.4.6 β-catenin levels were reduced in compound *prp1^ua5003/ua5003*; *appa^ua5005/ua5005*
mutants and there appeared to be less β-catenin at the center of neuromast rosettes

Hair cell number was reduced in *prp2* morphants (Huc-Brandt et al., 2014), leading us to speculate that the rosette structure within the primordium (Figure 4.1C Part 3) might be disrupted. While the hair cells appeared to be arranged in bundles in *prp1^ua5003/ua5003*; *appa^ua5005/ua5005* mutants as in wild type fish, there appeared to be reduced β-catenin levels in the cell membranes of hair cells and surrounding cells in the 6 *prp1^ua5003/ua5003*;*appa^ua5005/ua5005* fish examined compared to the 6 wild type fish examined. Further, less β-catenin was found at the apical surfaces of the hair cells (rosette center) in the 3dpf *prp1^ua5003/ua5003*;*appa^ua5005/ua5005*mutants compared to 3 dpf wild type fish. Representative images are shown in Figure 4.6A.

4.4.7 Hair cell numbers are not detectably different in the L2 neuromast of
compound *prp1^-/-*;*prp2^-/-* mutants or *prp1^-/-*;*appa^-/-* mutants

Activation of Wnt/beta catenin signaling in deposited neuromasts has been shown to increase hair cell number, presumably by inducing proliferation of support cells (Head et al., 2013; Jacques et al., 2014), while inhibition of Wnt signaling produces a reduction in lateral line hair cell number (Jacques et al., 2014). This, along with the observation that hair cell number was reduced in *prp2* morphants (Huc-Brandt et al., 2014), led us to speculate that reduced β catenin levels might influence hair cell number in deposited neuromasts. We therefore examined the number of activated hair cells in compound *prp1^-/-*;*appa^-/-* mutants and compound *prp1^-/-*;*prp2^-/-* mutants using a fixable analog of the live cell stain Fm43, Fm43-Fx. Fm43 is a styryl dye that is taken up through mechanotransduction channels in mature hair cells (Seiler and Nicolson, 1999). Hair cell number was unchanged in the L2 neuromast of both compound *prp1^ua5003/ua5003-*; *prp2^ua5001/ua5001* mutants and *prp1^ua5003/ua5003*; *appa^ua5005/ua5005* mutants (Figure 4.6 B-C). The latter result is not surprising given that combined loss of *prp1* and *prp2* produces an apparent rescue of neuromast number, compared to what is observed in single *prp1^-/-* or *prp2^-/-* mutants.
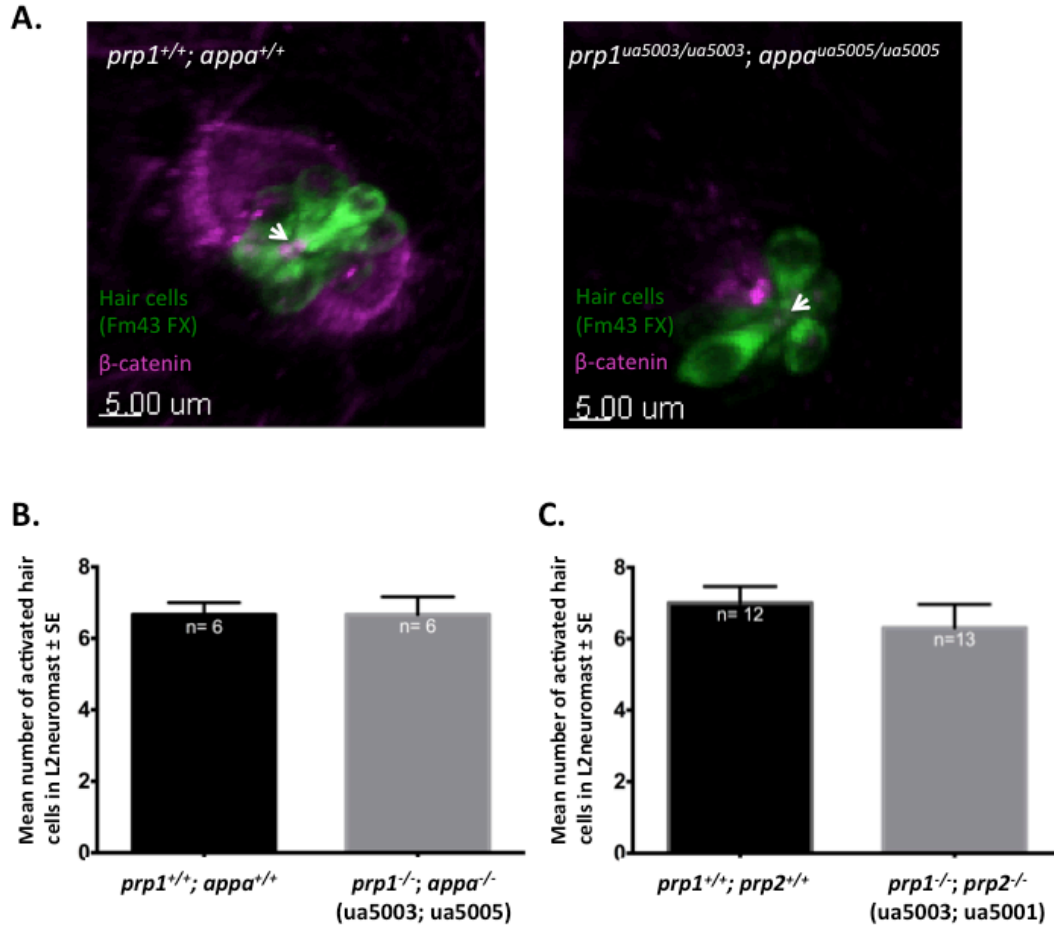
Figure 4.6. Combined loss of _prp1_ and _appa_ appeared to influence levels of β-catenin, but the number of activated hair cells per neuromast appears unchanged in compound _prp1^-/-_; _appa^-/-_ and _prp1^-/-_; _prp2^-/-_ mutants

A. Wild type fish (left panel) have dense β-catenin staining at the base of the hair cells of the L2 neuromast, while _prp1^ua5003/ua5003_; _appa^ua5005/ua5005_ fish (right panel) appear to have less □-catenin at the base of the hair cells and in the plasma membranes of surrounding cells. Fish were stained with β-catenin antibody and Alexafluor 555 secondary antibody (pseudo-coloured magenta) along with Fm43fx (pseudo-coloured green) to label the neuromast hair cells. Topro 3 channel is not shown. **B.** No difference was observed in the number of activated hair cells in the L2 neuromast of wild type (_prp1^+/+_; _appa^+/+_ fish) versus the L2 neuromast of _prp1^ua5003/ua5003_; _appa^ua5005/ua5005_ fish. n= number of fish. **C.** No difference was observed in the number of activated hair cells in the L2 neuromast of wild type (_prp1^+/+_; _prp2^+/+_ fish) versus the L2 neuromast of _prp1^ua5003/ua5003_; _prp2^ua5001/ua5001_ fish. n= number of fish.

4.5 Discussion

4.5.1 Prion proteins contribute to neuromast patterning within the zebrafish PLL

We hypothesized that the zebrafish prp1 and prp2 would have redundant functions in PLL development. We found that both prp1 and prp2 contributed to neuromast patterning, but they appeared to have opposing roles: loss of prp1 (in *prp1⁻ᐟ⁻* mutants) led to a reduced number of neuromasts, consistent with the phenotype previously observed in *prp2* morphants (Huc-Brandt et al., 2014), while loss of Prp2 in (in *prp2⁻ᐟ⁻* mutants) led to an increase in neuromast number and premature deposition of the L1 neuromast. These results countered our expectation that prp1 and prp2 would be redundant in development of the PLL.

4.5.2 Hypothetical mechanisms underlying abnormal neuromast patterning in zebrafish PrP mutants

Zebrafish prp1 or prp2 loss-of-function could interfere with neuromast formation/deposition at multiple levels. First, loss of prp1 function could reduce neuromast number at the level of Wnt/β catenin-signaling. Under normal conditions, Wnt proteins bind to a Frizzled/LRP5/6 complex and stabilize cytosolic β-catenin by preventing its phosphorylation by GSK-3β and destruction by the proteasome (reviewed in (Komiya and Habas, 2008)). β-catenin then translocates to the nucleus to activate transcription of *fgf3* and *fgf10*, which activate FGF signaling in the trailing zone of the primordium ((Aman and Piotrowski, 2008), Figure 4.1C). Disruption of FGF signaling could interfere with proneuromast rosette formation, leading to the reduced number of neuromasts observed in *prp1⁻ᐟ⁻* mutants. PrP^C has been shown to inactivate GSK-3β through caveolin/Lyn (Hernandez-Rapp et al., 2014). Further, an increase in the active (non-phosphorylated) form of GSK-3β and an increase in phosphorylated β-catenin (the form targeted for degradation) were also observed in the brains of Scrapie infected mice (Sun et al., 2015). Reduction in neuromast number in *prp1⁻ᐟ⁻* mutants, therefore, could be due to increased degradation of β-catenin and subsequent reduction in β-catenin induced FGF signaling.

Loss of prp2 function could increase neuromast number at the level of Notch signaling. Since Notch signaling restricts hair cell progenitor formation (Matsuda and

Chitnis, 2010), it may also restrict the number of proneuromast rosettes present at a time in the PLL primordium since apical adhesions between hair cell progenitors and its associated support cells precedes proneuromast rosette formation ((Hava et al., 2009), Figure 4.1C). Thus it is possible that prp2 loss-of-function causes an increase in neuromast number and premature deposition of the L1 neuromast through a disruption in Delta/Notch signaling and a subsequent increase in the number of hair cell progenitors in the primordium.

Finally, differential localization and/or levels of cell adhesion molecules in $prp1^{-/-}$ and $prp2^{-/-}$ mutants may influence proneuromast rosette structure (and hence neuromast number and patterning). In $prp1^{-/-}$ mutants, it is possible that some rosette adhesions are weak causing the cells to be dispersed as interneuromast cells. In $prp2^{-/-}$ mutants, it is possible that the adhesions between some cells are strong enough to maintain a rosette structure but the first rosette (L1) splits in two. Although one half of this split rosette would lack a hair cell progenitor, one of the support cells in this half becomes a hair cell progenitor in the absence of Delta-Notch inhibition. E-cadherin is one candidate cell adhesion protein that may be mislocalized in $prp1^{-/-}$ and/or $prp2^{-/-}$ mutants. PrP^C downregulation has been shown to contribute to abnormal adherens junctions in Human A431 epidermoid carcinoma cells (Solis et al., 2012). Loss of PrP^C reduces adherens junction formation and organization and reduces movement of adherens junctions to the apical cell contact sites. As PrP^C colocalizes with reggies, E-cadherin and epidermal growth factor receptor in macropinosomes, the authors proposed that PrP^C may interact with reggies to activate Src kinases. This may promote endocytosis of EGFR, which normally triggers macropinocytosis of E-cadherin, thereby reducing E-cadherin recycling from adherens junctions (Solis et al., 2012).

4.5.3 Hypothetical mechanisms to explain the apparent rescue of neuromast patterning in compound $prp1^{-/-}$; $prp2^{-/-}$ compound mutants

One alternative hypothesis to explain the apparent rescue of neuromast patterning in compound $prp1^{-/-}$; $prp2^{-/-}$ mutants is that prp1 and prp2 act at different stages of proneuromast development (i.e. have sub-functionalized roles in neuromast patterning), and a disruption in one phase of proneuromast development is countered by a second

disruption later in development. For example, loss of prp1 may cause a partial reduction in Wnt/β-catenin signaling leading to an initial reduction in the number of proneuromast rosettes in the primordium. Later, however, loss of prp2 function may reduce Delta/Notch lateral inhibition producing an extra hair cell progenitor (and eventually an extra rosette) in the trailing edge of the primordium.

A second series of alternative hypotheses is that prp1 and prp2 differentially regulate a hypothetical cell membrane receptor, denoted here as 'Receptor Y' (Figure 4.7). In wild type fish, prp2 might regulate prp1 (through direct binding) as prp1 binds to and activates 'Receptor Y' (Figure 4.7A). Alternatively, prp1 binding to 'Receptor Y' might activate a signaling pathway, while prp2 competes for binding sites on 'Receptor Y' and partially activates or inhibits a signaling pathway as depicted in Figure 4.7C. In $prp2^{-/-}$ mutants, prp1 is not regulated by prp2 and thus over-activates 'Receptor Y' (Figure 4.7B). Conversely, in $prp1^{-/-}$ mutants; prp2 inhibits or reduces the activity of 'Receptor Y' (Figure 4.7C). Finally, in compound $prp1^{-/-} prp2^{-/-}$ mutants, a compensatory protein activates 'Receptor Y (Figure 4.7D). Hypothetically, 'Receptor Y' activation could represent Caveolin1- mediated activation of Lyn. If this were the case, prp1 binding to Caveolin 1 would be regulated by prp2 in wild type fish leading to normal levels of Lyn activation (see Figure 4.7A). Lyn would then phosphorylate GSK-3β, and normal levels of β-catenin would then go on to activate transcription of FGF signaling activators (eg. $fgf3$ and $fgf10$). In $prp2^{-/-}$ larvae, activation of Lyn by prp1 would not be properly regulated (Figure 4.7B). This might lead to an over-abundance of β-catenin and $fgf10$ transcripts. Overexpression of $fgf10$ in the leading edge of the primordium might cause an increase in the number of trailing edge cells that become hair cell progenitors, hence increasing neuromast number. In $prp1^{-/-}$ larvae, Lyn activation would be reduced or inhibited (Figure 4.7C). This would cause more β-catenin to be marked for destruction in $prp1^{-/-}$ mutants than in wild type fish. Reduced activation of FGF signaling would then limit the number of proneuromast rosettes formed in the trailing edge of the PLL primordium. In sum, a variety of molecular mechanisms could be investigated to explain the apparent rescue of neuromast number in compound $prp1^{-/-}$;$prp2^{-/-}$ mutants.
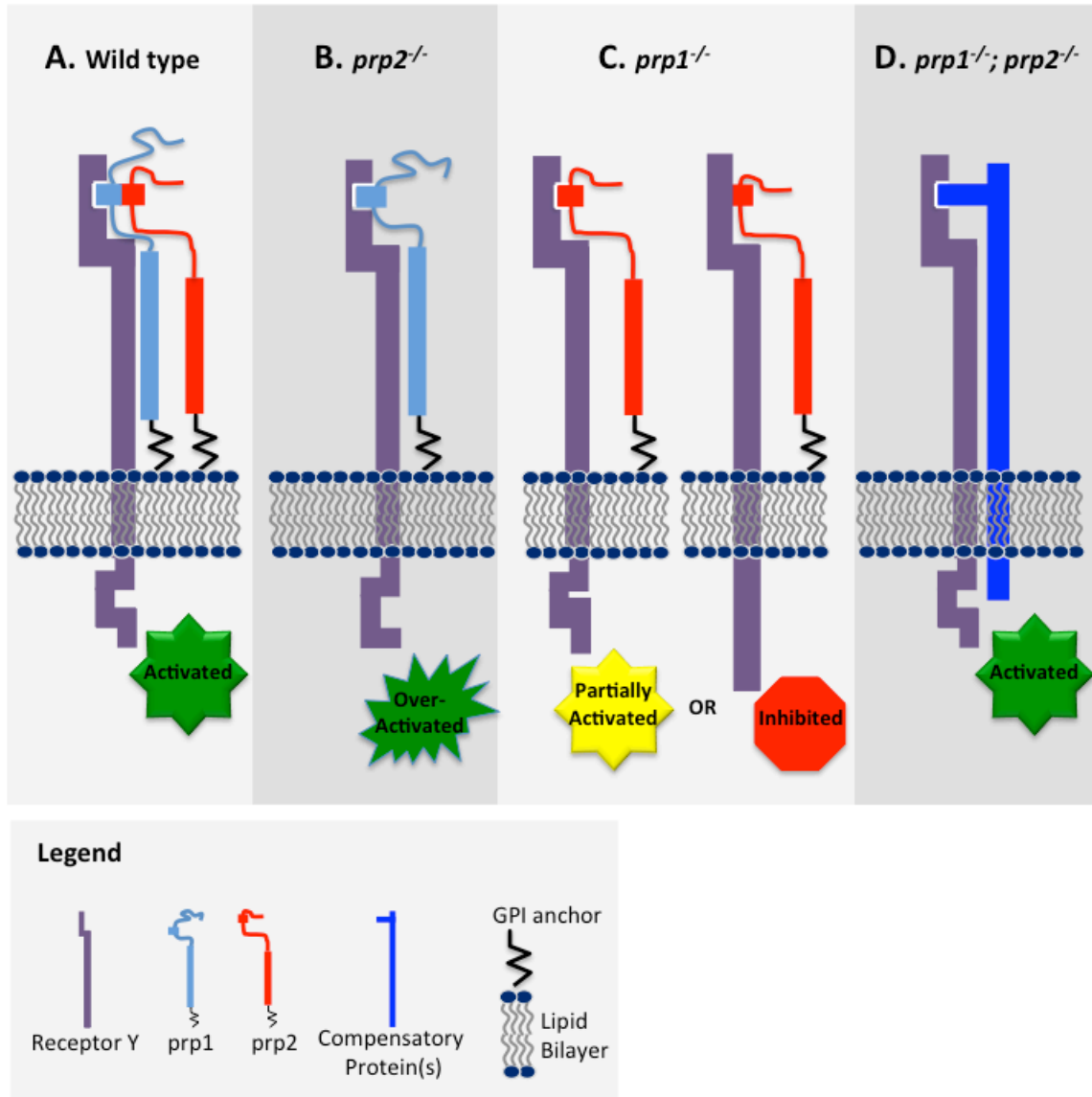
Figure 4.7. Hypothetical model to explain the differential effects of *prp1* and *prp2* loss-of-function on neuromast number and the apparent rescue of both phenotypes in *prp1/prp2* compound mutants

A. In this hypothetical model, prp1 binds to a membrane receptor, an unknown 'Receptor Y,' thereby activating it in wild type fish. Prp2 regulates this activity by direct binding to prp1 (shown here) or by competing with prp1 for access to 'Receptor Y' (as depicted in panel C). **B.** When prp2 is absent, prp1 over-activates 'Receptor Y'. **C.** When prp1 is absent, prp2 outcompetes other substrates for access to 'Receptor Y'. Prp2 binding to 'Receptor Y' may reduce or inhibit its normal function. **D.** Absence of prp1 and prp2

causes transcription of compensatory genes. Compensatory proteins that may have been present in *prp1$^{-/-}$* fish can now access 'Receptor Y' because prp2 is no longer blocking the receptor-binding site.

4.5.4 Role of APP in PLL neuromast patterning remains ambiguous

We were interested in determining whether appa also contributes to neuromast patterning in the PLL because we previously found that *appa* and *prp1* interact during zebrafish development (Kaiser et al., 2012). We found that some *appa* loss-of-function alleles (*is22gt*, *ua5006* and *ua5007*) yielded reductions in neuromast number, whereas the *appa ua5005* loss-of-function allele did not alter neuromast number relative to wild type *appa*. The differences observed between these *appa* loss-of-function alleles could be due to differences in genetic background: the *appa*$^{is22gt/is22gt}$ and *appa*$^{ua5006/ua5007}$ larvae had both AB and Wik as background strains, whereas the *appa*$^{ua5005/ua5005}$ fish were maintained on an AB background. Differences in the strength of the *appa* alleles might also contribute. The *appa is22gt* allele is hypomorphic (some normally spliced *appa* is still produced) (Liao et al., 2012), whereas *appa* transcript levels in maternal zygotic *appa*$^{ua5005/ua5005}$ fish (see Chapter 2) suggest that the *appa ua5005* allele is a null allele. Transcript levels were not measured in the *appa*$^{ua5006/ua5007}$ larvae. It is possible that gene compensation is triggered in fish with the *appa ua5005* allele, but not in fish with the *appa is22gt* allele because the *ua5005* allele is a null; however this does not explain why neuromast patterning is normal in heterozygous *appa*$^{+/ua5005}$ fish. Loss of appa did not modify the phenotypes observed in *prp1*$^{-/-}$ or *prp2*$^{-/-}$ mutants, therefore this protein does not appear to interact with prion proteins at this level of PLL development. It is quite possible that appb can compensate for the loss of appa as appb has been shown to participate in neurogenesis (Banote et al., 2016).

4.5.5 Future Outlook and Disease Relevance

Since the PLL is an accessible neural system, it is worth the continued effort to identify the stages of PLL development wherein prp1 and prp2 exert their effects on neuromast number, and whether loss of prp1 and prp2 influence neuromast development after their deposition. To address the hypothesis that prp1 and prp2 modulate Wnt/β-catenin signaling, we could attempt to rescue the reduced neuromast number in *prp1*$^{-/-}$ mutant embryos with the GSK-3β inhibitor, 1-azakenpaullone. Along this line, we could also attempt to rescue the increased number in *prp2*$^{-/-}$ mutant embryos by inhibiting Wnt signaling. To do this, we could cross the Tg(hsp70:dkk1b-GFP) transgenic line (Stoick-

Cooper et al., 2007) into *prp2*^{-/-} mutants. Tg(hsp70:dkk1b-GFP) fish express the Wnt inhibitor, dkk1b, when they are incubated at 38°C (i.e. heat-shocked). Thus we could use this transgene determine whether inhibiting Wnt signaling in early stages of primordium migration would restore the normal neuromast deposition pattern in *prp2*^{-/-} mutants. Preliminary examination of neuromasts in *prp1*^{-/-}*; prp2*^{-/-} compound mutants and *prp1*^{-/-}*; appa*^{-/-} compound mutants using the activated hair cell dye Fm43-fx did not reveal obvious defects in hair cell number or organization. We did, however, observe reduced levels of the adherens junction protein β-catenin at the center of L2 neuromasts in 3dpf *prp1*^{-/-}*; appa*^{-/-} compound mutants, and further investigation may reveal further structural deficits in the neuromasts of these mutants. It will also be important to study whether single genetic mutants of *prp2*, *prp1*, and *appa*^{-/-} also have mislocalization of cell adhesion proteins, such as β-catenin, to assess whether interactions among these proteins are involved in proneuromast rosette stabilization.

Furthermore, it will be important to determine whether differences in neuromast patterning (and possible deficits in neuromast integrity) in *prp1*^{-/-} and *prp2*^{-/-} fish have functional consequences. For example, it is conceivable that the reduced neuromast number in *prp1*^{-/-} mutants partially impairs their ability to detect water currents and predators/prey. To test this, we could use a picospritzer to direct a small spray of water towards the trunks of wild type and *prp1*^{-/-} mutants and compare their swim responses (i.e. escape responses).

In summary, we have shown that zebrafish prion proteins participate in neural cell migration. If PrP[C] participates in neural development, loss of functional PrP[C] during prion disease and AD may also impair adult neurogenesis thereby producing disease symptoms such as memory loss. Further study of the mechanisms through which prion proteins contribute to neuromast patterning in the zebrafish lateral line will provide new insights into PrP[C]'s role in neural development and maintenance. Given the subversion of PrP[C]'s function in both prion disease and AD (discussed in Chapter 1), these studies will likely uncover putative therapeutic targets for prion diseases and AD.

Chapter 4 References

Aman, A., Piotrowski, T., 2008. Wnt/beta-catenin and Fgf signaling control collective cell migration by restricting chemokine receptor expression. Dev Cell. 15**,** 749-61.

Banote, R. K., et al., 2016. beta-Amyloid precursor protein-b is essential for Mauthner cell development in the zebrafish in a Notch-dependent manner. Dev Biol. 413**,** 26-38.

Beraldo, F. H., et al., 2011. Metabotropic glutamate receptors transduce signals for neurite outgrowth after binding of the prion protein to laminin gamma1 chain. FASEB J. 25**,** 265-79.

Cotto, E., et al., 2005. Molecular characterization, phylogenetic relationships, and developmental expression patterns of prion genes in zebrafish (Danio rerio). FEBS Journal. 272**,** 500-513.

Dambly-Chaudiere, C., et al., 2007. Control of cell migration in the development of the posterior lateral line: antagonistic interactions between the chemokine receptors CXCR4 and CXCR7/RDC1. BMC Dev Biol. 7**,** 23.

Dijkgraaf, S., 1963. The functioning and significance of the lateral-line organs. Biol Rev Camb Philos Soc. 38**,** 51-105.

Fleisch, V., et al., 2013. Targeted mutation of the gene encoding prion protein in zebrafish reveals a conserved role in neuron excitability. Neurobiol Dis. 55**,** 11-25.

Ghysen, A., Dambly-Chaudiere, C., 2007. The lateral line microcosmos. Genes Dev. 21**,** 2118-30.

Go, W., et al., 2010. atp2b1a regulates Ca(2+) export during differentiation and regeneration of mechanosensory hair cells in zebrafish. Cell Calcium. 48**,** 302-13.

Gompel, N., et al., 2001. Pattern formation in the lateral line of zebrafish. Mech Dev. 105**,** 69-77.

Graner, E., et al., 2000. Cellular prion protein binds laminin and mediates neuritogenesis. Brain Res Mol Brain Res. 76**,** 85.

Haas, P., Gilmour, D., 2006. Chemokine signaling mediates self-organizing tissue migration in the zebrafish lateral line. Dev Cell. 10**,** 673-80.

Hava, D., et al., 2009. Apical membrane maturation and cellular rosette formation during morphogenesis of the zebrafish lateral line. J Cell Sci. 122**,** 687-95.

Head, J. R., et al., 2013. Activation of canonical Wnt/beta-catenin signaling stimulates proliferation in neuromasts in the zebrafish posterior lateral line. Dev Dyn. 242**,** 832-46.

Hernandez-Rapp, J., et al., 2014. A PrP(C)-caveolin-Lyn complex negatively controls neuronal GSK3beta and serotonin 1B receptor. Sci Rep. 4**,** 4881.

Huc-Brandt, S., et al., 2014. Zebrafish prion protein PrP2 controls collective migration process during lateral line sensory system development. PLoS One. 9**,** e113331.

Jacques, B. E., et al., 2014. The role of Wnt/beta-catenin signaling in proliferation and regeneration of the developing basilar papilla and lateral line. Dev Neurobiol. 74**,** 438-56.

Kaiser, D., et al., 2012. Amyloid beta precursor protein and prion protein have a conserved interaction affecting cell adhesion and CNS development. PloS one. 7.

Komiya, Y., Habas, R., 2008. Wnt signal transduction pathways. Organogenesis. 4**,** 68-75.

Lecaudey, V., et al., 2008. Dynamic Fgf signaling couples morphogenesis and migration in the zebrafish lateral line primordium. Development. 135**,** 2695-705.

Liao, H. K., et al., 2012. Tol2 gene trap integrations in the zebrafish amyloid precursor protein genes appa and aplp2 reveal accumulation of secreted APP at the embryonic veins. Dev Dyn. 241**,** 415-425.

Ma, E. Y., Raible, D. W., 2009. Signaling pathways regulating zebrafish lateral line development. Curr Biol. 19**,** R381-6.

Malaga-Trillo, E., et al., 2009. Regulation of Embryonic Cell Adhesion by the Prion Protein. Plos Biology. 7**,** 576-590.

Matsuda, M., Chitnis, A. B., 2010. Atoh1a expression must be restricted by Notch signaling for effective morphogenesis of the posterior lateral line primordium in zebrafish. Development. 137**,** 3477-87.

Mehrabian, M., et al., 2015. The Prion Protein Controls Polysialylation of Neural Cell Adhesion Molecule 1 during Cellular Morphogenesis. PLoS One. 10**,** e0133741.

Musa, A., et al., 2001. Distinct expression patterns of two zebrafish homologues of the human APP gene during embryonic development. Dev Genes Evol. 211, 563.

Nicolas, M., Hassan, B. A., 2014. Amyloid precursor protein and neural development. Development. 141, 2543-8.

Pantera, B., et al., 2009. PrPc activation induces neurite outgrowth and differentiation in PC12 cells: role for caveolin-1 in the signal transduction pathway. J Neurochem. 110, 194-207.

Santuccione, A., et al., 2005. Prion protein recruits its neuronal receptor NCAM to lipid rafts to activate p59fyn and to enhance neurite outgrowth. J Cell Biol. 169, 341-54.

Schmitt-Ulms, G., et al., 2001. Binding of neural cell adhesion molecules (N-CAMs) to the cellular prion protein. J Mol Biol. 314, 1209.

Schmitz, M., et al., 2014. Impact of the cellular prion protein on amyloid-beta and 3PO-tau processing. J Alzheimers Dis. 38, 551-65.

Seiler, C., Nicolson, T., 1999. Defective calmodulin-dependent rapid apical endocytosis in zebrafish sensory hair cell mutants. J Neurobiol. 41, 424-34.

Solis, G. P., et al., 2012. Reggies/flotillins regulate E-cadherin–mediated cell contact formation by affecting EGFR trafficking. Mol Biol Cell. 23, 1812-1825.

Stoick-Cooper, C. L., et al., 2007. Distinct Wnt signaling pathways have opposing roles in appendage regeneration. Development. 134, 479-89.

Sun, J., et al., 2015. Remarkable impairment of Wnt/beta-catenin signaling in the brains of the mice infected with scrapie agents. J Neurochem. 136, 731-40.

Thomas, E. D., et al., 2015. There and back again: development and regeneration of the zebrafish lateral line system. Wiley Interdiscip Rev Dev Biol. 4, 1-16.

Villablanca, E. J., et al., 2006. Control of cell migration in the zebrafish lateral line: implication of the gene "tumour-associated calcium signal transducer," tacstd. Dev Dyn. 235, 1578-88.

Watts, J. C., et al., 2009. Interactome Analyses Identify Ties of PrPC and Its Mammalian Paralogs to Oligomannosidic N-Glycans and Endoplasmic Reticulum-Derived Chaperones. PloS Pathogens. 5.

Chapter 5. An Ancient Conserved Role for Prion Protein in Learning and Memory[19]

---

[19] A version of Chapter 5 has been prepared for submission to Dis Model Mech. as outlined in the Preface.

5.1 Summary

The misfolding of cellular prion protein (PrP^C) to form PrP Scrapie (PrP^{Sc}) is an exemplar of toxic gain-of-function mechanisms inducing propagated protein misfolding and progressive devastating neurodegeneration. Despite this, PrP^C function in the brain is also reduced and subverted during prion disease progression; thus understanding the normal function of PrP^C in healthy brains is key. Disrupting PrP^C in mice has led to a myriad of controversial functions that sometimes map onto disease symptoms, including a proposed role in memory or learning. Intriguingly, PrP^C's interaction with amyloid beta (Aβ) oligomers at synapses has also linked its function to Alzheimer's disease (AD) and dementia in recent years. We set out to test the involvement of PrP^C in memory using a disparate animal model, the zebrafish. Here we document an age-dependent memory decline in *prp2$^{-/-}$* zebrafish, pointing to a conserved and ancient role of PrP^C in memory. Specifically, we found that aged (3-year old) *prp2$^{-/-}$* fish performed poorly in an object recognition task relative to age-matched *prp2$^{+/+}$* fish or 1-year old *prp2$^{-/-}$* fish. Further, using a novel object approach (NOA) test, we found that aged (3-year old) *prp2$^{-/-}$* fish approached the novel object more than either age-matched *prp2$^{+/+}$* fish or 1-year old *prp2$^{-/-}$* fish, but did not have decreased anxiety when we tested them in a novel tank diving test. Taken together, the results of the novel object approach and novel tank diving tests suggest an altered cognitive appraisal of the novel object in the 3-year old *prp2$^{-/-}$* fish. The learning paradigm established here enables a path forward to study PrP^C interactions of relevance to AD and prion diseases, and to screen for candidate therapeutics for these diseases. The findings underpin a need to consider the relative contributions of loss- *vs*. gain-of-function of PrP^C during AD and prion diseases, and have implications upon the prospects of several promising therapeutic strategies.

5.2. Introduction

Prion diseases are a unique class of neurological diseases that naturally affect a number of mammalian species including humans (eg. Creutzfeld Jakob Disease, Fatal Familial Insomnia), cattle (Bovine Spongiform Encephalopathy; commonly known as mad cow disease), sheep (scrapie), as well as deer and other cervids (Chronic Wasting Disease). The devastating impacts of these diseases span from the well being of

individuals to the socioeconomics of various industries and ecosystems. In these diseases, normal proteins (Cellular prion protein, or PrP^C) are converted to misfolded forms (prions), and the resulting prions propagate the diseases to neighbouring cells and tissues and infect new hosts. Despite identification of prions as disease agents in the early 1980s (Prusiner, 1982) and the creation of multiple lines of PrP^C knockout mice (Bueler et al., 1992; Manson et al., 1994; Moore et al., 1995; Rossi et al., 2001; Sakaguchi et al., 1995; Yokoyama et al., 2001), the normal functions of PrP^C remain ambiguous. PrP^C is a GPI anchored protein that is present within synapses (Sales et al., 1998; Stahl et al., 1987). It is highly expressed in several brain regions including the cortex, hippocampus, striatum and in the olfactory bulb to a lesser extent, suggesting that it plays a role in cognition (Sales et al., 1998). Some Creutzfeld-Jakob Disease patients have memory impairments (Caine et al., 2015), and PrP^C may contribute to cognitive decline in AD (reviewed in (Kostylev et al., 2015)). Briefly, some forms of Aβ oligomers exhibit high-affinity binding to PrP^C (first reported in (Lauren et al., 2009)), ultimately leading to one of many modes of Aβ oligomer-mediated synaptic dysfunction (reviewed in (Kostylev et al., 2015)). In prion diseases and AD, pathologies underlying memory impairments and other symptoms are thought to be mediated in part by PrP^C loss-of-function (for review see (Leighton and Allison, 2016)).

Several rodent behavioural studies have reported roles for PrP^C in memory and learning, though this has been controversial. Short-term social recognition memory was lower in the Zurich I line of $Prnp^{-/-}$ mice (ZrchI $Prnp^{-/-}$ mice) than in wild type mice at 3 months of age, and PrP overexpression in Tg20 mice improved social recognition memory in 11-month old mice relative to age-matched wild type mice (Rial et al., 2009). Tg20 mice (transgenic line overexpressing $Prnp$) also had increased levels of synaptophysin compared to ZrchI $Prnp^{-/-}$ mice or wild type mice (Rial et al., 2009). ZrchI $Prnp^{-/-}$ mice exhibited reduced object recognition memory at 9 and 20 months of age compared to age-matched $Prnp^{+/+}$ mice, and both genotypes exhibited age-related memory impairments (Schmitz et al., 2014a). Additionally, the Nagasaki line of $Prnp^{-/-}$ mice displayed an age-related decline in memory and/or latent learning in a water-finding test. This was not observed in age-matched $Prnp^{+/+}$ mice (Nishida et al., 1997). Further, multiple lines of $Prnp^{-/-}$ knockout mice show impairments in conditioned memory tasks,

particularly in the 6-20 month age range (Coitinho et al., 2003; Criado et al., 2005; Nishida et al., 1997; Rial et al., 2009; Schmitz et al., 2014a). In contrast, while 3-month old ZrchI $Prnp^{-/-}$ mice performed comparably to age-matched $Prnp^{+/+}$ in a water maze spatial learning task, they exhibited a delay in learning when the platform position was changed (Bueler et al., 1992). Impaired spatial learning was more apparent in 5-6 month old Edinburgh $Prnp^{-/-}$ mice using the Barnes Maze, and these impairments were rescued by transgenic expression of PrP^C in neurons (Criado et al., 2005). Fear conditioning tests have also produced mixed results in 3-6 month $Prnp^{-/-}$ mice (Coitinho et al., 2003; Nishida et al., 1997; Rial et al., 2009; Roesler et al., 1999; Schmitz et al., 2014a), but there have been consistent reports of learning deficits in older (9-20 month old mice) $Prnp^{-/-}$ mice compared to age-matched $Prnp^{+/+}$ mice (Coitinho et al., 2003; Rial et al., 2009; Schmitz et al., 2014a). The finding that 9-month old rats treated with α-PrP^C antibody exhibit deficits in fear-conditioned learning demonstrates that PrP^C has a role in learning in other closely related rodents (Coitinho et al., 2003). This result should be interpreted with caution, however, because some α-PrP^C antibodies are inherently toxic (Herrmann et al., 2015).

There have been mixed reports in the field regarding whether PrP^C contributes to anxiogenic behaviour (Coitinho et al., 2003; Rial et al., 2009; Roesler et al., 1999; Schmitz et al., 2014a). It has consistently been reported that 3-month old ZrchI $Prnp^{-/-}$ mice do not behave differently than age-matched $Prnp^{+/+}$ mice (Coitinho et al., 2003; Rial et al., 2009; Roesler et al., 1999; Schmitz et al., 2014a); however one study using older animals reported that $Prnp^{-/-}$ mice spent significantly more time in the open arms than $Prnp^{+/+}$ animals (Schmitz et al., 2014a) , while others found no difference between genotypes (Coitinho et al., 2003; Rial et al., 2009). Age-related reductions in anxiety were found in ZrchI $Prnp^{-/-}$ mice and $Prnp^{+/+}$ mice in two studies (Rial et al., 2009; Schmitz et al., 2014a), but were not found in Tg20 mice, which overexpress PrP^C (Rial et al., 2009). In a third study, however, no age-related changes in anxiety were found in either ZrchI $Prnp^{-/-}$ mice or $Prnp^{+/+}$ mice, nor in rats treated with an α –PrP antibody (Coitinho et al., 2003).

An opportunity to reassess the role of PrP^C in memory emerged from our recent engineering of $prp2^{-/-}$ zebrafish (Fleisch et al., 2013). These $prp2^{-/-}$ zebrafish are thought

to be null mutants and, like *Prnp* knockout mice, display no overt phenotypes into adulthood (Figure 5.1). *Prp2*$^{-/-}$ zebrafish have altered NMDA receptor kinetics (Fleisch et al., 2013), and given that NMDA receptors play critical roles in learning and memory in various animals (reviewed in (Morris, 2013)), including in zebrafish (Swain et al., 2004), we predicted that fish lacking *prp2* would display memory impairments. Further, *prp2*$^{-/-}$ zebrafish have increased susceptibility to convulsants (Fleisch et al., 2013) and alterations in neural development (Huc-Brandt et al., 2014), encouraging the suggestion that synaptic function might be disrupted in a manner consistent with memory deficits. Zebrafish are an attractive model system for the study of disease because they reproduce in large numbers, can be deployed in high-throughput *in vivo* drug screens, have a sequenced annotated genome and are accessible for genetic manipulation (Norton and Bally-Cuif, 2010; Tierney, 2011). Regarding aging, zebrafish typically reach adulthood (sexual maturity) at about three months of age and display reduced fecundity after their second year, but often live to be four or five years old (Gerhard et al., 2002; Kishi et al., 2003). Although some important differences in brain structures exist between fish and mammals, the overall brain structure, cellular architectures and neurotransmitter systems are highly comparable between fish and mammals (Norton and Bally-Cuif, 2010; Panula et al., 2010; Rodriguez et al., 2002a). A growing number of cognitive tests are being developed for use in zebrafish (Tierney, 2011), including those that assess both spatial and associative learning (reviewed in (Norton and Bally-Cuif, 2010)).
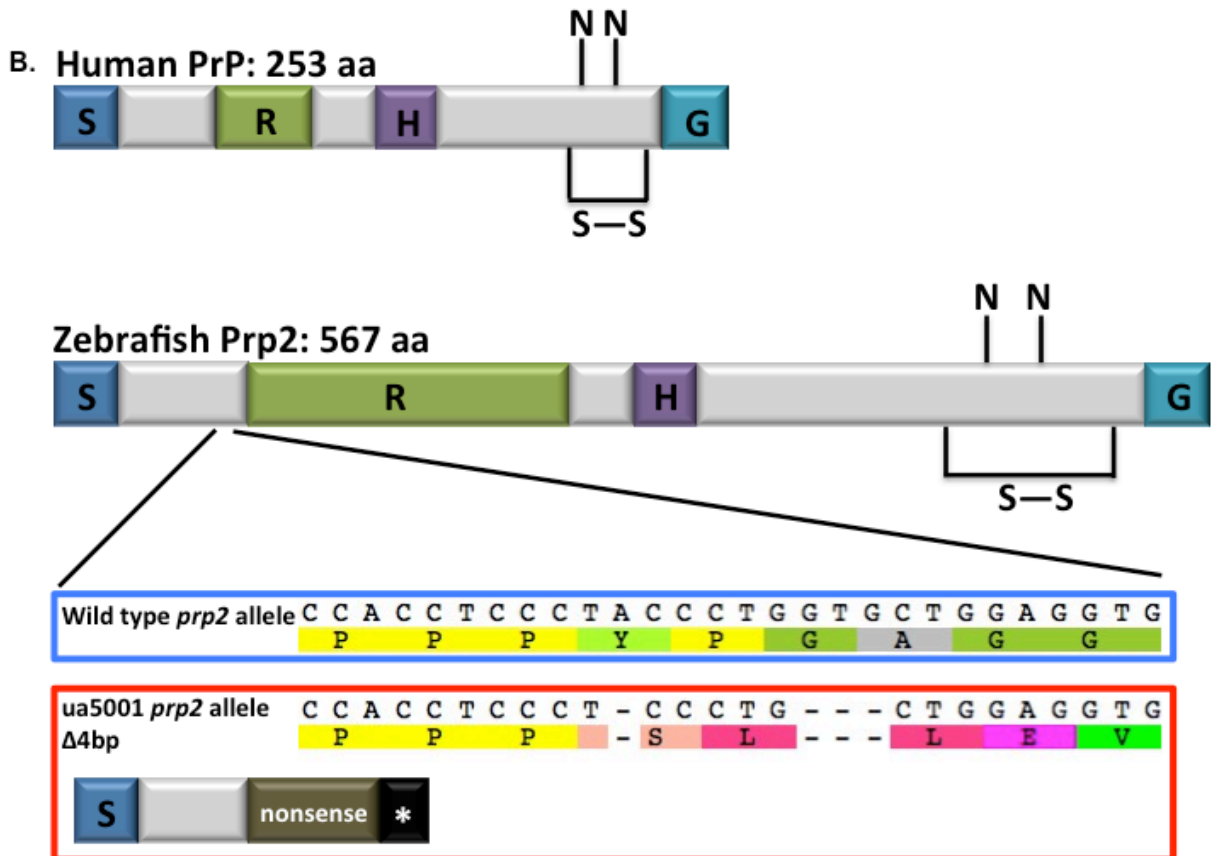
Figure 5.1. *prp2⁻/⁻* fish develop normally and display no overt phenotypes during adulthood

A. A young adult (~1-year old) $prp2^{+/+}$ fish is pictured on top, while a young adult $prp2^{-/-}$ fish is pictured on the bottom. **B.** Zebrafish prp2 is conserved with mammalian PrP^C at the protein domain level. Both have a signal peptide (S), a repeat region (R; though the repetitive region in zebrafish is longer and less patterned than the octarepeats in mammals), a hydrophobic domain (H) and are attached to the cell surface by a GPI anchor (G). Like mammalian PrP^C, zebrafish prp2 also has putative N-linked glycosylation sites (N) and a disulphide bond (S—S) within its C-terminus. The zebrafish *prp2* ua5001 allele has a 4 base pair deletion (frameshift), which produces an early stop codon and a putative nonsense protein.

Object recognition memory has been used as a model of declarative memory (memory of facts, events, and places) in rodents and zebrafish (Hammond et al., 2004; May et al., 2016). In rats it has been experimentally demonstrated that object recognition over short retention intervals involves the perirhinal cortex (Aggleton et al., 2010; Hannesson et al., 2004; Winters et al., 2011), while recognition over longer retention intervals requires the hippocampus (Hammond et al., 2004). The object recognition/preference test is a working memory test (Ennaceur and Delacour, 1988) that is commonly used in rodents (Hammond et al., 2004). Advantages of the object recognition test include its relative simplicity to perform (as it is a test of one-trial learning), and repetitive training with reinforcers are not required (Ennaceur and Delacour, 1988). Some of us recently established an object recognition test for adult zebrafish, and we found that wild type zebrafish prefer the familiar object over the novel object, providing evidence for a functional object recognition memory system in zebrafish (May et al., 2016).

Methods to reliably test anxiety behaviour in zebrafish have also been introduced in recent years. Like rodents, zebrafish exhibit anxiety-like behaviour when exposed to novel environments. Novel tank diving tests and open-field tests are standard methods for measuring anxiety in zebrafish and have been evaluated pharmacologically (Maximino et al., 2010). The novel tank diving test exploits the innate tendency of several zebrafish strains to seek protection when exposed to novel environments (Egan et al., 2009). In this test, fish are typically placed in a narrower tank and bottom dwelling activity is used as the main output of anxiety (sometimes along with other measures such as erratic swimming, swimming bouts and thigmotaxis) (Maximino et al., 2010). In the open-field test, fish are placed in a novel (usually circular arena) and exploratory behaviour and thigmotaxis (wall hugging) are measured (Champagne et al., 2010; Maximino et al., 2010). The novel object approach (NOA) test (also known as the boldness test) is a variation of the open field test where an object is introduced into a circular arena after an acclimation period (Moretz et al., 2007; Ogwang, 2008; Wright et al., 2006; Wright et al., 2003). Time spent near the object and away from the object (in the thigmotaxis zone) is then quantified. In a different test used to assess fear, computer simulated images of natural predators and select geometric shapes induced responses in domesticated zebrafish including freezing, erratic movement and more time spent on the side of the

arena away from the stimulus (Ahmed et al., 2012). Thus avoidance of the novel object in the NOA test may be interpreted as an innate response to a perceived threat.

In this study we deployed our previously established object recognition/preference test (May et al., 2016) and found that zebrafish engineered to lack *prp2* show age-related declines in familiar object preference, suggesting their object recognition memory system is compromised. *Prp2*$^{+/+}$ and *prp2*$^{-/-}$ fish did not display differences in anxiety in the novel tank diving test. Using the novel object approach test, however, we found that 3-year old *prp2*$^{-/-}$ fish approached the novel object more than the 3-year old *prp2*$^{+/+}$ fish, likely indicating an age-dependent change in cognitive appraisal of the object.

5.3 Methods

5.3.1 Zebrafish strains and husbandry

Zebrafish of the AB strain were used as the wild type fish in this study. The *prp2*$^{ua5001/ua5001}$ zebrafish mutants (ZFIN ID: ZDB-ALT-130724-2) that we previously engineered (Fleisch et al., 2013), denoted as *prp2*$^{-/-}$ throughout this text, were generated and maintained on an AB strain background. *prp2*$^{-/-}$ zebrafish are thought to be null mutants, engineered by targeted mutagenesis to have a 4 base pair deletion in the beginning of the *prp2* coding region (which is contained within a single exon) leading to a protein that is predicted to be truncated and lack all recognizable prion protein domains; (Fleisch et al., 2013) (Figure 5.1). In these mutants the *prp2* gene product is greatly reduced in abundance presumably by nonsense-mediated decay (Fleisch et al., 2013). *Prp2*$^{-/-}$ fish used in the current study were maternal zygotic mutants at the *prp2* gene locus, but previous generations of fish were genotyped using a restriction fragment length polymorphism (RFLP) assay as described below and in Chapter 2. Wild type zebrafish, denoted *prp2*$^{+/+}$ (AB background fish from the same stock as *prp2*$^{-/-}$ fish, such that mutants and wild types were closely related but not siblings), were tested for comparison. The mean lifespan of laboratory raised zebrafish is ~40 months (3.3 years) (Gerhard et al., 2002; Gilbert et al., 2014). In the current study, both young adult zebrafish (1-year old) and aged zebrafish (3-year old) were used. Fish of both ages displayed normal health and movement. The fish were raised and maintained within the University of Alberta fish facility at 28°C under a 14/10 light/dark cycle as previously described (Fleisch et al.,

2013). Fish were transferred across town (4 kilometers) to the MacEwan University fish facility at least 2 weeks prior to the initiation of behavioural tests, where they were maintained as described in (May et al., 2016). All protocols were approved by the University of Alberta's Animal Care and Use Committee: Biosciences and the MacEwan University Animal Research Ethics Board (AREB), in compliance with the Canadian Council on Animal Care (CCAC).

5.3.2 Genotyping

An RFLP assay was developed to genotype zebrafish at the *prp2* gene locus wherein the ua5001 mutation disrupted an *MvaI* cut site. Genomic DNA was amplified using *prp2* RFLP primers (Forward primer 5'-TCC CCT GGA AAC TAT CCT CGC CAA C-3'; reverse primer 5'-TGG GTT AGA GCC TGC TGG TGG-3'), and then digested with Fast Digest *Mva I* (Thermo Fischer Scientific catalogue #FD0554). PCR products from mutant and wild type DNA produced different banding patterns on an Ethidium bromide agarose gel (*prp2* wild type allele yields 3 bands with sizes of 21, 36 and 54 base pairs; *prp2*^-/- ua5001 allele yields 2 bands with sizes of 36 and 71 base pairs; See Figure 2.3C).

5.3.3 Object Preference/Recognition Test

The object preference/recognition test is designed to measure object recognition memory, and was structured to be a minor variant on the 'novel object recognition' (NOR) test that is prevalent in rodent research. The method exploits the observation that zebrafish presented with a novel and a familiar object spent more time near the familiar object relative to the novel object. Thus, similar to rodent research where innate preferences of novel objects are exploited to test memory, in our method the time zebrafish spent amongst novel and familiar objects is interpreted as familiar object preference and is considered a proxy for object recognition (i.e. memory) (May et al., 2016). The object preference test was performed between the hours of 09:00-17:00 as previously described (May et al., 2016). Prior to experimentation, the holding and testing tanks (29 cm x 14cm x 18cm) were filled to a depth of ~6 cm with habitat water. The temperature of the water was maintained by placing the tanks on top of a seedling-heating mat (HydroFarm Horticultural Products, Pentaluma, CA, USA). During the experiments, fish were first placed in a holding tank for 5 minutes to acclimate. Fish were then netted

and moved to a new tank that was identical to the holding tank, except for including the presence two identical objects for the zebrafish to explore (all objects devised from LEGO$^{□}$ pieces; see (May et al., 2016)) for a 10-minute training trial (T1). Next, fish were moved back to the holding tank for either a 1-minute or 5-minute retention interval (RI). During this time an identical object in the trial tank was replaced with a novel object. The objects were randomly counterbalanced such that the object designated as familiar vs. novel was randomized amongst fish. Finally, fish were moved back into the trial tank for a 10-minute testing trial (Figure 5.2A). Position and movement of zebrafish was recorded by an overhead camera and tracked in Ethovision XT. To quantify the object preference for each fish we used the discrimination indices D1, D2, and D3 (Table 5.1) for the time fish spent in close proximity to the objects (8.4 cm^2 boxes were placed over the objects in Ethovision) (May et al., 2016). Positive values of D1 and D2 that were significantly different from zero were interpreted to indicate a familiar object preference (negative values indicate a novel object preference). Values of D3 that were significantly different from 0.5 were also interpreted to indicate an object preference (greater than 0.5 indicates a familiar object preference whereas a value less than 0.5 indicates a novel object preference).

A. Object Preference Test

1. Habituation	2. Training	3. Memory Retention	4. Preference test
Holding tank	O1 / Testing tank / O1	Holding tank	O1 / Testing tank / O2

29 cm

14 cm

B. Novel Object Approach (NOA) Test

Thigmotaxis

Middle

Center

N

6 cm   5.5 cm   11 cm

34 cm

C. Novel Tank Diving Test

Top Zone

Middle Zone

Bottom Zone

18.1 cm

4.8 cm

24.5 cm
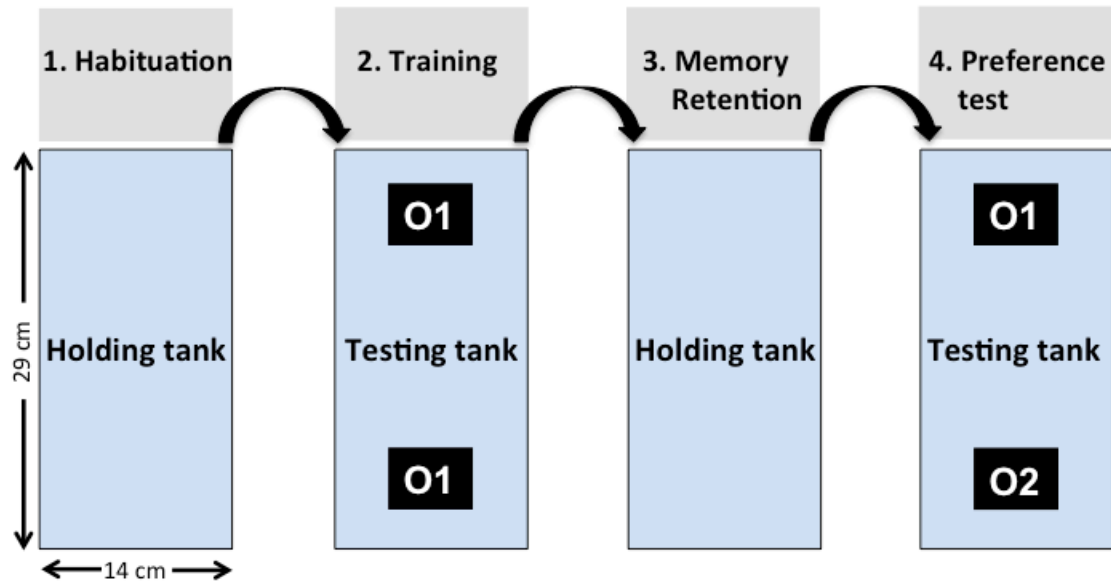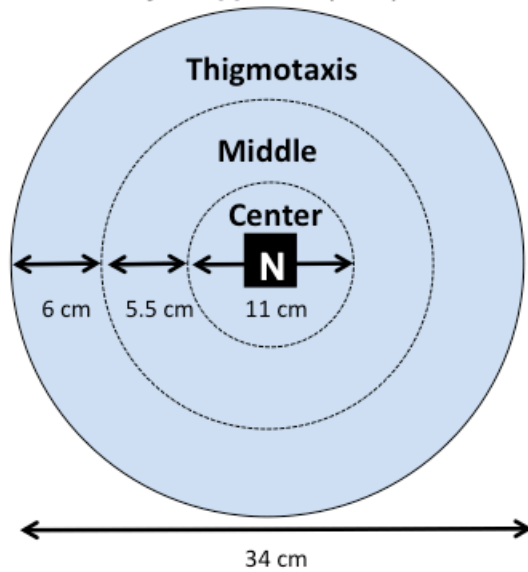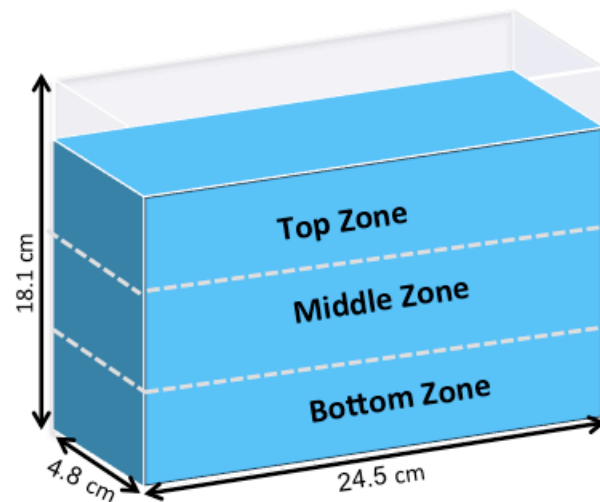
Figure 5.2. Overview of the behavioural tests used in the study

A. Flowchart summarizing the sequence of events in the object preference test. 1) Fish were first habituated to a tank of the same size as the testing arena (the holding tank). 2) Fish were then netted and moved to the testing tank containing two identical objects (O1) for the 10-minute training phase. 3) Fish were then moved back to the holding tank for a

1 or 5-minute period (memory retention interval), during which time one of the familiar objects in the testing tank was replaced with a novel object (O2). 4) Finally, fish were placed back into the testing tank for the 10-minute object preference test. **B.** Schematic of the Novel Object Approach (NOA) setup. Fish were netted and placed into a circular arena, where they acclimated for 15 minutes. After this time, a novel object (N) was placed into the center of the arena and the activity of the fish was recorded for 5 minutes. The arena was virtually divided into center, middle, and thigmotaxis zones for data analysis. **C.** Schematic of the tank diving test. Fish were netted and placed into the novel tank (narrower and deeper than the home tank) and activity of the fish was recorded for 5 minutes. The tank was virtually divided into bottom, middle and top zones for data analysis.

Table 5.1. Formulae used to assess object exploration and object discrimination indices

Exploration	Discrimination
$E_{T1}=A1+A2$	$D1=A3-B$
$E_{T2}=A3+B$	$D2=D1/E_{T2}$
	$D3=A3/E_{T2}$

A1 and A2 are defined as the time spent near each of the two identical objects in Trial 1 (T1), a measure of exploration (E). In Trial 2 (T2), values A3 and B are defined as the time spent near the familiar object and the novel object, respectively.

5.3.4 Novel Object Approach (NOA) Test

The Novel Object Approach (NOA) test is a two- phase test designed to measure the anxiety levels in a zebrafish exposed to a novel object. In the first phase of this test, the zebrafish were introduced using a small net into a circular arena (34 cm in diameter) filled with habitat water maintained between 26-28°C to a height of 5 cm. The trial was recorded using an overhead camera and tracked using using Ethovision XT motion tracking software. This allowed for quantification of locomotion and thigmotaxis (wall hugging). After the first 15 minutes, phase two was initiated by the introduction of a novel object (as above, (Ou et al., 2015)) in the center of the arena. The zebrafish was then recorded for an additional 5 minutes before terminating the trial. The circular arena was divided into 3 radial zones; the outer thigmotaxis zone, the middle (transition) zone, and the center (object) zone (Figure 5.2B). Increased anxiety is inferred from fish spending more time in the outer thigmotaxis zone and decreased boldness is inferred from fish spending less time near the object.

5.3.5 Novel Tank Diving Test

Anxiety levels of the zebrafish were also assessed using the novel tank diving test (Bencan et al., 2009; Egan et al., 2009; Parker et al., 2014). In this test zebrafish were netted and transferred into a tall, narrow, but deep rectangular arena measuring 24.9 cm x 4.8 cm x 18.1 cm, with glass walls 0.7 cm thick. The arena was filled with habitat water maintained between 26-28°C. We chose to use a rectangular rather than trapezoidal arena

used in other studies (Egan et al., 2009; Parker et al., 2014) because we housed zebrafish in a trapezoidal tanks (Aquatic Habitats) so our choice of a 'novel tank' for the diving test would be relatively more novel than a thinner trapezoidal tank. The location of the fish was recorded, using a camera positioned at the side of the tank, and analyzed with Ethovision XT motion tracking software for 5- minute trials. The arena was divided into 3 equal latitudinal zones; the Top Zone, Middle Zone, and Bottom Zone (Figure 5.2C). Zebrafish that spend more time in the bottom of the arena, similar to rodents spending more time in the closed arms of an elevated plus maze or near the walls of an open field arena, were considered to have elevated anxiety relative to fish that explored the upper areas of the arena.

5.3.6 Statistics

Data were analyzed using GraphPad Prism Software (San Diego, CA). For one sample testing, normality was first assessed using D'Agostino & Pearson omnibus normality tests. Parametric data were analyzed using one sample t-tests, and nonparametric data were analyzed using Wilcoxon signed rank tests. For multiple sample comparisons, variances were first assessed using F-tests. Parametric data were then analyzed with unpaired t-tests, and nonparametric data were analyzed with Mann-Whitney tests. Well-established discrimination indices typical of object recognition tests (D1, D2, and D3) were used to assess object preference as described previously (Table 5.1) (May et al., 2016).

5.4 Results

5.4.1 *prp2*^{-/-} fish displayed an age-dependent decline in familiar object preference

Object preference tests were performed to assess memory in young (1-year-old) versus old (3-year old) *prp2*^{-/-} fish and to compare memory capacity (object recognition) between *prp2*^{-/-} and *prp2*^{+/+} fish. In these tests, the fish were first individually exposed to two identical objects on opposite sides of the tank (training phase). The fish were then removed for a specified period of time representing the memory retention interval. Finally, the fish were tested in the same tank with an original (familiar) object on one side of the tank and a novel object on the other side; this represents the test phase. We quantified the amount of time each fish spent near each object during the test phase and

calculated discrimination indices as described in Table 1. D1 is a discrimination index that measures the difference between time spent near the familiar object and the time spent near the novel object. The D2 and D3 discrimination indices account for the total time that the fish spend exploring the objects during the test phase.

The first series of tests used a 1-minute retention interval between the training and testing trials. These assays demonstrated that 1-year old $prp2^{-/-}$ fish had learning and memory capabilities in a range typically observed in zebrafish (i.e. displayed object preference after a memory retention interval of 1 minute) (May et al., 2016). Thus 1-year old $prp2^{-/-}$ fish had D1 and D2 discrimination indices >0 (Figure 5.3 A-B; $p<0.05$) and D3 discrimination indices >0.5 (Figure 5.4A; $p<0.05$). This was in contrast to 3-year old $prp2^{-/-}$ zebrafish, which did not display object preference after a 1-minute retention interval (Figure 5.3 C-D). This was not simply due to age, because 3-year old wild type $prp2^{+/+}$ fish displayed familiar object preference as measured by the D1 discrimination index (but not D2 or D3) (Figure 5.3 C-D, Figure 5.4B; $p<0.05$). Comparing the D1 and D2 discrimination indices of the 1-year old $prp2^{-/-}$ fish to those of the 3-year old $prp2^{-/-}$ fish, revealed a small (though not significantly different) trend towards reduced familiar object preference with age (Figure 5.3 E-F, a re-plotting of the values in Figure 5.3 panels A-D). This encouraged us to next challenge the fish with more difficult memory tasks in the form of longer retention intervals, i.e. more time between training and test phases.
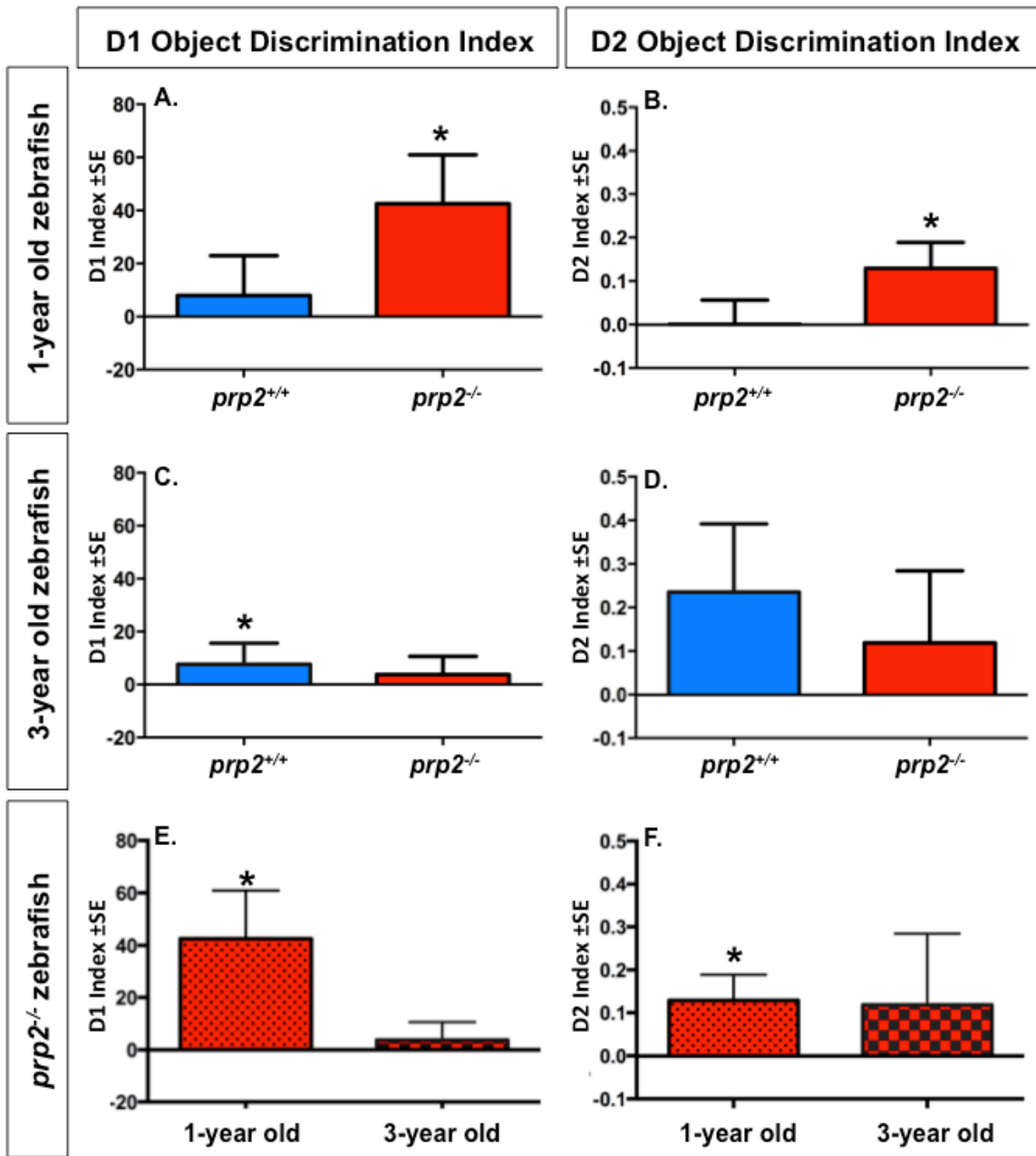
Figure 5.3. Zebrafish lacking *prp2* showed a trend towards a reduction in familiar object preference with age, following a 1-minute retention interval

Prp2^{-/-} fish showed a trend towards an age-dependent decline in familiar object preference with the object preference test after a 1-minute retention interval. **A-B**. 1-year old *prp2*^{-/-} zebrafish displayed familiar object preference following a 1-minute retention

interval, while the 1-year old $prp2^{+/+}$ fish did not as revealed by the D1 and D2 discrimination indices of object preference (panels A and B, respectively; *p <0.05 with the one sample t-test; n=29 $prp2^{+/+}$ fish, n=28 $prp2^{-/-}$ fish). **C.** 3-year old $prp2^{+/+}$ fish displayed familiar object preference while 3-year old $prp2^{-/-}$ fish did not (D1 discrimination index, *p<0.05 with the Wilcoxon signed rank test; n=16 fish/genotype). **D.** 3-year old fish of both genotypes ($prp2^{+/+}$ and $prp2^{-/-}$) failed to show object preference following a 1-minute retention interval using the D2 discrimination index. **E-F.** Zebrafish lacking prion protein ($prp2^{-/-}$) displayed a small, though not statistically significant reduction in familiar object preference with age as measured by D1 and D2 (values replotted from Figure 5.3 A-D).
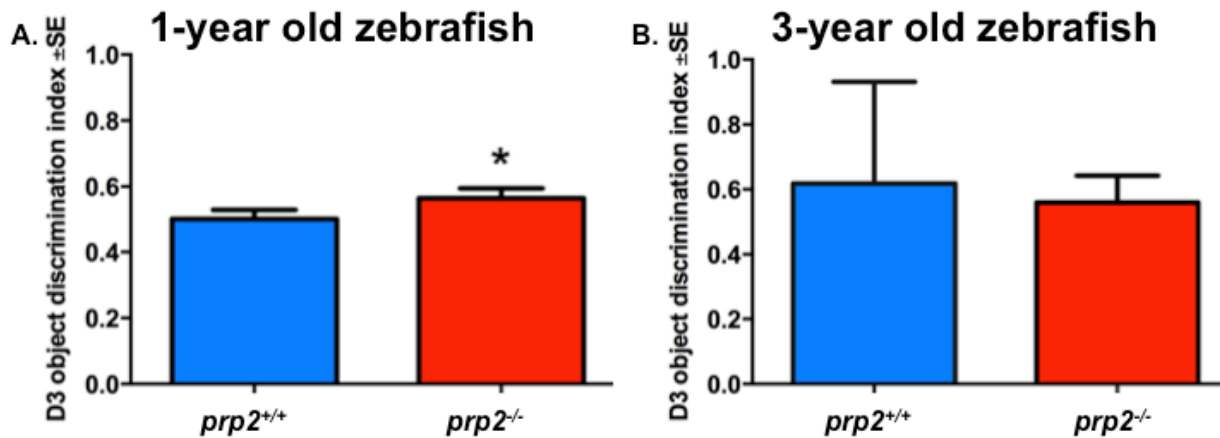
Figure 5.4. After a 1-minute retention interval, 1-year old *prp2$^{-/-}$* fish displayed familiar object preference with the object preference test, but 3-year old *prp2$^{-/-}$* fish did not

A. The D3 discrimination index revealed that 1-year old *prp2$^{-/-}$* fish displayed familiar object preference after a 1-minute retention interval, but 1-year old *prp2$^{+/+}$* fish did not (*$p<0.05$ with one-sample t-test; n=29 *prp2$^{+/+}$* fish, n=28 *prp2$^{-/-}$* fish). **B.** At 3 years of age neither genotype (*prp2$^{+/+}$* or *prp2$^{-/-}$*) displayed object preference after a 1-minute retention interval as revealed by the D3 discrimination index (n=16 fish/genotype).

Considering the trends towards genotype-and age-specific differences in memory above, we next asked whether a more challenging memory test, using a longer (5-minute) retention interval in the familiar object preference test, would accentuate the observed differences. In these tests some individual 1-year old *prp2*$^{-/-}$ fish again displayed robust memory as revealed by preference for the familiar object over the novel object during the test phase (Figure 5.5A), however, as a group they did not display significant object preference (D1, D2 Figure 5.5B-C; D3 Figure 5.6A). Neither 3-year old *prp2*$^{+/+}$ nor 3-year old *prp2*$^{-/-}$ fish (Figure 5.5D) displayed object preference after a 5-minute retention interval (D1, D2 Figure 5.5 E-F; D3 Figure 5.6B). As for the 1-minute retention interval, the 3-year old *prp2*$^{-/-}$ fish had a small (though not significantly different) reduction in memory (familiar object preference) compared to 1-year old *prp2*$^{-/-}$ fish (Figure 5.5G; this is a re-plotting of values from Figure 5.5 panels C and F). Unexpectedly, 1-year-old *prp2*$^{+/+}$ fish did not display object preference after a 1-minute or 5-minute memory retention interval, contrasting with previous results ((Figures 5.3 A-B, 5.4A, 5.5 B-C, 5.6A) (May et al., 2016)).
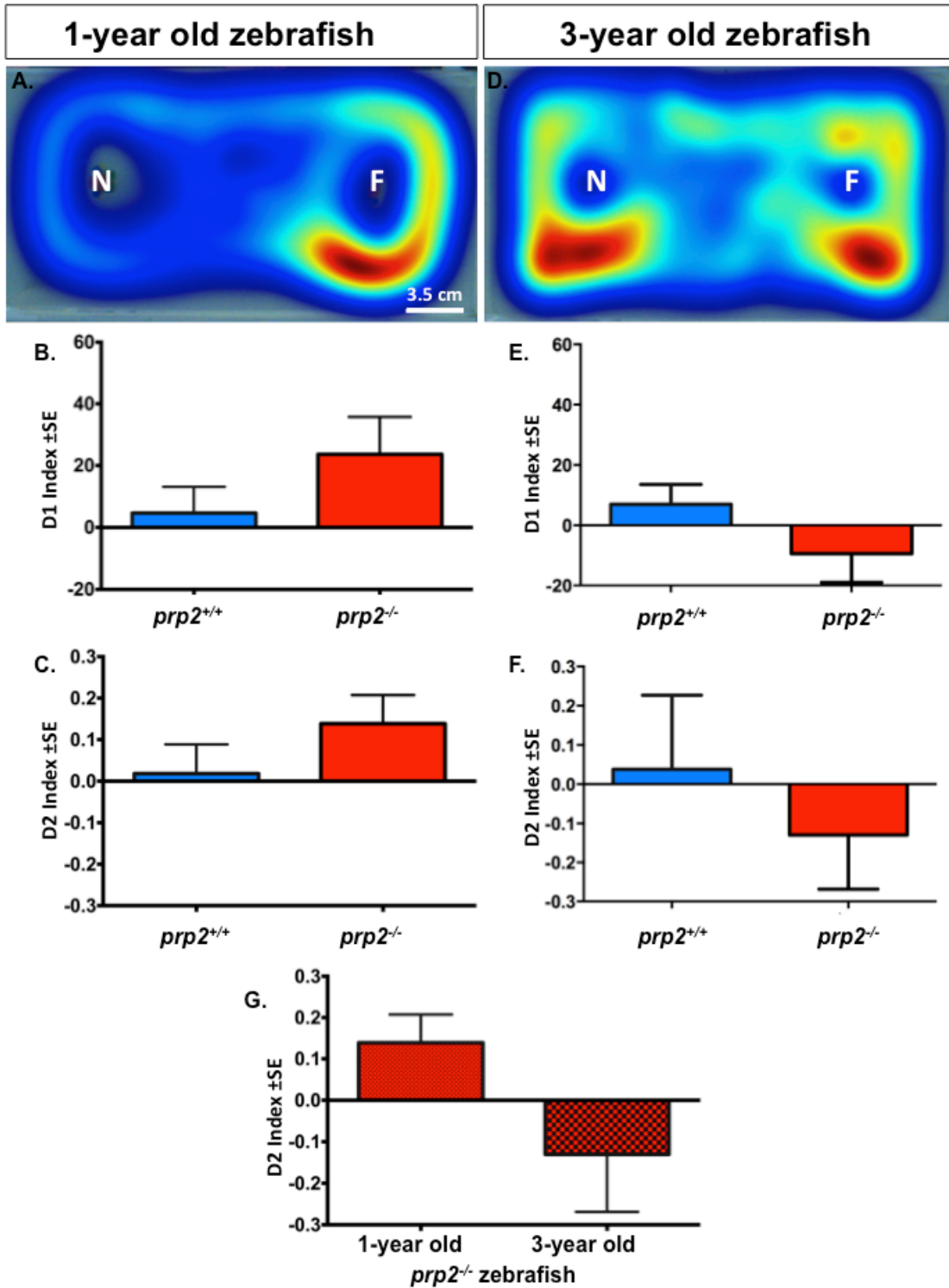
Figure 5.5. *prp2*$^{+/+}$ and *prp2*$^{-/-}$ fish did not display significant object preference after a 5-minute retention interval

Familiar object preference tests after a 5-minute retention interval were expected to be more challenging than memory tests reported in Figure 5.3-5.4. **A.** Sample heat map of a 1-year old *prp2*$^{-/-}$ fish that exhibited familiar object preference during the test phase. The view is looking down on the test tank, wherein fish can swim around the novel object (N) and/or the familiar object (F). Warm colours (yellows and reds) in the heat map indicate this individual fish spent more time near the familiar object, which was interpreted herein as indicating the fish remembered this object from its earlier training phase (see Methods and assumptions therein). Scale bar = 3.5 cm (the approximate size of an adult zebrafish). **B-C.** Neither 1-year old *prp2*$^{+/+}$ zebrafish nor 1-year old *prp2*$^{-/-}$ fish showed familiar object preference following a 5-minute retention interval (D1 and D2 discrimination indices in panels B and C respectively; n=26 *prp2*$^{+/+}$ fish, n=28 *prp2*$^{-/-}$ fish). **D.** Sample heat map of a 3-year old *prp2*$^{-/-}$ fish that did not display familiar object preference during the test phase. The view is the same as described in part A. **E-F.** 3-year old zebrafish of both genotypes (*prp2*$^{+/+}$ and *prp2*$^{-/-}$) failed to show object preference following a 5-minute retention interval (D1 and D2 discrimination indices plotted in panels E and F respectively; n=16 *prp2*$^{+/+}$ fish, n=15 *prp2*$^{-/-}$ fish). **G.** *prp2*$^{-/-}$ zebrafish appeared to display a reduction in familiar object preference with age (as determined by the D2 discrimination index), but this did not reach statistical significance (p=0.2269 with an unpaired t-test; data in panel G is data re-plotted from Figure 5.5C and 5.5F).
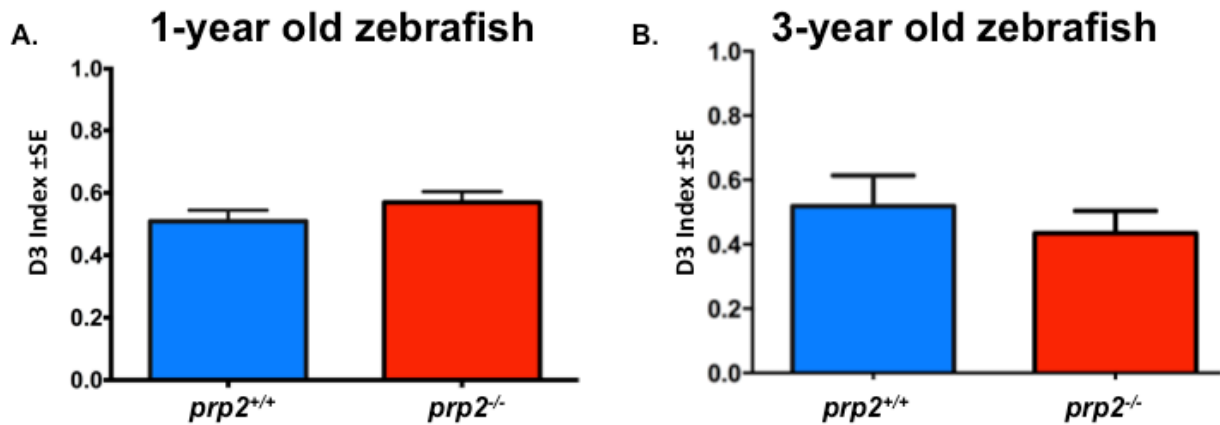
Figure 5.6. After a 5-minute retention interval, neither _prp2_⁺/⁺ nor _prp2_⁻/⁻ fish displayed significant object preference as measured using the D3 discrimination index

A. The D3 discrimination index revealed that neither 1-year old $prp2^{-/-}$ fish nor 1-year old $prp2^{+/+}$ fish displayed significant familiar object preference after a 5-minute retention interval (n=26 $prp2^{+/+}$ fish, n=28 $prp2^{-/-}$ fish). **B.** At 3 years of age neither genotype ($prp2^{+/+}$ or $prp2^{-/-}$) displayed object preference after a 5-minute retention interval as revealed by the D3 discrimination index (n=16 $prp2^{+/+}$ fish, n=15 $prp2^{-/-}$ fish).

5.4.2 *prp2*$^{-/-}$ fish showed an age-dependent increase in approach to the novel object

A typical interpretation of the data from the object preference test using the 1-minute retention interval (Figures 5.3-5.4 above) is that zebrafish lacking prion protein have reduced memory at old age. An alternative explanation for a lack of object preference among 3-year old *prp2*$^{-/-}$ fish is that they perceive the objects differently compared to 3-year old wild type fish and 1-year old *prp2*$^{-/-}$ fish. In such an instance the novel objects might not invoke an innate anxious response or the zebrafish might not cognitively perceive the novel object as a threat. We addressed this hypothesis using the Novel Object Approach (NOA) test. In this test, zebrafish were first acclimated to a circular arena for 15 minutes and a novel object was then introduced into the center of the arena for the last 5 minutes of the trial. The amount of time the fish spent in the object (center) zone, middle zone, and thigomotaxis zone (outer edge of the arena) was calculated. Zebrafish spending more time in the center of the arena near the object were interpreted to be less anxious or perhaps displaying deficits in cognitive appraisal compared to zebrafish exhibiting thigomotaxis.

Among young (1-year old) fish, there was no significant difference between genotypes in time spent in the object (center) zone during the NOA test (Figure 5.7A). Old (3-year old) *prp2*$^{-/-}$ fish spent significantly more time in the object (center) zone during the NOA test than 3-year old *prp2*$^{+/+}$ fish (Figure 5.7B; $p<0.05$). There were no differences in time spent in the middle zone or thigmotaxis zone between genotypes (data not shown). 3-year old fish also spent significantly more time in the object (center) zone than 1-year old *prp2*$^{-/-}$ fish (Figure 5.7C; $p<0.05$; a re-plotting of the values from Figure 5.7 A-B). Because no difference in time spent in the thigmotaxis zone was observed (an index of anxiety), but time spent in the center (object) zone was significantly increased (an index of boldness of object appraisal), this was suggestive of an age-dependent difference in object appraisal in the *prp2*$^{-/-}$ fish. Further assessments of anxiety were performed to assess this interpretation, below.
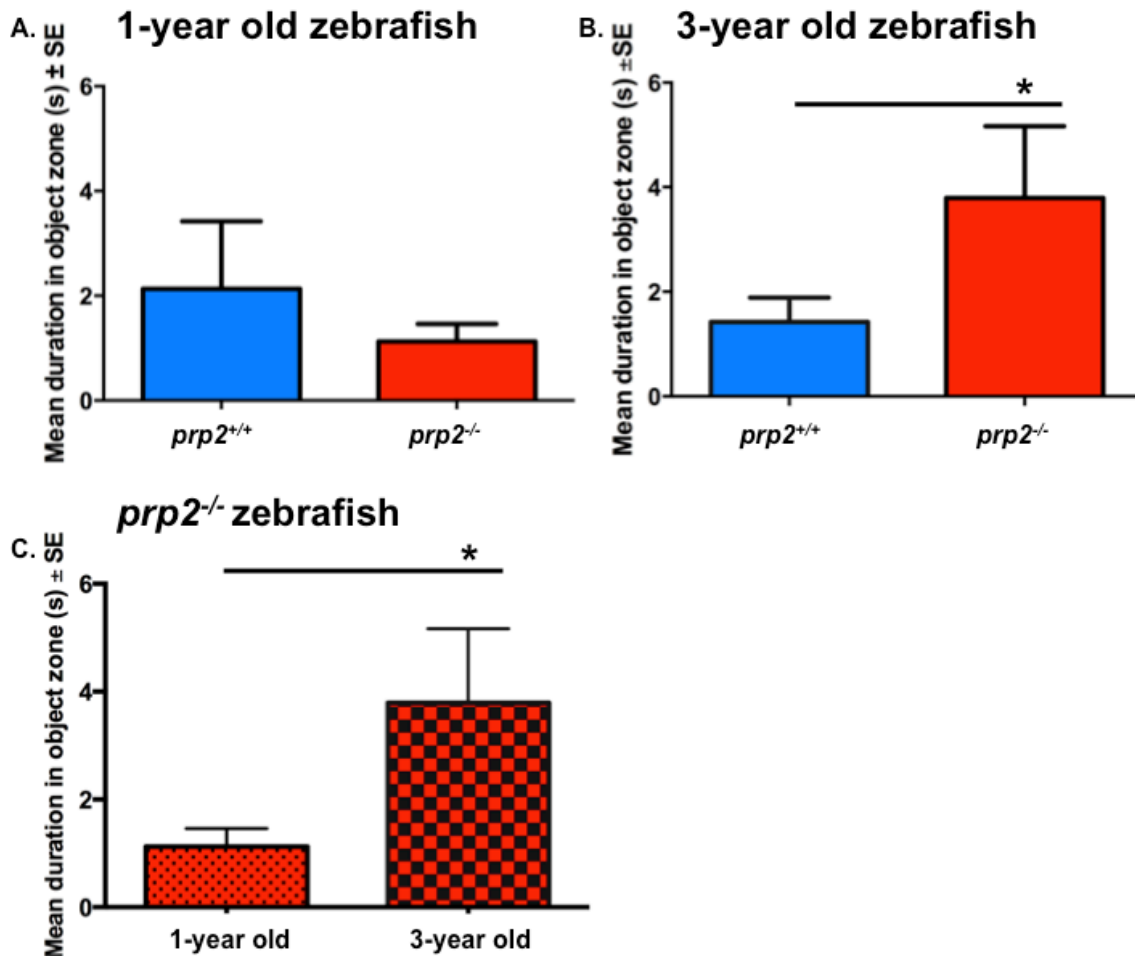
Figure 5.7. Zebrafish lacking *prp2* exhibited an age-dependent difference in object appraisal

3-year old *prp2*-/- fish spent more time in close proximity to the novel object than 1-year old *prp2*-/- fish in the NOA test. **A.** Amongst 1-year old fish, there was no significant difference between genotypes (*prp2*+/+ and *prp2*-/-) in time spent in the object (center) zone (n=33 *prp2*+/+ fish, n=29 *prp2*-/- fish). **B.** Time spent in the object (center) zone with significantly greater for the 3-year old *prp2*-/- fish than for the 3-year old *prp2*+/+ fish (*p<0.05 with one-tailed Mann-Whitney test, n=16 fish/genotype). **C.** 3-year old *prp2* -/- fish spent a significantly greater period of time in the object (center) zone than 1-year old *prp2*-/- fish (*p<0.05 with the Mann-Whitney test; a re-plotting the values from Figure 5.7A and 5.7B).

5.4.3 No differences in anxiety were detectable with age or between *prp2*^{+/+} and *prp2*^{-/-} fish genotypes using the novel tank diving test

The novel tank diving test, an established and sensitive anxiety test (Maximino et al., 2010), was deployed to determine differences in anxiety. Such differences might have accounted for reduced object preference and increased novel object approach observed with age or between genotypes. The zebrafish were exposed to a tank that was narrower and deeper than their home tank; the time the fish spent in the bottom, middle and top third of the tank was recorded. In this test, 'bottom dwelling' is considered an anxious response. Consistent with previous reports (Bencan et al., 2009), our wild type (*prp2*^{+/+}) fish of both ages exhibited an anxious response to the novel environment: they spent proportionally more time in the bottom zone than in the top zone of the novel tank (Figure 5.8 A-B). No differences were found between genotypes (*prp2*^{+/+} versus *prp2*^{-/-}) of young (1-year old) zebrafish in the novel tank diving test, indicating that 1-year old *prp2*^{-/-} zebrafish had anxiety levels comparable to those of *prp2*^{+/+} fish (Figure 5.8A). There were also no significant differences between aged (3-year old) fish of the *prp2*^{-/-} and *prp2*^{+/+} genotypes in the top zone, middle zone or bottom zone of the tank during the novel tank diving test (Figure 5.8B). Further, there were no age-dependent differences in the time the *prp2*^{-/-} fish spent in the bottom zone (Figure 5.8C), suggesting that the fish displayed no age-dependent changes in anxiety.
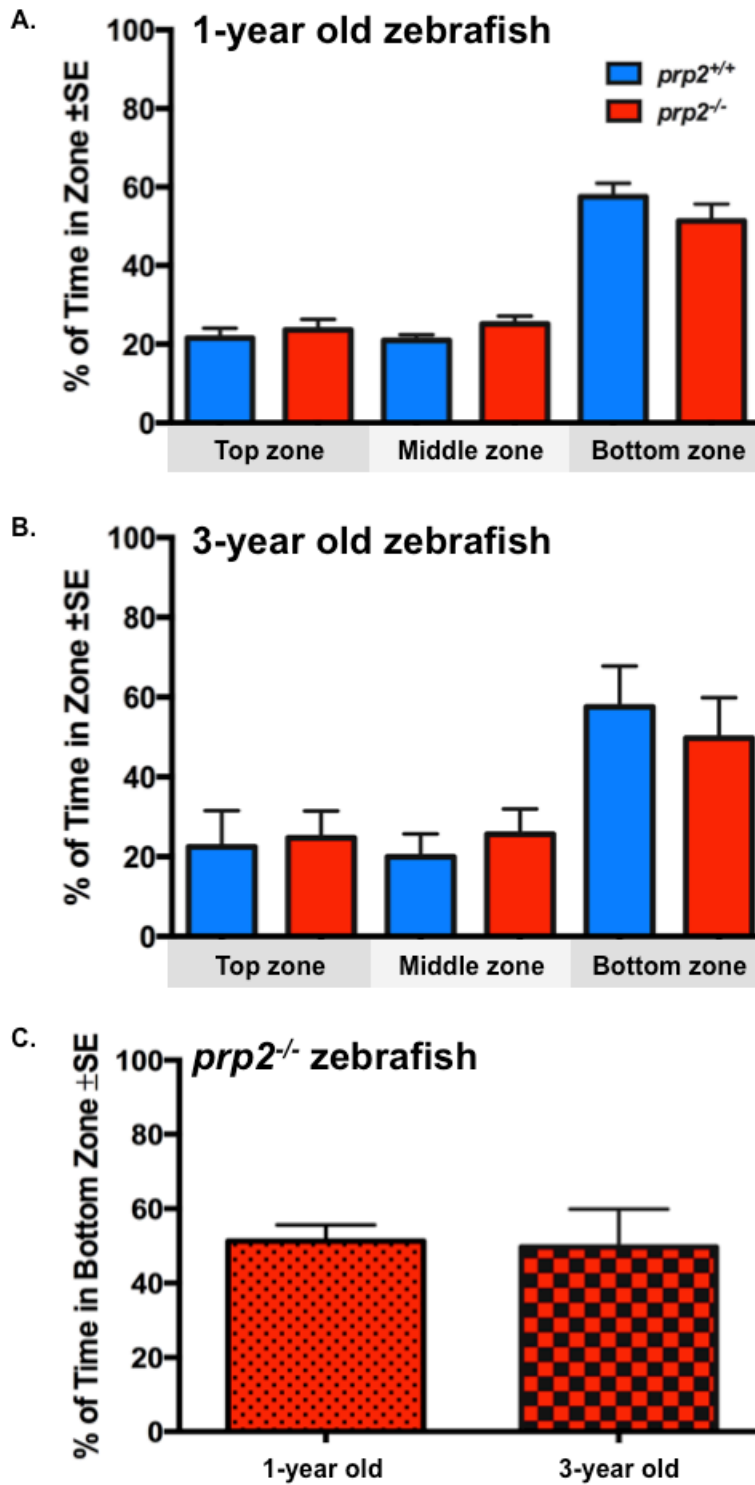
Figure 5.8. There were no differences in anxiety between *prp2*$^{+/+}$ and *prp2*$^{-/-}$ fish or age-related changes in anxiety using the novel tank diving test

All groups of fish displayed the typical bottom dwelling response to tank novelty. **A.** Among 1-year old fish, there were no significant differences between genotypes in time spent in the top zone, middle zone, or bottom zone (n=34 *prp2*$^{+/+}$ fish, n=29 *prp2*$^{-/-}$ fish). **B.** Among 3-year old fish, there were no significant differences between genotypes in time spent in the top zone, middle zone, or bottom zone (n=11 *prp2*$^{+/+}$ fish, n=10 *prp2*$^{-/-}$ fish). **C.** 1-year old *prp2*$^{-/-}$ fish and 3-year old *prp2*$^{-/-}$ fish spent a comparable proportion of time in the bottom zone (re-plotted from Figures 5.8A and 5.8B).

5.5 Discussion

The goal of our study was to determine whether PrP^C has a conserved role underlying memory and anxious behaviour. We also sought to characterize a zebrafish PrP^C loss-of-function model that could be used for testing potential prion disease and AD therapeutics in the future. There are many advantages of using zebrafish as a model for drug testing that include 1) water soluble drugs can be applied directly to the tank water and thus drug delivery is not invasive; and 2) drugs can be applied continuously, aiding study of drug pharmacokinetics (Kedikian et al., 2013).

5.5.1 PrP^C influences object preference in zebrafish, a role that is conserved in mice

We used a zebrafish object preference paradigm (May et al., 2016) to assess object recognition memory in our recently engineered $prp2^{-/-}$ fish (Fleisch et al., 2013). Similar to rodent novel object preference paradigms (Dodart et al., 1997; Ennaceur and Delacour, 1988), we analyzed the time the fish spent exploring (i.e. in close proximity to) a novel object compared to time spent exploring a familiar object. We used previously established discrimination indices (Table 1, (Akkerman et al., 2012; May et al., 2016)) to assess novel object preference in young (1-year old) and aged (3-year old) $prp2^{-/-}$ fish. With the first test (novel object preference with a 1 minute retention interval), we found that 1-year old $prp2^{-/-}$ fish displayed preference for the familiar object using the D1, D2, and D3 discrimination indices. We interpret this familiar object preference as a response to recognizing the familiar object. Using the D1 discrimination index, we found that 3-year old $prp2^{+/+}$ zebrafish displayed familiar object preference after a 1-minute retention interval, while 3-year old $prp2^{-/-}$ fish did not. When taking exploration time into account using the D2 and D3 discrimination indices, however, the 3-year old $prp2^{+/+}$ fish also did not display familiar object preference. When we challenged the fish with a more difficult task (object recognition test with a 5 minute retention interval), none of the groups of fish showed significant object preference. However, when we compared the D1 and D2 indices of the 1-year-old $prp2^{-/-}$ fish to those of the 3-year-old $prp2^{-/-}$ fish, we found a trend (though not significant) towards reduced object preference among the older fish after both 1-minute and 5-minute retention intervals. This suggests that $prp2^{-/-}$ fish exhibit age-dependent memory decline. This age-dependent decline in object discrimination is

comparable to what has been reported in *Prnp*$^{-/-}$ mice using a novel object recognition paradigm (Schmitz et al., 2014a).

5.5.2 PrP influences object recognition and cognitive appraisal in zebrafish

While object preference has been previously used as a proxy for object recognition, alternative explanations for the age-dependent decline in object preference among *prp2*$^{-/-}$ fish include changes in cognitive appraisal and/or anxiety. In the novel object approach test the aged (3-year old) *prp2*$^{-/-}$ fish spent more time exploring the novel object than the 3-year old *prp2*$^{+/+}$ fish and the young (1-year old) *prp2*$^{-/-}$ fish. In this test, fish that keep distance from the object and spend time in the thigmotaxis zone could be interpreted as a proxy for fear of a predator (Maximino et al., 2010), and it is possible that the fish fear the object due to its relative size (May et al., 2016). If this were the case, the older *prp2*$^{-/-}$ fish would be interpreted as having adopted a more risky/bold behaviour, or they may not appraise the object as being one to fear. It was previously found that *Prnp*$^{-/-}$ mice exhibited less anxiety in an elevated plus maze than *Prnp*$^{+/+}$ mice following acute stress (foot shock or swimming in a tank of water) (Nico et al., 2005). This may mean that PrP^{C} is involved in adapting to conditions of stress (Nico et al., 2005). However, the interpretation that the 3-year old *prp2*$^{-/-}$ fish have decreased anxiety is not consistent with our results from the novel tank diving test. In this test we saw no significant differences in bottom dwelling time (a proxy for increased anxiety) or top dwelling time (a proxy for decreased anxiety) in the 3-year old *prp2*$^{-/-}$ fish compared to age matched *prp2*$^{+/+}$ fish or 1-year old *prp2*$^{-/-}$ fish. The novel tank diving test is considered to be a more sensitive anxiety test compared to the novel approach test (Loh et al., *in prep*) so it is unlikely that the *prp2*$^{-/-}$ fish are less anxious. An alternate explanation is that the 3-year old *prp2*$^{-/-}$ fish have lost their ability to cognitively discern whether the novel object appears to be a predator. In other words, they may not recognize that the object is something to be afraid of.

Interestingly, the 1-year old wild type fish used in our study did not perform as well in the novel object preference test as young wild type fish used in a previous study (May et al., 2016). This difference in behaviour of the wild type fish could be due to being handled more during early adult life (eg. Set up more often to breed), or may be related to an idiosyncrasy of the home tank environment. Regardless, our most valid comparison is

between the 1-year old and 3-year old *prp2*$^{-/-}$ fish, which demonstrated a loss of object recognition memory and cognitive appraisal.

In sum, we interpret our results as supporting the hypothesis that prion protein of zebrafish is required for learning and memory functions, and ruled out alternative explanation for the data that invoke differences in anxiety levels between genotypes. This is similar to the effects of *Prnp* loss on novel object recognition demonstrated previously in mice, supporting a conserved, ancient (and thus presumably important) role for prion protein in learning and memory.

5.5.3 Potential cellular mechanisms linking PrP^C to memory and cognitive appraisal

PrP^C is a known interaction partner of many other membrane proteins and may contribute to memory formation through multiple mechanisms. PrP^C interactions with Sti1 and Laminin-γ1 have been shown to be involved in a memory paradigm in rats (Coitinho et al., 2006; Coitinho et al., 2007), and these interactions activate PKA and ERK 1/2 signalling (Beraldo et al., 2010; Coitinho et al., 2006). The PrP^C-Sti1 complex also interacts with the α7 nicotinic acetylcholine receptor (Beraldo et al., 2010), which is a known regulator of long-term memory (reviewed in (Jeong and Park, 2015)). Low doses of nicotine enhance spatial recognition in zebrafish and antagonists of several zebrafish nicotinic acetylcholine receptors are available (Braida et al., 2014). Thus it would be possible to treat zebrafish *prp2*$^{-/-}$ fish with nicotine and nicotinic receptor antagonists to determine whether interactions between PrP^C and nicotinic receptors are important for memory retention. NMDA receptors have also been shown to be involved in zebrafish memory (Swain et al., 2004), and given that PrP^C regulates NMDA receptors, including in zebrafish, (Fleisch et al., 2013; Khosravani et al., 2008; Stys et al., 2012) it would be interesting to investigate the effect of this regulation on object recognition memory.

A potential explanation for reduced cognitive appraisal in older *prp2*$^{-/-}$ fish could be reduced activity of nitric oxide synthase. Both scrapie-infected mice and PrP$^{-/-}$ mice exhibit alterations in the localization and activity of nitric oxide synthase (Keshet et al., 1999), and inhibition of nitric oxide synthase has been shown to increase exploratory behaviour of mice in an elevated plus maze, including time spent in the open arms and number of entries into the open arms (Volke et al., 1995). This altered behaviour may

also be due to loss of regulation of nicotinic receptors by PrP^C. Low doses of nicotine enhance cognitive functions, including memory, in zebrafish and mammals (reviewed in (Levin et al., 2006)). Thus if PrP^C's interaction with nicotinic acetylcholine receptors (Beraldo et al., 2010) enhances memory, nicotinic receptor agonists may counteract memory deficits in aged *prp2$^{-/-}$* fish. In turn, nicotine would be predicted to have a greater effect in *prp2$^{+/+}$* fish than in *prp2$^{-/-}$* fish.

5.5.4 Conclusions and future outlook

Here we have demonstrated that zebrafish have object recognition memory and that this memory is disrupted by targeted mutagenesis of one of the zebrafish *Prnp* paralogs. We have recently engineered compound *prp1$^{-/-}$*; *prp2$^{-/-}$* zebrafish and when they have aged it will be important to determine whether loss of *prp1* exacerbates the age-dependent deficits in memory that we observed in our *prp2$^{-/-}$* fish. Our zebrafish paradigm is relatively simple and well suited for testing which PrP^C interacting partners are important for mediating memory and synaptic plasticity *in vivo*, since drugs (eg. Nicotine, nicotinic receptor antagonists, MK-801) can be delivered by adding them to the tank water. Knowledge gathered from the object recognition memory paradigm will be applied to conditional learning paradigms to assess the roles of PrP^C and its interaction partners in learning. As PrP^C is associated with prion diseases as well as AD (through its interactions with APP and Aβ oligomers), knowledge gained from these studies will accelerate/enhance the development and screening of prion disease and AD therapeutics.

Further, our data strongly support the growing list of phenotypes observed in prion loss-of-function models that map with high fidelity onto prion disease symptomology (Leighton and Allison, 2016). Thus, in contradistinction to the simplifying assumption that protein gain-of-function is largely responsible for disease outcomes, we infer that the etiology of prion diseases likely requires prion protein function to be at least partially lost or subverted on the path to dementia.

Chapter 5 References

Aggleton, J. P., et al., 2010. Lesions of the rat perirhinal cortex spare the acquisition of a complex configural visual discrimination yet impair object recognition. Behav Neurosci. 124, 55-68.

Ahmed, T. S., et al., 2012. Effects of animated images of sympatric predators and abstract shapes on fear responses in zebrafish. Behaviour 149, 1125-1153.

Akkerman, S., et al., 2012. Object recognition testing: statistical considerations. Behav Brain Res. 232, 317-22.

Bencan, Z., et al., 2009. Buspirone, chlordiazepoxide and diazepam effects in a zebrafish model of anxiety. Pharmacol Biochem Behav. 94, 75-80.

Beraldo, F. H., et al., 2010. Role of alpha7 nicotinic acetylcholine receptor in calcium signaling induced by prion protein interaction with stress-inducible protein 1. J Biol Chem. 285, 36542-50.

Braida, D., et al., 2014. Role of neuronal nicotinic acetylcholine receptors (nAChRs) on learning and memory in zebrafish. Psychopharmacology (Berl). 231, 1975-85.

Bueler, H., et al., 1992. Normal development and behaviour of mice lacking the neuronal cell-surface PrP protein. Nature. 356, 577-582.

Caine, D., et al., 2015. The cognitive profile of prion disease: a prospective clinical and imaging study. Ann Clin Transl Neurol. 2, 548-58.

Champagne, D. L., et al., 2010. Translating rodent behavioral repertoire to zebrafish (Danio rerio): relevance for stress research. Behav Brain Res. 214, 332-42.

Coitinho, A. S., et al., 2006. The interaction between prion protein and laminin modulates memory consolidation. Eur J Neurosci. 24, 3255-64.

Coitinho, A. S., et al., 2007. Short-term memory formation and long-term memory consolidation are enhanced by cellular prion association to stress-inducible protein 1. Neurobiol Dis. 26, 282-90.

Coitinho, A. S., et al., 2003. Cellular prion protein ablation impairs behavior as a function of age. Neuroreport. 14, 1375-9.

Criado, J. R., et al., 2005. Mice devoid of prion protein have cognitive deficits that are rescued by reconstitution of PrP in neurons. Neurobiol Dis. 19, 255-65.

Dodart, J. C., et al., 1997. Scopolamine-induced deficits in a two-trial object recognition task in mice. Neuroreport. 8**,** 1173-8.

Egan, R. J., et al., 2009. Understanding behavioral and physiological phenotypes of stress and anxiety in zebrafish. Behav Brain Res. 205**,** 38-44.

Ennaceur, A., Delacour, J., 1988. A new one-trial test for neurobiological studies of memory in rats. 1: Behavioral data. Behav Brain Res. 31**,** 47-59.

Fleisch, V., et al., 2013. Targeted mutation of the gene encoding prion protein in zebrafish reveals a conserved role in neuron excitability. Neurobiol Dis. 55**,** 11-25.

Gerhard, G. S., et al., 2002. Life spans and senescent phenotypes in two strains of Zebrafish (Danio rerio). Exp Gerontol. 37**,** 1055-68.

Gilbert, M. J., et al., 2014. Zebrafish (Danio rerio) as a model for the study of aging and exercise: physical ability and trainability decrease with age. Exp Gerontol. 50**,** 106-13.

Hammond, R. S., et al., 2004. On the delay-dependent involvement of the hippocampus in object recognition memory. Neurobiol Learn Mem. 82**,** 26-34.

Hannesson, D. K., et al., 2004. Interaction between perirhinal and medial prefrontal cortex is required for temporal order but not recognition memory for objects in rats. J Neurosci. 24**,** 4596-604.

Herrmann, U. S., et al., 2015. Prion infections and anti-PrP antibodies trigger converging neurotoxic pathways. PLoS Pathog. 11**,** e1004662.

Huc-Brandt, S., et al., 2014. Zebrafish prion protein PrP2 controls collective migration process during lateral line sensory system development. PLoS One. 9**,** e113331.

Jeong, J. K., Park, S. Y., 2015. Neuroprotective effect of cellular prion protein (PrPC) is related with activation of alpha7 nicotinic acetylcholine receptor (alpha7nAchR)-mediated autophagy flux. Oncotarget. 6**,** 24660-74.

Kedikian, X., et al., 2013. Behavioral and molecular analysis of nicotine-conditioned place preference in zebrafish. PLoS One. 8**,** e69453.

Keshet, G. I., et al., 1999. Scrapie-infected mice and PrP knockout mice share abnormal localization and activity of neuronal nitric oxide synthase. J Neurochem. 72**,** 1224-31.

Khosravani, H., et al., 2008. Prion protein attenuates excitotoxicity by inhibiting NMDA receptors. J Cell Biol. 181**,** 551-565.

Kishi, S., et al., 2003. The zebrafish as a vertebrate model of functional aging and very gradual senescence. Exp Gerontol. 38**,** 777-86.

Kostylev, M. A., et al., 2015. Prion-Protein-interacting Amyloid-beta Oligomers of High Molecular Weight Are Tightly Correlated with Memory Impairment in Multiple Alzheimer Mouse Models. J Biol Chem. 290**,** 17415-38.

Lauren, J., et al., 2009. Cellular prion protein mediates impairment of synaptic plasticity by amyloid-beta oligomers. Nature. 457**,** 1128-U84.

Leighton, P. L., Allison, W. T., 2016. Protein Misfolding in Prion and Prion-Like Diseases: Reconsidering a Required Role for Protein Loss-of-Function. J Alzheimers Dis. 54**,** 3-29.

Levin, E. D., et al., 2006. Timing of nicotine effects on learning in zebrafish. Psychopharmacology (Berl). 184**,** 547-52.

Manson, J. C., et al., 1994. 129/Ola mice carrying a null mutation in PrP that abolishes mRNA production are developmentally normal. Mol Neurobiol. 8**,** 121-7.

Maximino, C., et al., 2010. Measuring anxiety in zebrafish: a critical review. Behav Brain Res. 214**,** 157-71.

May, Z., et al., 2016. Object recognition memory in zebrafish. Behav Brain Res. 296**,** 199-210.

Moore, R. C., et al., 1995. Double replacement gene targeting for the production of a series of mouse strains with different prion protein gene alterations. Biotechnology (N Y). 13**,** 999-1004.

Moretz, J. A., et al., 2007. Behavioral syndromes and the evolution of correlated behavior in zebrafish. Behav Ecol. 18**,** 556-562.

Morris, R. G., 2013. NMDA receptors and memory encoding. Neuropharmacology. 74**,** 32-40.

Nico, P. B., et al., 2005. Altered behavioural response to acute stress in mice lacking cellular prion protein. Behav Brain Res. 162**,** 173-81.

Nishida, N., et al., 1997. Prion protein is necessary for latent learning and long-term memory retention. Cell Mol Neurobiol. 17**,** 537-45.

Norton, W., Bally-Cuif, L., 2010. Adult zebrafish as a model organism for behavioural genetics. BMC Neurosci. 11**,** 90.

Ogwang, S. P., Inspection of a novel object by wild and laboratory Zebrafish (Danio rerio H.) in the presence and absence of alarm substance. Biology, Vol. M.Sc. The University of Bergen, Bergen, Norway, 2008, pp. 68.

Ou, M., et al., 2015. Responses of pink salmon to CO_2-induced aquatic acidification. Nat Clim Change. 5**,** 950-955.

Panula, P., et al., 2010. The comparative neuroanatomy and neurochemistry of zebrafish CNS systems of relevance to human neuropsychiatric diseases. Neurobiol Dis. 40**,** 46-57.

Parker, M. O., et al., 2014. The utility of zebrafish to study the mechanisms by which ethanol affects social behavior and anxiety during early brain development. Prog Neuropsychopharmacol Biol Psychiatry. 55**,** 94-100.

Prusiner, S. B., 1982. Novel proteinaceous infectious particles cause scrapie. Science. 216**,** 136-44.

Rial, D., et al., 2009. Cellular prion protein modulates age-related behavioral and neurochemical alterations in mice. Neuroscience. 164**,** 896-907.

Rodriguez, F., et al., 2002. Spatial memory and hippocampal pallium through vertebrate evolution: insights from reptiles and teleost fish. Brain Res Bull. 57**,** 499-503.

Roesler, R., et al., 1999. Normal inhibitory avoidance learning and anxiety, but increased locomotor activity in mice devoid of PrP(C). Brain Res Mol Brain Res. 71**,** 349-53.

Rossi, D., et al., 2001. Onset of ataxia and Purkinje cell loss in PrP null mice inversely correlated with Dpl level in brain. EMBO J. 20**,** 694-702.

Sakaguchi, S., et al., 1995. Accumulation of proteinase K-resistant prion protein (PrP) is restricted by the expression level of normal PrP in mice inoculated with a mouse-adapted strain of the Creutzfeldt-Jakob disease agent. J Virol. 69**,** 7586-92.

Sales, N., et al., 1998. Cellular prion protein localization in rodent and primate brain. Eur J Neurosci. 10**,** 2464-71.

Schmitz, M., et al., 2014. Loss of Prion Protein Leads to Age-Dependent Behavioral Abnormalities and Changes in Cytoskeletal Protein Expression. Mol Neurobiol.

Stahl, N., et al., 1987. Scrapie prion protein contains a phosphatidylinositol glycolipid. Cell. 51**,** 229-40.

Stys, P. K., et al., 2012. Copper-dependent regulation of NMDA receptors by cellular prion protein: implications for neurodegenerative disorders. J Physiol. 590**,** 1357-68.

Swain, H. A., et al., 2004. Effects of dizocilpine (MK-801) on circling behavior, swimming activity, and place preference in zebrafish (Danio rerio). Neurotoxicol Teratol. 26**,** 725-9.

Tierney, K. B., 2011. Behavioural assessments of neurotoxic effects and neurodegeneration in zebrafish. Biochim Biophys Acta. 1812**,** 381-389.

Volke, V., et al., 1995. Inhibition of nitric oxide synthase causes anxiolytic-like behaviour in an elevated plus-maze. Neuroreport. 6**,** 1413-6.

Winters, B. D., et al., 2011. On the dynamic nature of the engram: evidence for circuit-level reorganization of object memory traces following reactivation. J Neurosci. 31**,** 17719-28.

Wright, D., et al., 2006. QTL analysis of behavioral and morphological differentiation between wild and laboratory zebrafish (Danio rerio). Behav Genet. 36**,** 271-84.

Wright, D., et al., 2003. Inter and intra-population variation in shoaling and boldness in the zebrafish (Danio rerio). Naturwissenschaften. 90**,** 374-7.

Yokoyama, T., et al., 2001. In vivo conversion of cellular prion protein to pathogenic isoforms, as monitored by conformation-specific antibodies. J Biol Chem. 276**,** 11265-71.

Chapter 6. Conclusions and Future Directions

6.1 Summary

Understandably, much of the work on PrP^C and APP biology has focused on the contributions of their misfolded forms or aggregated metabolites to prion diseases and Alzheimer's disease (AD), respectively. It is, however, equally important to understand the normal physiology of these proteins as subversion/partial loss of some normal functions likely contribute to the disease states, and restoring said functions represent therapeutic avenues. While attempts have been made to study the function of these proteins in healthy organisms, progress has been thwarted by the lack of overt phenotypes in *Prnp* and *APP* knockout mice (Bueler et al., 1992; Manson et al., 1994; Muller et al., 1994; Zheng et al., 1995). As discussed in Chapter 1, an abundance of putative functions have been ascribed to both PrP^C and APP, with protective effects against convulsants (Rangel et al., 2007; Steinbach et al., 1998; Walz et al., 1999), and roles in synaptic transmission (Khosravani et al., 2008; Wang et al., 2005) and cognition (Coitinho et al., 2003; Dawson et al., 1999; Muller et al., 1994) being common to both proteins. Further, mammalian PrP^C and APP can physically interact (Kaiser et al., 2012; Schmitz et al., 2014b), leading us to hypothesize that these proteins also have functional interactions. Zebrafish are an attractive model organism for uncovering conserved (and hence important) functions of PrP^C and APP because their CNS resembles that of mammals, and their genetic tractability can be harnessed to identify protein functional domains (eg. by 'rescuing' a phenotype in loss-of-function mutants with modified mRNAs). Here we confirmed our previous finding that zebrafish homologs of *PRNP* and *APP*, *prp1* and *appa*, interact during early zebrafish development (Kaiser et al., 2012). We also found that *prp1* and *prp2* have redundant, protective roles during exposure to the convulsant, PTZ. Further, both *prp1* and *prp2* participate in the development of the zebrafish lateral line neuromasts, but their functions appear to have diverged (i.e. sub-functionalized). Finally, we showed that zebrafish lacking the *prp2* paralog have age-dependent deficits in object recognition memory and cognitive appraisal.

6.2 PrP^C and APP interact during early zebrafish development

Previously, severe developmental defects were observed in zebrafish embryos when *prp1* or *appa* were transiently knocked down, sharply contrasting the lack of overt

phenotypes in *Prnp* and *APP* knockout mice; therefore we reasoned that zebrafish loss-of-function *prp1* and *appa* mutants might reveal functions of PrP^C and APP at later developmental stages. Transient loss of *prp1* through delivery of a high dose (4 ng) of *prp1* morpholino led to developmental arrest of zebrafish embryos during gastrulation (Malaga-Trillo et al., 2009), and effective doses (1 ng) of either *prp1* MO or *appa* MO induced apoptosis and CNS malformations (Kaiser et al., 2012). Further, co-knockdown of *prp1* and *appa* with subeffective doses of each morpholino (0.5 ng) also produced fish with high levels of apoptosis and CNS malformations (Kaiser et al., 2012). Interestingly, in Chapter 2, we found that maternal zygotic *prp1*$^{-/-}$ mutants (those lacking *prp1* mRNA in the egg cell), maternal zygotic *appa*$^{-/-}$ mutants and compound maternal zygotic *prp1*$^{-/-}$; *appa*$^{-/-}$ mutants developed into adulthood without signs of overt phenotypes. Further work is needed to unambiguously demonstrate that the generated mutant alleles are null alleles (for example, western blots showing absence of appa and prp1; however available data support a substantive loss of function in these alleles). In the meantime, we performed experiments to address the hypothesis that selection pressure, possibly due to gene compensation or use of alternate biological pathways in some individual fish, contributed to the lack of overt phenotypes in the compound *prp1*$^{-/-}$; *appa*$^{-/-}$ mutants.

We reasoned that an absence of phenotypes in zygotic *prp1*$^{-/-}$; *appa*$^{-/-}$ mutants might be due to selection of fish capable of surviving to adulthood without *prp1* or *appa*, and that phenotypes might appear if acute loss of one gene was combined with a loss-of-function mutant of the other gene (i.e. in *appa*/*prp1* morphomutants). Indeed, we found that acute loss of *appa* in maternal zygotic *prp1*$^{ua5003/ua5003}$ and *prp1*$^{ua5004/ua5004}$ mutants produced embryos with severe body axis abnormalities and necrotic appearance, which could be reversed with either mouse *Prnp* or *prp1* mRNA. Though it will be important to perform the converse experiments (i.e. *prp1* morpholino into *appa*$^{-/-}$ embyros), these results confirm our previous findings that *appa* and *prp1* genetically interact during early development and that interactions between PrP^C and APP are conserved (Kaiser et al., 2012). RNA sequencing comparing wild type fish, compound *prp1*$^{-/-}$;*appa*$^{-/-}$ mutants, *appa*$^{-/-}$ mutants injected with *prp1* MO and *appa*$^{-/-}$ mutants injected with *prp1* MO would yield a list of candidate genes capable of replacing *prp1* in its interaction with *appa*, and

would inspire new hypotheses on the molecular nature of the genetic interaction between *prp1* and *appa.*

6.3 Zebrafish homologs of PrP^C reduce susceptibility to convulsants

An alternative idea to explain the lack of overt phenotypes in the zebrafish prion protein and *appa*$^{-/-}$ mutants described in Chapter 2, are that the primary roles of these genes are to protect against environmental stressors (Makzhami et al., 2014). The idea that mammalian PrP^{C} is neuroprotective is supported by findings that *Prnp* knockout mice are more sensitive to treatment with PTZ, kainic acid and NMDA than wild type mice and that N2A cells with reduced *Prnp* expression (through siRNA knockdown) are more sensitive to kainic acid than control-transfected N2A cells (reviewed in (Carulla et al., 2015)). In Chapter 3, we aimed to use an established model of zebrafish seizure susceptibility- treatment of zebrafish with pentylenetetrazole (PTZ) doses known to produce Type II and Type III seizures (Baraban et al., 2005) to test the hypothesis that protection against drug-induced seizures is a conserved function of PrP^{C}. We found that endogenous *prp2* had a protective effect by suppressing PTZ-induced hyperactivity. Others in the lab found that *prp1* and *prp2* are redundant in this role since our *prp1*$^{-/-}$ mutants also showed an increase in hyperactivity upon treatment with PTZ compared to wild type fish. We also found that endogenous *prp1* and *prp2* suppress *c-fos* expression in PTZ-treated larvae, which indirectly indicates that *prp1* and *prp2* have redundant roles in regulating neural activity. Further, preliminary data suggests that mouse *Prnp* mRNA can suppress *c-fos* expression in PTZ-treated 2dpf compound maternal zygotic *prp1*$^{-/-}$;*prp2*$^{-/-}$ treated with PTZ, hence producing a rescue effect and supporting the hypothesis that neuroprotection is a conserved function of PrP^{C}.

As *c-fos* expression is an indirect measure of neural activity (and includes muscle activity), and variability in *c-fos* induction with PTZ in control (un-injected) fish made it difficult to suppress/rescue *c-fos* levels in PTZ-treated zebrafish prion protein mutants, others in our lab have started working with CaMPARI technology (Fosque et al., 2015). In CaMPARI transgenic fish, the photoactivatable fluorescent protein, CaMPARI, changes its fluorescence from green to red in the presence of calcium and simultaneous stimulation with a violet light. Hence, neural activity can be directly measured through

changes in intracellular calcium levels, indicated by changes in green to red fluorescence (Fosque et al., 2015). CaMPARI transgenes have been bred into our $prp1^{-/-}$, $prp2^{-/-}$ and compound $prp1^{-/-};prp2^{-/-}$ mutants, and others in our lab will attempt to suppress PTZ-induced activity in these fish (i.e. rescue drug-induced neural activation) with cognate mRNA and mouse *Prnp* mRNA. It will also be informative for AD research to determine whether PTZ-induced neural excitability is exacerbated in compound $prp1^{-/-};appa^{-/-}$ mutants compared to neural excitability in $prp1^{-/-}$ and $appa^{-/-}$ single mutants.

Further, Jason Rihel (our colleague at University College London) is currently using established high throughput behavioural assays (Rihel et al., 2010a; Rihel et al., 2010b; Rihel and Schier, 2012) to assess whether our *prnp* mutant zebrafish larvae are hyperactive and/or exhibit sleep-wake disruptions. The activity 'fingerprints' generated by our mutants will be compared to 'fingerprints' previously generated in zebrafish larvae exposed to a panel of neuroactive drugs. Identification of drugs that mimic *prnp* loss-of-function will provide insights into the molecular pathways PrP^C participates in to regulate neural activity.

6.4 *Prp2$^{-/-}$* fish exhibit age-dependent decline in object recognition and appraisal

In Chapter 3 we found that zebrafish prion protein mutants were hyperactive and had increased neural activity in the presence of a drug. It follows then, that subtler changes in neural activity may be occurring through disruption of PrP^C function under normal environmental conditions in animals lacking PrP^C, manifesting as behavioural changes. Indeed, deficits in social recognition (Rial et al., 2009) and novel object recognition (Schmitz et al., 2014a), as well as impaired performance in conditioned memory tasks (Coitinho et al., 2003; Criado et al., 2005; Nishida et al., 1997; Rial et al., 2009; Schmitz et al., 2014a) have been observed in mouse *Prnp* knockouts. We performed an object recognition test with adult wild type and $prp2^{-/-}$ zebrafish to test the hypothesis that PrP^C has a conserved role in memory. We found that aged (3-year old) $prp2^{-/-}$ zebrafish did not perform as well in the object preference test as aged-matched $prp2^{+/+}$ fish or younger (1-year old) $prp2^{-/-}$ fish. The aged $prp2^{-/-}$ zebrafish also approached the novel object more than the aged-matched $prp2^{+/+}$ fish or younger (1-year old) $prp2^{-/-}$ fish, in the novel

object approach test, but performed similarly to these other groups in a test of anxiety (tank diving test). Altogether, these results suggested that the aged $prp2^{-/-}$ fish exhibit altered cognitive appraisal of the novel object.

We hypothesize that *prp1* and *prp2* have redundant roles in memory; thus we expect that compound $prp1^{-/-};prp2^{-/-}$ fish will exhibit further reductions in object recognition memory than $prp2^{-/-}$ mutants. It will also be interesting to determine whether decline in object recognition and appraisal correlates with loss of neurons. Others in our lab are adapting a technique called Isotropic Fractionator (Herculano-Houzel and Lent, 2005) to count the total number of cells and neurons in the zebrafish brain, and it will be interesting to determine whether decline in object recognition and appraisal in aged $prp2^{-/-}$ fish coincides with a reduction in neurons. A reduction in neurons could be due to a combination of neuron death and deficits in adult neurogenesis. As adult neurogenesis uses similar biological pathways as those employed during nervous system development (Schmidt et al., 2013), in the next section we discuss roles for *prp1* and *prp2* in neural development.

6.5 Zebrafish *prp1* and *prp2* contribute to neural development

PrP^C is found in the developing CNS of mice (Halliez et al., 2015) and zebrafish *prnp* paralogs are expressed during early zebrafish development (Cotto et al., 2005; Malaga-Trillo et al., 2009). This, together with findings PrP^C participates in cell adhesion and neural outgrowth in primary neuronal cultures, prompted us to investigate contributions of *prp1* and *prp2* to zebrafish neural development (Beraldo et al., 2011; Chen et al., 2003; Santuccione et al., 2005). Specifically, PrP^C is localized to stem cells and progenitors of the CNS in mouse embryos by embryonic day 8.25 and is found in the presumptive brain, floor plate and neural tube by embryonic day 9 (Halliez et al., 2015), and PrP^C mediates neurite outgrowth through interactions with laminin and NCAM (Beraldo et al., 2011; Santuccione et al., 2005).

The zebrafish lateral line is an accessible neural system for studies of neural cell migration and cohesion, with structures sharing homology with the inner ear of mammals-the neuromasts (Thomas et al., 2015). Thus in Chapter 4, we studied neuromast deposition in zebrafish prion protein loss-of-function mutants. We predicted that *prp1*

and *prp2* would have redundant function in neuromast patterning, but instead we found that loss of *prp1* reduced the number of posterior lateral line neuromasts, while loss of *prp2* yielded an increase in the number of trunk neuromasts. One hypothesis to explain this (discussed in more detail in Chapter 4) is that *prp1* and *prp2* have sub-functionalized and participate at different stages of proneuromast development in the primordium. Alternatively, prp1 and prp2 differentially regulate a hypothetical membrane receptor (See Figure 4.7). As discussed in Chapter 4, prp1 and prp2 could potentially interact with several signalling pathways, including Wnt signalling, Fgf signalling and Notch signalling, in the developing lateral line primordium to influence neuromast number. Since parallels exist between the early stages of primordium development (i.e. progenitor cell proliferation and specification of hair cells) and neurogenesis in both adult zebrafish and mammals (Table 6.1), uncovering the molecular mechanisms through which PrP^C influences neuromast number might also be relevant to adult neurogenesis and have some bearing on the cognitive deficits observed in aged *prp2$^{-/-}$* fish.

Table 6.1. Parallels exist between development neuromasts in the zebrafish lateral line primordium and adult neurogenesis in zebrafish and mammals

	Zebrafish lateral line primordium	Adult zebrafish telencephalon	Mammalian subgranular zone of dentate gyrus
Wnt signalling	Promotes cell proliferation in the leading edge[1]	?	Promotes proliferation and differentiation of neural stem cells[4]
Fgf signalling	Cell fate determination of rosette cells in trailing edge[2]	Increase proliferation of stem cells (some of the daughter cells later become neuroblasts)[3]	?
Notch signalling	Inhibit neuroblast formation (restricts # of hair cells to 1/rosette)[2]	Keeps stem cells in the quiescent stage (thus preventing formation of neuroblasts)[3]	Inhibits neural stem cell proliferation and neuronal differentiation[4]

Table 6.1 References:

[1]reviewed in (Thomas et al., 2015), [2](Matsuda and Chitnis, 2010), [3]reviewed in (Schmidt et al., 2013), [4]Reviewed in (Benarroch, 2013)

We also observed a reduced number of neuromasts in fish with some appa loss-of-function alleles, but loss/reduction of *appa* in *appa*$^{-/-}$*;prp1*$^{-/-}$ and *appa*$^{is22gt/is22gt}$*;prp2*$^{-/-}$ larvae did not have an additive or synergistic affect compared to loss of *prp1* or *prp2* alone. As discussed in Chapter 2, however, this may be due to selection of mutants able to survive to adulthood, and acute loss of *appa* in *prp1*$^{-/-}$ mutants might further reduce the neuromast number. Likewise, acute loss of *appa* in *prp2*$^{-/-}$ mutants might reduce neuromast number towards those observed in wild type larvae. Thus future experiments might yet reveal an interaction between *appa* (and *appb*) and zebrafish prion proteins in lateral line development.

6.6 Zebrafish paradigms are applicable to treatment of neurodegenerative diseases

The zebrafish paradigms that we have developed and described in this thesis can be used to uncover the molecular mechanisms underlying AD and prion diseases. Information obtained from the proposed experiments in the section below will help to uncover the consequences of partial loss-of PrP^C and/or APP function in disease states and aid in the development of effective therapeutics.

Messenger RNA 'rescue' experiments in PTZ-treated, $prp1^{-/-}$, $prp2^{-/-}$ and compound $prp1^{-/-};prp2^{-/-}$ mutants (with either *c-fos* levels or CaMPARI photoconversion as outputs) can be used to determine which regions of PrP^C are protective against convulsant-induced neuroactivity, and whether this function is subverted by familial prion disease mutations. Recently, it was found that PrP^C must be anchored to the cell membrane to mediate its protective affects against kainic acid insults (Carulla et al., 2015). It was found that transfection of N2A cells with PrPΔ32-134 produced a reduction in viability of N2A cells treated with kainic acid compared to cells transfected with PrP^C. Further, an increased number of mice with the PrPΔ32-134 transgene died when treated with 8 mg/kg kainic acid than either kainic acid-treated wild type or $Prnp^{-/-}$ mice and PrPΔ32-134 had more cell death as measured with Fluoro Jade staining (Carulla et al., 2015). It will be interesting to determine whether these findings extend to regulation of neural activity because such findings would implicate neuronal dysregulation as a mechanism of cell death. This can be tested by introducing mouse *Prnp* without the GPI anchor or mouse *Prnp* Δ32-134 to PTZ-treated CaMPARI $prp1^{-/-}$, $prp2^{-/-}$ and compound $prp1^{-/-};prp2^{-/-}$ mutant larvae. Similar 'rescue' experiments could be performed to determine which regions of prp1 and prp2 are critical for neuromast patterning, but 'rescue' with cognate mRNA and/or mouse *Prnp* mRNA are prerequisites for these analyses.

Molecular mechanisms underlying neural hyperexcitability may also underpin the memory and cognitive deficits in aged $prp2^{-/-}$ mutants, and PrP^C's main interactors could be identified by applying a battery of drugs in concert with the adult novel object preference test. Learning tasks in larval zebrafish may also reveal deficits in prion protein mutants that can be rescued with mRNA treatment. NMDA receptors are known to be involved in memory (reviewed in (Swain et al., 2004)), and given that PrP^C has been

shown to regulate NMDA receptors (Fleisch et al., 2013; Khosravani et al., 2008; Stys et al., 2012) it is possible that the deficits in object recognition in aged $prp2^{-/-}$ zebrafish is due to dysregulation of NMDA receptors. Thus it is possible that a low dose of the NMDA receptor antagonist, MK801, might improve performance of aged $prp2^{-/-}$ zebrafish in the object recognition task. The α7 nicotinic acetylcholine receptor is also a regulator of long-term memory (reviewed in (Jeong and Park, 2015)) and has been shown to interact with the PrP^C-Sti1 complex (Beraldo et al., 2010). Thus it will be interesting to test the hypothesis that interactions between the α7 nicotinic acetylcholine receptor and PrP^C are important for object recognition memory. To do this, we could determine whether nicotine or nicotinic receptor antagonists influence the performance of zebrafish prion protein mutants in the objection recognition task. Larvae as young at 4dpf are capable of habituation, a form of learning wherein an animal displays a reduced response to repeated stimuli. Habituation of the C-start response, an innate escape response, can be achieved by exposing larvae to repeated sound pulses and short-term habituation (25 minutes to 1 hour) is dependent on NMDA receptors (Roberts et al., 2011). If zebrafish prion protein mutants exhibit deficits in habituation, it may be possible to rescue such phenotypes with $Prnp$ mRNA (though rescue may not be possible at 4-5 dpf, depending on the half-life of the mRNA) or conditional expression of $Prnp$ using a Cre-Lox system (Hans et al., 2009).

Further, various mRNA 'rescue' experiments could be performed in $appa/prp1$ morphomutants to determine whether functions dependent on interactions between PrP^C and APP might be subverted in patients with familial prion diseases or AD, and to identify regions of APP and PrP that are important for functional interactions. For example, we could attempt to reverse the developmental phenotypes in $prp1^{-/-}$ mutants treated with $appa$ morpholino with mouse $Prnp$ mRNA harbouring FFI and GSS mutations (using wild type mouse $Prnp$ as a control), or phenotypes in $appa^{-/-}$ mutants treated with $prp1$ morpholino with human APP mRNA harbouring familial Alzheimer's AD mutations (using wild type human APP mRNA as a control), respectively. These experiments will directly test whether disease-associated mutations create protein loss-of-function. Further, given that $appa$ and $appb$ share 70% identity at the amino acid level (Musa et al., 2001) and that $prp1$ was previously shown to interact with $appa$ but not

appb, we could swap domains between appa and appb to determine which regions of appa mediate interactions with prp1. For example, if the N-terminus of appa (fused to the appb C-terminus) were required to rescue the developmental phenotype, it would suggest that direct or ligand-mediated interaction occurs between appa and prp1 at the cell surface. On the other hand, if the C-terminus of appa (fused to the appb C-terminus) were required to rescue the developmental phenotype, it would suggest that appa and prp1 interact indirectly through a cell-signalling pathway. Future insights on the nature of the PrP^C/APP interaction will be useful for the development of AD therapies.

6.7 Concluding remarks

The vast majority of the work in the prion and AD fields has focused on understanding the mechanisms underlying toxic gain-of-function induced by PrP^{Sc} and aggregates of Aβ and tau. While this work is crucial, it is also important to consider that partial loss or subversion of the normal functions of PrP^C and APP underlie disease symptoms. For example, loss of PrP^C function might contribute to seizures observed in some patients with familial prion diseases (Wieser et al., 2006) or tremors in cattle with BSE (Arai et al., 2009), memory impairments in prion disease patients (Caine et al., 2015), and sleep disturbances in FFI patients (Fiorino, 1996). It has been difficult to ascertain the normal biological functions of PrP^C because *Prnp* knockout mice lack overt phenotypes, and conflicting results have been obtained by experimenters using at least 7 independent lines of *Prnp* knockout mice (some with a 129/Ola genetic background, some with a C57BL background and some with mixed genetic backgrounds) (Nuvolone et al., 2016; Striebel et al., 2013). One of the most contested putative functions of PrP^C has been a role in regulating neural excitability, with some studies reporting that *Prnp*$^{-/-}$ mice are more susceptible to seizure-inducing drugs and others refuting this (reviewed in (Carulla et al., 2015)). We have clarified this point by demonstrating that PrP^C regulates neural activity in a disparate model organism, the zebrafish. Inconsistent results have also been reported surrounding a role for PrP^C in learning and memory (for examples see (Rial et al., 2009; Roesler et al., 1999; Schmitz et al., 2014a)). Here we found that *prp2*$^{-/-}$ fish have age-dependent deficits in object recognition memory. Overall, our results support ancient and conserved functions for PrP^C in regulating neural activity and in memory. Next it will be

important to determine which receptors PrP^C modulates to mediate these effects. NMDA receptors are ideal candidates to assay since we previously found that prp2 regulates NMDA receptors (Fleisch et al., 2013), and it will be important to determine whether this finding extends to prp1.

We have also confirmed that zebrafish *prp1* and *appa* interact, thus subversion of APP function in AD might disrupt some functions of PrP^C (described above), contributing to memory loss and other AD symptoms. Interestingly, we have shown that acute (but not chronic) loss of *appa* in the context of PrP^C loss of function produces overt developmental deficits in zebrafish embryos. As a relatively acute loss of APP and PrP^C function (relative to the lifespan of the individual) is expected in patients with sporadic forms of AD, it will be important to follow up on the effects of acute versus long term loss of these proteins. To do this, a Cre-Lox system (Hans et al., 2009) could be used to acutely inactivate *appa* and *prp1*, wherein CRISPR/Cas9 is used to introduce lox sites into the genome (Felker and Mosimann, 2016). In this system, fish with floxed *APP* and *Prnp* alleles would not exhibit *APP* or *Prnp* loss-of-function (or undergo selection pressure due to loss of App and Prp function) prior to being bred into fish with a Cre-driver line. The fish would then exhibit loss of appa and prp1 upon treatment with tamoxifen. This would allow acute loss of these proteins to be studied at developmental stages that are not accessible with morpholino gene knockdown.

In sum, we have contributed wholly unique genetic resources to the prion and AD fields (*prp1$^{-/-}$* mutants, compound *prp1$^{-/-}$;prp2$^{-/-}$* mutants, and *appa$^{-/-}$* mutants), which expand the powerful utility of zebrafish in resolving the normal physiology of PrP^C and APP and how these proteins interact during AD. We have also combined these genetic tools with assays to assess neurodevelopment, neural activity and behaviour that can now be used to dissect the functional domains of PrP^C and APP. This knowledge will be important for the development of therapies that can combat partial loss-of-function/ subversion of PrP^C and APP function during disease states.

Chapter 6 References

Arai, S., et al., 2009. Brainstem auditory evoked potentials in experimentally-induced bovine spongiform encephalopathy. Res Vet Sci. 87**,** 111-4.

Baraban, S. C., et al., 2005. Pentylenetetrazole induced changes in zebrafish behavior, neural activity and c-FoS expression. Neuroscience. 131**,** 759-768.

Benarroch, E. E., 2013. Adult neurogenesis in the dentate gyrus: general concepts and potential implications. Neurology. 81**,** 1443-52.

Beraldo, F. H., et al., 2011. Metabotropic glutamate receptors transduce signals for neurite outgrowth after binding of the prion protein to laminin gamma1 chain. FASEB J. 25**,** 265-79.

Beraldo, F. H., et al., 2010. Role of alpha7 nicotinic acetylcholine receptor in calcium signaling induced by prion protein interaction with stress-inducible protein 1. J Biol Chem. 285**,** 36542-50.

Bueler, H., et al., 1992. Normal development and behaviour of mice lacking the neuronal cell-surface PrP protein. Nature. 356**,** 577-582.

Caine, D., et al., 2015. The cognitive profile of prion disease: a prospective clinical and imaging study. Ann Clin Transl Neurol. 2**,** 548-58.

Carulla, P., et al., 2015. Involvement of PrP(C) in kainate-induced excitotoxicity in several mouse strains. Sci Rep. 5**,** 11971.

Chen, S., et al., 2003. Prion protein as trans-interacting partner for neurons is involved in neurite outgrowth and neuronal survival. Mol Cell Neurosci. 22**,** 227-33.

Coitinho, A. S., et al., 2003. Cellular prion protein ablation impairs behavior as a function of age. Neuroreport. 14**,** 1375-9.

Cotto, E., et al., 2005. Molecular characterization, phylogenetic relationships, and developmental expression patterns of prion genes in zebrafish (Danio rerio). FEBS Journal. 272**,** 500.

Criado, J. R., et al., 2005. Mice devoid of prion protein have cognitive deficits that are rescued by reconstitution of PrP in neurons. Neurobiol Dis. 19**,** 255-65.

Dawson, G. R., et al., 1999. Age-related cognitive deficits, impaired long-term potentiation and reduction in synaptic marker density in mice lacking the beta-amyloid precursor protein. Neuroscience. 90**,** 1-13.

Felker, A., Mosimann, C., 2016. Contemporary zebrafish transgenesis with Tol2 and application for Cre/lox recombination experiments. Methods Cell Biol. 135, 219-44.

Fiorino, A. S., 1996. Sleep, genes and death: fatal familial insomnia. Brain Res Brain Res Rev. 22, 258-64.

Fleisch, V., et al., 2013. Targeted mutation of the gene encoding prion protein in zebrafish reveals a conserved role in neuron excitability. Neurobiol Dis. 55, 11-25.

Fosque, B. F., et al., 2015. Neural circuits. Labeling of active neural circuits in vivo with designed calcium integrators. Science. 347, 755-60.

Halliez, S., et al., 2015. Prion protein localizes at the ciliary base during neural and cardiovascular development, and its depletion affects alpha-tubulin post-translational modifications. Sci Rep. 5, 17146.

Hans, S., et al., 2009. Temporally-controlled site-specific recombination in zebrafish. PLoS One. 4, e4640.

Herculano-Houzel, S., Lent, R., 2005. Isotropic fractionator: a simple, rapid method for the quantification of total cell and neuron numbers in the brain. J Neurosci. 25, 2518-21.

Jeong, J. K., Park, S. Y., 2015. Neuroprotective effect of cellular prion protein (PrPC) is related with activation of alpha7 nicotinic acetylcholine receptor (alpha7nAchR)-mediated autophagy flux. Oncotarget. 6, 24660-74.

Kaiser, D., et al., 2012. Amyloid beta precursor protein and prion protein have a conserved interaction affecting cell adhesion and CNS development. PloS One. 7.

Khosravani, H., et al., 2008. Prion protein attenuates excitotoxicity by inhibiting NMDA receptors. J Cell Biol. 181, 551-565.

Makzhami, S., et al., 2014. The prion protein family: a view from the placenta. Front Cell Dev Biol. 2, 35.

Malaga-Trillo, E., et al., 2009. Regulation of Embryonic Cell Adhesion by the Prion Protein. PloS Biology. 7, 576-590.

Manson, J. C., et al., 1994. 129/Ola mice carrying a null mutation in PrP that abolishes mRNA production are developmentally normal. Mol Neurobiol. 8, 121-7.

Matsuda, M., Chitnis, A. B., 2010. Atoh1a expression must be restricted by Notch signaling for effective morphogenesis of the posterior lateral line primordium in zebrafish. Development. 137**,** 3477-87.

Muller, U., et al., 1994. Behavioral and anatomical deficits in mice homozygous for a modified beta-amyloid precursor protein gene. Cell. 79**,** 755-65.

Musa, A., et al., 2001. Distinct expression patterns of two zebrafish homologues of the human APP gene during embryonic development. Dev Genes Evol. 211**,** 563.

Nishida, N., et al., 1997. Prion protein is necessary for latent learning and long-term memory retention. Cell Mol Neurobiol. 17**,** 537-45.

Nuvolone, M., et al., 2016. Strictly co-isogenic C57BL/6J-Prnp-/- mice: A rigorous resource for prion science. J Exp Med. 213**,** 313-27.

Rangel, A., et al., 2007. Enhanced susceptibility of Prnp-deficient mice to kainate-induced seizures, neuronal apoptosis, and death: Role of AMPA/kainate receptors. J Neurosci Res. 85**,** 2741-55.

Rial, D., et al., 2009. Cellular prion protein modulates age-related behavioral and neurochemical alterations in mice. Neuroscience. 164**,** 896-907.

Rihel, J., et al., 2010a. Zebrafish behavioral profiling links drugs to biological targets and rest/wake regulation. Science. 327**,** 348-51.

Rihel, J., et al., 2010b. Monitoring sleep and arousal in zebrafish. Methods Cell Biol. 100**,** 281-94.

Rihel, J., Schier, A. F., 2012. Behavioral screening for neuroactive drugs in zebrafish. Dev Neurobiol. 72**,** 373-85.

Roberts, A. C., et al., 2011. Habituation of the C-start response in larval zebrafish exhibits several distinct phases and sensitivity to NMDA receptor blockade. PLoS One. 6**,** e29132.

Roesler, R., et al., 1999. Normal inhibitory avoidance learning and anxiety, but increased locomotor activity in mice devoid of PrP(C). Brain Res Mol Brain Res. 71**,** 349-53.

Santuccione, A., et al., 2005. Prion protein recruits its neuronal receptor NCAM to lipid rafts to activate p59fyn and to enhance neurite outgrowth. J Cell Biol. 169**,** 341-54.

Schmidt, R., et al., 2013. Neurogenesis in zebrafish – from embryo to adult. Neural Dev. 8**,** 3.

Schmitz, M., et al., 2014a. Loss of Prion Protein Leads to Age-Dependent Behavioral Abnormalities and Changes in Cytoskeletal Protein Expression. Mol Neurobiol. 50, 923-36.

Schmitz, M., et al., 2014b. Impact of the cellular prion protein on amyloid-beta and 3PO-tau processing. J Alzheimers Dis. 38**,** 551-65.

Steinbach, J. P., et al., 1998. Hypersensitivity to seizures in beta-amyloid precursor protein deficient mice. Cell Death Differ. 5**,** 858-66.

Striebel, J. F., et al., 2013. Prion protein and susceptibility to kainate-induced seizures: genetic pitfalls in the use of PrP knockout mice. Prion. 7**,** 280-5.

Stys, P. K., et al., 2012. Copper-dependent regulation of NMDA receptors by cellular prion protein: implications for neurodegenerative disorders. J Physiol. 590**,** 1357-68.

Swain, H. A., et al., 2004. Effects of dizocilpine (MK-801) on circling behavior, swimming activity, and place preference in zebrafish (Danio rerio). Neurotoxicol Teratol. 26**,** 725-9.

Thomas, E. D., et al., 2015. There and back again: development and regeneration of the zebrafish lateral line system. Wiley Interdiscip Rev Dev Biol. 4**,** 1-16.

Walz, R., et al., 1999. Increased sensitivity to seizures in mice lacking cellular prion protein. Epilepsia. 40**,** 1679-1682.

Wang, P., et al., 2005. Defective neuromuscular synapses in mice lacking amyloid precursor protein (APP) and APP-Like protein 2. J Neurosci. 25**,** 1219-25.

Wieser, H. G., et al., 2006. EEG in Creutzfeldt-Jakob disease. Clin Neurophysiol. 117**,** 935-51.

Zheng, H., et al., 1995. beta-Amyloid precursor protein-deficient mice show reactive gliosis and decreased locomotor activity. Cell. 81**,** 525-31.

Cumulative Bibliography

Prevalence and Monetary Costs of Dementia in Canada: Population Health Expert Panel. In: L. W. Chambers, et al., (Eds.). Alzheimer Society of Canada Toronto, Ontario, 2016, pp. 1-71.

Abramsson, A., et al., 2013. The zebrafish amyloid precursor protein-b is required for motor neuron guidance and synapse formation. Dev Biol. 381, 377-88.

Aggleton, J. P., et al., 2010. Lesions of the rat perirhinal cortex spare the acquisition of a complex configural visual discrimination yet impair object recognition. Behav Neurosci. 124, 55-68.

Aguzzi, A., et al., 2007. Insights into prion strains and neurotoxicity. Nat Rev Mol Cell Biol. 8, 552-61.

Aguzzi, A., Rajendran, L., 2009. The transcellular spread of cytosolic amyloids, prions, and prionoids. Neuron. 64, 783-90.

Ahmed, T. S., et al., 2012. Effects of animated images of sympatric predators and abstract shapes on fear responses in zebrafish. Behaviour. 149, 1125-1153.

Ahmed, Z., et al., 2014. A novel in vivo model of tau propagation with rapid and progressive neurofibrillary tangle pathology: the pattern of spread is determined by connectivity, not proximity. Acta Neuropathol. 127, 667-83.

Akkerman, S., et al., 2012. Object recognition testing: statistical considerations. Behav Brain Res. 232, 317-22.

Alonso, A. C., et al., 1994. Role of abnormally phosphorylated tau in the breakdown of microtubules in Alzheimer disease. Proc Natl Acad Sci U S A. 91, 5562-6.

Altmeppen, H. C., et al., 2012. Proteolytic processing of the prion protein in health and disease. Am J Neurodegener Dis. 1, 15-31.

Aman, A., Piotrowski, T., 2008. Wnt/beta-catenin and Fgf signaling control collective cell migration by restricting chemokine receptor expression. Dev Cell. 15**,** 749-61.

Ambrose, C. M., et al., 1994. Structure and expression of the Huntington's disease gene: evidence against simple inactivation due to an expanded CAG repeat. Somat Cell Mol Genet. 20**,** 27-38.

Arai, S., et al., 2009. Brainstem auditory evoked potentials in experimentally-induced bovine spongiform encephalopathy. Res Vet Sci. 87**,** 111-4.

Arendash, G. W., et al., 2004. Multi-metric behavioral comparison of APPsw and P301L models for Alzheimer's disease: linkage of poorer cognitive performance to tau pathology in forebrain. Brain Res. 1012**,** 29-41.

Asante, E. A., et al., 2015. A naturally occurring variant of the human prion protein completely prevents prion disease. Nature. 522**,** 478-81.

Auer, T. O., et al., 2014. Highly efficient CRISPR/Cas9-mediated knock-in in zebrafish by homology-independent DNA repair. Genome Res. 24**,** 142-53.

Aula, P., et al., 1973. Partial trisomy 21. Clin Genet. 4**,** 241-51.

Ayers, J. I., et al., 2014. Experimental transmissibility of mutant SOD1 motor neuron disease. Acta Neuropathol. 128**,** 791-803.

Bai, Y., et al., 2008. The in Vivo brain interactome of the amyloid precursor protein. Mol Cell Proteomics. 7**,** 15-34.

Baier, M., et al., 2008. Prion infection of mice transgenic for human APPSwe: increased accumulation of cortical formic acid extractable Abeta(1-42) and rapid scrapie disease development. Int J Dev Neurosci. 26**,** 821-4.

Banote, R. K., et al., 2016. beta-Amyloid precursor protein-b is essential for Mauthner cell development in the zebrafish in a Notch-dependent manner. Dev Biol. 413**,** 26-38.

Baraban, S., et al., 2007. A large-scale mutagenesis screen to identify seizure-resistant zebrafish. Epilepsia. 48, 1151-1157.

Baraban, S. C., et al., 2005. Pentylenetetrazole induced changes in zebrafish behavior, neural activity and c-FoS expression. Neuroscience. 131, 759-768.

Baumann, F., et al., 2007. Lethal recessive myelin toxicity of prion protein lacking its central domain. EMBO J. 26, 538-47.

Baxendale, S., et al., 2012. Identification of compounds with anti-convulsant properties in a zebrafish model of epileptic seizures. Dis Model Mech. 5, 773-84.

Bayer, T. A., et al., 1999. It all sticks together--the APP-related family of proteins and Alzheimer's disease. Mol Psychiatry. 4, 524-8.

Bedell, V. M., et al., 2011. Lessons from morpholino-based screening in zebrafish. Brief Funct Genomics. 10, 181-8.

Beland, M., et al., 2014. Abeta induces its own prion protein N-terminal fragment (PrPN1)-mediated neutralization in amorphous aggregates. Neurobiol Aging. 35, 1537-48.

Beland, M., et al., 2012. PrP(C) homodimerization stimulates the production of PrPC cleaved fragments PrPN1 and PrPC1. J Neurosci. 32, 13255-63.

Benarroch, E. E., 2013. Adult neurogenesis in the dentate gyrus: general concepts and potential implications. Neurology. 81, 1443-52.

Bencan, Z., et al., 2009. Buspirone, chlordiazepoxide and diazepam effects in a zebrafish model of anxiety. Pharmacol Biochem Behav. 94, 75-80.

Benestad, S. L., et al., 2012. Healthy goats naturally devoid of prion protein. Vet Res. 43, 87.

Benestad, S. L., et al., 2016. First case of chronic wasting disease in Europe in a Norwegian free-ranging reindeer. Vet Res. 47, 88.

Beraldo, F. H., et al., 2011. Metabotropic glutamate receptors transduce signals for neurite outgrowth after binding of the prion protein to laminin gamma1 chain. FASEB J. 25**,** 265-79.

Beraldo, F. H., et al., 2010. Role of alpha7 nicotinic acetylcholine receptor in calcium signaling induced by prion protein interaction with stress-inducible protein 1. J Biol Chem. 285**,** 36542-50.

Beraldo, F. H., et al., 2013. Stress-inducible phosphoprotein 1 has unique cochaperone activity during development and regulates cellular response to ischemia via the prion protein. FASEB J. 27**,** 3594-607.

Bhinder, G., Tierney, K. B., 2012. Olfactory-Evoked Activity Assay for Larval Zebrafish. Zebrafish Protocols for Neurobehavioral Research. 66**,** 71-84.

Bidhendi, E. E., et al., 2016. Two superoxide dismutase prion strains transmit amyotrophic lateral sclerosis-like disease. J Clin Invest.126, 2249-53.

Birch, A. M., 2014. The contribution of astrocytes to Alzheimer's disease. Biochem Soc Trans. 42**,** 1316-20.

Black, S. A., et al., 2014. Cellular prion protein and NMDA receptor modulation: protecting against excitotoxicity. Front Cell Dev Biol. 2**,** 45.

Black, S. E., et al., 2010. Canadian Alzheimer's disease caregiver survey: baby-boomer caregivers and burden of care. Int J Geriatr Psychiatry. 25**,** 807-13.

Boch, J., et al., 2009. Breaking the code of DNA binding specificity of TAL-type III effectors. Science. 326**,** 1509-12.

Bodrikov, V., et al., 2011. Prion protein promotes growth cone development through reggie/flotillin-dependent N-cadherin trafficking. J Neurosci. 31**,** 18013-25.

Bogdanove, A. J., Voytas, D. F., 2011. TAL effectors: customizable proteins for DNA targeting. Science. 333**,** 1843-6.

Bolkan, B. J., Kretzschmar, D., 2014. Loss of Tau results in defects in photoreceptor development and progressive neuronal degeneration in Drosophila. Dev Neurobiol. 74, 1210-25.

Bolton, D. C., et al., 1982. Identification of a protein that purifies with the scrapie prion. Science. 218, 1309-11.

Bonaccorsi di Patti, M. C., et al., 2002. Analysis of Cu,ZnSOD conformational stability by differential scanning calorimetry. Methods Enzymol. 349, 49-61.

Borchelt, D. R., et al., 1994. Superoxide dismutase 1 with mutations linked to familial amyotrophic lateral sclerosis possesses significant activity. Proc Natl Acad Sci U S A. 91, 8292-6.

Bourdet, I., et al., 2015. The full-length form of the Drosophila amyloid precursor protein is involved in memory formation. J Neurosci. 35, 1043-51.

Braida, D., et al., 2014. Role of neuronal nicotinic acetylcholine receptors (nAChRs) on learning and memory in zebrafish. Psychopharmacology (Berl). 231, 1975-85.

Brandner, S., et al., 1996. Normal host prion protein necessary for scrapie-induced neurotoxicity. Nature. 379, 339-43.

Bremer, J., et al., 2010. Axonal prion protein is required for peripheral myelin maintenance. Nat Neurosci. 13, 310-8.

Broom, H. R., et al., 2015. Destabilization of the dimer interface is a common consequence of diverse ALS-associated mutations in metal free SOD1. Protein Sci. 24, 2081-2089.

Bruce, M., et al., 1994. Transmission of bovine spongiform encephalopathy and scrapie to mice: strain variation and the species barrier. Philos Trans R Soc Lond B Biol Sci. 343, 405-11.

Bruijn, L. I., et al., 1998. Aggregation and motor neuron toxicity of an ALS-linked SOD1 mutant independent from wild-type SOD1. Science. 281**,** 1851-4.

Brundin, P., et al., 2010. Prion-like transmission of protein aggregates in neurodegenerative diseases. Nat Rev Mol Cell Biol. 11**,** 301-7.

Budka, H., et al., 1995. Neuropathological diagnostic criteria for Creutzfeldt-Jakob disease (CJD) and other human spongiform encephalopathies (prion diseases). Brain Pathol. 5**,** 459-66.

Bueler, H., et al., 1992. Normal development and behaviour of mice lacking the neuronal cell-surface PrP protein. Nature. 356**,** 577-582.

Bueler, H., et al., 1994. High prion and PrPSc levels but delayed onset of disease in scrapie-inoculated mice heterozygous for a disrupted PrP gene. Mol Med. 1**,** 19-30.

Burns, C. S., et al., 2002. Molecular features of the copper binding sites in the octarepeat domain of the prion protein. Biochemistry. 41**,** 3991-4001.

Bustin, S. A., et al., 2009. The MIQE guidelines: minimum information for publication of quantitative real-time PCR experiments. Clin Chem. 55**,** 611-22.

Caetano, F. A., et al., 2011. Amyloid-beta oligomers increase the localization of prion protein at the cell surface. J Neurochem. 117**,** 538-53.

Caine, D., et al., 2015. The cognitive profile of prion disease: a prospective clinical and imaging study. Ann Clin Transl Neurol. 2**,** 548-58.

Calzolai, L., et al., 2005. Prion protein NMR structures of chickens, turtles, and frogs. Proc Natl Acad Sci U S A. 102**,** 651-5.

Campeau, J. L., et al., 2013. Early increase and late decrease of purkinje cell dendritic spine density in prion-infected organotypic mouse cerebellar cultures. PLoS One. 8**,** e81776.

Cao, X., Sudhof, T. C., 2001. A transcriptionally [correction of transcriptively] active complex of APP with Fe65 and histone acetyltransferase Tip60. Science. 293**,** 115-20.

Carulla, P., et al., 2011. Neuroprotective role of PrPC against kainate-induced epileptic seizures and cell death depends on the modulation of JNK3 activation by GluR6/7-PSD-95 binding. Mol Biol Cell. 22**,** 3041-54.

Carulla, P., et al., 2015. Involvement of PrP(C) in kainate-induced excitotoxicity in several mouse strains. Sci Rep. 5**,** 11971.

Cattaneo, E., et al., 2005. Normal huntingtin function: an alternative approach to Huntington's disease. Nat Rev Neurosci. 6**,** 919-30.

Champagne, D. L., et al., 2010. Translating rodent behavioral repertoire to zebrafish (Danio rerio): relevance for stress research. Behav Brain Res. 214**,** 332-42.

Chang, N., et al., 2013. Genome editing with RNA-guided Cas9 nuclease in zebrafish embryos. Cell Res. 23**,** 465-72.

Chasseigneaux, S., Allinquant, B., 2012. Functions of Abeta, sAPPalpha and sAPPbeta : similarities and differences. J Neurochem. 120 Suppl 1**,** 99-108.

Chattopadhyay, M., et al., 2008. Initiation and elongation in fibrillation of ALS-linked superoxide dismutase. Proc Natl Acad Sci U S A. 105**,** 18663-8.

Chen, G., et al., 2000. A learning deficit related to age and beta-amyloid plaques in a mouse model of Alzheimer's disease. Nature. 408**,** 975-9.

Chen, S., et al., 2003. Prion protein as trans-interacting partner for neurons is involved in neurite outgrowth and neuronal survival. Mol Cell Neurosci. 22**,** 227-33.

Chen, S., et al., 2013. A large-scale in vivo analysis reveals that TALENs are significantly more mutagenic than ZFNs generated using context-dependent assembly. Nucleic Acids Res. 41**,** 2769-78.

Chesebro, B., et al., 2010. Fatal transmissible amyloid encephalopathy: a new type of prion disease associated with lack of prion protein membrane anchoring. PLoS Pathog. 6, e1000800.

Chesebro, B., et al., 2005. Anchorless prion protein results in infectious amyloid disease without clinical scrapie. Science. 308, 1435-1439.

Chia, R., et al., 2010. Superoxide dismutase 1 and tgSOD1 mouse spinal cord seed fibrils, suggesting a propagative cell death mechanism in amyotrophic lateral sclerosis. PLoS One. 5, e10627.

Chiarini, L. B., et al., 2002. Cellular prion protein transduces neuroprotective signals. EMBO J. 21, 3317-26.

Chishti, M. A., et al., 2001. Early-onset amyloid deposition and cognitive deficits in transgenic mice expressing a double mutant form of amyloid precursor protein 695. J Biol Chem. 276, 21562-21570.

Chung, E., et al., 2010. Anti-PrPC monoclonal antibody infusion as a novel treatment for cognitive deficits in an Alzheimer's disease model mouse. BMC Neurosci. 11, 130.

Citron, M., et al., 1992. Mutation of the beta-amyloid precursor protein in familial Alzheimer's disease increases beta-protein production. Nature. 360, 672-674.

Clavaguera, F., et al., 2013. Brain homogenates from human tauopathies induce tau inclusions in mouse brain. Proc Natl Acad Sci U S A. 110, 9535-40.

Clavaguera, F., et al., 2009. Transmission and spreading of tauopathy in transgenic mouse brain. Nat Cell Biol. 11, 909-13.

Cohen, F. E., et al., 1994. Structural clues to prion replication. Science. 264, 530-1.

Coitinho, A. S., et al., 2006. The interaction between prion protein and laminin modulates memory consolidation. Eur J Neurosci. 24, 3255-64.

Coitinho, A. S., et al., 2007. Short-term memory formation and long-term memory consolidation are enhanced by cellular prion association to stress-inducible protein 1. Neurobiol Dis. 26**,** 282-90.

Coitinho, A. S., et al., 2003. Cellular prion protein ablation impairs behavior as a function of age. Neuroreport. 14**,** 1375-9.

Collins, S. J., et al., 2004. Transmissible spongiform encephalopathies. Lancet. 363**,** 51-61.

Come, J. H., et al., 1993. A kinetic model for amyloid formation in the prion diseases: importance of seeding. Proc Natl Acad Sci U S A. 90**,** 5959-63.

Conforti, P., et al., 2013. Lack of huntingtin promotes neural stem cells differentiation into glial cells while neurons expressing huntingtin with expanded polyglutamine tracts undergo cell death. Neurobiol Dis. 50**,** 160-70.

Costanzo, M., et al., 2013. Transfer of polyglutamine aggregates in neuronal cells occurs in tunneling nanotubes. J Cell Sci. 126**,** 3678-85.

Costanzo, M., Zurzolo, C., 2013. The cell biology of prion-like spread of protein aggregates: mechanisms and implication in neurodegeneration. Biochem J. 452**,** 1-17.

Cotto, E., et al., 2005. Molecular characterization, phylogenetic relationships, and developmental expression patterns of prion genes in zebrafish (Danio rerio). FEBS Journal. 272**,** 500.

Criado, J. R., et al., 2005. Mice devoid of prion protein have cognitive deficits that are rescued by reconstitution of PrP in neurons. Neurobiol Dis. 19**,** 255-65.

Culbertson, M. R., 1999. RNA surveillance. Unforeseen consequences for gene expression, inherited genetic disorders and cancer. Trends Genet. 15**,** 74-80.

Dambly-Chaudiere, C., et al., 2007. Control of cell migration in the development of the posterior lateral line: antagonistic interactions between the chemokine receptors CXCR4 and CXCR7/RDC1. BMC Dev Biol. 7, 23.

Daude, N., et al., 2012. Knockout of the prion protein (PrP)-like Sprn gene does not produce embryonic lethality in combination with PrP(C)-deficiency. Proc Natl Acad Sci U S A. 109, 9035-40.

Dawson, G. R., et al., 1999. Age-related cognitive deficits, impaired long-term potentiation and reduction in synaptic marker density in mice lacking the beta-amyloid precursor protein. Neuroscience. 90, 1-13.

Dawson, H. N., et al., 2001. Inhibition of neuronal maturation in primary hippocampal neurons from tau deficient mice. J Cell Sci. 114, 1179-87.

deCarvalho, T. N., et al., 2013. Aversive cues fail to activate fos expression in the asymmetric olfactory-habenula pathway of zebrafish. Front Neural Circuits. 7, 98.

Diack, A. B., et al., 2014. Variant CJD. 18 years of research and surveillance. Prion. 8, 286-95.

Dijkgraaf, S., 1963. The functioning and significance of the lateral‐line organs. Biol Rev Philos Soc. 38, 51-105.

Distel, M., et al., 2009. Optimized Gal4 genetics for permanent gene expression mapping in zebrafish. Proc Natl Acad Sci U S A. 106, 13365-70.

Dodart, J. C., et al., 1997. Scopolamine-induced deficits in a two-trial object recognition task in mice. Neuroreport. 8, 1173-8.

Doyon, Y., et al., 2008. Heritable targeted gene disruption in zebrafish using designed zinc-finger nucleases. Nat Biotechnol. 26, 702-8.

Dragatsis, I., et al., 2000. Inactivation of Hdh in the brain and testis results in progressive neurodegeneration and sterility in mice. Nat Genet. 26, 300-6.

DuVal, M. G., et al., 2014. Growth differentiation factor 6 as a putative risk factor in neuromuscular degeneration. PLoS One. 9, e89183.

Egan, R. J., et al., 2009. Understanding behavioral and physiological phenotypes of stress and anxiety in zebrafish. Behav Brain Res. 205, 38-44.

Eisen, J. S., Smith, J. C., 2008. Controlling morpholino experiments: don't stop making antisense. Development. 135, 1735-43.

Ennaceur, A., Delacour, J., 1988. A new one-trial test for neurobiological studies of memory in rats. 1: Behavioral data. Behav Brain Res. 31, 47-59.

Felker, A., Mosimann, C., 2016. Contemporary zebrafish transgenesis with Tol2 and application for Cre/lox recombination experiments. Methods Cell Biol. 135, 219-44.

Fiorino, A. S., 1996. Sleep, genes and death: fatal familial insomnia. Brain Res Brain Res Rev. 22, 258-64.

Fischer, L. R., et al., 2011. SOD1 targeted to the mitochondrial intermembrane space prevents motor neuropathy in the Sod1 knockout mouse. Brain. 134, 196-209.

Fischer, L. R., et al., 2012. Absence of SOD1 leads to oxidative stress in peripheral nerve and causes a progressive distal motor axonopathy. Exp Neurol. 233, 163-71.

Flechsig, E., et al., 2003. Expression of truncated PrP targeted to Purkinje cells of PrP knockout mice causes Purkinje cell death and ataxia. EMBO J. 22, 3095-101.

Fleisch, V., et al., 2013. Targeted mutation of the gene encoding prion protein in zebrafish reveals a conserved role in neuron excitability. Neurobiol Dis. 55, 11-25.

Fluharty, B. R., et al., 2013. An N-terminal fragment of the prion protein binds to amyloid-beta oligomers and inhibits their neurotoxicity in vivo. J Biol Chem. 288, 7857-66.

Fonseca, M. B., et al., 2013. Amyloid beta peptides promote autophagy-dependent differentiation of mouse neural stem cells: Abeta-mediated neural differentiation. Mol Neurobiol. 48**,** 829-40.

Fosque, B. F., et al., 2015. Neural circuits. Labeling of active neural circuits in vivo with designed calcium integrators. Science. 347**,** 755-60.

Fraser, B., et al., 2013. Regeneration of cone photoreceptors when cell ablation is primarily restricted to a particular cone subtype. PLoS One. 8**,** e55410.

Fraser, H., et al., 1992a. Transmission of bovine spongiform encephalopathy and scrapie to mice. J Gen Virol. 73**,** 1891-7.

Fraser, P. E., et al., 1992b. Fibril formation by primate, rodent, and Dutch-hemorrhagic analogues of Alzheimer amyloid beta-protein. Biochemistry. 31**,** 10716-23.

Frost, B., Diamond, M. I., 2010. Prion-like mechanisms in neurodegenerative diseases. Nat Rev Neurosci. 11**,** 155-9.

Fujio, K., et al., 2007. 14-3-3 proteins and protein phosphatases are not reduced in tau-deficient mice. Neuroreport. 18**,** 1049-52.

Gamblin, T. C., et al., 2003. Modeling tau polymerization in vitro: a review and synthesis. Biochemistry. 42**,** 15009-17.

Games, D., et al., 1995. Alzheimer-type neuropathology in transgenic mice overexpressing V717F beta-amyloid precursor protein. Nature. 373**,** 523-7.

Gasperini, L., et al., 2015. Prion protein and copper cooperatively protect neurons by modulating NMDA receptor through S-nitrosylation. Antioxid Redox Signal. 22**,** 772-84.

Gauthier, L. R., et al., 2004. Huntingtin controls neurotrophic support and survival of neurons by enhancing BDNF vesicular transport along microtubules. Cell. 118**,** 127-38.

Geoghegan, J. C., et al., 2009. Trans-dominant inhibition of prion propagation in vitro is not mediated by an accessory cofactor. PLoS Pathog. 5**,** e1000535.

Gerhard, G. S., et al., 2002. Life spans and senescent phenotypes in two strains of Zebrafish (Danio rerio). Exp Gerontol. 37**,** 1055-68.

Ghysen, A., Dambly-Chaudiere, C., 2007. The lateral line microcosmos. Genes Dev. 21**,** 2118-30.

Gilbert, M. J., et al., 2014. Zebrafish (Danio rerio) as a model for the study of aging and exercise: physical ability and trainability decrease with age. Exp Gerontol. 50**,** 106-13.

Glenner, G. G., 2012. Reprint of "Alzheimer's disease: Initial report of the purification and characterization of a novel cerebrovascular amyloid protein". Biochem Biophys Res Commun. 425**,** 534-539.

Go, W., et al., 2010. atp2b1a regulates Ca(2+) export during differentiation and regeneration of mechanosensory hair cells in zebrafish. Cell Calcium. 48**,** 302-13.

Goate, A., et al., 1991. Segregation of a missense mutation in the amyloid precursor protein gene with familial Alzheimer's disease. Nature. 349**,** 704-706.

Goedert, M., et al., 2014. Prion-like mechanisms in the pathogenesis of tauopathies and synucleinopathies. Curr Neurol Neurosci Rep. 14**,** 495.

Goedert, M., et al., 1988. Cloning and sequencing of the cDNA encoding a core protein of the paired helical filament of Alzheimer disease: identification as the microtubule-associated protein tau. Proc Natl Acad Sci U S A. 85**,** 4051-5.

Golanska, E., et al., 2009. Earlier onset of Alzheimer's disease: risk polymorphisms within PRNP, PRND, CYP46, and APOE genes. J Alzheimers Dis. 17**,** 359-68.

Goldgaber, D., et al., 1987. Characterization and chromosomal localization of a cDNA encoding brain amyloid of Alzheimer's disease. Science. 235**,** 877-80.

Gompel, N., et al., 2001. Pattern formation in the lateral line of zebrafish. Mech Dev. 105, 69-77.

Grad, L. I., Cashman, N. R., 2014. Prion-like activity of Cu/Zn superoxide dismutase: implications for amyotrophic lateral sclerosis. Prion. 8, 33-41.

Grad, L. I., et al., 2015. From molecule to molecule and cell to cell: Prion-like mechanisms in amyotrophic lateral sclerosis. Neurobiol Dis. 77,257-65.

Grad, L. I., et al., 2011. Intermolecular transmission of superoxide dismutase 1 misfolding in living cells. Proc Natl Acad Sci U S A. 108, 16398-403.

Grad, L. I., et al., 2014a. Exosome-dependent and independent mechanisms are involved in prion-like transmission of propagated Cu/Zn superoxide dismutase misfolding. Prion. 8, 331-5.

Grad, L. I., et al., 2014b. Intercellular propagated misfolding of wild-type Cu/Zn superoxide dismutase occurs via exosome-dependent and -independent mechanisms. Proc Natl Acad Sci U S A. 111, 3620-5.

Graffmo, K. S., et al., 2013. Expression of wild-type human superoxide dismutase-1 in mice causes amyotrophic lateral sclerosis. Hum Mol Genet. 22, 51-60.

Graner, E., et al., 2000. Cellular prion protein binds laminin and mediates neuritogenesis. Brain Res Mol Brain Res. 76, 85.

Greer, P. L., Greenberg, M. E., 2008. From synapse to nucleus: calcium-dependent gene transcription in the control of synapse development and function. Neuron. 59, 846-60.

Gu, X., et al., 2015. N17 Modifies mutant Huntingtin nuclear pathogenesis and severity of disease in HD BAC transgenic mice. Neuron. 85, 726-41.

Guillot-Sestier, M. V., et al., 2009. The alpha-secretase-derived N-terminal product of cellular prion, N1, displays neuroprotective function in vitro and in vivo. J Biol Chem. 284, 35973-86.

Guillot-Sestier, M. V., et al., 2012. alpha-Secretase-derived fragment of cellular prion, N1, protects against monomeric and oligomeric amyloid beta (Abeta)-associated cell death. J Biol Chem. 287, 5021-32.

Gurney, M. E., et al., 1994. Motor neuron degeneration in mice that express a human Cu,Zn superoxide dismutase mutation. Science. 264, 1772-5.

Haas, P., Gilmour, D., 2006. Chemokine signaling mediates self-organizing tissue migration in the zebrafish lateral line. Dev Cell. 10, 673-80.

Hall, G. F., Patuto, B. A., 2012. Is tau ready for admission to the prion club? Prion. 6, 223-33.

Halliez, S., et al., 2015. Prion protein localizes at the ciliary base during neural and cardiovascular development, and its depletion affects alpha-tubulin post-translational modifications. Sci Rep. 5, 17146.

Hammond, R. S., et al., 2004. On the delay-dependent involvement of the hippocampus in object recognition memory. Neurobiol Learn Mem. 82, 26-34.

Hannesson, D. K., et al., 2004. Interaction between perirhinal and medial prefrontal cortex is required for temporal order but not recognition memory for objects in rats. J Neurosci. 24, 4596-604.

Hans, S., et al., 2009. Temporally-controlled site-specific recombination in zebrafish. PLoS One. 4, e4640.

Harada, A., et al., 1994. Altered microtubule organization in small-calibre axons of mice lacking tau protein. Nature. 369, 488-91.

Haraguchi, T., et al., 1989. Asparagine-linked glycosylation of the scrapie and cellular prion proteins. Arch Biochem Biophys. 274**,** 1-13.

Hardy, J., 2006. A hundred years of Alzheimer's disease research. Neuron. 52**,** 3-13.

Hardy, J., Allsop, D., 1991. Amyloid Deposition as the Central Event in the Etiology of Alzheimers-Disease. Trends Pharmacol Sci. 12**,** 383-8.

Hava, D., et al., 2009. Apical membrane maturation and cellular rosette formation during morphogenesis of the zebrafish lateral line. J Cell Sci. 122**,** 687-95.

Hay, B., et al., 1987a. Biogenesis and transmembrane orientation of the cellular isoform of the scrapie prion protein [published errratum appears in Mol Cell Biol 1987 May;7(5):2035]. Mol Cell Biol. 7**,** 914-20.

Hay, B., et al., 1987b. Evidence for a secretory form of the cellular prion protein. Biochemistry. 26**,** 8110-5.

Head, J. R., et al., 2013. Activation of canonical Wnt/beta-catenin signaling stimulates proliferation in neuromasts in the zebrafish posterior lateral line. Dev Dyn. 242**,** 832-46.

Heber, S., et al., 2000. Mice with combined gene knock-outs reveal essential and partially redundant functions of amyloid precursor protein family members. J Neurosci. 20**,** 7951-7963.

Herculano-Houzel, S., Lent, R., 2005. Isotropic fractionator: a simple, rapid method for the quantification of total cell and neuron numbers in the brain. J Neurosci. 25**,** 2518-21.

Herms, J., et al., 2004. Cortical dysplasia resembling human type 2 lissencephaly in mice lacking all three APP family members. EMBO J. 23**,** 4106-15.

Hernandez-Rapp, J., et al., 2014. A PrP(C)-caveolin-Lyn complex negatively controls neuronal GSK3beta and serotonin 1B receptor. Sci Rep. 4**,** 4881.

Herrmann, U. S., et al., 2015. Prion infections and anti-PrP antibodies trigger converging neurotoxic pathways. PLoS Pathog. 11**,** e1004662.

Hesse, L., et al., 1994. The beta A4 amyloid precursor protein binding to copper. FEBS Lett. 349**,** 109-16.

Hewitt, P. E., et al., 2006. Creutzfeldt-Jakob disease and blood transfusion: results of the UK Transfusion Medicine Epidemiological Review study. Vox Sang. 91**,** 221-30.

Hiolski, E. M., et al., 2014. Chronic low-level domoic acid exposure alters gene transcription and impairs mitochondrial function in the CNS. Aquat Toxicol. 155**,** 151-9.

Hornshaw, M. P., et al., 1995. Copper binding to the N-terminal tandem repeat regions of mammalian and avian prion protein. Biochem Biophys Res Commun. 207**,** 621-629.

Horwich, A. L., Weissman, J. S., 1997. Deadly conformations--protein misfolding in prion disease. Cell. 89**,** 499-510.

Huang, P., et al., 2011. Heritable gene targeting in zebrafish using customized TALENs. Nat Biotechnol. 29**,** 699-700.

Huang, P., et al., 2012. Reverse genetic approaches in zebrafish. J Genet Genomics. 39**,** 421-33.

Huang, Y., Mucke, L., 2012. Alzheimer mechanisms and therapeutic strategies. Cell. 148**,** 1204-22.

Huc-Brandt, S., et al., 2014. Zebrafish prion protein PrP2 controls collective migration process during lateral line sensory system development. PLoS One. 9**,** e113331.

Hurt, J. A., et al., 2003. Highly specific zinc finger proteins obtained by directed domain shuffling and cell-based selection. Proc Natl Acad Sci U S A. 100**,** 12271-6.

Hwang, W. Y., et al., 2013. Efficient genome editing in zebrafish using a CRISPR-Cas system. Nat Biotechnol. 31**,** 227-9.

Iba, M., et al., 2013. Synthetic tau fibrils mediate transmission of neurofibrillary tangles in a transgenic mouse model of Alzheimer's-like tauopathy. J Neurosci. 33**,** 1024-37.

Iba, M., et al., 2015. Tau pathology spread in PS19 tau transgenic mice following locus coeruleus (LC) injections of synthetic tau fibrils is determined by the LC's afferent and efferent connections. Acta Neuropathol. 130**,** 349-62.

Ikegami, S., et al., 2000. Muscle weakness, hyperactivity, and impairment in fear conditioning in tau-deficient mice. Neurosci Lett. 279**,** 129-32.

Irizarry, M. C., et al., 1997. Abeta deposition is associated with neuropil changes, but not with overt neuronal loss in the human amyloid precursor protein V717F (PDAPP) transgenic mouse. J Neurosci. 17**,** 7053-9.

Jacobsen, J. C., et al., 2011. HD CAG-correlated gene expression changes support a simple dominant gain of function. Hum Mol Genet. 20**,** 2846-60.

Jacques, B. E., et al., 2014. The role of Wnt/beta-catenin signaling in proliferation and regeneration of the developing basilar papilla and lateral line. Dev Neurobiol. 74**,** 438-56.

Jeong, J. K., Park, S. Y., 2015. Neuroprotective effect of cellular prion protein (PrPC) is related with activation of alpha7 nicotinic acetylcholine receptor (alpha7nAchR)-mediated autophagy flux. Oncotarget. 6**,** 24660-74.

Jin, L. W., et al., 1994. Peptides containing the RERMS sequence of amyloid beta/A4 protein precursor bind cell surface and promote neurite extension. J Neurosci. 14**,** 5461-70.

Jonsson, P. A., et al., 2004. Minute quantities of misfolded mutant superoxide dismutase-1 cause amyotrophic lateral sclerosis. Brain. 127**,** 73-88.

Joshi, P., et al., 2009. Amyloid precursor protein is required for convergent-extension movements during Zebrafish development. Dev Biol. 335, 1-11.

Joyce, P. I., et al., 2011. SOD1 and TDP-43 animal models of amyotrophic lateral sclerosis: recent advances in understanding disease toward the development of clinical treatments. Mamm Genome. 22, 420-48.

Joyce, P. I., et al., 2015. A novel SOD1-ALS mutation separates central and peripheral effects of mutant SOD1 toxicity. Hum Mol Genet. 24, 1883-97.

Kaden, D., et al., 2008. Homophilic interactions of the amyloid precursor protein (APP) ectodomain are regulated by the loop region and affect beta-secretase cleavage of APP. J Biol Chem. 283, 7271-7279.

Kaiser, D., et al., 2012. Amyloid beta precursor protein and prion protein have a conserved interaction affecting cell adhesion and CNS development. PloS One. 7.

Kane, M. D., et al., 2000. Evidence for seeding of beta -amyloid by intracerebral infusion of Alzheimer brain extracts in beta -amyloid precursor protein-transgenic mice. J Neurosci. 20, 3606-11.

Kang, J., et al., 1987. The precursor of Alzheimer's disease amyloid A4 protein resembles a cell-surface receptor. Nature. 325, 733-6.

Karran, E., De Strooper, B., 2016. The amyloid cascade hypothesis: are we poised for success or failure? J Neurochem. 139, 237-252.

Kawakami, K., et al., 2004. A transposon-mediated gene trap approach identifies developmentally regulated genes in zebrafish. Dev Cell. 7, 133-44.

Kawas, C., et al., 2000. Age-specific incidence rates of Alzheimer's disease: the Baltimore Longitudinal Study of Aging. Neurology. 54, 2072-7.

Kedikian, X., et al., 2013. Behavioral and molecular analysis of nicotine-conditioned place preference in zebrafish. PLoS One. 8, e69453.

Keshet, G. I., et al., 1999. Scrapie-infected mice and PrP knockout mice share abnormal localization and activity of neuronal nitric oxide synthase. J Neurochem. 72**,** 1224-31.

Khare, S. D., et al., 2006. FALS mutations in Cu, Zn superoxide dismutase destabilize the dimer and increase dimer dissociation propensity: a large-scale thermodynamic analysis. Amyloid. 13**,** 226-35.

Khosravani, H., et al., 2008. Prion protein attenuates excitotoxicity by inhibiting NMDA receptors. J Cell Biol. 181**,** 551-565.

Kim, H. S., et al., 2003. C-terminal fragments of amyloid precursor protein exert neurotoxicity by inducing glycogen synthase kinase-3beta expression. FASEB J. 17**,** 1951-3.

Kim, J. W., et al., 2016. Recruitment of Rod Photoreceptors from Short-Wavelength-Sensitive Cones during the Evolution of Nocturnal Vision in Mammals. Dev Cell. 37**,** 520-32.

Kim, Y. G., et al., 1996. Hybrid restriction enzymes: zinc finger fusions to Fok I cleavage domain. Proc Natl Acad Sci U S A. 93**,** 1156-60.

Kimberly, W. T., et al., 2005. Physiological regulation of the beta-amyloid precursor protein signaling domain by c-Jun N-terminal kinase JNK3 during neuronal differentiation. J Neurosci. 25**,** 5533-43.

Kinoshita, A., et al., 2002. The gamma secretase-generated carboxyl-terminal domain of the amyloid precursor protein induces apoptosis via Tip60 in H4 cells. J Biol Chem. 277**,** 28530-6.

Kishi, S., et al., 2003. The zebrafish as a vertebrate model of functional aging and very gradual senescence. Exp Gerontol. 38**,** 777-86.

Kok, F. O., et al., 2015. Reverse genetic screening reveals poor correlation between morpholino-induced and mutant phenotypes in zebrafish. Dev Cell. 32**,** 97-108.

Komiya, Y., Habas, R., 2008. Wnt signal transduction pathways. Organogenesis. 4, 68-75.

Kostylev, M. A., et al., 2015. Prion-Protein-interacting Amyloid-beta Oligomers of High Molecular Weight Are Tightly Correlated with Memory Impairment in Multiple Alzheimer Mouse Models. J Biol Chem. 290, 17415-38.

Kuffer, A., et al., 2016. The prion protein is an agonistic ligand of the G protein-coupled receptor Adgrg6. Nature. 536, 464-8.

Kurt, T. D., Sigurdson, C. J., 2016. Cross-species transmission of CWD prions. Prion. 10, 83-91.

Kuznetsova, A., et al., 2014. Potential role of soil properties in the spread of CWD in western Canada. Prion. 8, 92-99.

Kwan, K. M., et al., 2007. The Tol2kit: a multisite gateway-based construction kit for Tol2 transposon transgenesis constructs. Dev Dyn. 236, 3088.

Langheinrich, U., et al., 2002. Zebrafish as a model organism for the identification and characterization of drugs and genes affecting p53 signaling. Curr Biol. 12, 2023-8.

Lansbury, P. T., Jr., Caughey, B., 1995. The chemistry of scrapie infection: implications of the 'ice 9' metaphor. Chem Biol. 2, 1-5.

Lasagna-Reeves, C. A., et al., 2010. Preparation and characterization of neurotoxic tau oligomers. Biochemistry. 49, 10039-41.

Lasagna-Reeves, C. A., et al., 2012. Alzheimer brain-derived tau oligomers propagate pathology from endogenous tau. Sci Rep. 2, 700.

Lauren, J., 2014. Cellular prion protein as a therapeutic target in Alzheimer's disease. J Alzheimers Dis. 38, 227-44.

Lauren, J., et al., 2009. Cellular prion protein mediates impairment of synaptic plasticity by amyloid-beta oligomers. Nature. 457**,** 1128-U84.

Law, S. H., Sargent, T. D., 2014. The serine-threonine protein kinase PAK4 is dispensable in zebrafish: identification of a morpholino-generated pseudophenotype. PLoS One. 9**,** e100268.

Le Roy, D. G., Klein, K. K., 2003. Apocalypse Cow: The effect of BSE on Canada's beef industry. In Western Economics Forum (Vol. 2, No. 2, pp. 20-27). Western Agricultural Economics Association.

Leavitt, B. R., et al., 2001. Wild-type huntingtin reduces the cellular toxicity of mutant huntingtin in vivo. Am J Hum Genet. 68**,** 313-24.

Lecaudey, V., et al., 2008. Dynamic Fgf signaling couples morphogenesis and migration in the zebrafish lateral line primordium. Development. 135**,** 2695-705.

Lee, Y. H., et al., 2013. Strain characterization of the Korean CWD cases in 2001 and 2004. J Vet Med Sci. 75**,** 95-8.

Lei, P., et al., 2012. Tau deficiency induces parkinsonism with dementia by impairing APP-mediated iron export. Nat Med. 18**,** 291-5.

Lei, P., et al., 2014. Motor and cognitive deficits in aged tau knockout mice in two background strains. Mol Neurodegener. 9**,** 29.

Leighton, P. L., Allison, W. T., 2016. Protein Misfolding in Prion and Prion-Like Diseases: Reconsidering a Required Role for Protein Loss-of-Function. J Alzheimers Dis. 54**,** 3-29.

Leiss, W., Nicol, A. M., 2006. A Tale of Two Food Risks: BSE and Farmed Salmon in Canada. J Risk Res. 9**,** 891-910.

Leissring, M. A., et al., 2002. A physiologic signaling role for the gamma -secretase-derived intracellular fragment of APP. Proc Natl Acad Sci U S A. 99**,** 4697-702.

Levin, E. D., et al., 2006. Timing of nicotine effects on learning in zebrafish. Psychopharmacology (Berl). 184**,** 547-52.

Lewis, J., et al., 2001. Enhanced neurofibrillary degeneration in transgenic mice expressing mutant tau and APP. Science. 293**,** 1487-91.

Lewis, J., et al., 2000. Neurofibrillary tangles, amyotrophy and progressive motor disturbance in mice expressing mutant (P301L) tau protein. Nat Genet. 25**,** 402-5.

Li, A., et al., 2007. Neonatal lethality in transgenic mice expressing prion protein with a deletion of residues 105-125. EMBO J. 26**,** 548-58.

Li, A., et al., 2000. Identification of a novel gene encoding a PrP-like protein expressed as chimeric transcripts fused to PrP exon 1/2 in ataxic mouse line with a disrupted PrP gene. Cell Mol Neurobiol. 20**,** 553-67.

Liao, H. K., et al., 2012. Tol2 gene trap integrations in the zebrafish amyloid precursor protein genes appa and aplp2 reveal accumulation of secreted APP at the embryonic veins. Dev Dyn. 241**,** 415-425.

Lieschke, G. J., Currie, P. D., 2007. Animal models of human disease: zebrafish swim into view. Nat Rev Genet. 8**,** 353-67.

Lindberg, M. J., et al., 2002. Common denominator of Cu/Zn superoxide dismutase mutants associated with amyotrophic lateral sclerosis: decreased stability of the apo state. Proc Natl Acad Sci U S A. 99**,** 16607-12.

Luo, L., et al., 1992. Human amyloid precursor protein ameliorates behavioral deficit of flies deleted for Appl gene. Neuron. 9**,** 595-605.

Ma, E. Y., Raible, D. W., 2009. Signaling pathways regulating zebrafish lateral line development. Curr Biol. 19**,** R381-6.

Ma, Q. L., et al., 2014. Loss of MAP function leads to hippocampal synapse loss and deficits in the Morris Water Maze with aging. J Neurosci. 34**,** 7124-36.

Magara, F., et al., 1999. Genetic background changes the pattern of forebrain commissure defects in transgenic mice underexpressing the beta-amyloid-precursor protein. Proc Natl Acad Sci U S A. 96**,** 4656-61.

Makzhami, S., et al., 2014. The prion protein family: a view from the placenta. Front Cell Dev Biol. 2**,** 35.

Malaga-Trillo, E., et al., 2009. Regulation of Embryonic Cell Adhesion by the Prion Protein. Plos Biology. 7**,** 576.

Mali, P., et al., 2013. RNA-guided human genome engineering via Cas9. Science. 339**,** 823-6.

Mallm, J. P., et al., 2010. Generation of conditional null alleles for APP and APLP2. Genesis. 48**,** 200-6.

Mallucci, G., et al., 2003. Depleting neuronal PrP in prion infection prevents disease and reverses spongiosis. Science. 302**,** 871-4.

Manson, J. C., et al., 1994. 129/Ola mice carrying a null mutation in PrP that abolishes mRNA production are developmentally normal. Mol Neurobiol. 8**,** 121-7.

Marc, D., et al., 2007. Scavenger, transducer, RNA chaperone? What ligands of the prion protein teach us about its function. Cell Mol Life Sci. 64**,** 815-29.

Marciniuk, K., et al., 2013. Evidence for prion-like mechanisms in several neurodegenerative diseases: potential implications for immunotherapy. Clin Dev Immunol. 2013**,** 473706.

Marotta, C. A., et al., 1992. Molecular and cellular biology of Alzheimer amyloid. J Mol Neurosci. 3**,** 111-25.

Masters, C. L., et al., 1985a. Neuronal origin of a cerebral amyloid: neurofibrillary tangles of Alzheimer's disease contain the same protein as the amyloid of plaque cores and blood vessels. EMBO J. 4**,** 2757-63.

Masters, C. L., et al., 1985b. Amyloid plaque core protein in Alzheimer disease and Down syndrome. Proc Natl Acad Sci U S A. 82, 4245-9.

Matsuda, M., Chitnis, A. B., 2010. Atoh1a expression must be restricted by Notch signaling for effective morphogenesis of the posterior lateral line primordium in zebrafish. Development. 137, 3477-87.

Maurer, K., et al., 1997. Auguste D and Alzheimer's disease. Lancet. 349, 1546-9.

Maximino, C., et al., 2010. Measuring anxiety in zebrafish: a critical review. Behav Brain Res. 214, 157-71.

May, Z., et al., 2016. Object recognition memory in zebrafish. Behav Brain Res. 296, 199-210.

Mays, C. E., et al., 2014. Prion disease tempo determined by host-dependent substrate reduction. J Clin Invest. 124, 847-58.

McCord, J. M., Fridovich, I., 1969. Superoxide dismutase. An enzymic function for erythrocuprein (hemocuprein). J Biol Chem. 244, 6049-55.

McDonald, A. J., et al., 2014. A new paradigm for enzymatic control of alpha-cleavage and beta-cleavage of the prion protein. J Biol Chem. 289, 803-13.

McGown, A., et al., 2013. Early interneuron dysfunction in ALS: insights from a mutant sod1 zebrafish model. Ann Neurol. 73, 246-58.

McLachlan, S. M., Yestrau, M., 2008. From the ground up: holistic management and grassroots rural adaptation to bovine spongiform encephalopathy across western Canada. Mitig Adapt Strat for Gl. 14, 299-316.

McLennan, N., et al., 2004. Prion protein accumulation and neuroprotection in hypoxic brain damage. Am J Pathol. 165, 227-235.

Meeker, N. D., et al., 2007. Method for isolation of PCR-ready genomic DNA from zebrafish tissues. Biotechniques. 43, 610.

Mehrabian, M., et al., 2015. The Prion Protein Controls Polysialylation of Neural Cell Adhesion Molecule 1 during Cellular Morphogenesis. PLoS One. 10**,** e0133741.

Meng, X., et al., 2008. Targeted gene inactivation in zebrafish using engineered zinc-finger nucleases. Nat Biotechnol. 26**,** 695-701.

Mercer, R. C., et al., 2013. The prion protein modulates A-type K+ currents mediated by Kv4.2 complexes through dipeptidyl aminopeptidase-like protein 6. J Biol Chem. 288**,** 37241-55.

Meyer-Luehmann, M., et al., 2006. Exogenous induction of cerebral beta-amyloidogenesis is governed by agent and host. Science. 313**,** 1781-4.

Miesbauer, M., et al., 2006. Prion protein-related proteins from zebrafish are complex glycosylated and contain a glycosylphosphatidylinositol anchor. Biochem Biophys Res Commun. 341**,** 218-24.

Miller, J. C., et al., 2011. A TALE nuclease architecture for efficient genome editing. Nat Biotechnol. 29**,** 143-8.

Millhauser, G. L., 2007. Copper and the prion protein: Methods, structures, function, and disease. Annu Rev Phys Chem. 58**,** 299-320.

Minikel, E. V., et al., 2016. Quantifying prion disease penetrance using large population control cohorts. Sci Transl Med. 8**,** 322ra9.

Mo, H., et al., 2001. Two different neurodegenerative diseases caused by proteins with similar structures. Proc Natl Acad Sci U S A. 98**,** 2352-7.

Montag-Sallaz, M., Buonviso, N., 2002. Altered odor-induced expression of c-fos and arg 3.1 immediate early genes in the olfactory system after familiarization with an odor. J Neurobiol. 52**,** 61-72.

Moore, H. A., Whitmore, D., 2014. Circadian rhythmicity and light sensitivity of the zebrafish brain. PLoS One. 9**,** e86176.

Moore, R. C., et al., 1999. Ataxia in prion protein (PrP)-deficient mice is associated with upregulation of the novel PrP-like protein doppel. J Mol Biol. 292, 797-817.

Moore, R. C., et al., 1995. Double replacement gene targeting for the production of a series of mouse strains with different prion protein gene alterations. Biotechnology (N Y). 13, 999-1004.

Morales, R., et al., 2015. Prion-like features of misfolded Abeta and tau aggregates. Virus Res. 207, 106-12.

Morales, R., et al., 2010. Molecular cross talk between misfolded proteins in animal models of Alzheimer's and prion diseases. J Neurosci. 30, 4528-35.

Moretz, J. A., et al., 2007. Behavioral syndromes and the evolution of correlated behavior in zebrafish. Behav Ecol. 18, 556-562.

Morris, R. G., 2013. NMDA receptors and memory encoding. Neuropharmacology. 74, 32-40.

Moussavi Nik, S. H., et al., 2012. The BACE1-PSEN-AbetaPP regulatory axis has an ancient role in response to low oxygen/oxidative stress. J Alzheimers Dis. 28, 515-30.

Mullan, M., et al., 1992. A pathogenic mutation for probable Alzheimer's disease in the APP gene at the N-terminus of beta-amyloid. Nat Genet. 1, 345-7.

Muller, U., et al., 1994. Behavioral and anatomical deficits in mice homozygous for a modified beta-amyloid precursor protein gene. Cell. 79, 755-65.

Multhaup, G., et al., 1996. The amyloid precursor protein of Alzheimer's disease in the reduction of copper(II) to copper(I). Science. 271, 1406-9.

Murrell, J., et al., 1991. A mutation in the amyloid precursor protein associated with hereditary Alzheimer's disease. Science. 254, 97-9.

Musa, A., et al., 2001. Distinct expression patterns of two zebrafish homologues of the human APP gene during embryonic development. Dev Genes Evol. 211**,** 563-567.

Mussolino, C., et al., 2011. A novel TALE nuclease scaffold enables high genome editing activity in combination with low toxicity. Nucleic Acids Res. 39**,** 9283-93.

Nakao, N., et al., 1995. Trophic and protective actions of brain-derived neurotrophic factor on striatal DARPP-32-containing neurons in vitro. Brain Res Dev Brain Res. 90**,** 92-101.

Nico, P. B., et al., 2005. Altered behavioural response to acute stress in mice lacking cellular prion protein. Behav Brain Res. 162**,** 173-81.

Nicolas, M., Hassan, B. A., 2014. Amyloid precursor protein and neural development. Development. 141**,** 2543-8.

Ninomiya, H., et al., 1993. Amino acid sequence RERMS represents the active domain of amyloid beta/A4 protein precursor that promotes fibroblast growth. J Cell Biol. 121**,** 879-86.

Nishida, N., et al., 1997. Prion protein is necessary for latent learning and long-term memory retention. Cell Mol Neurobiol. 17**,** 537-45.

Nishimoto, I., et al., 1993. Alzheimer amyloid protein precursor complexes with brain GTP-binding protein G(o). Nature. 362**,** 75-9.

Norton, W., Bally-Cuif, L., 2010. Adult zebrafish as a model organism for behavioural genetics. BMC Neurosci. 11**,** 90.

Nourizadeh-Lillabadi, R., et al., 2010. Early Embryonic Gene Expression Profiling of Zebrafish Prion Protein (Prp2) Morphants. Plos One. 5.

Novak, P., et al., 2011. Tauons and prions: infamous cousins? J Alzheimers Dis. 26**,** 413-30.

Nussbaum, J. M., et al., 2012. Prion-like behaviour and tau-dependent cytotoxicity of pyroglutamylated amyloid-beta. Nature. 485, 651-5.

Nuvolone, M., et al., 2016. Strictly co-isogenic C57BL/6J-Prnp-/- mice: A rigorous resource for prion science. J Exp Med. 213, 313-27.

Oddo, S., et al., 2003. Triple-transgenic model of Alzheimer's disease with plaques and tangles: intracellular Abeta and synaptic dysfunction. Neuron. 39, 409-21.

Oesch, B., et al., 1985. A cellular gene encodes scrapie PrP 27-30 protein. Cell. 40, 735-46.

Ogwang, S. P., Inspection of a novel object by wild and laboratory Zebrafish (Danio rerio H.) in the presence and absence of alarm substance. Biology, Vol. M.Sc. The University of Bergen, Bergen, Norway, 2008, pp. 68.

Ohsawa, I., et al., 2001. Fibulin-1 binds the amino-terminal head of beta-amyloid precursor protein and modulates its physiological function. J Neurochem. 76, 1411-20.

Ou, M., et al., 2015. Responses of pink salmon to CO2-induced aquatic acidification. Nat Clim Change. 5, 950-955.

Oueslati, A., et al., 2014. Protein Transmission, Seeding and Degradation: Key Steps for alpha-Synuclein Prion-Like Propagation. Exp Neurobiol. 23, 324-36.

Pan, K. M., et al., 1993. Conversion of alpha-helices into beta-sheets features in the formation of the scrapie prion proteins. Proc Natl Acad Sci U S A. 90, 10962-6.

Pantera, B., et al., 2009. PrPc activation induces neurite outgrowth and differentiation in PC12 cells: role for caveolin-1 in the signal transduction pathway. J Neurochem. 110, 194-207.

Panula, P., et al., 2010. The comparative neuroanatomy and neurochemistry of zebrafish CNS systems of relevance to human neuropsychiatric diseases. Neurobiol Dis. 40**,** 46-57.

Parker, M. O., et al., 2014. The utility of zebrafish to study the mechanisms by which ethanol affects social behavior and anxiety during early brain development. Prog Neuropsychopharmacol Biol Psychiatry. 55**,** 94-100.

Parkin, E. T., et al., 1999. Amyloid precursor protein, although partially detergent-insoluble in mouse cerebral cortex, behaves as an atypical lipid raft protein. Biochem J. 344**,** 23.

Parkin, E. T., et al., 2007. Cellular prion protein regulates beta-secretase cleavage of the Alzheimer's amyloid precursor protein. Proc Natl Acad Sci U S A. 104**,** 11062-11067.

Pearce, M. M., et al., 2015. Prion-like transmission of neuronal huntingtin aggregates to phagocytic glia in the Drosophila brain. Nat Commun. 6**,** 6768.

Peeraer, E., et al., 2015. Intracerebral injection of preformed synthetic tau fibrils initiates widespread tauopathy and neuronal loss in the brains of tau transgenic mice. Neurobiol Dis. 73**,** 83-95.

Pillay, L. M., et al., 2013. Evaluating the Mutagenic Activity of Targeted Endonucleases Containing a Sharkey FokI Cleavage Domain Variant in Zebrafish. Zebrafish. 10, 353-64.

Poggiolini, I., et al., 2013. Prion protein misfolding, strains, and neurotoxicity: an update from studies on Mammalian prions. Int J Cell Biol. 2013**,** 910314.

Pokrishevsky, E., et al., 2012. Aberrant localization of FUS and TDP43 is associated with misfolding of SOD1 in amyotrophic lateral sclerosis. PLoS One. 7**,** e35050.

Porteus, M. H., Carroll, D., 2005. Gene targeting using zinc finger nucleases. Nat Biotechnol. 23**,** 967-73.

Premzl, M., et al., 2003. Shadoo, a new protein highly conserved from fish to mammals and with similarity to prion protein. Gene. 314, 89-102.

Prince, M., et al., 2013. The global prevalence of dementia: a systematic review and metaanalysis. Alzheimers Dement. 9, 63-75 e2.

Provost, E., et al., 2007. Viral 2A peptides allow expression of multiple proteins from a single ORF in transgenic zebrafish embryos. Genesis (New York, N.Y.: 2000). 45, 625.

Prudencio, M., et al., 2010. An examination of wild-type SOD1 in modulating the toxicity and aggregation of ALS-associated mutant SOD1. Hum Mol Genet. 19, 4774-89.

Prusiner, S., 1991. Molecular biology of prion diseases. Science. 252, 1515-1522.

Prusiner, S. B., 1982. Novel proteinaceous infectious particles cause scrapie. Science. 216, 136-44.

Prusiner, S. B., 1989. Scrapie prions. Annu Rev Microbiol. 43, 345-74.

Prusiner, S. B., et al., 1984. Purification and structural studies of a major scrapie prion protein. Cell. 38, 127-34.

Prusiner, S. B., et al., 1990. Transgenetic studies implicate interactions between homologous PrP isoforms in scrapie prion replication. Cell. 63, 673-86.

Pun, S., et al., 2006. Selective vulnerability and pruning of phasic motoneuron axons in motoneuron disease alleviated by CNTF. Nat Neurosci. 9, 408-19.

Pushie, M. J., et al., 2011. Prion protein expression level alters regional copper, iron and zinc content in the mouse brain. Metallomics. 3, 206-14.

Qi, L. S., et al., 2013. Repurposing CRISPR as an RNA-guided platform for sequence-specific control of gene expression. Cell. 152, 1173-83.

Radovanovic, I., et al., 2005. Truncated prion protein and Doppel are myelinotoxic in the absence of oligodendrocytic PrPC. J Neurosci. 25**,** 4879-88.

Rakhit, R., et al., 2004. Monomeric Cu,Zn-superoxide dismutase is a common misfolding intermediate in the oxidation models of sporadic and familial amyotrophic lateral sclerosis. J Biol Chem. 279**,** 15499-504.

Rambold, A. S., et al., 2008. Stress-protective signalling of prion protein is corrupted by scrapie prions. EMBO J. 27**,** 1974-84.

Ramesh, T., et al., 2010. A genetic model of amyotrophic lateral sclerosis in zebrafish displays phenotypic hallmarks of motoneuron disease. Dis Model Mech. 3**,** 652-62.

Rangel, A., et al., 2007. Enhanced susceptibility of Prnp-deficient mice to kainate-induced seizures, neuronal apoptosis, and death: Role of AMPA/kainate receptors. J Neurosci Res. 85**,** 2741-55.

Ratte, S., et al., 2011. Threshold for epileptiform activity is elevated in prion knockout mice. Neuroscience. 179**,** 56-61.

Rauk, A., 2009. The chemistry of Alzheimer's disease. Chem Soc Rev. 38**,** 2698-715.

Rea, M. A., 1989. Light increases Fos-related protein immunoreactivity in the rat suprachiasmatic nuclei. Brain Res Bull. 23**,** 577-81.

Reaume, A. G., et al., 1996. Motor neurons in Cu/Zn superoxide dismutase-deficient mice develop normally but exhibit enhanced cell death after axonal injury. Nat Genet. 13**,** 43-7.

Redler, R. L., Dokholyan, N. V., 2012. The complex molecular biology of amyotrophic lateral sclerosis (ALS). Prog Mol Biol Transl Sci. 107**,** 215-62.

Reinhard, C., et al., 2005. The amyloid-beta precursor protein: integrating structure with biological function. EMBO J. 24**,** 3996-4006.

Relano-Gines, A., et al., 2013. Prion replication occurs in endogenous adult neural stem cells and alters their neuronal fate: involvement of endogenous neural stem cells in prion diseases. PLoS Pathog. 9**,** e1003485.

Requena, J. R., Wille, H., 2014. The structure of the infectious prion protein: experimental data and molecular models. Prion. 8**,** 60-6.

Rial, D., et al., 2009. Cellular prion protein modulates age-related behavioral and neurochemical alterations in mice. Neuroscience. 164**,** 896-907.

Richt, J. A., et al., 2007. Production of cattle lacking prion protein. Nat Biotechnol. 25**,** 132-8.

Rihel, J., et al., 2010a. Zebrafish behavioral profiling links drugs to biological targets and rest/wake regulation. Science. 327**,** 348-51.

Rihel, J., et al., 2010b. Monitoring sleep and arousal in zebrafish. Methods Cell Biol. 100**,** 281-94.

Rihel, J., Schier, A. F., 2012. Behavioral screening for neuroactive drugs in zebrafish. Dev Neurobiol. 72**,** 373-85.

Roberson, E. D., et al., 2007. Reducing endogenous tau ameliorates amyloid beta-induced deficits in an Alzheimer's disease mouse model. Science. 316**,** 750-4.

Roberts, A. C., et al., 2011. Habituation of the C-start response in larval zebrafish exhibits several distinct phases and sensitivity to NMDA receptor blockade. PLoS One. 6**,** e29132.

Robu, M. E., et al., 2007. p53 activation by knockdown technologies. Plos Genetics. 3**,** 787-801.

Rodriguez, F., et al., 2002a. Spatial memory and hippocampal pallium through vertebrate evolution: insights from reptiles and teleost fish. Brain Res Bull. 57**,** 499-503.

Rodriguez, J. A., et al., 2002b. Familial amyotrophic lateral sclerosis-associated mutations decrease the thermal stability of distinctly metallated species of human copper/zinc superoxide dismutase. J Biol Chem. 277**,** 15932-7.

Roesler, R., et al., 1999. Normal inhibitory avoidance learning and anxiety, but increased locomotor activity in mice devoid of PrP(C). Brain Res Mol Brain Res. 71**,** 349-53.

Rosenkranz, S. C., et al., 2013. Amyloid-precursor-protein-lowering small molecules for disease modifying therapy of Alzheimer's disease. PLoS One. 8**,** e82255.

Rossi, A., et al., 2015. Genetic compensation induced by deleterious mutations but not gene knockdowns. Nature. 524**,** 230-3.

Rossi, D., et al., 2001. Onset of ataxia and Purkinje cell loss in PrP null mice inversely correlated with Dpl level in brain. EMBO J. 20**,** 694-702.

Rothstein, J. D., et al., 1995. Selective loss of glial glutamate transporter GLT-1 in amyotrophic lateral sclerosis. Ann Neurol. 38**,** 73-84.

Saccon, R. A., et al., 2013. Is SOD1 loss of function involved in amyotrophic lateral sclerosis? Brain. 136**,** 2342-58.

Safar, J. G., et al., 2005. Prion clearance in bigenic mice. J Gen Virol. 86**,** 2913-23.

Sakaguchi, S., et al., 1995. Accumulation of proteinase K-resistant prion protein (PrP) is restricted by the expression level of normal PrP in mice inoculated with a mouse-adapted strain of the Creutzfeldt-Jakob disease agent. J Virol. 69**,** 7586-92.

Sakudo, A., et al., 2005. Octapeptide repeat region and N-terminal half of hydrophobic region of prion protein (PrP) mediate PrP-dependent activation of superoxide dismutase. Biochem Biophys Res Commun. 326**,** 600-6.

Sakurai-Yamashita, Y., et al., 2005. Female-specific neuroprotection against transient brain ischemia observed in mice devoid of prion protein is abolished by ectopic expression of prion protein-like protein. Neuroscience. 136, 281-7.

Sales, N., et al., 1998. Cellular prion protein localization in rodent and primate brain. Eur J Neurosci. 10, 2464-71.

Salta, E., et al., 2014. Assessing proteinase K resistance of fish prion proteins in a scrapie-infected mouse neuroblastoma cell line. Viruses. 6, 4398-421.

Sander, J. D., et al., 2011. Targeted gene disruption in somatic zebrafish cells using engineered TALENs. Nat Biotechnol. 29, 697-8.

Santuccione, A., et al., 2005. Prion protein recruits its neuronal receptor NCAM to lipid rafts to activate p59fyn and to enhance neurite outgrowth. J Cell Biol. 169, 341-54.

Sarradin, P., et al., 2015. Transgenic Rabbits Expressing Ovine PrP Are Susceptible to Scrapie. PLoS Pathog. 11, e1005077.

Scheltens, P., et al., 2016. Alzheimer's disease. Lancet. 388, 505-17.

Schmidt, R., et al., 2013. Neurogenesis in zebrafish – from embryo to adult. Neural Dev. 8, 3.

Schmitt-Ulms, G., et al., 2004. Time-controlled transcardiac perfusion cross-linking for the study of protein interactions in complex tissues. Nat Biotechnol. 22, 724-731.

Schmitt-Ulms, G., et al., 2001. Binding of neural cell adhesion molecules (N-CAMs) to the cellular prion protein. J Mol Biol. 314, 1209.

Schmitz, M., et al., 2014a. Loss of Prion Protein Leads to Age-Dependent Behavioral Abnormalities and Changes in Cytoskeletal Protein Expression. Mol Neurobiol. 50, 923-36.

Schmitz, M., et al., 2014b. Impact of the cellular prion protein on amyloid-beta and 3PO-tau processing. J Alzheimers Dis. 38**,** 551-65.

Schwartz, P. J., et al., 1998. Effects of over- and under-expression of Cu,Zn-superoxide dismutase on the toxicity of glutamate analogs in transgenic mouse striatum. Brain Res. 789**,** 32-9.

Scott, A. C., et al., 1990. Bovine spongiform encephalopathy: detection and quantitation of fibrils, fibril protein (PrP) and vacuolation in brain. Vet Microbiol. 23**,** 295-304.

Scott, M., et al., 1989. Transgenic mice expressing hamster prion protein produce species-specific scrapie infectivity and amyloid plaques. Cell. 59**,** 847-57.

Seiler, C., Nicolson, T., 1999. Defective calmodulin-dependent rapid apical endocytosis in zebrafish sensory hair cell mutants. J Neurobiol. 41**,** 424-34.

Selkoe, D. J., 2011. Resolving controversies on the path to Alzheimer's therapeutics. Nat Med. 17**,** 1060-5.

Sempou, E., et al., 2016. Activation of zebrafish Src family kinases by the prion protein is an amyloid-beta-sensitive signal that prevents the endocytosis and degradation of E-cadherin/beta-catenin complexes in vivo. Mol Neurodegener. 11**,** 18.

Shamchuk, A. L., Tierney, K. B., 2012. Phenotyping stimulus evoked responses in larval zebrafish. Behaviour. 149**,** 1177-1203.

Shefner, J. M., et al., 1999. Mice lacking cytosolic copper/zinc superoxide dismutase display a distinctive motor axonopathy. Neurology. 53**,** 1239-46.

Shmerling, D., et al., 1998. Expression of amino-terminally truncated PrP in the mouse leading to ataxia and specific cerebellar lesions. Cell. 93**,** 203-14.

Shyu, W. C., et al., 2005. Overexpression of PrPC by adenovirus-mediated gene targeting reduces ischemic injury in a stroke rat model. J Neurosci. 25**,** 8967-77.

Small, D. H., et al., 1999. Neurite-outgrowth regulating functions of the amyloid protein precursor of Alzheimer's disease. J Alzheimers Dis. 1**,** 275-85.

Small, D. H., et al., 1994. A heparin-binding domain in the amyloid protein precursor of Alzheimer's disease is involved in the regulation of neurite outgrowth. J Neurosci. 14**,** 2117-27.

Smart, N., Riley, P. R., 2013. Thymosin beta4 in vascular development response to research commentary. Circ Res. 112**,** e29-30.

Soba, P., et al., 2005. Homo- and heterodimerization of APP family members promotes intercellular adhesion. EMBO Journal. 24**,** 3624.

Solis, G. P., et al., 2013. Conserved roles of the prion protein domains on subcellular localization and cell-cell adhesion. PLoS One. 8**,** e70327.

Solis, G. P., et al., 2012. Reggies/flotillins regulate E-cadherin–mediated cell contact formation by affecting EGFR trafficking. Mol Biol Cell. 23**,** 1812-1825.

Solomon, I. H., et al., 2010. Prion neurotoxicity: insights from prion protein mutants. Curr Issues Mol Biol. 12**,** 51-61.

Song, P., Pimplikar, S. W., 2012. Knockdown of amyloid precursor protein in zebrafish causes defects in motor axon outgrowth. PLoS One. 7**,** e34209.

Southwell, A. L., et al., 2013. A fully humanized transgenic mouse model of Huntington disease. Hum Mol Genet. 22**,** 18-34.

Spires, T. L., Hyman, B. T., 2005. Transgenic models of Alzheimer's disease: learning from animals. NeuroRx. 2**,** 423-37.

Stahl, N., et al., 1987. Scrapie prion protein contains a phosphatidylinositol glycolipid. Cell. 51**,** 229-40.

Stathopulos, P. B., et al., 2006. Calorimetric analysis of thermodynamic stability and aggregation for apo and holo amyotrophic lateral sclerosis-associated Gly-93 mutants of superoxide dismutase. J Biol Chem. 281, 6184-93.

Steele, A. D., et al., 2006. Prion protein (PrPc) positively regulates neural precursor proliferation during developmental and adult mammalian neurogenesis. Proc Natl Acad Sci U S A. 103, 3416-21.

Steele, A. D., et al., 2007. The prion protein knockout mouse: a phenotype under challenge. Prion. 1, 83-93.

Steinbach, J. P., et al., 1998. Hypersensitivity to seizures in beta-amyloid precursor protein deficient mice. Cell Death Differ. 5, 858-66.

Stoick-Cooper, C. L., et al., 2007. Distinct Wnt signaling pathways have opposing roles in appendage regeneration. Development. 134, 479-89.

Striebel, J. F., et al., 2013. Prion protein and susceptibility to kainate-induced seizures: genetic pitfalls in the use of PrP knockout mice. Prion. 7, 280-5.

Stys, P. K., et al., 2012. Copper-dependent regulation of NMDA receptors by cellular prion protein: implications for neurodegenerative disorders. J Physiol. 590, 1357-68.

Sun, J., et al., 2015. Remarkable impairment of Wnt/beta-catenin signaling in the brains of the mice infected with scrapie agents. J Neurochem. 136, 731-740.

Sun, Y., et al., 2001. Polyglutamine-expanded huntingtin promotes sensitization of N-methyl-D-aspartate receptors via post-synaptic density 95. J Biol Chem. 276, 24713-8.

Sunyach, C., et al., 2007. The C-terminal products of cellular prion protein processing, C1 and C2, exert distinct influence on p53-dependent staurosporine-induced caspase-3 activation. J Biol Chem. 282, 1956-63.

Suzuki, N., et al., 1994. An increased percentage of long amyloid beta protein secreted by familial amyloid beta protein precursor (beta APP717) mutants. Science. 264, 1336-40.

Swain, H. A., et al., 2004. Effects of dizocilpine (MK-801) on circling behavior, swimming activity, and place preference in zebrafish (Danio rerio). Neurotoxicol Teratol. 26, 725-9.

Takei, Y., et al., 2000. Defects in axonal elongation and neuronal migration in mice with disrupted tau and map1b genes. J Cell Biol. 150, 989-1000.

Tanzi, R. E., et al., 1988. Protease inhibitor domain encoded by an amyloid protein precursor mRNA associated with Alzheimer's disease. Nature. 331, 528-30.

Tarr, P. E., et al., 2002. Tyrosine phosphorylation of the beta-amyloid precursor protein cytoplasmic tail promotes interaction with Shc. J Biol Chem. 277, 16798-804.

Telling, G. C., et al., 1996. Interactions between wild-type and mutant prion proteins modulate neurodegeneration in transgenic mice. Genes Dev. 10, 1736-1750.

Telling, G. C., et al., 1995. Prion propagation in mice expressing human and chimeric PrP transgenes implicates the interaction of cellular PrP with another protein. Cell. 83, 79-90.

Teng, Y., et al., 2010. Knockdown of zebrafish Lgi1a results in abnormal development, brain defects and a seizure-like behavioral phenotype. Hum Mol Genet. 19, 4409-20.

Thomas, E. D., et al., 2015. There and back again: development and regeneration of the zebrafish lateral line system. Wiley Interdiscip Rev Dev Biol. 4, 1-16.

Thomas, J. G., et al., 2013. Iatrogenic Creutzfeldt-Jakob disease via surgical instruments. J Clin Neurosci. 20, 1207-12.

Tierney, K. B., 2011. Behavioural assessments of neurotoxic effects and neurodegeneration in zebrafish. Biochim Biophys Acta. 1812**,** 381-389.

Tobler, I., et al., 1996. Altered circadian activity rhythms and sleep in mice devoid of prion protein. Nature. 380**,** 639-42.

Turk, E., et al., 1988. Purification and properties of the cellular and scrapie hamster prion proteins. Eur J Biochem. 176**,** 21-30.

Turner, B. J., Talbot, K., 2008. Transgenics, toxicity and therapeutics in rodent models of mutant SOD1-mediated familial ALS. Prog Neurobiol. 85**,** 94-134.

Urwin, P. J., et al., 2016. Creutzfeldt-Jakob disease and blood transfusion: updated results of the UK Transfusion Medicine Epidemiology Review Study. Vox Sang. 110**,** 310-6.

Van Cauwenberghe, C., et al., 2016. The genetic landscape of Alzheimer disease: clinical implications and perspectives. Genet Med. 18**,** 421-30.

van der Kant, R., Goldstein, L. S., 2015. Cellular Functions of the Amyloid Precursor Protein from Development to Dementia. Dev Cell. 32**,** 502-515.

Vázquez-Fernández, E., et al., 2016. The Structural Architecture of an Infectious Mammalian Prion Using Electron Cryomicroscopy. PLoS Pathog. 12**,** e1005835.

Villablanca, E. J., et al., 2006. Control of cell migration in the zebrafish lateral line: implication of the gene "tumour-associated calcium signal transducer," tacstd. Dev Dyn. 235**,** 1578-88.

Volke, V., et al., 1995. Inhibition of nitric oxide synthase causes anxiolytic-like behaviour in an elevated plus-maze. Neuroreport. 6**,** 1413-6.

Walker, F. O., 2007. Huntington's disease. Lancet. 369**,** 218-28.

Walker, L. C., et al., 2013. Mechanisms of protein seeding in neurodegenerative diseases. JAMA Neurol. 70**,** 304-10.

Walsh, D. M., et al., 2002. Naturally secreted oligomers of amyloid beta protein potently inhibit hippocampal long-term potentiation in vivo. Nature. 416, 535-9.

Walsh, D. M., et al., 1997. Amyloid beta-protein fibrillogenesis. Detection of a protofibrillar intermediate. J Biol Chem. 272, 22364-72.

Walz, R., et al., 1999. Increased sensitivity to seizures in mice lacking cellular prion protein. Epilepsia. 40, 1679-1682.

Wang, P., et al., 2005. Defective neuromuscular synapses in mice lacking amyloid precursor protein (APP) and APP-Like protein 2. J Neurosci. 25, 1219-25.

Wang, Z. L., et al., 2009. Presynaptic and Postsynaptic Interaction of the Amyloid Precursor Protein Promotes Peripheral and Central Synaptogenesis. J Neurosci. 29, 10788.

Ward, H. J., et al., 2006. Risk factors for variant Creutzfeldt-Jakob disease: a case-control study. Ann Neurol. 59, 111-20.

Watt, N. T., et al., 2012. Prion protein facilitates uptake of zinc into neuronal cells. Nat Commun. 3, 1134.

Watts, J. C., et al., 2014. Serial propagation of distinct strains of Abeta prions from Alzheimer's disease patients. Proc Natl Acad Sci U S A. 111, 10323-8.

Watts, J. C., et al., 2009. Interactome Analyses Identify Ties of PrPC and Its Mammalian Paralogs to Oligomannosidic N-Glycans and Endoplasmic Reticulum-Derived Chaperones. PloS Pathogens. 5.

Watts, J. C., Prusiner, S. B., 2014. Mouse models for studying the formation and propagation of prions. J Biol Chem. 289, 19841-9.

Wei, C., et al., 2013. TALEN or Cas9 - Rapid, Efficient and Specific Choices for Genome Modifications. J Genet Genomics. 40, 281-9.

Weise, J., et al., 2006. Deletion of cellular prion protein results in reduced Akt activation, enhanced postischemic caspase-3 activation, and exacerbation of ischemic brain injury. Stroke. 37**,** 1296-300.

Weissmann, C., et al., 1994. Susceptibility to scrapie in mice is dependent on PrPC. Philos Trans R Soc Lond B Biol Sci. 343**,** 431-3.

Westerfield, M., 2000. The Zebrafish Book. A Guide for the Laboratory Use of Zebrafish (Danio rerio). University of Oregon Press, Eugene, OR.

Westergard, L., et al., 2011. A naturally occurring C-terminal fragment of the prion protein (PrP) delays disease and acts as a dominant-negative inhibitor of PrPSc formation. J Biol Chem. 286**,** 44234-42.

Whitehouse, I. J., et al., 2010. Prion Protein is Reduced in Aging and in Sporadic but not in Familial Alzheimer's Disease. J Alzheimers Dis. 22**,** 1023-1031.

Whitehouse, I. J., et al., 2013. Prion protein is decreased in Alzheimer's brain and inversely correlates with BACE1 activity, amyloid-beta levels and Braak stage. PLoS One. 8**,** e59554.

Wienholds, E., et al., 2002. Target-selected inactivation of the zebrafish rag1 gene. Science. 297**,** 99-102.

Wieser, H. G., et al., 2006. EEG in Creutzfeldt-Jakob disease. Clin Neurophysiol. 117**,** 935-51.

Will, R. G., et al., 1996. A new variant of Creutzfeldt-Jakob disease in the UK. Lancet. 347**,** 921-5.

Williams, E. S., Young, S., 1980. Chronic wasting disease of captive mule deer: a spongiform encephalopathy. J Wildl Dis. 16**,** 89-98.

Winklhofer, K. F., et al., 2008. The two faces of protein misfolding: gain- and loss-of-function in neurodegenerative diseases. EMBO J. 27**,** 336-49.

Winters, B. D., et al., 2011. On the dynamic nature of the engram: evidence for circuit-level reorganization of object memory traces following reactivation. J Neurosci. 31, 17719-28.

Wong, P. C., et al., 1995. An adverse property of a familial ALS-linked SOD1 mutation causes motor neuron disease characterized by vacuolar degeneration of mitochondria. Neuron. 14, 1105-16.

Wood, J. L., et al., 1997. Neuropathology of scrapie: a study of the distribution patterns of brain lesions in 222 cases of natural scrapie in sheep, 1982-1991. Vet Rec. 140, 167-74.

Wright, D., et al., 2006. QTL analysis of behavioral and morphological differentiation between wild and laboratory zebrafish (Danio rerio). Behav Genet. 36, 271-84.

Wright, D., et al., 2003. Inter and intra-population variation in shoaling and boldness in the zebrafish (Danio rerio). Naturwissenschaften. 90, 374-7.

Yokoyama, T., et al., 2001. In vivo conversion of cellular prion protein to pathogenic isoforms, as monitored by conformation-specific antibodies. J Biol Chem. 276, 11265-71.

You, H., et al., 2012. Abeta neurotoxicity depends on interactions between copper ions, prion protein, and N-methyl-D-aspartate receptors. Proc Natl Acad Sci U S A. 109, 1737-42.

Young, R., et al., 2009. The prion or the related Shadoo protein is required for early mouse embryogenesis. FEBS Lett. 583, 3296-300.

Yu, G., et al., 2009. Generation of goats lacking prion protein. Mol Reprod Dev. 76, 3.

Zahn, R., et al., 2000. NMR solution structure of the human prion protein. Proc Natl Acad Sci U S A. 97, 145-50.

Zanata, S. M., et al., 2002. Stress-inducible protein 1 is a cell surface ligand for cellular prion that triggers neuroprotection. EMBO J. 21**,** 3307-16.

Zeineddine, R., et al., 2015. SOD1 protein aggregates stimulate macropinocytosis in neurons to facilitate their propagation. Mol Neurodegener. 10**,** 57.

Zhang, B., et al., 2012. The microtubule-stabilizing agent, epothilone D, reduces axonal dysfunction, neurotoxicity, cognitive deficits, and Alzheimer-like pathology in an interventional study with aged tau transgenic mice. J Neurosci. 32**,** 3601-11.

Zheng, H., et al., 1995. beta-Amyloid precursor protein-deficient mice show reactive gliosis and decreased locomotor activity. Cell. 81**,** 525-31.

Zuccato, C., et al., 2001. Loss of huntingtin-mediated BDNF gene transcription in Huntington's disease. Science. 293**,** 493-8.

**Appendix A. Towards creating a zebrafish model of Alzheimer's Disease**

A1.1 Summary

We endeavoured to create a zebrafish model of Alzheimer's disease (AD) that would enable us to study the mechanisms underlying AD and to study the physiological consequences of the recently reported interaction between Aβ oligomers and PrP^C (Lauren et al., 2009). We were unable to generate a stable transgenic zebrafish line expressing human APP. We did, however, create zebrafish lines capable of driving Kal4 in neurons under the *Enolase 2* promoter that can be used to activate other UAS transgenes.

A1.2 Introduction

We aimed to create a zebrafish model of AD that would facilitate study of the pathophysiological effects of Aβ peptide fragments. Existing animal models of AD do not display all features of AD (reviewed in (Spires and Hyman, 2005)), thus a zebrafish model of AD might help to fill this gap. Further, zebrafish larvae exhibiting features of AD would be an *in vivo* system accessible to high throughput drug screening (reviewed in (Lieschke and Currie, 2007)). Some familial AD mutations in the Amyloid Precursor Protein (APP) including the Swedish mutations (K595N, M596L, (Mullan et al., 1992)) and the Indiana mutation (V642F in APP695, (Murrell et al., 1991)) increase the production of Aβ peptides from APP (Citron et al., 1992; Suzuki et al., 1994). We therefore set out to create transgenic zebrafish that would produce the 695 isoform of APP with the Swedish and Indiana mutations, hereafter referred to as huAPP695$^{Swe/Ind}$. We hypothesized that these transgenic fish would produce human Aβ peptides and would exhibit pathological features of AD including signs of neuron loss, tau hyperphosphorylation and synapse loss (reviewed in (Spires and Hyman, 2005)). We used a Kaloop expression system inspired by (Distel et al., 2009) wherein Kal4 is expressed by a gene specific promoter (Enolase 2 for expression in neurons or GFAP for expression in glia), while a transgene containing the gene of interest (in this case *APP$^{Swe/Ind}$*) fused to Viral 2A peptide-KalTA4 is activated by the binding of Kal4 to a 4xupstream activating element (4xUAS; Figure A.1). The Viral 2A peptide is expected to interrupt translation so that APP$^{Swe/Ind}$ and Kal4 become separate proteins (Provost et al., 2007). The advantage of this approach over directly driving huAPP695$^{Swe/Ind}$ with a gene

specific promoter is that huAPP695$^{Swe/Ind}$ cannot be expressed until fish containing this transgene are crossed with a driver line. Therefore, we predicted that production of stable lines that express a fairly active transgene, despite the potential toxicity of huAPP695$^{Swe/Ind}$, would be possible. We were successful in creating *Enolase 2* (*Eno2*) driver lines that could activate mCherry under 4xUAS, but unfortunately were unable to generate stable lines that were validated as expressing appreciable levels of *4xUAS-APP$^{Swe/Ind}$-V2AKalTA4.*
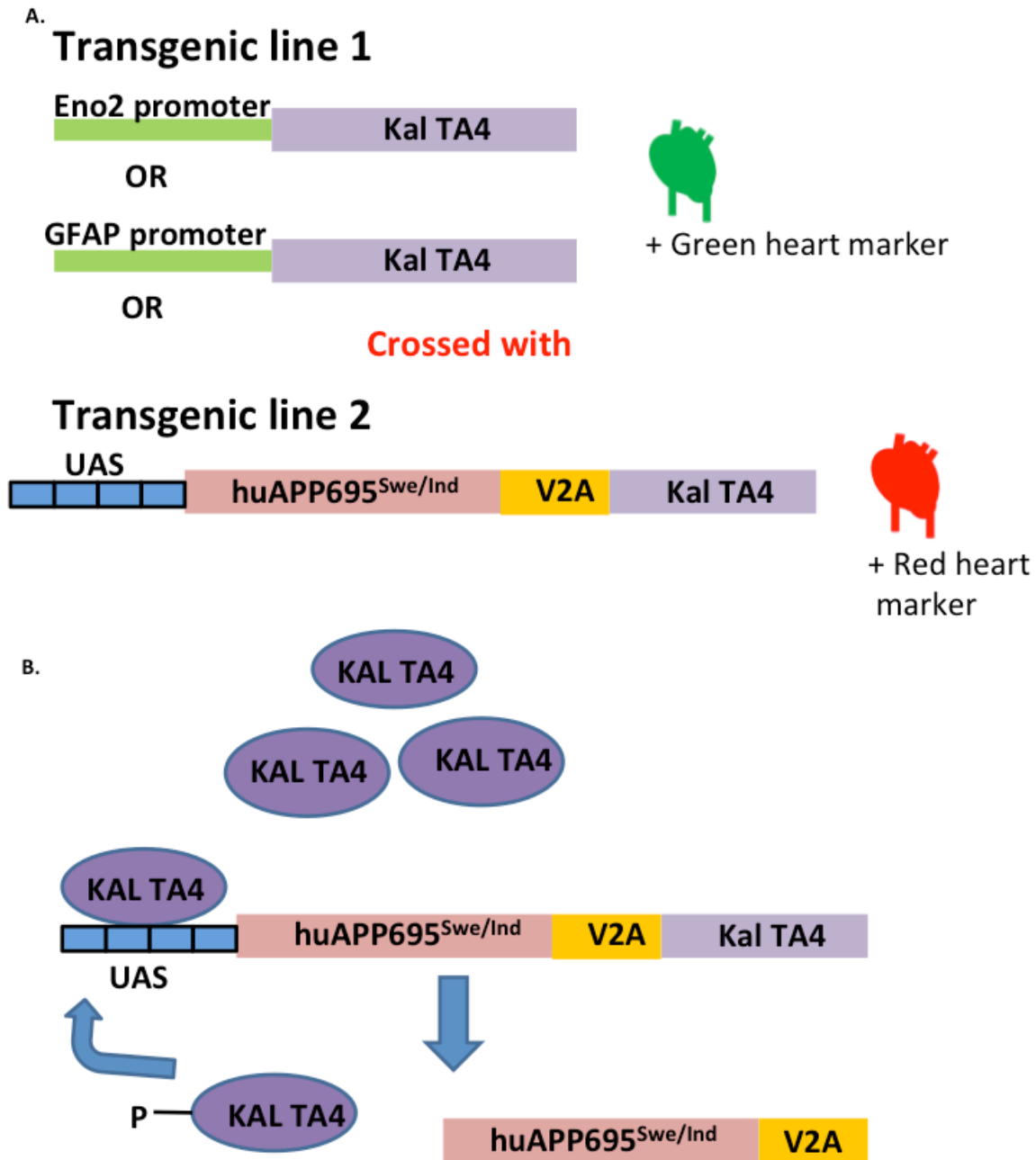
Figure A.1. Schematic of the Kaloop model used to produce huAPP695$^{Swe/Ind}$

A. In these models, fish with a cell specific promoter (Eno2 or GFAP) driving KalTA4 are crossed to lines with Human APP$^{Swe/Ind}$ under the control of an upstream activating sequence (UAS). **B.** KalTA4 expression is first driven by a cell specific promoter. KalTA4 then binds to the UAS to activate transcription of Human APP$^{Swe/Ind}$-V2A-KalTA4. During translation, the viral 2A peptide (V2A) splits the Human APP$^{Swe/Ind}$ from

KalTA4, producing two separate proteins. The resulting KalTA4 binds to UAS to continue the feed forward loop of KalTA4 and Human APP$^{Swe/Ind}$ production.

A1.3 Methods

Engineering Tol-2 based transgenic constructs

Multi-site Gateway Cloning and Tol2 systems were used as previously described (Fraser et al., 2013; Kwan et al., 2007) to engineer the following constructs:

1) pDestTol2CG2.eno2:KalTA4.pA-2 (Allison Lab Glycerol Stock #a6a-42)

2) pDestTol2CG2.GFAP:KalTA4.pA-2 (Allison Lab Glycerol Stock #a6a-41)

3) pDestTol2CR2-4xuas-huAPP695$^{Swe/Ind}$-T2AKalTA4 (Allison Lab Glycerol Stock #a6a-53)

Creation of pDestTol2CR2-4xuas-huAPP695$^{Swe/Ind}$-T2AKalTA4:
Amplifying huAPP695$^{Swe/Ind}$ from an existing pCDNA plasmid obtained from David Westaway's laboratory served as the starting point for generating pMe-huAPP695Swe/Ind entry vector. The PCR reaction added the attb1 and attb2 adapter sequences required for the Gateway BP reaction. The reverse primer included a base pair substitution to remove the stop codon. The BP reaction was then performed using BP Clonase II (Invitrogen Life Technologies/Thermo Fisher Scientific 11789-020, Waltham MA, USA).

The 3p-V2AKalTA4 entry vector was generated by amplifying V2AKalTA4 from the unpublished pDestTol2CR2-4xuas-zebrafishBri-humanAβ42 construct. The PCR reaction added attb2 and attb3 adapter sequences for the Gateway BP reaction. Primers used for the construction of the entry vectors can be found in Table A.1. The Gateway LR reaction was used to combine the p5e-4xuas (Distel, 2009: PNAS) pME-huAPP695$^{Swe/Ind}$, and p3e-V2AKalTA4 entry vectors with pDestTol2CR2. The reaction was performed using LR clonase II plus (Invitrogen Life Technologies/Thermo Fisher Scientific 12538-120, Waltham MA, USA). pDestTol2CR2 is a modification of the pDestTol2CG2 vector in which mCherry replaces GFP. Fluorescent red heart muscle is a marker of successful integration of the transgene (Kim et al., 2016).

Table A.1. Primers used to generate the pME-huAPP695$^{Swe/Ind}$ entry vector

| Entry vector	Forward primer	Reverse primer
pME-huAPP695$^{Swe/Ind}$	5'-GGGGACAAGTTTGTACAAAAAAGCAGGCTCCATGCTGCCCGGTTTGGCACTG-3'	5'-GGGGACCACTTTGTACAAGAAAGCTGGGTCCTGGTTCTGCATCTGCTCAAAGAA-3'

Generating transgenic zebrafish

The three constructs described above were individually microinjected into 1-4 cell stage AB strain or AB/Wik strain zebrafish embryos at a 50-75 pg dose/embryo along with 25 pg of *Tol2*mRNA as previously described (Kwan et al., 2007). Larvae injected with the pDestTol2CG2.eno2:KalTA4.pA-2 and pDestTol2CG2.GFAP:KalTA4.pA-2 constructs were screened for the green heart marker and larvae injected with the pDestTol2CR2-4xuas-huAPP695$^{Swe/Ind}$-T2AKalTA4 construct were screened for the red heart marker. F0 generation fish expressing the appropriate markers were grown to adulthood. F0 generation fish were bred and F1 generation larvae were screened for the appropriate transgenic marker. F1 generation fish expressing the transgenic marker were then grown to adulthood. Transgenic alleles were maintained in the Allison lab fish facility by crossing F1 fish to AB-strain wild type zebrafish.

A1.4 Results and Discussion

Three stable lines of Eno2-KalTA4 (ua3112, ua3119, and ua3120) were identified and lines ua3112 and ua3119 were found to drive expression of UAS-mCherry (Figure A.2). Several stable lines of GFAP-KalTA4 (ua3114, ua3126-ua3134), but their ability to drive a UAS-construct have not yet been demonstrated. The 4xuas-huAPP$^{Swe/Ind}$ construct proved to be toxic to the fish. Later batches of pDestTol2CR2-4xuas-huAPP$^{Swe/Ind}$-T2AKalTA4 injected embryos were co-injected with lower doses of *transposase* mRNA (5 or 15 pg/embryo), but the embryo survival was still low. Some 4xuas-huAPP$^{Swe/Ind}$-T2AKalTA4 transient transgenic (F0 generation) fish survived to adulthood, but germline transmission of the construct was not observed. The toxicity of the construct could indicate that there is leaky expression of the transgene, and fish that survive have less efficient transgene expression.

To conclude, the Eno2:KalTA4 transgenic lines produced here (and GFAP:KalTA4 lines following validation) can be used to drive expression of other 4xUAS transgenes, and other methods are being deployed to create a zebrafish model of AD. Alternate techniques for producing zebrafish that express *huAPP695*[Swe/Ind] include using a Cre-Lox system (Hans et al., 2009) or humanizing zebrafish *appb* using CRISPR knock-in techniques (Auer et al., 2014). A zebrafish model of AD will be informative in the study of the pathophysiological mechanisms of AD. For example, it could be used to study interactions between Aβ and PrP[C]. It could also serve as a tool for high throughput drug screening if zebrafish larvae exhibit features of AD.
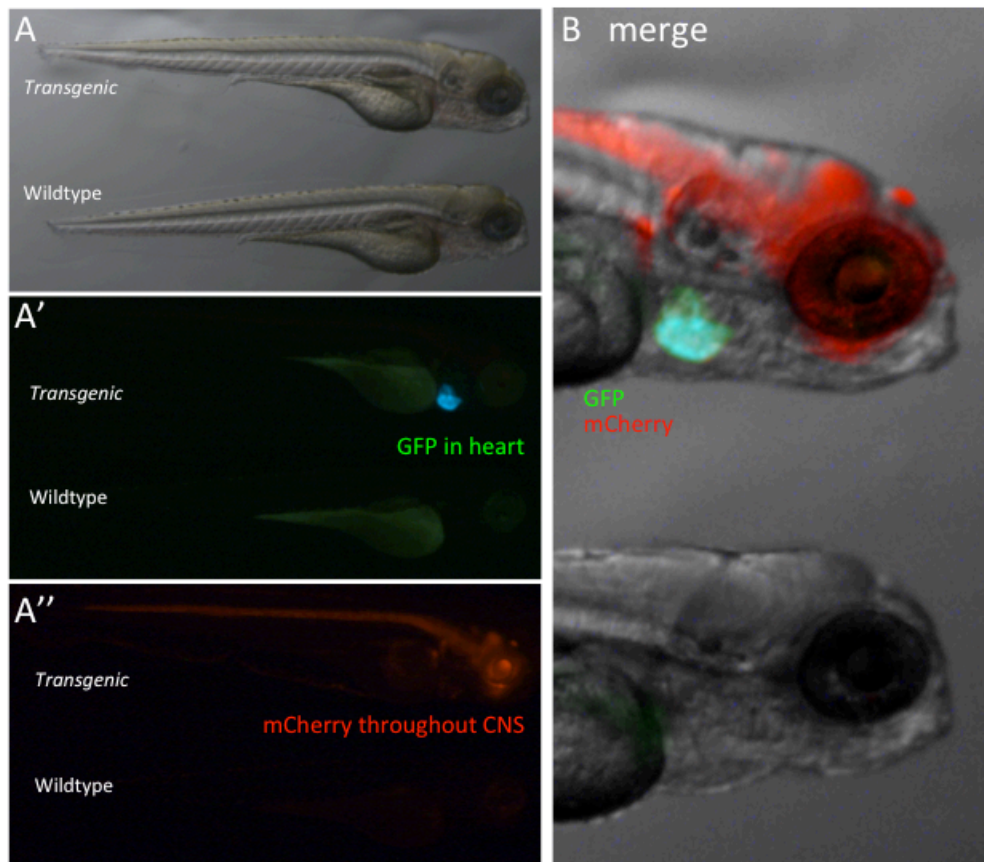
Figure A.2. Eno2Kal TA4 lines successfully drive expression of *UAS:mCherry*.

A. The top fish has two transgenes (Its heart has both red and green fluorescence markers) – one drives expression of *KalTA4* through the CNS (neuronal *Enolase 2* promoter) and the other expresses both *KalTA4 + mCherry* under control of the uas promoter. **B.** A merge of these images indicates a high level of expression of mCherry protein in the CNS, encouraging us that our strategy can lead to abundant expression of proteins.

Appendix A References

Auer, T. O., et al., 2014. Highly efficient CRISPR/Cas9-mediated knock-in in zebrafish by homology-independent DNA repair. Genome Res. 24**,** 142-53.

Citron, M., et al., 1992. Mutation of the beta-amyloid precursor protein in familial Alzheimer's disease increases beta-protein production. Nature. 360**,** 672-674.

Distel, M., et al., 2009. Optimized Gal4 genetics for permanent gene expression mapping in zebrafish. Proc Natl Acad Sci U S A. 106**,** 13365-70.

Fraser, B., et al., 2013. Regeneration of cone photoreceptors when cell ablation is primarily restricted to a particular cone subtype. PLoS One. 8**,** e55410.

Hans, S., et al., 2009. Temporally-controlled site-specific recombination in zebrafish. PLoS One. 4**,** e4640.

Kim, J. W., et al., 2016. Recruitment of Rod Photoreceptors from Short-Wavelength-Sensitive Cones during the Evolution of Nocturnal Vision in Mammals. Dev Cell. 37**,** 520-32.

Kwan, K. M., et al., 2007. The Tol2kit: a multisite gateway-based construction kit for Tol2 transposon transgenesis constructs. Dev Dyn. 236**,** 3088.

Lauren, J., et al., 2009. Cellular prion protein mediates impairment of synaptic plasticity by amyloid-beta oligomers. Nature. 457**,** 1128-U84.

Lieschke, G. J., Currie, P. D., 2007. Animal models of human disease: zebrafish swim into view. Nat Rev Genet. 8**,** 353-67.

Mullan, M., et al., 1992. A pathogenic mutation for probable Alzheimer's disease in the APP gene at the N-terminus of beta-amyloid. Nat Genet. 1**,** 345-7.

Murrell, J., et al., 1991. A mutation in the amyloid precursor protein associated with hereditary Alzheimer's disease. Science. 254**,** 97-9.

Provost, E., et al., 2007. Viral 2A peptides allow expression of multiple proteins from a single ORF in transgenic zebrafish embryos. Genesis (New York, N.Y.: 2000). 45**,** 625.

Spires, T. L., Hyman, B. T., 2005. Transgenic models of Alzheimer's disease: learning from animals. NeuroRx. 2**,** 423-37.

Suzuki, N., et al., 1994. An increased percentage of long amyloid beta protein secreted by familial amyloid beta protein precursor (beta APP717) mutants. Science. 264**,** 1336-40.